COMBINING IMINIUM ION-MEDIATED CATALYSIS AND PHOTOCHEMISTRY TO DEVELOP ENANTIOSELECTIVE RADICAL PROCESSES

Pablo Bonilla Dominguez

UNIVERSITAT ROVIRA i VIRGILI

Combining Iminium Ion-Mediated Catalysis and Photochemistry to Develop Enantioselective Radical Processes

Pablo Bonilla Dominguez

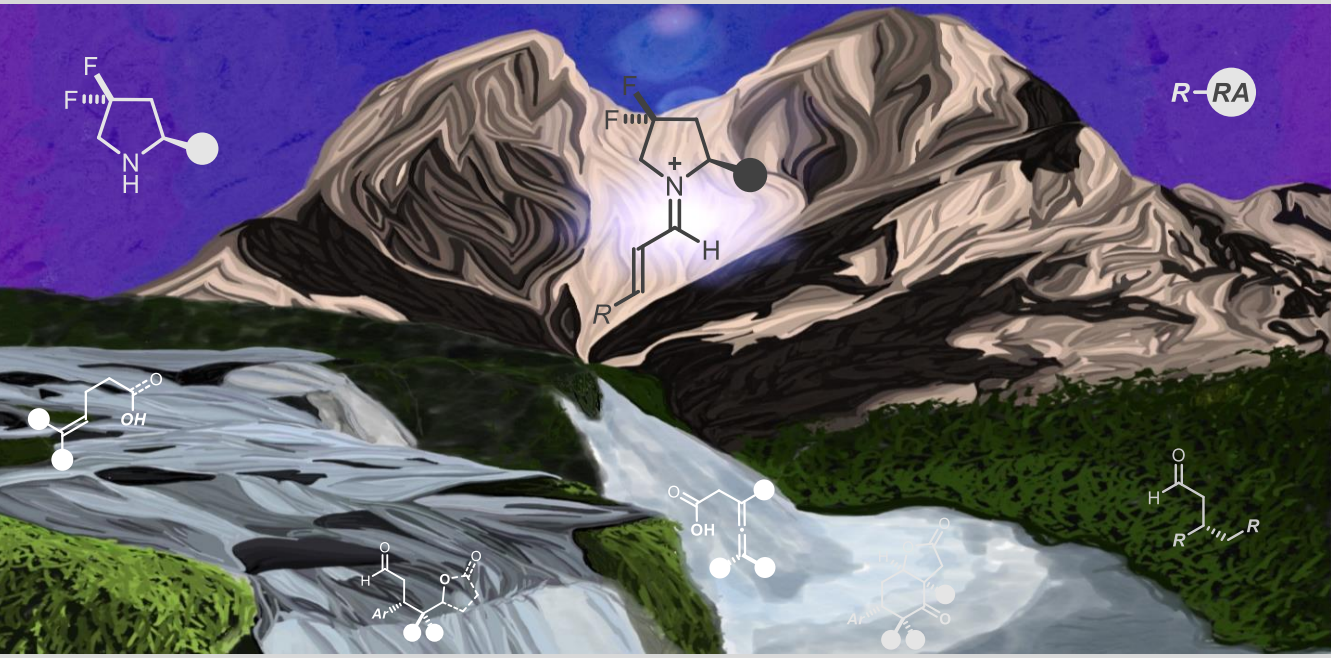

DOCTORAL THESIS
2020

UNIVERSITAT ROVIRA I VIRGILI
COMBINING IMINIUM ION-MEDIATED CATALYSIS AND PHOTOCHEMISTRY TO DEVELOP ENANTIOSELECTIVE RADICAL PROCESSES
Pablo Bonilla Domínguez

UNIVERSITAT ROVIRA I VIRGILI
COMBINING IMINIUM ION-MEDIATED CATALYSIS AND PHOTOCHEMISTRY TO DEVELOP ENANTIOSELECTIVE RADICAL PROCESSES
Pablo Bonilla Domínguez

Pablo Bonilla Domínguez

Combining Iminium Ion-Mediated Catalysis and Photochemistry to Develop Enantioselective Radical Processes

Doctoral Thesis

Supervised by Prof. Paolo Melchiorre

ICIQ – Institut Català d'Investigació Química

Tarragona

2020

UNIVERSITAT ROVIRA I VIRGILI
COMBINING IMINIUM ION-MEDIATED CATALYSIS AND PHOTOCHEMISTRY TO DEVELOP ENANTIOSELECTIVE RADICAL PROCESSES
Pablo Bonilla Domínguez

UNIVERSITAT ROVIRA i VIRGILI

ICIQ Institut Català d'Investigació Química

Prof. Paolo Melchiorre, ICREA Research Professor & ICIQ Group Leader

I STATE that the present study, entitled "Combining Iminium Ion-Mediated Catalysis and Photochemistry to Develop Enantioselective Radical Processes", presented by PABLO BONILLA DOMÍNGUEZ for the award of the degree of Doctor, has been carried out under my supervision at the Institut Català d'Investigació Química (ICIQ).

Tarragona, June 1st 2020

Doctoral Thesis Supervisor

Prof. Paolo Melchiorre

UNIVERSITAT ROVIRA I VIRGILI
COMBINING IMINIUM ION-MEDIATED CATALYSIS AND PHOTOCHEMISTRY TO DEVELOP ENANTIOSELECTIVE RADICAL PROCESSES
Pablo Bonilla Domínguez

Acknowledgments

This is probably one of the most important parts of the thesis, if not the most, since completing a PhD is not possible without the support of the people around you.

I would like to express my gratitude to *Prof. Paolo Melchiorre*, for giving me the opportunity to be part of his research group and for guiding me through this process of self-growth as a scientist.

All the former and current members of the Melchiorre group also deserve to be acknowledged for all the science and life we have share together. In particular, I'm grateful to *Catherine*, for helping me during my PhD by being always available to discuss anything (from science to psychology) and being there to support me and help me keep focus. To *Yannick*, for teaching me the importance of fundamental organic knowledge and precision. To *Luca Perego*, for sharing with me his wisdom. To *Emilien*, for making these last months of the thesis more entertaining and showing me that the French are not that bad. To *Daniele*, for coping with me during conferences, I will miss that loud clapping. To *Giulio*, for the patience and peace that he transmitted. To *Nurty*, for her infinite smile thanks to Lo-Fi and gossip. To *Ben*, for the perfectly pronounced "qué pasa, cab**n?". To *Giacomo,* for his unlimited energy, "colazione, chiquis?". To Giando, for tempting me to buy stuff I didnot need. To *Eugenio* and *Adriana* for welcoming me in the Italian corner of 2.10. To *Edu*, for defending the Spanish cuisine and the right pronunciation of Madriz. Special thanks to the proofreaders of this thesis that did a wonderful job: Ben, Dengke, Edu, Emilien, Eugenio, and Riccardo.

I am also grateful to *Núria Planella*, *Dr. Lorna Piazzi* and, *Maria Checa* for administrative support. I thank the research support units at ICIQ, in particular I am indebted to the NMR-staff, the X-ray unit, the spectroscopy unit and the chromatography unit.

I have to dedicate a special thanks to *Marine*, for the amazing design of the cover, and for putting up with all the details and changes I did to it. *Apéroooo*!

I also want to thank all the friends I have met in Tarragona that have become my family. To *Ani*, for being there with me since day 1 (literally) sharing life, problems, and happiness above all. To *Joan*, for teaching me so much about how to let go, be open, loving, honest, and trustworthy. To *Ángel*, for being yourself, bringing you contagious laugh into my life and increase my self-confidence every day. To *Adi* (mi amor platónico) and *Bruna*, for making one year feel like a life together. To Miguelito, for being as trustworthy as one can be. To *David*, for his uncontrollable energy, joy and his persistence to buy Iron Maiden tickets. To *Alba,* for being so much like me and controlling David. To *Cris* la ilicitana de Zaragoza, for always being one bit stronger than me so that I keep pushing. To *Jana*, for having the energy of a child and the strength of a Spartan. To *Jan*, for all the Becherovka that he made me drink. To *Jake* and *Anna*, for making everything smoother and easier. To *Ana Arroyo*, for expressing so much with her face. To *Cris M.*, for sharing and understanding my southern roots. To *Mauro*, for proving that you can reach the top in everything you do (even without feet). To *Enric*, bippez ici. To *Raul*, mi bro. To *Pau*, for enduring me in the house and providing amazing beer. To *Laia*, for the ideas and opportunities to do outreach. To the whole group of bous (*Rosie, Jeroen, Katia, Sope, Jessica, Marino, Marta*) for all the climbing and fun we shared.

Since I would not be who I am today without the people that have been my past and present, I have to thank the *Ftoseinos* (Almu, Fidel, David, Antuan, Borja, Delia y Gabi) for all the memories and fun during the past years. Almu, cara de seta. Also, to *Carlos*, my brother from another mother, who has always been there and always will be, reminding me of the jabato I am.

Por supuesto, también tengo que dar las gracias a aquellos que me han visto crecer, que me han criado y me han apoyado desde que nací. Aquellos cuyo amor y educación han hecho de mí el hombre que soy hoy en día y de los que considero que este logro es tan mío como suyo, mi madre, mi padre y mis hermanos. Gracias a mis tíos y primos por conseguir que me pase todo el año esperando las reuniones familiares para poder jugar y reírme como lo hago. Gracias también al pilar fundamental de mi familia, mi abuela, la mujer a la

que aspiro convertirme algún día para poder decir: “a mis 80 años soy feliz y no me arrepiento de nada”.

Por último, gracias a la persona con la que he compartido más de un tercio de mi vida y que me ha entregado todo su corazón cada minuto que hemos estado juntos. La misma que me ha apoyado en todas mis decisiones y ha hecho que estos últimos 10 años de mi vida hayan sido los más felices de mi vida. Gracias a ella me he descubierto mejor a mí mismo y a los que me rodean. No existen páginas ni palabras suficientes para explicar todo lo que te debo, así que voy a intentar devolvértelo de aquí el final de mis días. Te quiero pato.

I would also like to acknowledge the financial support from the Institute of Chemical Research of Catalonia (ICIQ) and from the European Research Council for the ERC consolidator grant, under the European Union’s Horizon 2020 research and innovation programme (grant agreement No 681840-CATA-LUX).

UNIVERSITAT ROVIRA I VIRGILI
COMBINING IMINIUM ION-MEDIATED CATALYSIS AND PHOTOCHEMISTRY TO DEVELOP ENANTIOSELECTIVE RADICAL PROCESSES
Pablo Bonilla Domínguez

List of publications

Some of the results presented in this thesis have been published:

- Bonilla, P.; Rey, Y. P.; Holden, C. M.; Melchiorre, P. "Photo-Organocatalytic Enantioselective Radical Cascade Reactions of Unactivated Olefins" *Angew. Chem. Int. Ed.,* **2018**, *57*, 12819.
- Perego, L. A.; Bonilla, P.; Melchiorre, P. "Photo-Organocatalytic Enantioselective Radical Cascade Enabled by Single-Electron Transfer Activation of Allenes" *Adv. Synth. Catal.,* **2020**, *362*, 302.

UNIVERSITAT ROVIRA I VIRGILI
COMBINING IMINIUM ION-MEDIATED CATALYSIS AND PHOTOCHEMISTRY TO DEVELOP ENANTIOSELECTIVE RADICAL PROCESSES
Pablo Bonilla Domínguez

"La suerte se busca, pero con los privilegios se nace"

UNIVERSITAT ROVIRA I VIRGILI
COMBINING IMINIUM ION-MEDIATED CATALYSIS AND PHOTOCHEMISTRY TO DEVELOP ENANTIOSELECTIVE RADICAL PROCESSES
Pablo Bonilla Domínguez

Table of Contents

UNIVERSITAT ROVIRA I VIRGILI
COMBINING IMINIUM ION-MEDIATED CATALYSIS AND PHOTOCHEMISTRY TO DEVELOP ENANTIOSELECTIVE RADICAL PROCESSES
Pablo Bonilla Domínguez

Chapter I

General Overview

1.1. Asymmetric Organocatalysis

All forms of life contain chiral molecules.[1] This notion has deeply influenced scientists and particularly chemists, who have devoted tremendous efforts towards new synthetic methods to access selectively a single enantiomer of a chiral molecule.[2] Historically, the development of enantioselective catalytic processes has relied on the use of organometallic reagents and enzymes.[3] Along with them, organocatalysis is nowadays recognized as the third main mode of activation for the stereoselective synthesis of chiral molecules.[4] Although some early examples were reported during the past century,[5] the field of enantioselective organocatalysis was not generally established until the seminal independent contributions from MacMillan[6] and List, Lerner and Barbas,[7] appeared in 2000. Since then, organocatalysis has experienced an exponential growth. The extensive use of organic catalysts in asymmetric catalysis was partially justified by their ready availability, low toxicity, and their tolerance to air and moisture.[8] Another key factor to the success of organocatalysis is that it offers generic modes of substrate activation based on the predictable interaction of a chiral catalyst with fundamental functional groups within the reagent, such as ketones, aldehydes, alkenes, or imines. The catalysts' interaction with the substrates generates chiral

[1] Yamamoto, H.; Carreira, E. M. (eds.) Comprehensive Chirality. Elsevier, **2012**.

[2] Ramón, D. J.; Yus, D. "In the Arena of Enantioselective Synthesis, Titanium Complexes Wear the Laurel Wreath Titanium" *Chem. Rev.* **2006**, *106*, 2126.

[3] Dalko, P. I. (ed.) Enantioselective Organocatalysis: Reactions and Experimental Procedures. Wiley-VCH, **2007**.

[4] Melchiorre, P.; Marigo, M.; Carlone, A.; Bartoli, G. "Asymmetric Aminocatalysis—Gold Rush in Organic Chemistry" *Angew. Chem. Int. Ed.*, **2008**, *47*, 6138.

[5] References therein: List, B. "Emil Knoevenagel and the Roots of Aminocatalysis" *Angew. Chem. Int. Ed.*, **2010**, *49*, 1730.

[6] Ahrendt, K. A.; Borths, C. J.; MacMillan, D. W. C. "New Strategies for Organic Catalysis: The First Highly Enantioselective Organocatalytic Diels-Alder Reaction" *J. Am. Chem. Soc.*, **2000**, *122*, 4243.

[7] List, B.; Lerner, R. A.; Barbas III, C. F. "Proline-Catalyzed Direct Asymmetric Aldol Reactions" *J. Am. Chem. Soc.*, **2000**, *122*, 2395.

[8] Holden, C. M.; Melchiorre, P. "Photochemistry and excited-state reactivity of organocatalytic intermediates" Photochemistry, **2020**, *47*, 344.

reactive intermediates that can trigger mechanistically-related but different reactions with high predictability and enantiocontrol.[9]

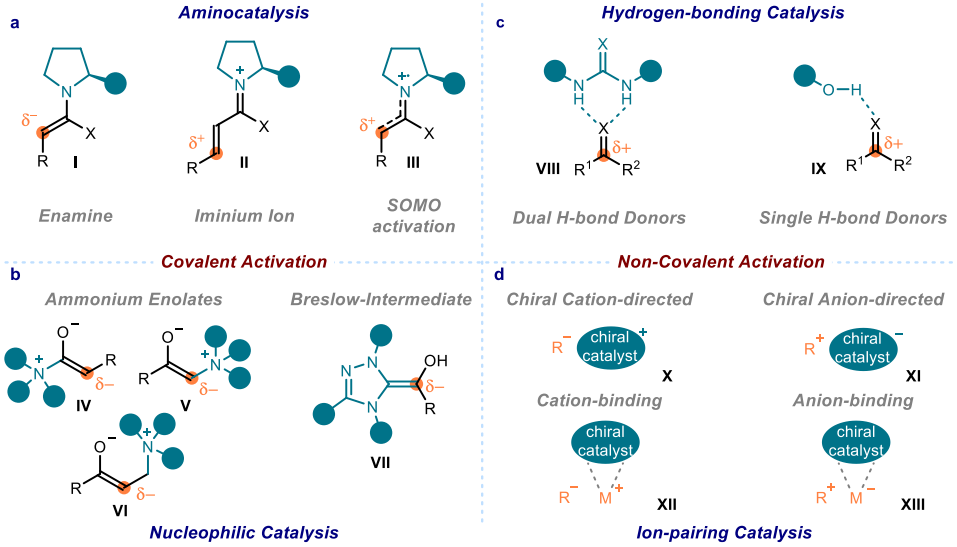

Figure 1.1. Activation modes in organocatalysis. Green circles represent different fragments of the chiral catalyst scaffolds. SOMO: singly occupied molecular orbital. X: N, O, S.

The different organocatalytic modes of substrate activation are generally classified based on the nature of the interaction between the chiral catalyst and the reactive functional group. Within the *covalent activation* methods (Figure 1.1, left part), chiral primary and secondary amines allow the functionalization of ketones and aldehydes *via* the formation of catalytic chiral enamines (**I**), iminium ions (**II**), and α-iminyl radical cation intermediates (**III**, Figure 1.1.a).[9] Chiral tertiary amines (**IV**-**VI**) enable the activation of complementary carbonyl compounds such as esters, amides, or nitriles through the generation of chiral enolate equivalents (Figure 1.1.b).[10] *N*-heterocyclic carbene catalysis infers an *umpolung* (inverted) reactivity[11] to aldehydes upon the formation of the Breslow intermediate (**VII**), which acts as an acyl anion equivalent.[12]

[9] MacMillan, D. W. "The Advent and Development of Organocatalysis" *Nature*, **2008**, *455*, 304.

[10] Johansson, C. C. C.; Gaunt, M. J. "Recent Developments in the Use of Catalytic Asymmetric Ammonium Enolates in Chemical Synthesis" *Chem. Rev.*, **2007**, *107*, 5596.

[11] Seebach, D. "Methods of Reactivity Umpolung" *Angew. Chem. Int. Ed.*, **1979**, *18*, 239.

[12] Enders, D.; Niemeier, O.; Henseler, A. "Organocatalysis by *N*-heterocyclic Carbenes" *Chem. Rev.*, **2007**, *107*, 5606.

Alternatively, *non-covalent activation* methods rely on several weak attractive interactions between the catalyst and the substrate (Figure 1.1, right part). On the one hand, hydrogen-bonding catalysis mimics some enzymatic activation methods to interact with substrates and delivers highly enantio-enriched chiral products (Figure 1.1.c).[13] On the other hand, ion-pairing catalysis depends on secondary structural elements to overcome their inherent less directionality compared to covalent or H-bonding interactions to ensure stereoselectivity (Figure 1.1.d).[14]

These organocatalytic modes of substrate activation were widely exploited in polar chemistry.[15] In comparison, less attention has been paid to the use of organocatalysis to control the stereoselectivity of radical processes.[16] This is partly because classical methods for radical generation require conditions not compatible with asymmetric organocatalysis (e.g. use of high temperatures or generation of a large amount of radicals employing stoichiometric initiators). The situation changed substantially when organocatalysis was merged with photochemical reactivity.[17] This combination paved the way for the incorporation of open-shell-based chemistry[18] and excited-state reactivity[19] into the portfolio of organocatalytic asymmetric transformations.

In 2008, David MacMillan's group[17] foresaw that this combination could solve one of the long-standing synthetic challenges of two-electron organocatalytic pathways, namely the direct asymmetric catalytic α-alkylation of carbonyl compounds.[20,21] To overcome the intrinsic modest reactivity of alkyl halides towards S_N2 pathways, chiral enamines[22] were used to intercept radicals, generated under very mild conditions from

---

[13] Doyle, A. G.; Jacobsen, E. N. "Small-Molecule H-Bond Donors in Asymmetric Catalysis" *Chem. Rev.*, **2007**, *107*, 5713.

[14] Brak, K.; Jacobsen, E. N. "Asymmetric Ion-Pairing Catalysis" *Angew. Chem. Int. Ed.*, **2013**, 52, 534.

[15] Pellissier, H. (ed.) Recent developments in asymmetric organocatalysis. Royal Society of Chemistry, **2010**.

[16] Silvi, M.; Melchiorre, P. "Enhancing the Potential of Enantioselective Organocatalysis with Light" *Nature*, **2018**, *554*, 41.

[17] Nicewicz, D. A.; MacMillan D. W. C. "Merging Photoredox Catalysis with Organocatalysis: The Direct Asymmetric Alkylation of Aldehydes" *Science*, **2008**, *322*, 77.

[18] Chatgilialoglu, C.; Studer, A. (ed) Encyclopedia of Radicals in Chemistry, Biology and Materials. Wiley-VCH, **2012**.

[19] Albini, A.; Fagnoni, M. (ed) Handbook of Synthetic Photochemistry. Wiley-VCH, **2010**.

[20] Melchiorre, P. "Light in Aminocatalysis: The Asymmetric Intermolecular α-Alkylation of Aldehydes" *Angew. Chem. Int. Ed.*, **2009**, *48*, 1360.

[21] List, B., Cŏrić, I.; Grygorenko, O. O.; Kaib, P. S. J.; Komarov, I.; Lee, A.; Leutzsch, M.; Chandra Pan, S.; Tymtsunik, A. V.; van Gemmeren, M. "The catalytic asymmetric α-benzylation of aldehydes" *Angew. Chem. Int. Ed.*, **2014**, *53*, 282.

[22] Beeson, T. D.; Mastracchio, A.; Hong, J.-B.; Ashton, K.; MacMillan, D.W.C. "Enantioselective Organocatalysis Using SOMO Activation" *Science*, **2007**, *316*, 582.

alkyl bromides using a photoredox catalyst (Figure 1.2).[23] Key to the implementation of this strategy was the use of a ruthenium-based polypyridyl photocatalyst ($[Ru(bpy)_3]^{2+}$, in which bpy is 2,2′ -bipyridine), which could form open-shell intermediates under conditions compatible with the enamine catalytic asymmetric regime (ambient temperature and using visible light irradiation). Before this point, $[Ru(bpy)_3]^{2+}$ had only been used sporadically in the synthetic chemistry area,[24] although its photophysical behavior was extensively studied[25] and its applications as single-electron transfer (SET) agent used for water splitting.[26] In the ground state, $[Ru(bpy)_3]^{2+}$ (Ru(II)) is a poor SET reductant and oxidant, while excitation by light converts it into a versatile and potent SET agent.[27]

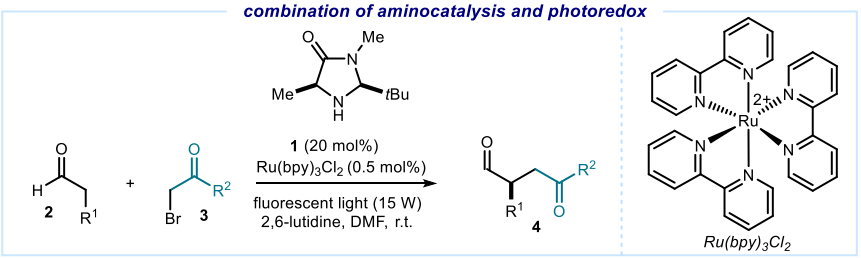

Figure 1.2. Asymmetric direct α-alkylation of aldehydes by merging organocatalysis and photoredox catalysis.

In the system developed by MacMillan, the reaction mechanism (Figure 1.3.a) merges two independent catalytic cycles. On one side, the photoredox catalytic cycle encompasses a Ru(I) intermediate, which acts as a SET reductant ($E_{red}(\mathbf{Ru^{2+}/Ru^{+}})$= -1.33 V) to generate electron-deficient radicals (**XVI**) from the alkyl bromides (**3**). The excited-state *Ru(II) ($E_{red}(\mathbf{*Ru^{2+}/Ru^{+}})$= +0.77 V), formed upon light irradiation, gives

[23] Nicewicz, D. A.; MacMillan D. W. C. "Merging Photoredox Catalysis with Organocatalysis: The Direct Asymmetric Alkylation of Aldehydes" *Science,* **2008**, *322*, 77

[24] a) Hedstrand, D. M.; Kruizinga, W. H.; Kellogg, R. M. "Light induced and dye accelerated reductions of phenacyl onium salts by 1,4-dihydropyridines" *Tetrahedron Lett.*, **1978**, *14*, 1255; b) van Bergen, T. J.; Hedstrand, D.M.; Kruizinga, W. H.; Kellogg, R. M. "Hydride Transfer from 1,4-Dihydropyridines to sp^3-Hybridized Carbon in Sulfonium Salts and Activated Halides. Studies with NAD(P)H Models" *J. Org. Chem.*, **1979**, *44*, 4953; c) Pac, C.; Ihama, M.; Yasuda, M.; Miyauchi, Y.; Sakurai, H. "$Ru(bpy)_3^{2+}$-Mediated Photoreduction of Olefins with 1-Benzyl-1,4-dihydronicotinamide: A Mechanistic Probe for Electron-Transfer Reactions of NAD(P)H-Model Compounds" *J. Am. Chem. Soc.*, **1981**, *103*, 6495.

[25] Juris, A.; Balzani, V.; Barigelletti, F.; Campagna, S.; Belser, P.; von Zelewsky, A. "Ru(II) polypyridine complexes: photophysics, photochemistry, electrochemistry, and chemiluminescence" *Coord. Chem. Rev.*, **1988**, *84*, 85.

[26] Meyer, T. J. "Chemical Approaches to Artificial Photosynthesis" *Acc. Chem. Res.*, **1989**, 22, 163.

[27] Prier, K. C.; Rankic, D. A.; MacMillan, D. W. C. "Visible Light Photoredox Catalysis with Transition Metal Complexes: Applications in Organic Synthesis" *Chem. Rev.*, **2013**, *113*, 5322.

one electron to the α-amino radical intermediate **XV** to generate the iminium ion **XV**, which is then prone to hydrolysis to liberate the catalyst and the final chiral product **4**. Concomitantly, the nucleophilic chiral enamine **XIV**, generated upon condensation of the chiral organocatalyst **1** with the carbonyl compound **2**, traps the radical **XVI** to forge the stereogenic center within intermediate **XV**, which after SET and hydrolysis yields the enantioenriched product **4**.

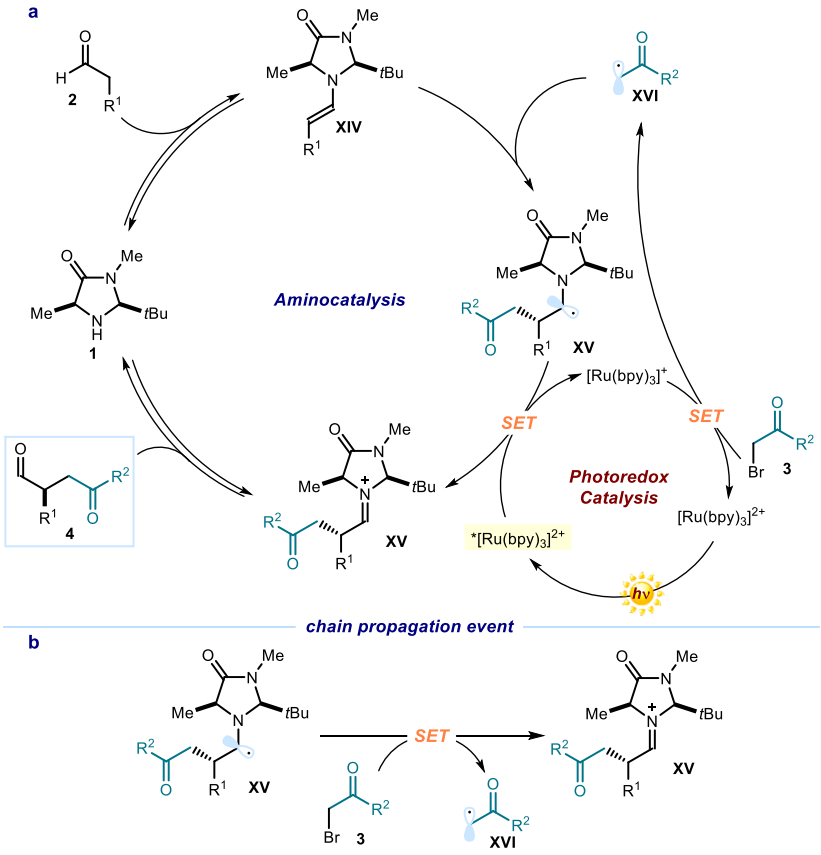

Figure 1.3. a) Mechanism of the asymmetric direct α-alkylation of aldehydes by merging organocatalysis and photoredox catalysis; b) main propagation event for the radical chain by single-electron transfer (SET) between **XV** and **3.**

Subsequent mechanistic investigations[28] established that the process was triggered by a self-propagating radical mechanism, where the photoredox catalyst served as an initiator for the first radical generation. The α-amino radical **XV** is the one reducing the organic bromide **3** to **XVI**, thus propagating the radical chain (Figure 1.3.b). The

[28] Cismesia, M. A.; Yoon, T. P. "Characterizing Chain Processes in Visible Light Photoredox Catalysis" *Chem. Sci.*, **2015**, *6*, 5426.

scope of this transformation was expanded to include other radical precursors suitable for the asymmetric α-alkylation of aldehydes, including trifluoromethylation,[29] benzylation,[30] cyanoalkylation,[31] and acylation[32] processes.

This study had a profound impact on the field of asymmetric catalysis. It demonstrated the possibility to perform asymmetric radical processes using classical organocatalytic tools. It also paved the way, along with concomitant studies by Yoon[33] and Stephenson,[34] to the field of photoredox catalysis.

1.1.1. Direct Excitation of Organocatalytic Intermediates

The combination of photoredox catalysis and organocatalysis allowed the development of transformations that were previously elusive via classical two-electron pathways, mainly because of the possibility to access radical intermediates under mild conditions. Another strategy to form radical effectively relies on the direct photoexcitation of chiral organic intermediates, which provided new possibilities to expand the synthetic potential of asymmetric organocatalysis.[16] The reaction depicted in Figure 1.2 was crucial to extend the reactivity of chiral enamines to the photochemical domain. When studying the asymmetric α-functionalization of aldehydes **5** with electron-poor alkyl bromides **6** catalyzed by the chiral amine **8** (Figure 1.4), our research group realized, by means of a control experiment, that the transformation could be promoted by direct light irradiation, without the need for an external photoredox catalyst.[35] This discovery unlocked new paths to mildly generate open-shell intermediates *via* SET mechanisms and engage them in asymmetric

[29] Nagib, D. A.; Scott, M. E; MacMillan, D. W. C. "Enantioselective α-Trifluoromethylation of Aldehydes Via Photoredox Organocatalysis" *J. Am. Chem. Soc.*, **2009**, *131*, 10875.

[30] Shih, H.-W.; Vander Wal, M. N.; Grange, R. L; MacMillan, D. W. C. "Enantioselective α-Benzylation of Aldehydes via Photoredox Organocatalysis" *J. Am. Chem. Soc.*, **2010**, *132*, 13600.

[31] Welin, E. R.; Warkentin, A. A.; Conrad, J. C.; MacMillan, D. W. C. "Enantioselective α-Alkylation of Aldehydes by Photoredox Organocatalysis: Rapid Access to Pharmacophore Fragments from β-Cyanoaldehydes" *Angew. Chem. Int. Ed.*, **2015**, *54*, 9668.

[32] Zhu, Y.; Zhang, L.; Luo, S. "Asymmetric α-Photoalkylation of β-Ketocarbonyls by Primary Amine Catalysis: Facile Access to Acyclic All-Carbon QuaternaryStereocenters" *J. Am. Chem. Soc.*, **2014**, *136*, 14642.

[33] Ischay, M. A.; Anzovino, M. E.; Du, J.; Yoon, T. P. "Efficient visible light photocatalysis of [2+2] enone cycloadditions" *J. Am. Chem. Soc.* **2008**, *130*, 12886.

[34] Narayanam, J. M. R.; Tucker, J. W.; Stephenson, C. R. J.; "Electron-Transfer Photoredox Catalysis: Development of a Tin-Free Reductive Dehalogenation Reaction" *J. Am. Chem. Soc.*, **2009**, *131*, 8756.

[35] Arceo, E.; Jurberg, I. D.; Alvarez-Fernández, A.; Melchiorre, P. "Photochemical Activity of a Key Donor–Acceptor Complex can Drive Stereoselective Catalytic α-Alkylation of Aldehydes" *Nat. Chem.*, **2013**, 5, 750.

transformations employing a single chiral organocatalyst. It also unveiled the rich photochemistry of classical organocatalytic intermediates, such as enamines.[16]

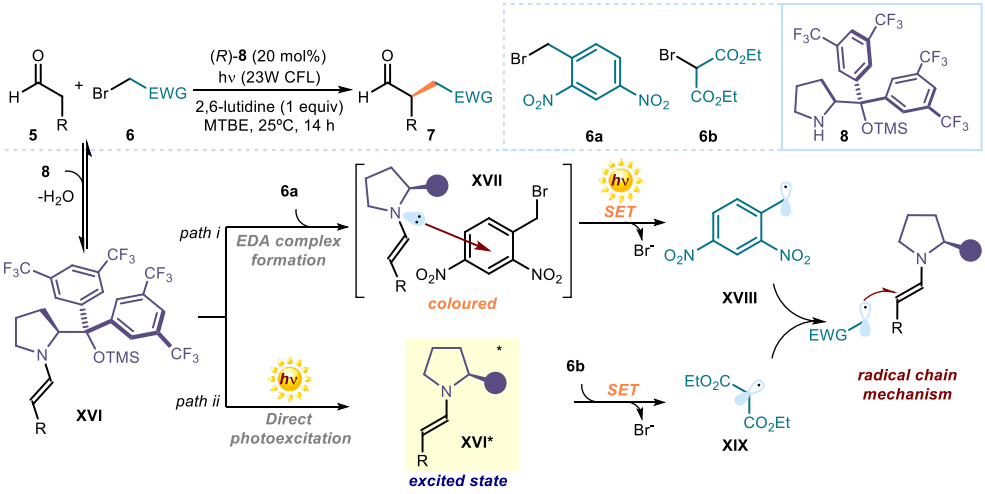

Figure 1.4. The photochemistry of enamines can generate radicals: a) Ground-state Electron Donor-Acceptor (EDA) complex formation and subsequent light irradiation of **XVI** generates radical **XVIII**; b) Direct photoexcitation of **XVI** generates a strong reductant that promotes the SET reduction of **6b** to form radical **XIX**.

Mechanistic investigations (Figure 1.4) established that two different pathways are available to the chiral enamines **XVI** to generate radicals, depending on the alkyl bromide **6** employed.[36] In the first mechanism (path *i* in Figure 1.4), the association of an electron-rich chiral enamine (**XVI**) and electron-poor benzyl bromide (**6a**) generated a ground-state colored electron donor-acceptor (EDA) complex **XVII**.[37] The EDA complex, contrary to the achromatic precursors **XVI** and **6a**, could absorb visible light to reach the excited state and subsequently inducing a SET to form the radical intermediate (**XVIII**).[35] The second mechanism, depicted in path *ii* in Figure 1.3, relied on the direct excitation by near UV-light (≈ 400 nm) of a chiral enamine intermediate (**XVI***), which behaved as a strong SET reductant in its excited state (E_{red}*(**XVI**$^{\bullet+}$/**XVI***)≈ -2.50 V, vs Ag/AgCl, NaCl sat.). The radical **XIX** was formed upon reductive cleavage of bromomalonate **6b**, a substrate which could not form an EDA

[36] Bahamonde, A.; Melchiorre, P. "Mechanism of The Stereoselective α-Alkylation of Aldehydes Driven by the Photochemical Activity of Enamines" *J. Am. Chem. Soc.*, **2016**, *138*, 8019.

[37] Mulliken, R. S. "Molecular Compounds and their Spectra. II" *J. Am. Chem. Soc.*, **1952**, *74*, 811; b) Rathore, R.; Kochi, J. K. "Donor/acceptor Organizations and the Electron-Transfer Paradigm for Organic Reactivity" *Adv. Phys. Org. Chem.*, **2000**, *35*, 193.

complex with the enamine (Figure 1.4.b).[38] In both mechanisms (paths *i* and *ii*), after the initial radical formation triggered by the photochemistry of enamines, intermediates **XVIII** and **XIX** sustained a self-propagating radical chain mechanism to deliver the enantioenriched chiral product **7**.[36]

The discovery that the catalytic functions of enamines could be expanded by exploiting their excited-state reactivity provided new opportunities for asymmetric catalysis with radicals using light-irradiated aminocatalytic intermediates. Following this idea, our research group demonstrated that another classical organocatalytic intermediate, the chiral iminium ion, can be used in the excited state to generate radicals and catalyze asymmetric processes not achievable via thermal pathways (Figure 1.5).[39] In this system, the condensation of a chiral secondary amine (**12** or **13**) to achromatic cinnamaldehyde (**13**) produced an electrophilic colored iminium ion **XX**. Visible-light irradiation promoted the formation of an electronic excited state (**XX***), turning the electrophilic iminium ion into a strong oxidant (E_{red}* (**XX***/ **XXI**) ≈ +2.40 V,[40] vs Ag/Ag$^+$ in CH_3CN).[41] SET from organosilane **10** to **XX*** triggered the formation of the silyl radical cation **XXII** along with the chiral β-enaminyl radical **XXI**. The irreversible fragmentation of the silyl group of **XXII** generated the neutral radical intermediate **XXIII**, hampering the unproductive back-electron transfer (BET). At this juncture, the stereocontrolled radical coupling between the two open-shell species **XXIII** and **XXI**, formed the new C-C bond while forging the stereogenic center. Upon hydrolysis, the resulting enamine intermediate **XXIV** regenerated the catalyst **12** while delivering the β-functionalized products **11**.

This methodology allowed the enantioselective β-functionalization of enals with substrates that were previously elusive to ground-state iminium ion reactivity. Key for the success of this methodology was the design of a new family of proline-based chiral secondary amine catalysts (**12** and **13**) bearing two geminal fluorine atoms on the pyrrolidine scaffold and a bulkier thexyldimethylsilane (TDS) protecting group on the oxygen.

---

[38] Silvi, M.; Arceo, E.; Jurberg, I. D.; Cassani, C.; Melchiorre, P. "Enantioselective organocatalytic alkylation of aldehydes and enals driven by the direct photoexcitation of enamines" *J. Am. Chem. Soc.*, **2015**, *137*, 6120.

[39] Silvi, M.; Verrier, C.; Rey, Y. P.; Buzzetti, L; Melchiorre, P. "Visible-light Excitation of Iminium Ions Enables the Enantioselective Catalytic β-Alkylation of Enals" *Nat. Chem.*, **2017**, *9*, 868.

[40] The value is estimated using the Rehm-Weller approximation. Rehm, D.; Weller, A. "Kinetics of Fluorescence Quenching by Electron and H-Atom Transfer" *Isr. J. Chem.*, **1970**, *8*, 259.

[41] Mariano, P. S. "Electron-Transfer Mechanisms in Photochemical Transformations of Iminium Salts" *Acc. Chem. Res.*, **1983**, *16*, 130.

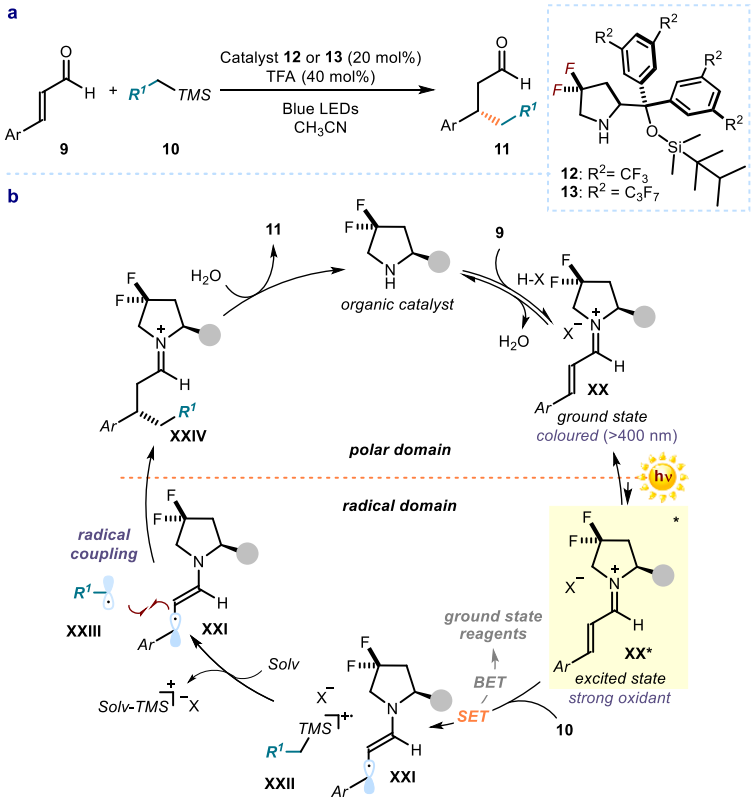

Figure 1.5. Direct photoexcitation of chiral iminium ions allows the asymmetric β-functionalization of cinnamaldehydes with non-nucleophilic silanes, which act as radical precursors.

The studies discussed in Figure 1.5 demonstrate the potential of chiral excited-state iminium ions to trigger the radical formation and deliver chiral products with high stereocontrol. The ground-state and excited-state reactivity of iminium ions will form the basis for the development of the catalytic asymmetric radical transformations explored in this research thesis.

1.2. General Objectives and Summary

The main scientific objective of my doctoral studies was to demonstrate the potential of organocatalysis to make chiral molecules with high stereoselectivity using the reactivity of photochemically generated radicals. The open-shell species were generated by two different approaches: i) upon direct excitation of chiral iminium ions while exploiting the ensuing (SET) mechanisms, or ii) by using an external photoredox catalyst.

Chapter II will detail the state-of-the-art in the field of enantioselective iminium ion organocatalysis and radical chemistry, detailing the reported strategies that exploit the combination of organocatalysis and light-driven processes to enantioselectively deliver chiral products. Then, I will focus on the research conducted during this thesis.

1.2.1. Photochemical Organocatalytic Cascade of Unactivated Alkenes

In *Chapter III,* I discuss the implementation of an asymmetric photochemical radical cascade. The high reactivity and selectivity of open-shell intermediates make radical chemistry perfectly suited for implementing cascades. However, the intrinsic challenge of carrying out reactions with radicals in a stereocontrolled fashion has greatly limited the development of enantioselective variants. Our system harnesses the great potential of visible-light excited chiral iminium ions (**XX***) to activate alkenes **16**, which are generally recalcitrant to thermal activation strategies, and form reactive radicals that trigger a stereocontrolled cascade (Figure 1.6). The overall process converts unactivated olefins **16** and α,β-unsaturated aldehydes into chiral adducts (**17**) in a single step through two sequential radical-based bond-forming events.

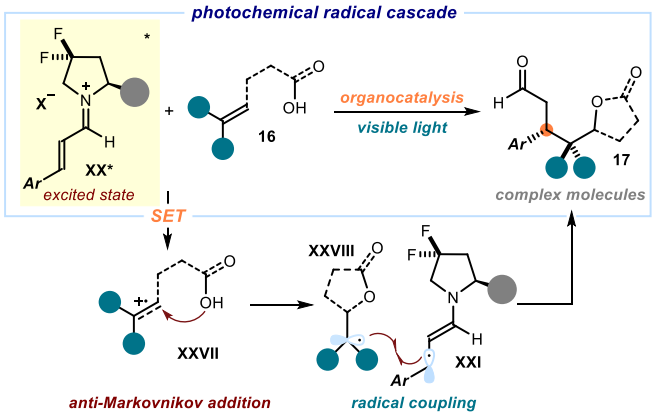

Figure 1.6 Photochemical organocatalytic radical cascade of unactivated alkenes. SET: single-electron transfer.

The enantioselective cascade process was successfully implemented, both inter- and intramolecularly, to afford complex lactones or tetrahydrofuran-containing scaffolds in a single-step with good yields and excellent enantioselectivities. These two

structural elements are present in numerous biologically active and naturally occurring molecules.[42]

This project was undertaken in collaboration with Dr. Yannick P. Rey, who was involved in the discovery and optimization of the process, and Dr. Catherine M. Holden, who assisted me in studying the scope of the intermolecular cascade process.

1.2.2. Activation of Allenes by Single Electron Transfer (SET)

After establishing that excited-state chiral iminium ions could successfully oxidize unactivated alkenes, we wondered if a similar strategy could be expanded to the underexplored activation of allenes. *Chapter IV* details the implementation of a visible-light-driven enantioselective organocatalytic process involving difficult-to-control allene radical cations.[43]

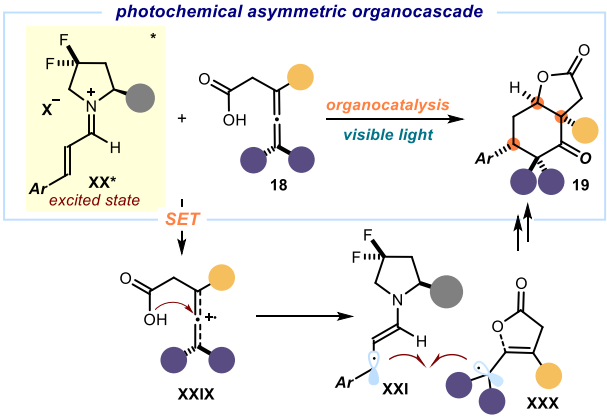

Figure 1.7. Photo-organocatalytic activation of allenes by SET oxidation to deliver complex polycyclic compounds.

In a similar way to the previous cascade, the photoexcited iminium ion **XX*** underwent SET oxidation to allene substrate (**18**) bearing a carboxylic acid moiety (Figure 1.7). Nucleophilic attack of the latter onto the allene radical cation **XXIX** induced the formation of radical lactone **XXX**, prone to a stereocontrolled radical coupling with **XXI**. The resulting intermediate could trigger an aldol-type cyclization followed by acyl migration to deliver the final product of the cascade, namely the complex bicyclic

[42] Bonilla, P.; Rey, Y. P.; Holden, C. M.; Melchiorre, P. "Photo-Organocatalytic Enantioselective Radical Cascade Reactions of Unactivated Olefins" *Angew. Chem. Int. Ed.*, **2018**, 57, 12819.

[43] Haddaway, K.; Somekawa, K.; Fleming, P.; Tossell, J. A.; Mariano, P. S. "The Chemistry of Allene Cation Radicals Probed by the Use of Theoretical and Electron-Transfer Photochemical Methods" *J. Org. Chem.*, **1987**, 52, 4239.

lactone **19**. Density Functional Theory (DFT) computational studies provided insights on the high diastereoselectivity of this process. This system engaged, for the first time, highly reactive allene radical cations into an asymmetric transformation.[44]

This project was carried out in collaboration with Dr. Luca A. Perego, who was involved in the discovery of the process and performed the computational studies on the mechanism.

1.2.3. A General Organocatalytic Method for the Asymmetric Radical Conjugate Addition to Enals

Chapter V details our efforts to establish a general method for the enantioselective radical conjugate addition to simple α,β-unsaturated aldehydes (Figure 1.8). Previous projects regarding the direct excitation of chiral iminium ions were intrinsically restricted to enals bearing an aromatic ring at the β position since an alkyl moiety disabled the excited-state reactivity. Seeking to overcome this limitation, we envisioned the use of a dual catalytic system in which the radical formation and the stereo-determining step were decoupled. By employing an external photocatalyst as an oxidant to generate a radical, we could intercept the radical with an electrophilic ground-state chiral iminium ion. We selectively irradiated the photocatalyst using a wavelength that the iminium ion could not absorb (λ=460 nm). This bypassed the need for the iminium ion to work in the excited state, allowing the use of alkyl enals.

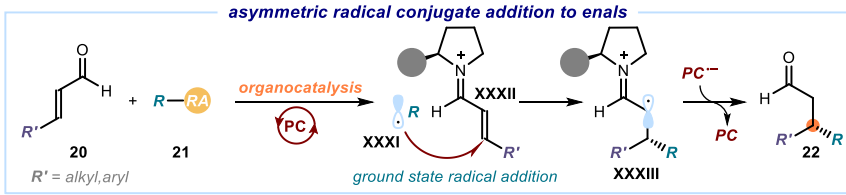

Figure 1.8 A general platform for the enantioselective 1,4-addition of radicals to simple alkyl and aryl enals.

Specifically, SET oxidation of a suitable substrate, bearing an oxidizable redox auxiliary (RA, **21**), from an organic photocatalyst generated the radical **XXXI**. The ensuing radical **XXXI** was stereoselectively intercepted by the ground-state electrophilic chiral iminium ion (**XXXII**). A final SET reduction of the 3π-enaminyl radical **XXXIII** by the reduced formed of the photocatalyst, followed by hydrolysis, provided the β-

[44] Perego, L. A.; Bonilla, P.; Melchiorre, P. "Photo-Organocatalytic Enantioselective Radical Cascade Enabled by Single-Electron Transfer Activation of Allenes" *Adv. Synth. Catal.*, **2020**, 362, 302.

functionalized chiral aldehyde **22**. The net reaction was an enantioselective radical conjugate addition.

This project was undertaken in collaboration with Dr. Catherine M. Holden, who was involved in the discovery and optimization of the process and Mr. Emilien LeSaux and Dr. Danilo M. Lustosa who carried out part of the scope.

UNIVERSITAT ROVIRA I VIRGILI
COMBINING IMINIUM ION-MEDIATED CATALYSIS AND PHOTOCHEMISTRY TO DEVELOP ENANTIOSELECTIVE RADICAL PROCESSES
Pablo Bonilla Domínguez

Chapter II

Introduction

2.1. Ground-State Iminium Ion Catalysis

The activation of α,β-unsaturated carbonyl substrates towards nucleophilic addition by condensation of an amine under acidic conditions is known as iminium ion activation.[1] In the year 2000, an enantioselective Diels-Alder process catalyzed by iminium ion was first reported by MacMillan (Figure 2.1.a)[2] and it intrinsically propelled the field of modern organocatalysis. This report demonstrated how the condensation of a chiral imidazolidinone **3** with α,β-unsaturated aldehydes **1** could trigger the reversible formation of the chiral electron-deficient iminium ion **I.** The electron-poor chiral intermediate **I**, acting as a chiral dienophile, underwent a Diel-Alder cycloaddition with diene **2** to afford the chiral cyclohexene product **4** in good yields (72-90%) and enantioselectivities (83-96 %).

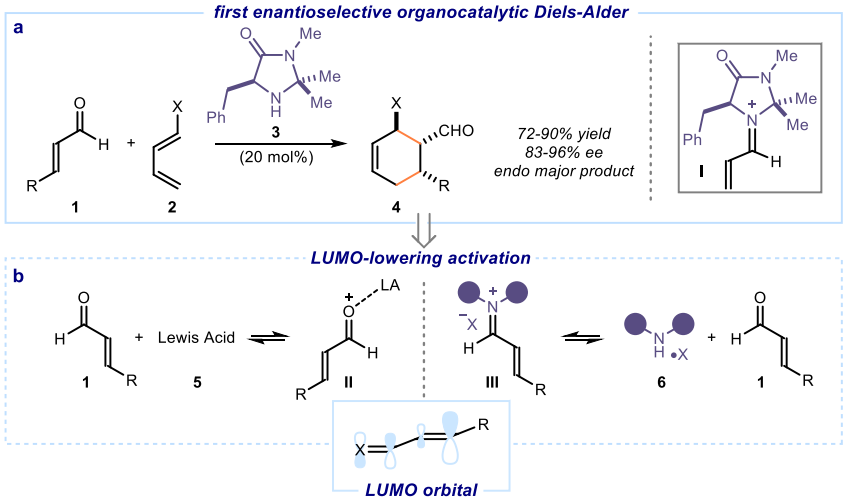

Figure 2.1. a) Iminium ion activation of enals using an imidazolidinone catalyst and the ensuing asymmetric Diels-Alder reaction; b) Comparison between Lewis Acid and amine activation of enals via LUMO-lowering strategy. LUMO: Lowest Unoccupied Molecular Orbital.

[1] Erkkilä, A.; Majander, I.; Pihko, P. M. "Iminium Catalysis" *Chem. Rev.*, **2007**, *107*, 5416.

[2] Ahrendt, K. A.; Borths, C. J.; MacMillan, D. W. C. "New Strategies for Organic Catalysis: The First Highly Enantioselective Organocatalytic Diels-Alder Reaction" *J. Am. Chem. Soc.* **2000**, *12*, 4243.

This publication established iminium ion-based catalysis as a general activation method (Figure 2.1.b) in which the condensation of an amine **6** with enals **1** enables an electron redistribution that lowers the energy of the LUMO (Lowest Unoccupied Molecular Orbital) of **1**, generating a highly electrophilic chiral π system **III**. Iminium ion activation resembles the equilibrium dynamics and the π-orbital electronics of the conventional Lewis acid-based strategy to activate carbonyl compounds. The organocatalytic LUMO lowering activation approach, in combination with the use of chiral imidazolidinone catalysts **3**,[3] was crucial for establishing the basis of asymmetric iminium ion catalysis.

A common mechanism of action for iminium ion-mediated asymmetric catalysis is depicted in Figure 2.2.a. First, the condensation of the chiral aminocatalyst with enal **7** generates the chiral electrophilic iminium ion intermediate **IV**. Nucleophilic addition on the most electrophilic β position of **IV** generates an enamine intermediate **V** that, upon α-protonation and hydrolysis, delivers the enantioenriched chiral β-functionalized aldehyde **9**. The generality of iminium ion activation is illustrated by the myriad of enantioselective transformations developed over the past twenty years (Figure 2.2.b).

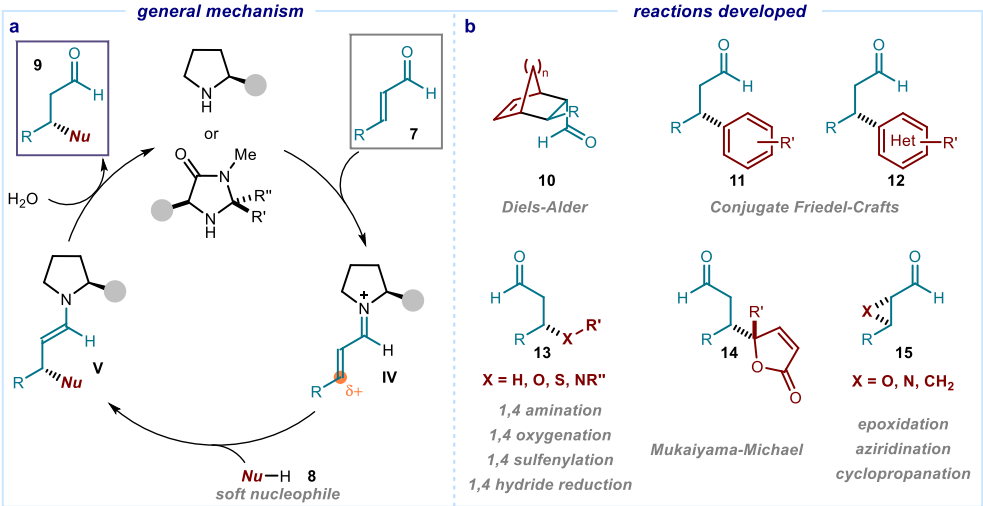

Figure 2.2. a) Common mechanism of action of iminium ion-mediated catalysis using secondary amines as chiral catalysts; b) examples of enantioselective transformations developed using iminium ion activation of enals.

[3] Naef, R.; Seebach, D. "Herstellung enantiomerenreiner *cis*- oder *trans*-konfigurierter 2-(tert-Butyl)-3-methyl imidazolidin-4-one aus den Aminosäuren (*S*)-Alanin, (*S*)-Phenylalanin, (*R*)-Phenylglycin, (*S*)-Methionin und (*S*)-Valin" *Helv. Chim. Acta*, **1985**, *68*, 135.

The pace of innovations was also sustained by the identification of diverse chiral amine catalysts that could expand the applicability of iminium ion catalysis (Figure 2.3.).

Primary amines derived from cinchona-alkaloids[4] (**16**) and aminoacids[5] (**17** and **18**) have been extensively used for the asymmetric functionalization of sterically hindered carbonyl compounds, such as α-branched enals and enones. A particular case of ion-pairing catalysis, ACDC (Asymmetric Counteranion-Directed Catalysis) in which an aminocatalysts (**19** and **20**) is merged with a chiral anion (**21**), secured asymmetric induction in multiple reactions proceeding via cationic iminium ion intermediates.[6] Regarding secondary amines, besides MacMillan's imidazolidinones (**22** and **23**), proline-based chiral secondary amines[7] (**24**-**27**), and particularly chiral diaryl prolinol ethers (**26** and **27**) popularized by Jorgensen (**27**)[8] and Hayashi (**26**),[9] occupy a prominent place as powerful motifs for iminium ion activation of enals.

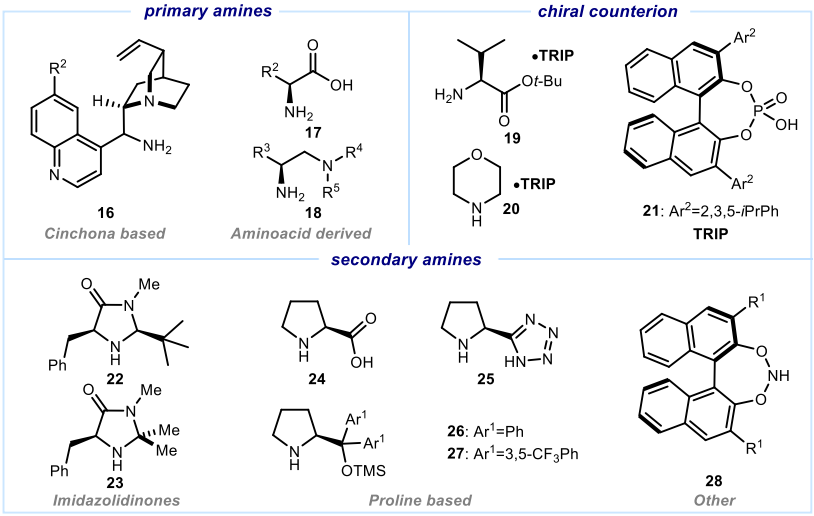

Figure 2.3. Selection of different chiral amines used as iminium catalysts.

---

[4] Melchiorre, P. "Cinchona-based Primary Amine Catalysis in the Asymmetric Functionalization of Carbonyl Compounds" *Angew. Chem. Int. Ed.*, **2012**, *51*, 9748.

[5] Xu, L.-W.; Lu, Y. "Non-Proline Amino Acid Catalysts" in Dalko, P. I. (ed.) Comprehensive Enantioselective Organocatalysis: Catalysts, Reactions, and Applications. Wiley-VCH, **2013**.

[6] Mahlau, M.; List, B. "Asymmetric Counteranion-Directed Catalysis: Concept, Definition, and Applications" *Angew. Chem. Int. Ed.*, **2013**, 52, 518.

[7] List, B.; Lerner, R. A.; Barbas III, C. F. "Proline-Catalyzed Direct Asymmetric Aldol Reactions" *J. Am. Chem. Soc.*, **2000**, *122*, 2395.

[8] Marigo, M.; Wabnitz, T. C; Fielenbach, D.; Jørgensen, K. A. "Enantioselective Organocatalyzed α Sulfenylation of Aldehydes" *Angew. Chem., Int. Ed.* **2005**, 44, 794.

[9] Hayashi, Y.; Gotoh, H.; Hayashi, T.; Shoji, M. "Diphenylprolinol Silyl Ethers as Efficient Organocatalysts for the Asymmetric Michael Reaction of Aldehydes and Nitroalkenes" *Angew. Chem. Int. Ed.* **2005**, 44, 4212.

2.1.1. Chiral Secondary Amines for Iminium Ion Enantioselective Catalysis

The success of chiral secondary amines as an efficient catalyst in iminium ion-mediated reactions builds upon several aspects: (i) their ability to undergo reversible iminium ion formation; (ii) their excellent configurational control over the iminium ion geometry; (iii) their control over the enantioselectivity of the process by selective shielding of one of the prochiral π-faces of the iminium ion.[10]

Given that the E geometry of the C=C bond is highly favorable, the main geometric elements to control are the C=N double bond (*E*/*Z* geometry) and the conformation of the single bond connecting the two unsaturations (s-*cis* and s-*trans* geometries, Figure 2.4). Due to steric repulsions between the catalyst substituents α to the nitrogen and the alkene fragment, the s-*cis* conformations (**VI** and **VII**, where both double bonds of the iminium ion sit *cis* to each other) are highly unfavored.[11] The same steric factor accounts for the preferential *E* geometry of the C=N double bond, which minimizes the steric clash between the α proton of the alkene and the stereogenic element of the catalyst. Overall, the *E*-s-*trans* iminium ion **IX** is the most favored conformation.[12] Experimental studies in solution have shown that noticeable amounts (3-10%) of undesired *Z*-isomer **VIII** are also present on the reaction media. Despite this, enantiomeric ratios over 95:5 are achievable in most cases. This indicates that nucleophilic attack on the *E*-s-*trans* is kinetically favored and consequently, the enantioenrichment of the final product does not correspond to the thermodynamic *E*/*Z*-ratio of the iminium-ion intermediate.[12]

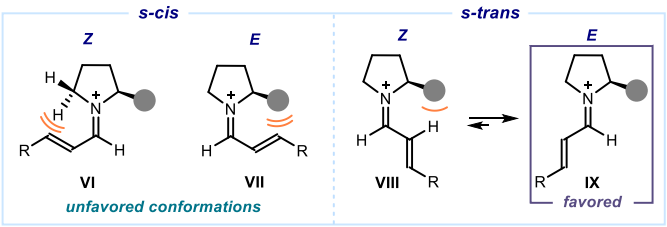

Figure 2.4. Possible geometries of the secondary amine-activated iminium ions.

[10] Jiang, H.; Albrecht, Ł.; Dickmeiss, G.; Jensen, K. L.; Jørgensen, K. A. "TMS-Prolinol Catalyst in Organocatalysis" in Dalko, P. I. (ed.) Comprehensive Enantioselective Organocatalysis: Catalysts, Reactions, and Applications. Wiley-VCH, **2013**.

[11] Grošelj, U.; Seebach D.; Badine, D. M.; Schweizer, W. B.; Beck, A. K.; Krossing, I.; Klose, P.; Hayashi, Y.; Uchimaru, T. "Structures of the Reactive Intermediates in Organocatalysis with Diarylprolinol Ethers" *Helv. Chim. Acta*, **2009**, 92, 1225.

[12] Seebach, D.; Gilmour, R.; Grošelj, U.; Deniau, G.; Sparr, C.; Ebert, M.-O.; Beck, A. K.; McCusker, L. B.; Šišak, D.; Uchimaru, T. "Stereochemical Models for Discussing Additions to α-β-Unsaturated Aldehydes Organocatalyzed by Diarylprolinol or Imidazolidinone Derivatives – Is There an (*E*)/(*Z*)-Dilemma?" *Helv. Chim. Acta*, **2010**, 93, 603

The exceptional enantiocontrol of iminium-ion-induced transformations is exerted by the sterically demanding fragment of the stereogenic element within the catalysts, which compels the nucleophile to attack from the least hindered face of the iminium ion (Figure 2.5). For example, when it comes to the chiral imidazolidinones **X**, the phenyl ring on C5 and the groups on C2 provide effective steric shielding of one of the prochiral faces of the iminium ion (Figure 2.5, left part).[13,14] Regarding the proline-based scaffolds **XI**, the stereoinduction was for a long time attributed to the effective steric shielding of the aryl groups.[10] However, NMR studies in solution, along with solid-state X-rays and DFT calculations,[11] revealed that the C-C bond between the diaryl(silyloxy)methyl group and the pyrrolidine-ring in iminium ion **XI** rests on a *synclinal-exo* conformation (Figure 2.5, right part). In this conformation, the OTMS substituent is positioned over the iminium ion and it is, therefore, the main responsible for the outstanding facial discrimination.

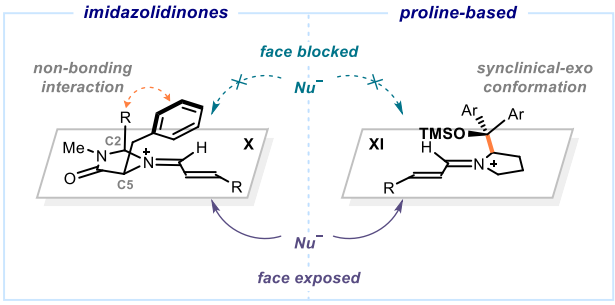

Figure 2.5. Origin of enantioselectivity for the two most common chiral secondary amine organocatalysts.

The electrophilicity of the iminium ion can be tuned by modifying the secondary amine scaffold. Extensive kinetic studies by the Mayr's group[15] established the electrophilicity

[13] For a review: b) Allemann, C.; Gordillo, R.; Clemente, F. R.; Cheong, P. H.-Y.; Houk, K. N. "Theory of Asymmetric Organocatalysis of Aldol and Related Reactions: Rationalizations and Predictions" *Acc. Chem. Res.*, **2004**, *37*, 558. For a comparison on the stabilizing interactions of C2 furyl catalyst and C2 tertbutyl catalyst: b) Gordillo, R.; Houk, K. N. "Origins of Stereoselectivity in Diels–Alder Cycloadditions Catalyzed by Chiral Imidazolidinones" *J. Am. Chem Soc.*, **2006**, *128*, 3543. For a study on the reaction with pyrroles as nucleophiles: c) Gordillo, R.; Carter, J.; Houk, K. N. "Theoretical Explorations of Enantioselective Alkylation Reactions of Pyrroles and Indoles Organocatalyzed by Chiral Imidazolidinones" *Adv. Synth. Catal.*, **2004**, *346*, 1175.

[14] Seebach, D.; Grošelj, U.; Schweizer, W. B.; Grimme, S.; Mück-Lichtenfeld, C. "Experimental and Theoretical Conformational Analysis of 5-Benzylimidazolidin-4-one Derivatives - a "Playground" for Studying Dispersion Interactions and a "Windshield-Wiper" Effect in Organocatalysis" *Helv. Chim. Acta*, **2016**, *93*, 1.

[15] Lakhdar, S.; Tokuyasu, T.; Mayr, H. "Electrophilic Reactivities of α, β-Unsaturated Iminium Ions" *Angew. Chem. Int. Ed.* **2008**, *47*, 8723; b) Lakhdar, S.; Ammer, J.; Mayr, H. "Generation of α,β-Unsaturated Iminium Ions by Laser Flash Photolysis" *Angew. Chem. Int. Ed.* **2011**, *50*, 9953.

(E) of a series of iminium ions (**XII**-**XIX**). This parameter experimentally accounts for the suitability of iminium ions to promote additions of weak nucleophiles, being particularly reactive those based on imidazolidinone scaffolds (Figure 2.6).

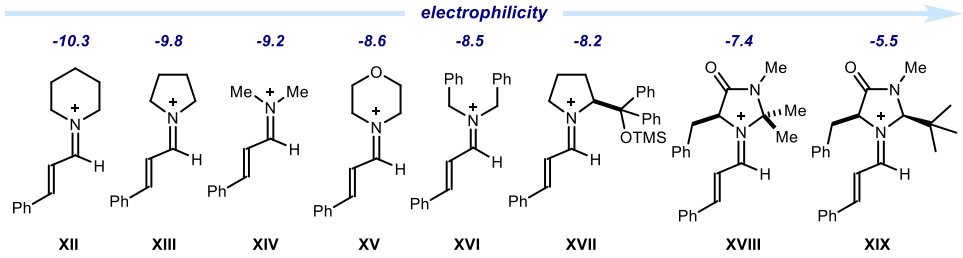

Figure 2.6. Scale of electrophilicity of a range of iminium ions

2.1.2. Secondary Aminocatalysis in Cascade Reactions

The ability of secondary aminocatalysts to tolerate many functional groups and to activate carbonyl compounds by lowering their Lowest Unoccupied Molecular Orbital (LUMO, iminium ion activation) and/or raising their Highest Occupied Molecular Orbital (HOMO, enamine activation) has been essential to developing effective cascade reactions.[16] Generally, the stereoselective nucleophilic addition to a chiral iminium ion (**IV**) results in the formation of an enamine intermediate **V** (Figure 2.7). The nucleophilic enamine **V** can subsequently undergo a stereoselective addition to an electrophilic substrate. Upon hydrolysis of **XX**, this reaction sequence allows for two consecutive bond-forming processes using a single catalyst to afford stereochemically dense α,β-disubstituted aldehydes **29**.[17]

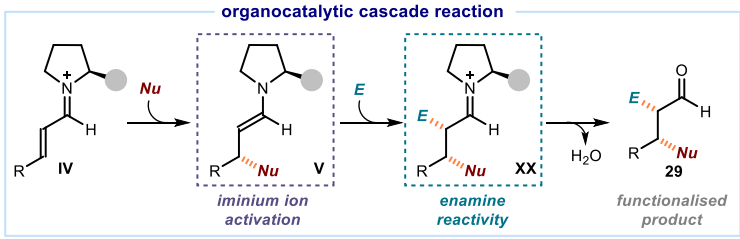

Figure 2.7. Combination of iminium ion and enamine activation modes to develop cascade processes. Nu: nucleophile; E: electrophile.

[16] Enders, D.; Grondal, C.; Hüttl, M. R. M. "Asymmetric Organocatalytic Domino Reactions" *Angew. Chem. Int. Ed.*, **2007**, 46, 1570.

[17] Pellissier, H. "Recent Developments in Asymmetric Organocatalytic Domino Reactions" *Adv. Synth. Catal.* **2012**, 354, 237.

In 2005, the Jørgensen group reported one of the first and representative examples of organocascade reactions using the iminium ion-enamine sequence. They developed the enantioselective epoxidation of α,β-unsaturated aldehydes (**30**) employing diaryl prolinol catalyst **27,** and hydrogen peroxide **31** as the oxygen source (Figure 2.8).[18] First, the condensation of catalyst **27** with enal **30** generates the iminium ion intermediate **IV**. Conjugate addition of **31** to the most electrophilic β-position of **IV** generates the enamine intermediate **XXI**. The nucleophilic enamine **XXI** attacks the peroxide unit to close the three-membered ring that upon hydrolysis of **XXII**, delivers enantioenriched epoxide **32**.

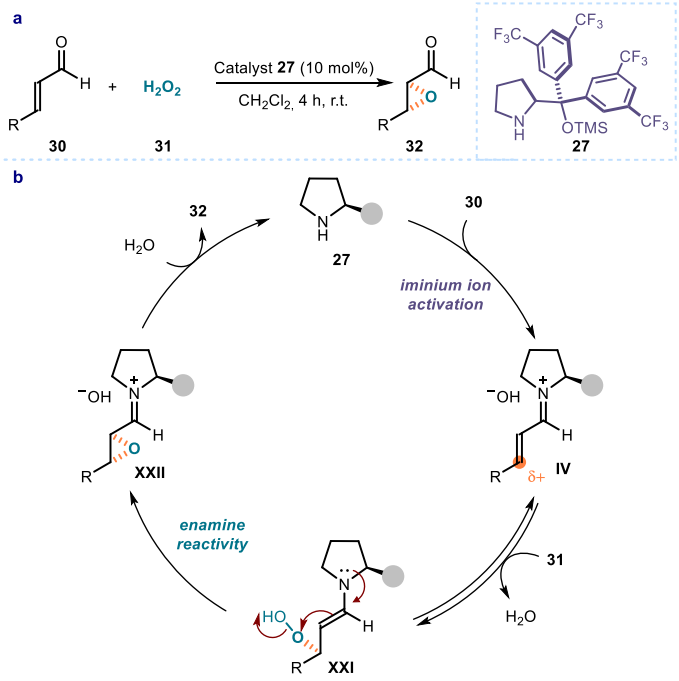

Figure 2.8. Organocatalytic epoxidation of α,β-unsaturated aldehydes with hydrogen peroxide employing an iminium ion-enamine tandem sequence.

These and many other examples[16,19] uncovered new possibilities for asymmetric aminocatalysis, leading to impressive growth in the development of catalytic organocascade methods. The strategy's experimental simplicity offers a rapid manner

[18] Marigo, M.; Franzen, J.; Poulsen, T. B.; Zhuang, W.; Jørgensen, K. A. "Asymmetric Organocatalytic Epoxidation of α,β-Unsaturated Aldehydes with Hydrogen Peroxide" *J. Am. Chem. Soc.* **2005,** *127*, 6964.

[19] For a pioneering example on a multicomponent cascade, see: b) Enders, D.; Hüttl, M. R. M.; Grondal, C.; Raabe, G. "Control of four stereocentres in a triple cascade organocatalytic reaction" *Nature*, **2006**, *441*, 861.

of increasing structural and stereochemical complexity starting from readily available substrates.

2.2. Excited-State Iminium Ion Catalysis

Our research group recently demonstrated that the reactivity of organocatalytic intermediates can be expanded beyond their ground-state reactivity to include the photochemical domain (Figure 2.9). For example, we used the iminium ion ability to absorb light in the visible region to generate an excited-state iminium ion **XXIII***, which behaves as a strong oxidant (E_{red}*(**XXIII***/**XXV**) ≈ 2.40 V, vs Ag/Ag$^+$, NaCl sat).[20] Single-electron transfer (SET) oxidation of a suitable donor substrate (organic silanes **34**) triggers the formation of the alkyl radical **XXIV** along with the chiral 5π-electron β-enaminyl radical intermediate **XXV**. The subsequent stereoselective radical coupling between **XXIV** and **XXV**[21] and hydrolysis led to the chiral β-benzylated aldehyde **35**.[22]

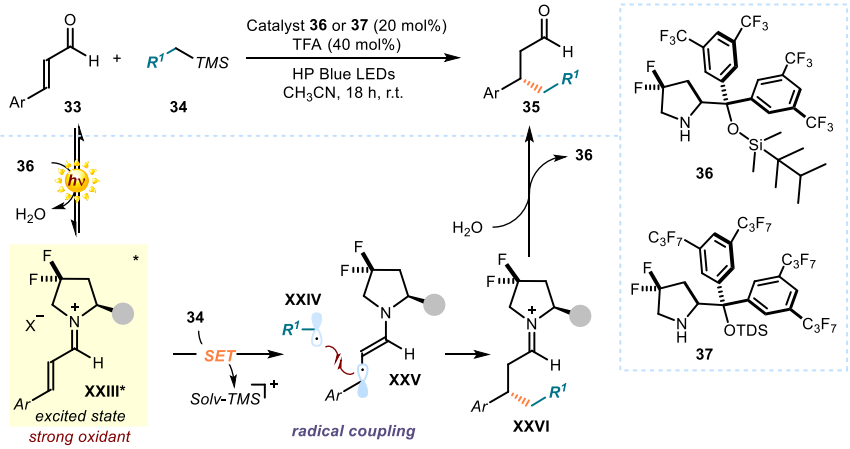

Figure 2.9. Reactivity of excited-state chiral iminium ions for the asymmetric β-functionalization of cinnamaldehydes with non-nucleophilic silanes. TDS: *tert*-hexyldimethylsilyl; TFA: trifluoroacetic acid.

[20] The value is estimated using the Rehm-Weller approximation. Rehm, D.; Weller, A. "Kinetics of Fluorescence Quenching by Electron and H-Atom Transfer" *Isr. J. Chem.*, **1970**, *8*, 259.

[21] The feasibility of the proposed stereoselective radical coupling relies on the persistent character of the chiral 5π-electron β-enaminyl radical intermediate **XXV**, which has a radical in a benzylic/allylic position. For a discussion on the importance of the persistent radical effect in radical coupling processes, see: Leifert, D.; Studer, A. "The Persistent Radical Effect in Organic Synthesis" *Angew. Chem. Int. Ed.*, **2020**, 59, 74.

[22] Silvi, M.; Verrier, C.; Rey, Y. P.; Buzzetti, L; Melchiorre, P. "Visible-light Excitation of Iminium Ions Enables the Enantioselective Catalytic β-Alkylation of Enals" *Nat. Chem.*, **2017**, 9, 868.

The capability of excited-state molecules to act as better electron donors and/or electron acceptors depends on thermodynamic factors.[23] In a simplified system depicted in Figure 2.10, light absorption of a ground-state molecule promotes an electron from the lower HOMO to the energetically higher LUMO, resulting in an excited-state electronic system. The promoted electron can then be more easily removed with respect to the ground-state electronic configuration, which means that the excited-state molecule has a smaller ionization potential (IP) than the original molecule. At the same time, the low-lying vacancy of the HOMO can easily accept an electron, which means that the excited state has a higher electron affinity (EA) than the ground state, and it is a better oxidant.[24]

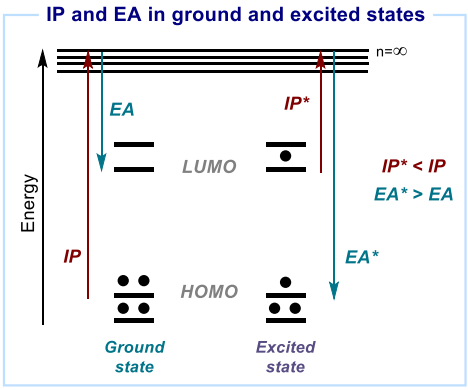

Figure 2.10. Excited-state molecules are better electron donors and acceptors than their corresponding ground-state partners due to decreased ionization potential (IP) and increased electron affinity (EA).

Translating this simple model to iminium ions implies that the excited state iminium ion has a greater tendency to accept an electron than its ground-state electrophilic partner, thus behaving as a strong oxidant.

The excited-state reactivity of chiral iminium ions was also used to activate different radical precursors other than organic silanes. The excited iminium ion **XXIII*** could oxidize dihydropyridines **38** bearing an alkyl group at C4 to form the corresponding unstable radical cation **38**$^{\bullet+}$ (Figure 2.11.a).[25] Fragmentation of the pyridine ring generated alkyl radicals **XXVII** that could engage in radical coupling with **XXV** to

[23] Kavarnos, G. J. "Fundamentals of Photoinduced Electron Transfer" VCH, **1993**.

[24] Balzani, V., Ceroni, P., Juris, A. "Photochemistry and photophysics: concepts, research, applications" Wiley & Sons., **2014**.

[25] Verrier, C.; Alandini, N.; Pezzetta, C.; Moliterno, M.; Buzzetti, L.; Hepburn, H. B.; Vega-Peñaloza, A.; Silvi, M.; Melchiorre, P. "Direct Stereoselective Installation of Alkyl Fragments at the β-Carbon of Enals via Excited Iminium Ion Catalysis" *ACS Catal.*, **2018**, *8*, 1062.

furnish β-functionalized enals **39**. Additionally, a multisite-PCET (proton-coupled electron transfer)[26] sequence, which combined the action of the photoexcited iminium ion **XXIII***, serving as an oxidant, and a counteranion, acting as a base, could generate the benzyl radical **XXVIII** from toluene **40** and its derivatives. The ensuing radical **XXVIII** was then intercepted by the chiral **XXV** to render the enantioenriched chiral products **41** (Figure 2.11.b).[27]

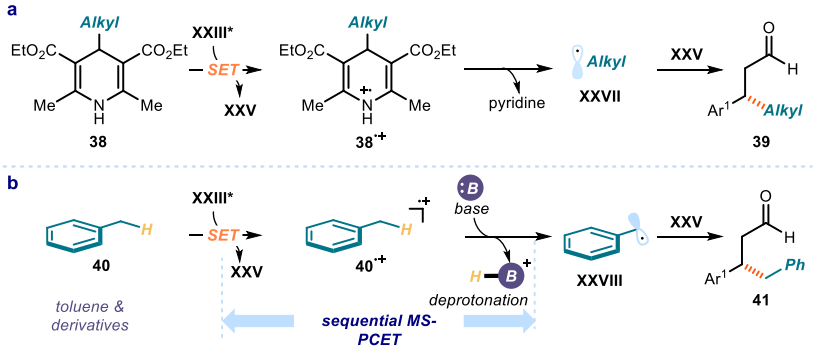

Figure 2.11. a) Generation of alkyl radicals **XXVII** from dihydropyridines **38** by excited-state iminium ion oxidation; b) Toluene C-H activation by a sequential SET/deprotonation for the functionalization of cinnamaldehydes. MS-PCET: multisite proton-coupled electron transfer; B: base.

We also envisioned that the excited-state reactivity of iminium ions could be useful to develop enantioselective organocatalytic cascades. In contrast to the well-known ground-state iminium ion-enamine sequence described in section 2.1.2, this approach combined the strong oxidizing power of chiral excited iminium ions with the ground-state enamine reactivity (Figure 2.12).[28] In this sequence, the photoexcited iminium ion **XXIII*** promotes the SET oxidation of cyclopropanols **42** to generate the radical cation **XXIX** and the β-enaminyl radical **XXV**. Subsequent ring-opening (**XXX**) and enantiocontrolled radical coupling with **XXV** delivered intermediate **XXXI** while forging the first stereogenic center. A final enamine-mediated aldol cyclization onto the electrophilic ketone delivers the final cyclopentanols **43**, containing three contiguous stereocenters, with excellent enantio- and diastereoselectivities.

[26] Warren, J. J.; Tronic, T. A.; Mayer, J. M. "Thermochemistry of Proton-Coupled Electron Transfer Reagents and its Implications" *Chem. Rev.*, **2010**, *110*, 6961.

[27] Mazzarella, D.; Crisenza, G. E. M.; Melchiorre, P. "Asymmetric Photocatalytic C–H Functionalization of Toluene and Derivatives" *J. Am. Chem. Soc.*, **2018**, *140*, 8439.

[28] Wozniak, Ł.; Magagnano, G.; Melchiorre, P. "Enantioselective Photochemical Organocascade Catalysis" *Angew. Chem. Int. Ed.*, **2018**, *57*, 1068.

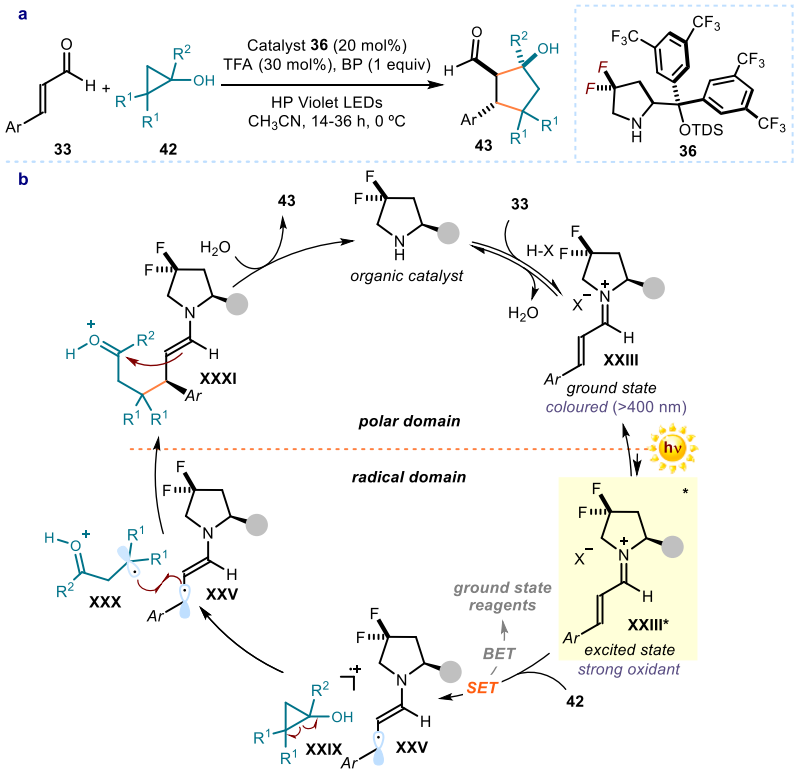

Figure 2.12. Enantioselective photo-organocatalytic cascade reaction with cyclopropanols triggered by excited-state iminium ions. BP: 1,1-biphenyl.

This new strategy opened new opportunities for reaction design providing a conceptually new approach to design organocascade catalytic processes while combining the fields of enantioselective photochemical radical reactions and classic polar ground-state organocatalysis.

UNIVERSITAT ROVIRA I VIRGILI
COMBINING IMINIUM ION-MEDIATED CATALYSIS AND PHOTOCHEMISTRY TO DEVELOP ENANTIOSELECTIVE RADICAL PROCESSES
Pablo Bonilla Domínguez

Chapter III

Photochemical Organocatalytic Asymmetric Radical Cascade Reactions of Unactivated Alkenes

Target

Developing a light-triggered organocatalytic strategy to perform cascade reactions with high stereoselectivity.

Tool

Using the excited-state reactivity of chiral iminium ions to activate alkenes and engage them in highly enantioselective radical cascades.[1]

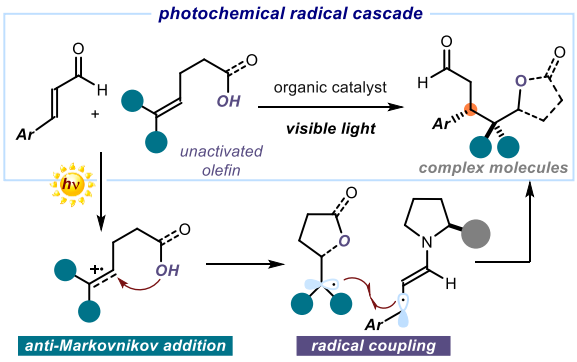

3.1. Introduction

Organic chemists strive to discover and implement efficient methods for the preparation of complex molecules. The goal of sustainable synthesis is to fulfill our needs by using the least resources and generating the least waste. Cascade processes are powerful strategies for rapidly increasing structural and stereochemical complexity while delivering complex chiral molecules in one step and from simple starting materials.[2] In these processes, multiple chemical steps proceed without any external intervention, and each sequential chemical reaction proceeds as a consequence of the functionality formed in the previous step.[3] The high reactivity and selectivity of radical

[1] The project discussed in this chapter has been conducted in collaboration with Dr. Yannick P. Rey, who was involved in the discovery and optimization of the process, and Dr. Catherine M. Holden, who was in charge of the scope of the intermolecular cascade process. I carried out the last round of optimization and investigated the scope on the intramolecular cascade. Part of this work has been published: Bonilla, P.; Rey, Y. P.; Holden, C. M.; Melchiorre, P. "Photo-Organocatalytic Enantioselective Radical Cascade Reactions of Unactivated Olefins" *Angew. Chem. Int. Ed.*, **2018**, 57, 12819.

[2] Tietze, L. F.; Brasche, G.; Gericke, K. M. Domino Reactions in Organic Synthesis. Wiley-VCH, **2006**.

[3] Tietze, L. F. "Domino Reactions in Organic Synthesis" *Chem. Rev.*, **1996**, 96, 115.

intermediates as well as their mechanistic differences with polar pathways[4] make them perfectly suited for cascade reactions.[5] However, the intrinsic challenge of carrying out reactions with radicals in a stereocontrolled fashion[6] has greatly limited the development of enantioselective variants so far.

3.2. Enantioselective Radical Chemistry

Radical intermediates were identified by Gomberg in 1900.[7] Because of their fleeting and uncontrollable nature, radicals were only considered as a simple "synthetic curiosity" for more than 80 years. This idea began to dissipate when chemists realized the difference between radical-radical coupling reactions, which often occur at the diffusion-controlled limit and lead to selectivity issues, and radical-molecule reactions, which have more predictable and controllable outcomes.[8] The intrinsic advantages of radical chemistry, including the neutral conditions and the large functional group tolerance, prompted scientists towards the study of such intermediates.[9] Studies carried out by physical organic chemists during the 1960s and 1970s[10] further expanded the knowledge on radical reactivity and laid the foundation for better exploitation of its synthetic potential. In the 1980s, many synthetic chemistry laboratories were very active in the field of radical chemistry,[11] and initial attempts to control the stereoselectivity of radical processes were made.[12] Since radical intermediates are mainly planar, a crucial aspect for controlling the enantioselectivity of the process is to ensure effective discrimination of the enantiotopic faces of the open-shell intermediate (Figure 3.1).[13] One way of achieving this target is based on a "reagent control" strategy, where chiral reagents (**1** or **2**) can selectively approach one of the

---

[4] Renaud, P.; Sibi, M. P. (ed.) Radicals in Organic Synthesis Volume 1: Basic Principles. Wiley-VCH, **2001**.

[5] Sebren, L. J.; Devery III, J. J.; Stephenson, C. R. J. "Catalytic Radical Domino Reactions in Organic Synthesis" *ACS Catal.*, **2014**, *4*, 703.

[6] Sibi, M. P.; Manyem, S.; Zimmerman, J. "Enantioselective Radical Processes" *Chem. Rev.*, **2003**, *103*, 3263.

[7] Gomberg, M. "An Instance of Trivalent Carbon: Triphenylmethyl" *J. Am. Chem. Soc.*, **1900**, 22, 757.

[8] Curran, D. P.; Porter, N. A.; Giese, B. (ed.) Stereochemistry of Radical Reactions: Concepts, Guidelines, and Synthetic Applications. Wiley-VCH, **1996**.

[9] Yang, Y.-H.; Sibi, M. P. "Stereoselective Radical Reactions" in Studer, A. (ed.) Encyclopedia of Radicals in Chemistry Biology and Materials. Wiley-VCH, **2012**.

[10] Kochi, J. (ed.) Free Radicals vol. 1 & 2, Wiley-VCH, **1973**.

[11] Renaud, P.; Sibi, M. P. (ed.) Radicals in Organic Synthesis Volume 1: Basic Principles. Wiley-VCH, **2001.**

[12] Porter, N. A.; Giese, B.; Curran, D. P. "Acyclic Stereochemical Control in Free-Radical Reactions" *Acc. Chem. Res.* **1991**, 24, 296.

[13] Parsons, A. "A radical revolution in synthesis" *Nat. Chem.* **2014**, *6*, 659.

faces of the open-shell species by minimizing the steric hindrance between the reagent chiral backbone and the structure of radical **I**. This strategy was mainly applied to induce asymmetry in processes based on H-atom transfer mechanisms (Figure 3.1.a).[9] Alternatively, the "complex control" approach relies on the use of stoichiometric chiral Lewis acids (**3** or **4**) that can coordinate the substrate. Upon complexation, the steric bulk of the scaffold on the Lewis acid differentiates the two diastereotopic faces of the radical complex **II** (Figure 3.1.b).[14] In combination with these two stoichiometric approaches, transition metal catalysis has also played a crucial role in the development of enantioselective radical reactions (Figure 3.1.c).[15] Metals such as titanium (**5**),[16] nickel (**6**),[17] copper (**7**),[18] and precious metals (Ir, Ru, Rh)[19] have been successfully employed in radical transformations. Generally, transition metals combined with different chiral ligands induce enantioselectivity by intercepting radicals and engaging them in classical organometallic cycles, in which the stereo-determining step is the final reductive elimination (Figure 3.1.c).

[14] Zimmerman, J.; Sibi, M. P. "Enantioselective Radical Reactions" *Top. Curr. Chem.,* **2006,** *263*, 107.

[15] Wanga, K.; Kong, W. "Recent Advances in Transition Metal-Catalyzed Asymmetric Radical Reactions" *Chin. J. Chem.,* **2018**, *36*, 247.

[16] Gansäuer, A.; Lauterbach, T; Bluhm, H.; Noltemeyer, M. "A Catalytic Enantioselective Electron Transfer Reaction: Titanocene-Catalyzed Enantioselective Formation of Radicals from meso-Epoxides" *Angew. Chem. Int. Ed.,* **1999**, *38*, 2909.

[17] a) Tellis, J. C.; Primer, D. N.; Molander, G. A. "Single-Electron Transmetalation in Organoboron Cross-Coupling by Photoredox/Nickel Dual Catalysis" *Science*, **2014**, *345*, 433; b) Zuo, Z.; Cong, H.; Li, W.; Choi, J.; Fu, G. C.; MacMillan, D. W. C. "Enantioselective Decarboxylative Arylation of α-Amino Acids via the Merger of Photoredox and Nickel Catalysis" *J. Am. Chem. Soc.,* **2016**, *138*, 1832; c) Amani, J.; Sodagar, E.; Molander, G. A. "Visible Light Photoredox Cross-Coupling of Acyl Chlorides with Potassium Alkoxymethyltrifluoroborates: Synthesis of α-Alkoxyketones" *Org. Lett.*, **2016**, *18*, 732; d) Stache, E. E.; Rovis, T.; Doyle, A. G. "Dual Nickel- and Photoredox-Catalyzed Enantioselective Desymmetrization of Cyclic meso-Anhydrides" *Angew. Chem. Int. Ed.*, **2017**, 56, 3679; e) Zhou, Q.-Q.; Lu, F.-D.; Liu, D.; Lu, L.-Q.; Xiao, W.-J. "Dual photoredox and nickel-catalyzed desymmetric C–O coupling reactions: visible light-mediated enantioselective synthesis of 1,4-benzodioxanes" *Org. Chem. Front*. **2018**, 5, 309; f) Gandolfo, E.; Tang, X.; Raha Roy, S.; Melchiorre, P. "Photochemical Asymmetric Nickel-Catalyzed Acyl Cross-Coupling" *Angew. Chem. Int. Ed.*, **2019**, *58*, 16854.

[18] Gu, Q.-S.; Li, Z.-L.; Liu, X.-Y "Copper(I)-Catalyzed Asymmetric Reactions Involving Radicals" *Acc. Chem. Res.*, **2020**, 53, 170.

[19] a) Zhang, L.; Meggers, E. "Steering Asymmetric Lewis Acid Catalysis Exclusively with Octahedral Metal-Centered Chirality" *Acc. Chem. Res.*, **2017**, 50, 320; b) Huang, X.; Meggers, E. "Asymmetric Photocatalysis with Bis-cyclometalated Rhodium Complexes" *Acc. Chem. Res.*, **2019**, 52, 833. For a pioneering example: c) Huo, H.; Shen, X.; Wang, C.; Zhang, L.; Röse, P.; Chen, L.-A.; Harms, K.; Marsch, M.; Hilt, G.; Meggers, E. "Asymmetric photoredox transition-metal catalysis activated by visible light" *Nature*, **2014**, *515*, 100.

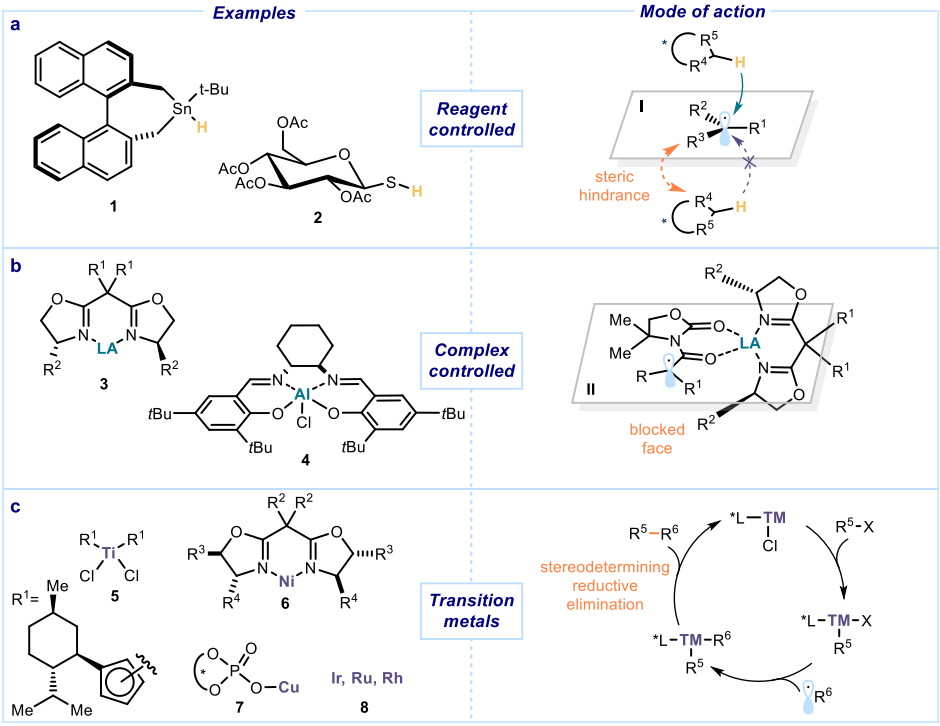

Figure 3.1. Approaches for inducing stereoselectivity in radical-based processes.

The synthetic potential of radical intermediates has also been harnessed to develop cascade processes. Many effective methodologies have been developed,[20] including catalytic variants[21] and their use in the total synthesis of natural products.[22] However, the intrinsic challenge of carrying out reactions with radicals in a stereocontrolled fashion limited the development of enantioselective variants.[6] The majority of the reported stereocontrolled strategies rely on either chiral substrates or stoichiometric ligands.[23] Some examples are discussed below.

[20] Yan, M.; Lo, J. C.; Edwards, J. T.; Baran, P. S. "Radicals: Reactive Intermediates with Translational Potential" *J. Am. Chem. Soc.*, **2016**, *138*, 12692.

[21] Studer, A.; Curran, D. P. "Catalysis of Radical Reactions: A Radical Chemistry Perspective" *Angew. Chem. Int. Ed.*, **2016**, 55, 58.

[22] Nicolau, K.C.; Edmonds, D.J.; Bulger, P.G., "Cascade Reactions in Total Synthesis" *Angew. Chem. Int. Ed.*, **2006**, *45*, 7134.

[23] a) Curran, D. P.; Porter, N. A.; Giese, B. (ed.) Stereochemistry of Radical Reactions Concepts, Guidelines, and Synthetic Applications. Wiley-VCH, **1996**; b) Miyabe, H.; Kawashima, A.; Yoshioka, E.; Kohtani, S. "Progress in Enantioselective Radical Cyclizations" *Chem. Eur. J.*, **2017**, 23, 6225; c) For a recent example, see: Kern, N.; Plesniak, M. P.; McDouall, J. J. W.; Procter, D. J. "Enantioselective Cyclizations and Cyclization Cascades of Samarium Ketyl Radicals" *Nat. Chem.* **2017**, 9, 1198.

3.3. Catalytic Asymmetric Radical Cascades

Recently, the field of photoredox catalysis has offered a flexible opportunity to develop asymmetric radical cascade processes by allowing the generation of radicals using single-electron transfer (SET) pathways.[24] Still, controlling the enantioselectivity of photo-induced radical processes through catalysis remained a difficult target, mainly for the challenge associated with the presence of a competitive racemic background reaction.[25] The high reactivity of radicals prompts them to react with substrates without the need for catalyst activation, therefore lowering the stereoselectivity of the overall process. Photoredox catalysis, however, offers an alternative to generate radicals in low amounts under highly controlled and mild conditions.

In 2014, Yoon's group devised a dual-catalyst system consisting of a visible-light absorbing photocatalyst ($Ru(bpy)_3^{2+}$) and a chiral Lewis acid cocatalyst that could promote highly enantioselective [2+2] cycloaddition **9** of α,β-unsaturated ketones to the corresponding cyclobutanes **11** (Figure 3.2).[26]

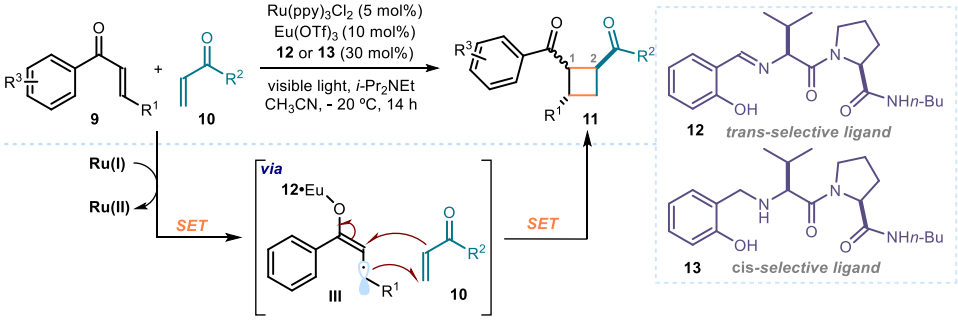

Figure 3.2. Asymmetric catalysis of [2+2] cycloadditions by the combination of chiral Lewis acid and photoredox catalysis.

The intermediate Ru(I), generated upon visible light irradiation of the photocatalyst Ru(II) complex and reductive quenching from an amine donor (not shown in Figure 3.2), can reduce the chiral Lewis acid-activated ketone **9** forming the radical intermediate **III**. Enantiocontrolled [2+2] cycloaddition between **III** and **10** delivers product **11**. Two different aspects prevented the uncatalyzed racemic background reaction. First, the photocatalyst was activated by visible light at wavelengths (λ_{max} =

[24] Plesniak, M.; Huang, H.-M.; Procter, D. J. "Radical cascade reactions triggered by single electron transfer" *Nat. Rev.*, **2017**, 77, 1.

[25] T.P. Yoon, "Photochemical Stereocontrol Using Tandem Photoredox-Chiral Lewis Acid Catalysis" *Acc. Chem. Res.*, **2016**, 49, 2307.

[26] Du, J.; Skubi, K. L.; Schultz, D. M.; Yoon, T. P. "A Dual-Catalysis Approach to Enantioselective [2+2] Photocycloadditions Using Visible Light" *Science*, **2014**, 344, 392.

450 nm) where the enones **9** and **10** did not absorb, preventing their direct photoexcitation and the background reaction to occur. Second, the Eu(III) cation activated **9** towards a SET reduction and stabilized the ensuing radical anion **III**. By decoupling the photochemical and stereocontrolling events, the chiral Lewis acid structure could be finely tuned to maximize the stereoselectivity of the process without perturbing the photoelectrochemistry of the photoredox catalyst.

The same catalytic strategy could also be applied for the asymmetric [3+2] cycloaddition reaction between aryl cyclopropyl ketone **14** and alkenes **15** (Figure 3.3).[27] In this system, the coordination of ketone **14** by a chiral Lewis acid complex, formed upon mixing Gd(III) and the chiral PyBOX ligand **17**, enabled the SET reduction by a photoredox Ru(I) complex. The resulting radical anion **IV** underwent reversible ring-opening (**V**) followed by slow stepwise cycloaddition with **15** to afford a ketyl radical (not shown). Final oxidation, either by the photogenerated amine radical cation *i*PrN$^{\bullet+}$Et or by chain-propagating electron transfer to another equivalent of **14**, delivered the enantioenriched chiral cyclopentane **16**.

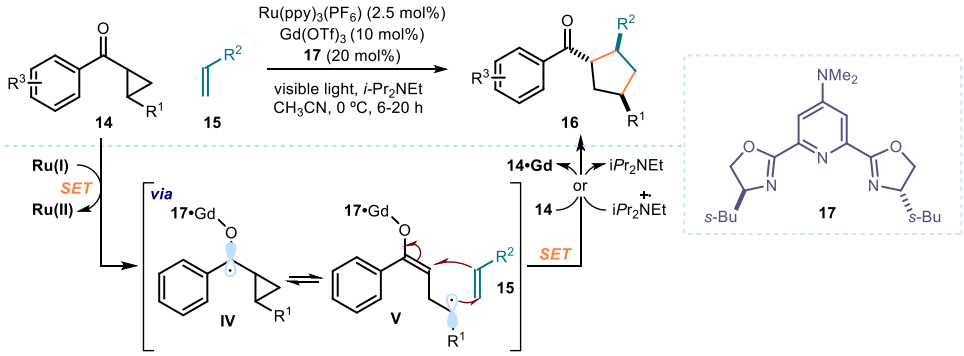

Figure 3.3. Enantioselective [3+2] cycloaddition between cyclopropyl ketones and alkenes.

Meggers considerably expanded the scope of this transformation by employing a different strategy, based on the use of a single rhodium chiral Lewis acid catalyst (Figure 3.4).[28] The octahedral chiral-at-metal rhodium(III) catalyst **21** is C_2-symmetrical but configurationally stable, which allows for the complex to induce asymmetry by coordination of a substrate to its two vacant sites.[29] Once the substrate

[27] Amador, A. G.; Sherbrook, E. M.; Yoon, T. P. "Enantioselective Photocatalytic [3+2] Cycloadditions of Aryl Cyclopropyl Ketones" *J. Am. Chem. Soc.* **2016**, *138*, 4722.

[28] Huang, X.; Lin, J.; Shen, T.; Harms, K.; Marchini, M.; Ceroni, P.; Meggers, E. "Asymmetric [3+2] Photocycloadditions of Cyclopropanes with Alkenes or Alkynes through Visible-Light Excitation of Catalyst-Bound Substrates" *Angew. Chem. Int. Ed.*, **2018**, *57*, 5454.

[29] Wang, C.; Chen, L.-A.; Huo, H.; Shen, X.; Harms, K.; Gong, L.; Meggers, E. "Asymmetric Lewis acid catalysis directed by octahedral rhodium centrochirality" *Chem. Sci.*, **2015**, *6*, 1094.

18 coordinates the Lewis acidic Rh catalyst **21**, photoexcitation of intermediate **VI** and reduction by a tertiary amine delivers the radical anion **VII**. Ring-opening (**VIII**) and subsequent enantiocontrolled radical addition and cyclization with electron-poor olefin **19** forms the ketyl radical **IX**. The highly reducing ketyl radical **IX** can give an electron to the oxidized amine radical cation or the photoexcited intermediate **VI***, propagating a radical chain. Finally, ligand exchange releases product **20** and regenerates complex **VI** completing the catalytic cycle. This system shows great functional group tolerance as well as high enantioselectivity levels (over 90% ee for the >40 examples reported).

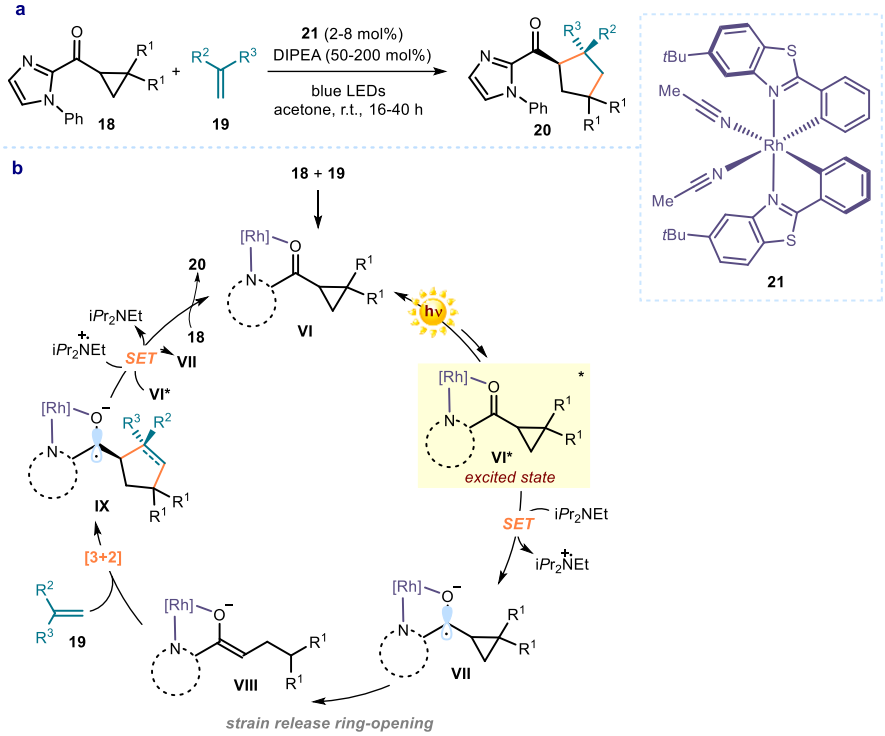

Figure 3.4. Asymmetric [3+2] photocycloadditions of cyclopropanes with alkenes using a single catalyst acting as chiral Lewis acid and photocatalyst.

The strategy was also applied to develop a catalytic asymmetric multicomponent radical reaction that, unlike previous examples, did not rely on a formal cycloaddition manifold (Figure 3.5).[30] In this sequence, photoexcitation of 4,4'-difluorobenzyl **25**, used as a photoredox organic catalyst, and reductive quenching by a sodium

[30] Ma, J.; Xie, X.; Meggers, E. "Catalytic Asymmetric Synthesis of Fluoroalkyl-Containing Compounds by Three-Component Photoredox Chemistry" *Chem. Eur. J.*, **2018**, 24, 259.

perfluoroalkyl sulfinate **23** generated perfluoroalkyl radical **XIV** along with ketyl radical **25**$^{\bullet-}$. The resulting electron-deficient radical **XIV** is then trapped by a vinyl ether **22** forming intermediate **XIII**, which contains an α-oxygen-stabilized radical. Conjugate radical addition of **XIII** to intermediate **X**, formed upon coordination of Lewis acid catalyst **21** to α,β-unsaturated ketones **18**, delivers the 3π-radical species **XI.** SET reduction of **XI** from **25**$^{\bullet-}$, and subsequent protonation and ligand exchange, yields the enantioenriched chiral product **24** and close the catalytic cycle. Although the results are remarkable in terms of yield and enantioselectivity, this system requires the preinstallation of an imidazole directing group α to the ketone, which serves as an anchor point for the catalyst.

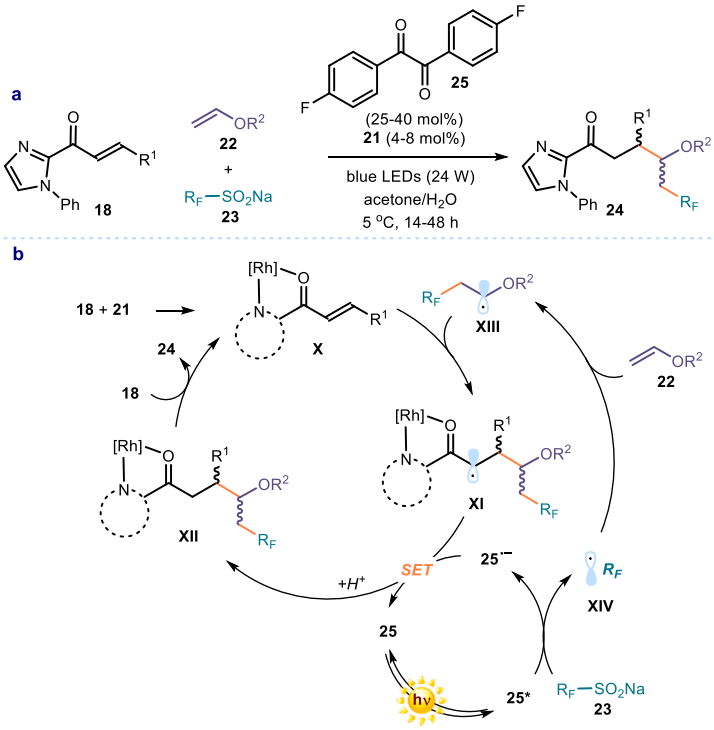

Figure 3.5. Catalytic asymmetric three-component radical reaction to synthesize fluoroalkyl-containing compounds.

The Nicewicz group reported an intramolecular enantioselective catalytic Diels-Alder reaction by combining photoredox catalysis and chiral counter-anion catalysis (Figure 3.6).[31] The highly oxidizing power of the oxypyrylium photocatalyst **29** was employed for the oxidation of electron-rich alkenes **26** to afford the radical cation **XV**. The chiral

[31] Morse, P. D.; Nguyen, T. M.; Cruz, C. L.; Nicewicz, D. A. "Enantioselective counter-anions in photoredox catalysis: The asymmetric cation radical Diels-Alder reaction" *Tetrahedron*, **2018**, *74*, 3266.

Brønsted acid **28** could then form a tight ion pair with **26** and promote the intramolecular enantioselective Diels-Alder reaction between the radical cation and the dienophile in **26**. SET reduction by the photocatalyst delivered product **27**. This strategy proved the feasibility of a new type of ion-paring between radical cation intermediates and chiral anions, albeit it afforded low yields, poor enantiocontrol, and limited substrate scope.

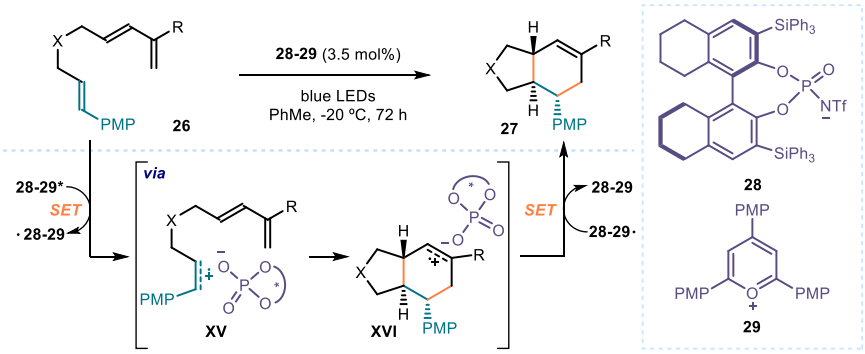

Figure 3.6. Enantioselective Diels-Alder reaction through ion pairing/photoredox catalysis.

In general, the reported catalytic asymmetric methods for radical cascade processes, based on the combination of photoredox catalysis and Lewis acid activation, were limited to formal [2+2] or [3+2] photocycloaddition reactions or cation radical Diels-Alder processes.

3.4. Targets of the Project

The implementation of enantioselective catalytic protocols constitutes a major challenge in the realm of radical cascade reactions. Our target was to expand the synthetic potential of enantioselective radical cascades beyond the reactivity constraints of formal cycloaddition chemistry. We wondered if the reactivity of photoexcited iminium ions, recently identified in our laboratories,[32,34] could be useful for this purpose.

Our group recently implemented a cascade protocol combining the strong oxidizing power of chiral excited iminium ions and ground-state enamine reactivity (Figure 3.7).[32] In this sequence, the photoexcited iminium ion **XVII*** performed SET oxidation of cyclopropanols **31** to generate a radical cation and the chiral β-enaminyl radical **XIX**.

[32] Wozniak, Ł.; Magagnano, G.; Melchiorre, P. "Enantioselective Photochemical Organocascade Catalysis" *Angew. Chem. Int. Ed.*, **2018**, *57*, 1068.

Subsequent ring-opening afforded radical **XVIII**, which was prone to an enantiocontrolled radical coupling with **XIX**. This step delivered intermediate **XX** while setting the first stereogenic center. A final ground-state enamine-mediated aldol cyclization onto the electrophilic ketone delivered the final cyclopentanols **32** containing three contiguous stereocenters with excellent enantio- and diastereoselectivity.

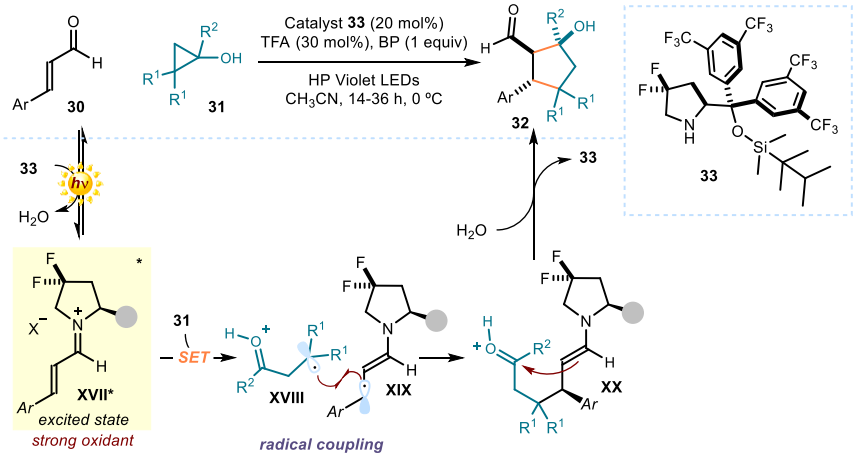

Figure 3.7. Enantioselective photo-organocatalytic cascade reaction with cyclopropanols triggered by excited-state iminium ions. BP: 1,1-biphenyl; TFA: trifluoroacetic acid.

However, while the first carbon-carbon bond-forming step in this cascade sequence was a radical process, the subsequent carbon-carbon bond formation followed a two-electron pathway. Our target was to apply the photochemistry of iminium ions to successfully implement an enantioselective catalytic radical cascade reaction that combines two sequential radical-based bond-forming processes without mechanistically relying on a cycloaddition manifold (Figure 3.8).

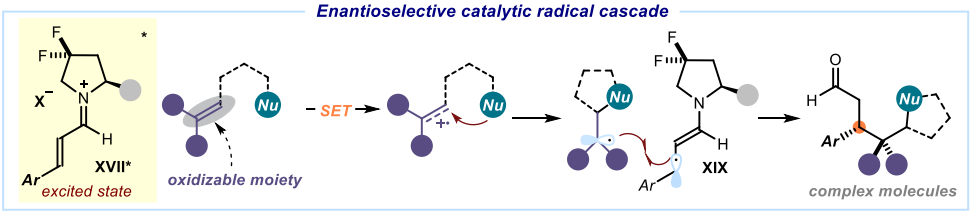

Figure 3.8. Our proposed design for a photochemical enantioselective radical cascade involving excited-state chiral iminium ions. The proposed cascade proceeds via two sequential radical steps: upon SET oxidation of an unactivated olefin, an *anti*-Markovnikov addition to the radical cation is followed by a stereocontrolled radical coupling.

Specifically, we envisioned that the SET oxidation of an alkene, adorned with a nucleophilic handle, could initiate a radical cascade. This organocatalytic photochemical process would convert readily available substrates, such as enals and unactivated olefins, into complex chiral molecules containing cyclic fragments.

3.5. SET Activation of Alkenes: the Choice of the Reaction Partner

Our plan required the ability of chiral iminium ions, formed upon condensation of enals with a chiral amine catalyst, to reach an excited state upon light absorption and then oxidize an alkene substrate. Our previous studies estimated that the excited iminium ions have a reduction potential E_{red}*(**XVII***/**XIX**) ≈ +2.40 V,[33] vs Ag/Ag$^+$ in CH_3CN.[34] This oxidizing power makes them amenable to accept one electron from different substrates, potentially including alkenes, whose oxidation potentials range between 1.0 and 2.5 V.[35]

Mariano already demonstrated that upon excitation, pre-formed cyclic iminium ion salts **XXI*** can activate alkenes through SET processes (Figure 3.9).[36]

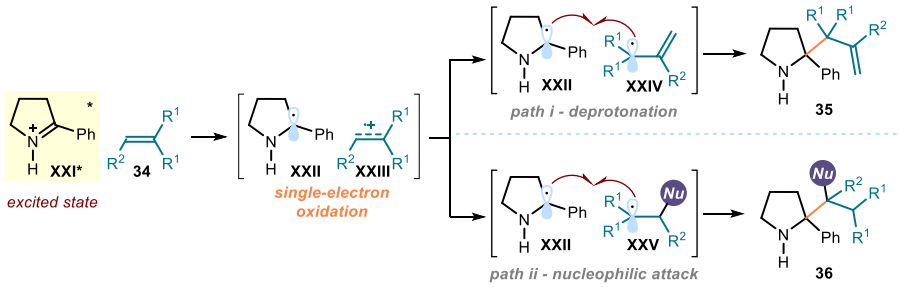

Figure 3.9. Oxidation of alkenes *via* SET from a photoexcited iminium ion reported by Mariano.

Upon excitation and SET from **XXI*** to **34**, a radical cation **XXIII** is formed. Depending on the solvent of the reaction, intermediate **XXIII** could follow two distinct pathways: (*path i*) deprotonation towards radical **XXIV** or, (*path ii*) nucleophilic attack by the

[33] The redox potential was estimated using the Rehm-Weller approximation. Rehm, D.; Weller, A. "Kinetics of Fluorescence Quenching by Electron and H-Atom Transfer" *Isr. J. Chem.*, **1970**, *8*, 259.

[34] Silvi, M.; Verrier, C.; Rey, Y. P.; Buzzetti, L; Melchiorre, P. "Visible-light Excitation of Iminium Ions Enables the Enantioselective Catalytic β-Alkylation of Enals" *Nat. Chem.*, **2017**, 9, 868.

[35] Nicewicz, D. A.; Roth, H. G.; Romero, N. A. "Experimental and Calculated Electrochemical Potentials of Common Organic Molecules for Applications to Single-Electron Redox Chemistry" *Synlett*, **2016**, *27*, 714.

[36] Stavinoha, J. L.; Mariano, P. S. "Novel Photochemical Addition Reactions of Iminium Salts. Electron Transfer Initiated Additions of Olefins to 2-Phenyl-l-pyrrolinium Perchlorate" *J. Am. Chem. Soc.*, **1978**, *100*, 1978; b) Stavinoha, J. L.; Mariano, P. S. "Electron-Transfer Photochemistry of Iminium Salts. Olefin Photoadditions to 2-Phenyl-1-pyrrolinium Perchlorate" *J. Am. Chem. Soc.*, **1981**, *103*, 3136.

solvent to deliver radical **XXV**. The final radical-radical coupling of any of these two intermediates with the reduced iminium ion yielded product **35** (*path i*) or **36** (*path ii*). However, these pioneering processes did suffer from poor regio-selectivity and narrow substrate scope.

More recently, the Nicewicz laboratories used photoredox catalysis to oxidize alkenes by SET.[37] The first example combined the use of the 9-mesityl-10-methylacridinium photocatalyst **39**[38] and a Hydrogen-Atom-Transfer (HAT) agent **40** to hydroetherificate alkenes with *anti*-Markovnikov selectivity (Figure 3.10).[39] Oxidation by the photoexcited **39** of the alkene moiety within **37** delivers radical cation **XXVI**. This intermediate could undergo intramolecular nucleophilic cyclization triggered by the nucleophilic oxygen handle, affording the most stable tertiary radical species **XXVII**. The process shows therefore an *anti*-Markovnikov selectivity. HAT from **40** to **XXVII** forms product **38** and radical **40•**, which oxidizes **39•** to **39** closing the photocatalytic cycle. This dual catalytic system demonstrated the possibility of controlling the selectivity of addition to alkenes under mild conditions. An asymmetric variant of this reaction was developed using an ion-pairing strategy.[40]

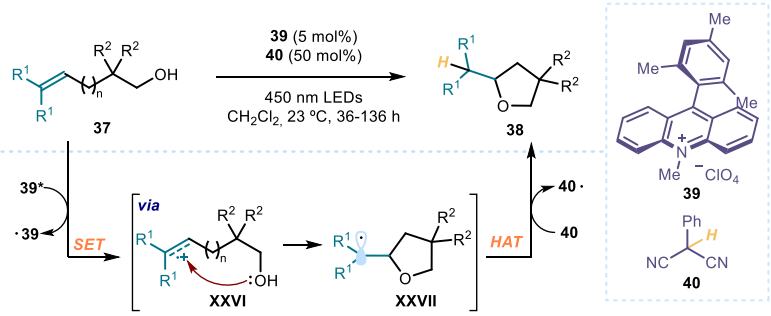

Figure 3.10. Intramolecular anti-Markovnikov hydroetherification reaction of alkenols.

[37] Margrey, K. A.; Nicewicz, D. A. "A General Approach to Catalytic Alkene Anti-Markovnikov Hydrofunctionalization Reactions via Acridinium Photoredox Catalysis" *Acc. Chem. Res.*, **2016**, *49*, 1997.

[38] Fukuzumi, S.; Kotani, H.; Ohkubo, K.; Ogo, S.; Tkachenko, N.V.; Lemmetyinen, H. "Photocatalytic Oxygenation of Anthracenes and Olefins with Dioxygen via Selective Radical Coupling Using 9-Mesityl-10-methylacridinium Ion as an Effective Electron-Transfer Photocatalyst" *J. Am. Chem. Soc.*, **2004**, *126*, 1600.

[39] Hamilton, D. S.; Nicewicz, D. A. "Direct Catalytic Anti-Markovnikov Hydroetherification of Alkenols" *J. Am. Chem. Soc.*, **2012**, *134*, 18577. For a mechanistic insight: b) Romero, N. A.; Nicewicz, D. A. "Mechanistic Insight into the Photoredox Catalysis of Anti-Markovnikov Alkene Hydrofunctionalization Reactions" *J. Am. Chem. Soc.*, **2014**, *136*, 17024.

[40] Yang, Z.; Li, H.; Li, S.; Zhang, M.-T.; Luo, S. "A chiral ion-pair photoredox organocatalyst: enantioselective anti-Markovnikov hydroetherification of alkenols" *Org. Chem. Front.*, **2017**, *4*, 1037.

The combined use of an acridinium photocatalyst and a hydrogen atom source was then applied by Nicewicz for the hydroamination of alkenes[41] and other intramolecular cyclization reactions.[42]

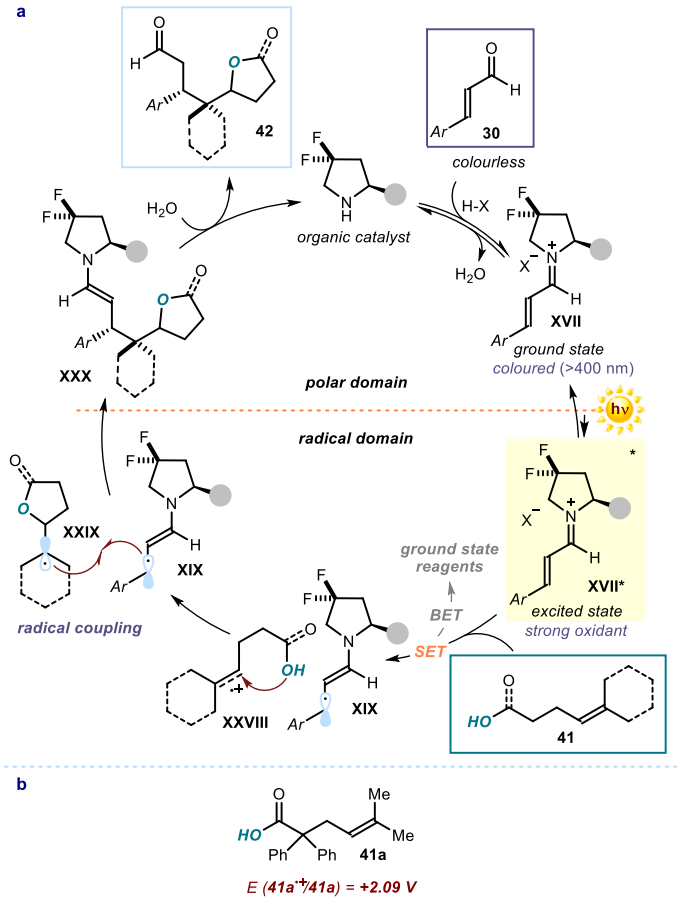

Figure 3.11. Our proposed plan for the development of a radical enantioselective cascade triggered by the photochemistry of chiral iminium ions.

[41] Nguyen, T. M.; Nicewicz, D. A. "Anti-Markovnikov Hydroamination of Alkenes Catalyzed by an Organic Photoredox System" *J. Am. Chem. Soc.*, **2013**, *135*, 9588.

[42] a) Grandjean, J.-M. M.; Nicewicz, D. A. "Synthesis of Highly Substituted Tetrahydrofurans by Catalytic Polar-Radical-Crossover Cycloadditions of Alkenes and Alkenols" *Angew. Chem. Int. Ed.*, **2013**, *52*, 3967; b) Zeller, M. A.; Riener, M.; Nicewicz, D. A. "Butyrolactone Synthesis via Polar Radical Crossover Cycloaddition Reactions: Diastereoselective Syntheses of Methylenolactocin and Protolichesterinic Acid" *Org. Lett.*, **2014**, *16*, 12822; c) Cavanaugh, C. L.; Nicewicz, D. A. "Synthesis of α-Benzyloxyamino-γ-butyrolactones via a Polar Radical Crossover Cycloaddition Reaction" *Org. Lett.*, **2015**, *17*, 6082; d) Gesmundo, N. J.; Grandjean, J.-M. M.; Nicewicz, D. A. "Amide and Amine Nucleophiles in Polar Radical Crossover Cycloadditions: Synthesis of γ-Lactams and Pyrrolidines" *Org. Lett.*, **2015**, *17*, 1316.

Based on these precedents, we identified alkenoic acid **41a** as a suitable candidate for implementing our light-triggered radical cascade. A detailed explanation of our designed plan is depicted in Figure 3.11. We envisioned a catalytic cycle wherein a chiral secondary aminocatalyst would condense with an enal **30** to form the colored iminium ion intermediate **XVII**. Selective excitation with violet light-emitting diode (LED) would render the strong oxidant **XVII***.[34] Therefore, **XVII*** can oxidize an alkenoic acid **41** adorned with a suitable oxygen nucleophilic handle. The SET transfer would concomitantly form the alkene radical cation **XXVIII** and the chiral 5π-intermediate **XIX**. The nucleophilic moiety of **XXVIII** would thus trigger a polar-radical-crossover cycloaddition exploiting the simultaneous polar and radical nature of such radical cation. This process would proceed with an *anti*-Markovnikov selectivity to afford the more stable tertiary radical intermediate **XXIX**. At this point, a stereo-controlled radical coupling with **XIX** would deliver the cascade product **42** with high enantioselectivity.

To confirm the propensity of **41a** towards SET, we measured its oxidation potential by cyclic voltammetry (E (**41a**$^{\bullet+}$/**41a**) = +2.09 V, vs Ag/Ag$^+$ in CH_3CN). This value falls within the oxidizing capability of the exited iminium ion, indicating the feasibility for alkene **41a** to undergo the proposed stereocontrolled SET oxidation-mediated *anti*-Markovnikov lactonization.

3.6. Results and discussion

3.6.1. Preliminary Results[43] and Optimization

To test the feasibility of our photochemical plan, we selected cinnamaldehyde **30a** in combination with 20 mol% of a chiral amine catalyst to form the iminium ion and the alkenoic acid **41a** as the reaction partner. (Figure 3.12.). An excess of cinnamaldehyde (3 equiv.) in the presence of 40 mol% of trifluoroacetic acid helped the formation of the chiral iminium ion. The reaction mixture was dissolved in acetonitrile and irradiated with 365 nm LED strip for 16 hours. From this initial screening, we observed that imidazolidinone-based catalyst **43** yielded 42% of the cascade product **42a** with a low enantiomeric excess (26% and 35% ee for each of the diastereoisomers, formed in a 1:1 ratio). The diarylprolinol-based catalyst **44** offered worse reactivity (24% yield) but substantially better levels of enantiocontrol (70% and 75% ee for each diastereoisomer).

[43] Preliminary investigations were conducted by Dr. Yannick P. Rey.

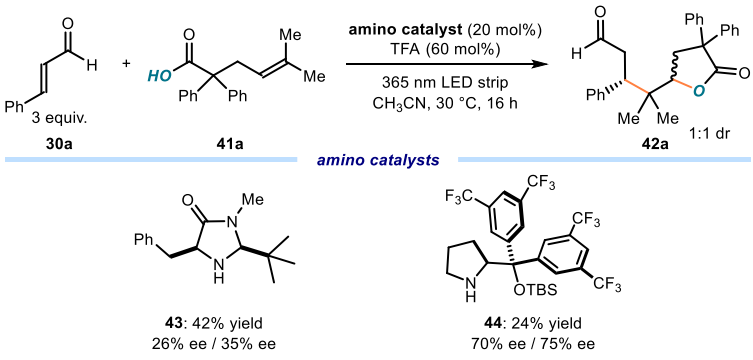

Figure 3.12. Initial results for the photochemical cascade reaction. TBS = *tert*-Butyldimethylsilyl.

Prompted by these results, we decided to evaluate other prolinol-based amino catalysts bearing different substitution patterns (Figure 3.13).

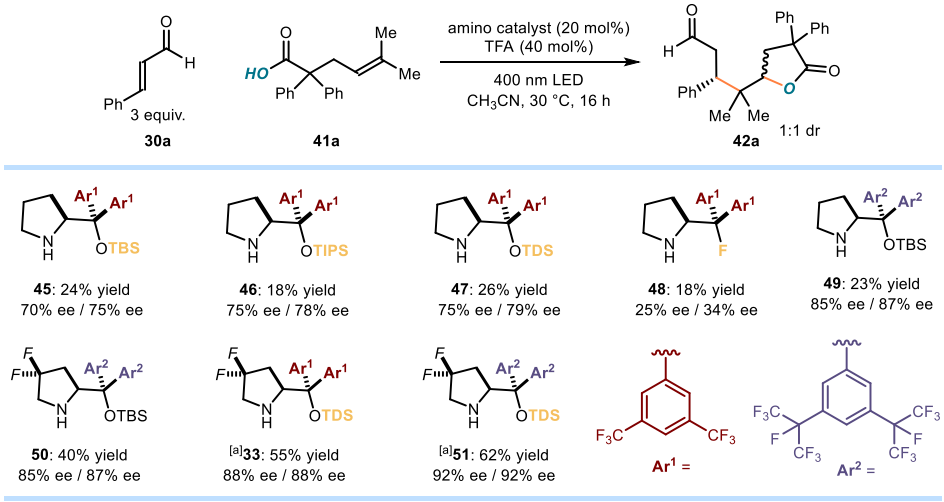

Figure 3.13. Screening of different secondary chiral amine catalysts. Reactions performed on a 0.1 mmol scale at 30 °C for 16 h using 0.2 mL of solvent under illumination by 400 nm LED strip. Enantiomeric excess determined by HPLC analysis on a chiral stationary phase. [a] Reaction performed under 420 nm High-power LED irradiation. TIPS = tri-*iso*-propylsilyl.

In these experiments, we used a high-power LED emitting at 400 nm. Modifying the TMS oxygen protecting group within the catalyst scaffold with other silicon compounds, such as triisopropylsilyl (TIPS) **46** or thexyldimethylsilyl (TDS) **47**, maintained similar levels of chemical yield while slightly improving the enantioselectivity (70-75% and 75-78% ee for each diastereoisomer). Replacing the oxygen by a fluorine **48** decreased substantially the enantiocontrol (25% and 34% ee for each diastereoisomer). Increasing the bulk on the aryl substituents (**49**) further

incremented the enantioselectivity (85% and 87% ee for each diastereoisomer). Catalysts **50**, bearing two geminal fluorine groups[34] on the proline ring, increased the product formation to 40% yield while maintaining the high levels of enantioselectivity. Catalysts **33** and **51**, carrying a TDS as the oxygen protecting group, substantially increased the product formation to 55% and 62% yield respectively, while maintaining high stereocontrol. The significant increase in reactivity observed with the fluorinated catalysts **33** and **51** is due to their improved stability under the highly oxidizing reaction conditions, which accounts for the main deactivation pathways of such kinds of reactions.[34] The better performance of the *gem*-difluorinated diarylprolinol silylether catalysts confirmed the observation, made in our original studies on the excitation of iminium ions,[34] that these amine catalysts better survived the reaction conditions. We finally used a more selective and powerful light source (420 nm high-power LED with an irradiance at 30 mW/cm², details of the experimental set-up, including irradiation and temperature control, are available in the experimental section 3.8.) to ensure efficient and selective irradiation of the chiral iminium ion. This reaction set-up provided the best results in terms of both yields (62%) and enantioselectivity (92%). In a final round of optimization (Table 3.1), an increased amount of TFA (entry 2 and 3) and the implementation of a two-phase solvent system (tetradecafluorohexane and CH_3CN in a 1:1 ratio), which secured a better solubility of the fluorinated chiral amine catalyst **51**, further increased the yield of the radical cascade reaction (entry 4).

Table 3.1. Final round of optimization. [a]

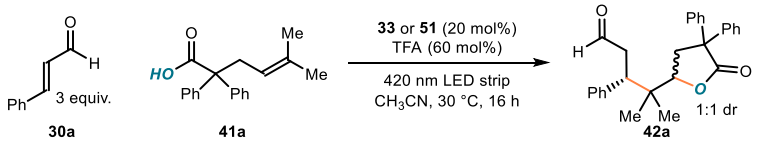

30a **41a** **42a**

Entry	Catalyst	Reaction conditions	Yield [%][b]	*ee* [%][c]
1	**33**	40 mol% TFA	55	88
2	**33**	60 mol% TFA	62	88
3	**51**	60 mol% TFA	63	91
4	**51**	CH_3CN:Hex_F 1:1	72	91
5	**33**	No light	0	--
6	--	No catalyst	0	--

[a] Reactions performed on a 0.1 mmol scale at 30 °C for 16 h using 0.2 mL of solvent under illumination by a single high-power (HP) LED (λ_{max}=420 nm) with an irradiance of 30 mWcm^{-2}. [b] Yield of **42a** determined by ^{1}H NMR analysis of the crude reaction mixture using trichloroethylene as the internal standard. [c] Enantiomeric excess determined by HPLC analysis on a chiral stationary phase. Hex_F=tetradecafluorohexane.

The improved reactivity in the two-phase solvent system was rationalized by the preferential solvation of catalyst **51** in the fluorinated phase (see Figure 3.14), which permits its slow release into the acetonitrile phase. This minimizes the oxidative degradation of the catalyst (E_p (**33**$^{\bullet+}$/**33**) = + 2.20 V, E_p (**51**$^{\bullet+}$/**51**) = + 2.40 V) by the photoexcited iminium ion **XVII***. Control experiments indicated that both the light and the amine catalyst are required for reactivity (entries 5 and 6).

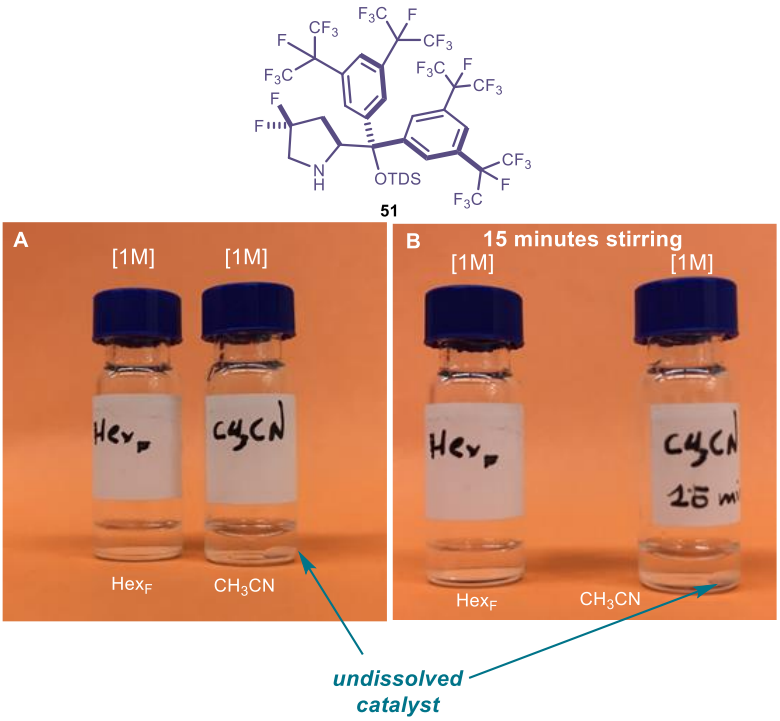

Figure 3.14. Catalyst **51** solubility experiments. A: 0.02 mmol of catalyst **51** (22.1 mg) was dissolved in 200 µL of solvent (same amount of catalyst and solvent used under optimized conditions). B: After 15 min stirring, catalyst **51** remains insoluble in CH_3CN.

3.6.2. Substrate Scope

With the optimized conditions for **42a** in hand (Table 3.1, entry 4), we then turned our attention to the scope of the photocatalytic asymmetric radical cascade process (Figure 3.15). We first evaluated the possibility of using different alkenoic acids **41**. The presence of geminal methyl groups at the α-position of **41** significantly improved the yield and gave slightly better enantioselectivity (product **42b**, 75% yield, and 94% ee). An ethyl fragment could also be installed (**42c**), while the incorporation of a cyclohexyl group provided the spirocyclic product **42d** in moderate yield but maintaining the same level of enantiocontrol. The lack of α-substituents in **41** did not significantly affect the overall efficiency (product **42e**), which indicates that the Thorpe–Ingold effect is

not critical for the cascade process.[44] Regarding the substitution of the alkene moiety, introducing a cyclohexyl in place of the *gem*-dimethyl moiety slightly increased the diastereoselectivity to 1.3:1 (**42f**) while maintaining high yield and enantioselectivity. Importantly, tetrahydrofuran derivatives **52a** and **52b** could also be synthesized when substituting the acid moiety with alcohol acting as the nucleophile.

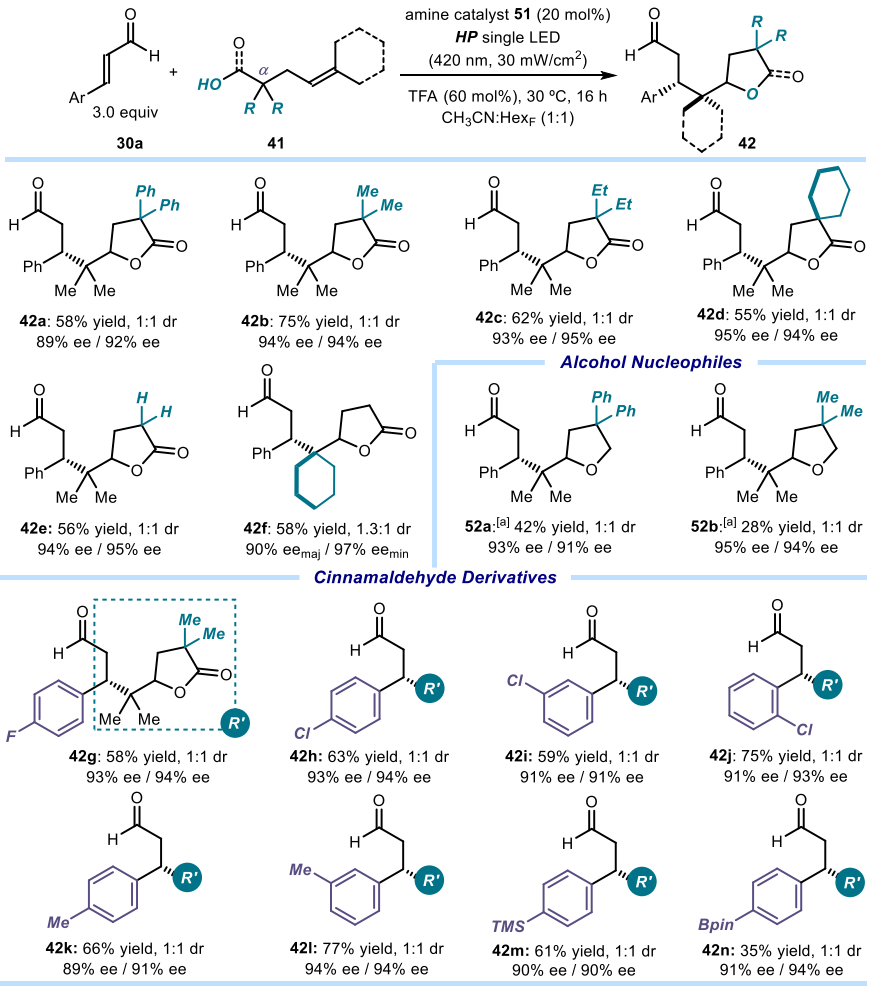

Figure 3.15. Survey of the alkenoic acids and alkenols that can participate in the radical cascade process with cinnamaldehydes. Reactions performed on 0.1 mmol scale using 1:1 mixture of acetonitrile and tetradecafluorohexane. Yields and enantiomeric excesses of the isolated products are indicated below each entry (average of two runs per substrate). Enantiomeric excesses measured on the enoate derivatives of **42** obtained upon olefination of the aldehyde with PPh_3CHCO_2Et. The dr was inferred by ^1H NMR analysis of the crude mixture. [a] Reaction performed using catalyst **33** in acetonitrile.

[44] Beesley, R. M.; Ingold, C. K.; Thorpe, J. F. "The Formation and Stability of spiro-Compounds. Part I. spiro-Compounds from cyclo-Hexane" *J. Chem. Soc.*, **1915**, *107*, 1117; b) Jung, M.E., Piizi, G. "gem-Disubstituent Effect Theoretical Basis and Synthetic Applications" *Chem. Rev.*, **2005**, *105*, 1735.

Concerning the scope of the α,β-unsaturated aldehydes **41**, moderately electron-donating, and electron-withdrawing groups on the aromatic ring are tolerated maintaining both the chemical yield and the enantioselectivity. The substituent can also be placed in different positions of the ring without impeding reactivity (**42g-n**). Remarkably, synthetically useful groups, amenable to further functionalization, were tolerated, including halogens (**42g-j**), trimethylsilyl (**42m**), and pinacolborane (**42n**). One inherent limitation of this reaction is that aliphatic enals, including *tert*-butylacroleine and (*E*)-2-octenal, remained unreacted.

Crystals from compound **42a** were suitable for X-ray crystallographic analysis (Flack parameter = 0.03(5)),[45] which established the stereochemical course of the radical cascade process (Figure 3.16).

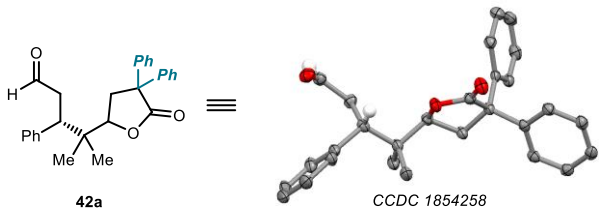

Figure 3.16. ORTEP representation of the X-ray crystal of **37a.**

3.6.3. Three-Component Reaction Scope[46]

After establishing the feasibility of our radical cascade protocol for a two-component system, we aimed to develop a more complex multi-component process using three different substrates. Specifically, we hypothesized that the excited iminium ion **XVII*** could oxidize amylene (**53**), an unfunctionalized alkene hydrocarbon (E_p (**53**$^{\bullet+}$/**53** = +2.03V, vs. Ag/Ag$^+$ in CH_3CN; Figure 3.17). The *anti*-Markovnikov intermolecular addition of a carboxylic acid **54** to the less substituted position of the resulting radical cation **53**$^{\bullet+}$ would then provide the tertiary radical intermediate **XXXI**, which would engage in a stereoselective radical coupling controlled by the chiral 5π-intermediate **XIX** (structure shown in Figure 3.17). This catalytic asymmetric cascade process, which combines two intermolecular radical steps, would provide one-step access to complex aldehydes **55**.

[45] CCDC 1854258 (**37a**) contains the supplementary crystallographic data for this paper. These data can be obtained free of charge from The Cambridge Crystallographic Data Centre.

[46] The initial results were obtained by Dr. Yannick P. Rey and the scope was carried out by Dr. Catherine M. Holden.

The key to the successful realization of this three-component cascade was the use of α,α-difluorinated acids **54**. The acids play a dual role in this transformation since they assist the iminium ion formation while acting as nucleophilic substrates in the three-component cascade. The aldehydic products had to be converted into enoates **55** to allow their isolation with moderate yields and enantioselectivities (Figure 3.17).

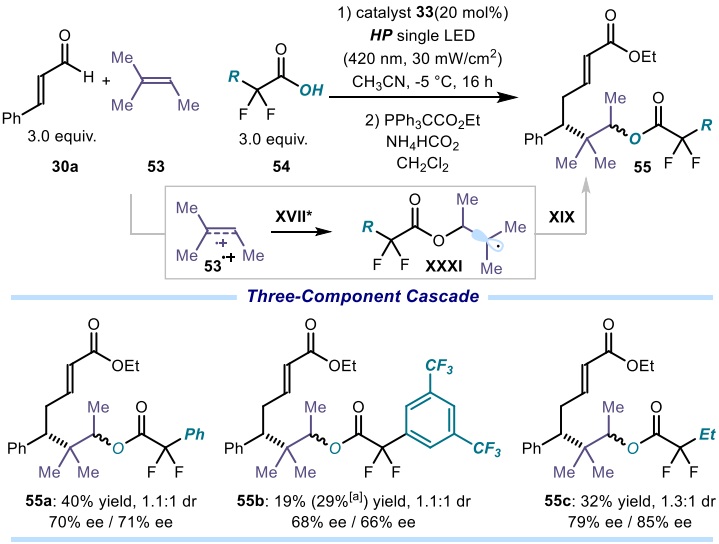

Figure 3.17. Catalytic enantioselective three-component radical cascade process that combines two intermolecular radical steps. Reactions performed on a 0.1 mmol scale in CH_3CN. Yields and enantiomeric excess given on the isolated enoate derivatives **55** obtained upon olefination of the aldehyde precursor (average of two experiments). The dr values were inferred by ^1H NMR analysis of the crude reaction mixture. [a] Yield of the isolated intermediate aldehyde.

3.6.4.Unsuccessful Substrates

During our survey of possible reactive alkenoic acids **50** for the two-component enantioselective cascade, we tested the reactivity of several substrates bearing different nucleophilic groups (Figure 3.18). Unfortunately, all the tested substrates, bearing an amide, tosylamines, or carbamate as nucleophilic moieties, offered very low yields and poor conversion of the starting materials (adducts **56a-g**). We also sought to expand the scope of the aromatic enals that could participate in the radical cascade. Placing strongly electron-donating or withdrawing groups within the aryl ring resulted in very poor yields and usually no conversion (**420-r**). The substitution of the phenyl ring by a heteroaromatic one (**42t-u**) or an extended aromatic ring (**42v**) completely inhibited the reactivity. These results showcased the limitation of the system regarding strong electronic changes in the aryl moiety of the enals.

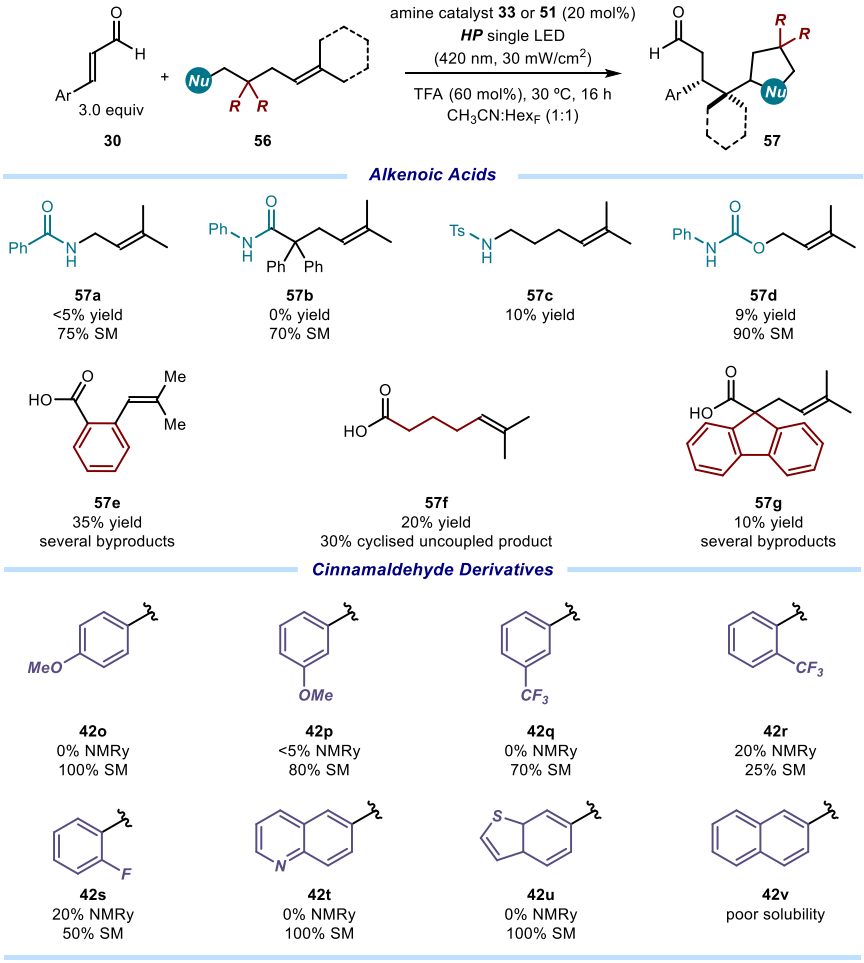

Figure 3.18. Survey of substrates that proved unsuccessful in the photochemical enantioselective radical cascade.

3.7. Conclusions

We have developed a visible-light-mediated organocatalytic strategy that exploits the excited-state reactivity of chiral iminium ions to trigger radical cascade reactions with high enantioselectivity. The method combines two sequential radical-based bond-forming events in a single step and converts unactivated olefins and α,β-unsaturated aldehydes into complex chiral products containing butyrolactone or tetrahydrofuran moieties. These two structural elements are present in numerous biologically active and naturally occurring molecules. We have further implemented an asymmetric three-component radical cascade variant that further demonstrates the complexity-generating power of this photochemical strategy.

3.8. Experimental

3.8.1. General Information

The ^{1}H NMR, ^{19}F NMR, ^{13}C NMR spectra, and HPLC or UPC2 traces are available in literature[1] and are not reported in the present dissertation.

The NMR spectra were recorded at 300 MHz, 400 MHz, and 500 MHz for ^{1}H or at 75 MHz, 101 MHz, and 126 MHz for ^{13}C, 376 MHz for ^{19}F, respectively. The chemical shifts (δ) for ^{1}H and $^{13}C\{^{1}H\}$ are given in ppm relative to residual signals of the solvents ($CHCl_3$ @ 7.26 ppm ^{1}H NMR, 77.00 ppm ^{13}C NMR). Coupling constants are given in Hz. The following abbreviations are used to indicate the multiplicity: s, singlet; d, doublet; t, triplet; q, quartet; m, multiplet; br s, broad singlet.

High-resolution mass spectra (HRMS) were obtained from the ICIQ High-Resolution Mass Spectrometry Unit on MicroTOF Focus and Maxis Impact (Bruker Daltonics) with electrospray ionization. X-ray data were obtained from the ICIQ X-Ray Unit using a Bruker-Nonius diffractometer equipped with an APPEX 2 4K CCD area detector. Optical rotations were measured on a Polarimeter Jasco P-1030 and are reported as follows: $[\alpha]_D$ ambient temperature (c in g per 100 mL, solvent). Cyclic voltammetry studies were carried out on a Princeton Applied Research PARSTAT 2273 potentiostat offering compliance voltage up to ± 100 V (available at the counter electrode), ± 10 V scan range and ± 2 A current range.

General Procedures. All reactions were set up under an argon atmosphere in oven-dried glassware using standard Schlenk techniques unless otherwise stated. Synthesis grade solvents were used as purchased. Anhydrous solvents were taken from a commercial solvent purification system (SPS) dispenser. Chromatographic purification of products was accomplished using flash column chromatography (FC) on silica gel (35-70 mesh). For thin-layer chromatography (TLC) analysis throughout this work, Merck precoated TLC plates (silica gel 60 GF_{254}, 0.25 mm) were used, using UV light as the visualizing agent and either phosphomolybdic acid in EtOH, dinitrophenylhydrazine in EtOH/H_2O, *p*-anisaldehyde or basic aqueous potassium permanganate ($KMnO_4$), and heat as developing agents. Organic solutions were concentrated under reduced pressure on a Büchi rotary evaporator (*in vacuo* at 40 °C, ~5 mbar).

Determination of Diastereomeric Ratio. The diastereomeric ratio was determined by ^{1}H NMR analysis of the crude reaction mixture through integration of diagnostic signals.

Determination of Enantiomeric Purity: HPLC analysis on a chiral stationary phase was performed on an Agilent 1200 series HPLC, using Daicel Chiralpak IC-3, ID-3, and IG columns with *n*-hexane: ^{i}PrOH as the eluent. UPC² analysis on a chiral stationary phase was performed on a Waters Acquity instrument using AMY1 and IG chiral columns. The exact conditions for the analyses are specified within the characterization section. HPLC and UPC² traces were compared to racemic samples prepared by running the reaction in the presence of a catalytic amount (20 mol%) of racemic 2-*tert*-butyl-3-methyl-5-benzyl-4-imidazolidinone, which is commercially available from Sigma Aldrich.

Materials: Commercial grade reagents and solvents were purchased at the highest commercial quality from Sigma Aldrich, Fluka, Acros Organics, Fluorochem, or Alfa Aesar and used as received unless otherwise stated. Chiral secondary amine catalysts **33** and **51** were prepared according to the reported literature.[34] Enals **30a** and **30k** are commercially available, and they were distilled prior to use. Enals **30g**, **30h**, and **30l** were prepared according to the literature procedure.[47] Enal **30i, 30j, 30m, 30n** were prepared according to the literature procedure.[34] Enal **30n** was prepared according to the literature procedure.[48] Alkenoic acids **41b**, **41c**, **41d** were synthesized according to a reported procedure.[49] The synthesis of other alkenoic acids **41** are outlined below. α-Difluoroacids **54a** and **54b** are commercially available.

3.8.2. Substrate Synthesis

Synthesis of acids 41

Acids **41b**, **41c**, **41d** were synthesized as shown in Figure 3.19 according to a reported procedure:[49]

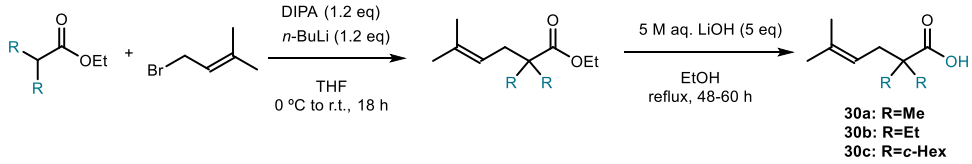

Figure 3.19. Preparation of gem-disubstituted acids.

---

[47] Battistuzzi, G.; Cacchi, S.; Fabrizi, G. "An Efficient Palladium-Catalyzed Synthesis of Cinnamaldehydes from Acrolein Diethyl Acetal and Aryl Iodides and Bromides" *Org. Lett.* **2003**, *5*, 777.

[48] Clary L.; Boiteau, J.-G.; Millois, B. C. "Novel Biaromatic Compounds which Activate Receptors of PPAR type and their Use in Cosmetic or Pharmaceutical Compositions" WO2006/018325, **2006.**

[49] Takenaka, K.; Akita, M.; Tanigaki, Y.; Takizawa, S.; Sasai, H. "Enantioselective Cyclization of 4-Alkenoic Acids via an Oxidative Allylic C–H Esterification" *Org. Lett.* **2011**, *13*, 3506.

To a solution of diisopropylamine (1.2 equiv., 20.2 mmol, 2.83 mL) in THF (20 mL) was added *n*-BuLi (2.6 M solution in hexane; 1.2 equiv., 20.2 mmol, 7.77 mL) dropwise at 0 °C. The solution was stirred at that temperature for 30 minutes and subsequently, the ester was added (1.0 equiv., 16.8 mmol). The reaction mixture was allowed to warm to ambient temperature and stirred for an additional 30 minutes. Then 1-bromo-3-methyl-2-butene (1.2 equiv., 2.46 g, 20.2 mmol) was added dropwise at 0 °C and the resulting solution was stirred at ambient temperature for 16 hours. The reaction was quenched by the addition of aq. HCl (1.0 M) and the mixture extracted with diethyl ether (3 times). The organic layer was washed with brine, dried over Mg_2SO_4, and concentrated *in vacuo*. The residue was re-dissolved in EtOH (30 mL) and aq. NaOH (5.0 M, 5 equiv., 16.3 mmol) was added to this solution. The mixture was refluxed for 48–72 h. After being cooled to ambient temperature, the mixture was extracted with EtOAc and the organic layer was washed with brine and dried over Na_2SO_4. The product was purified by column chromatography on silica gel to give the acid.

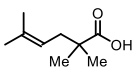

2,2,5-Trimethylhex-4-enoic acid (41b)

Prepared according to the general procedure using ethyl isobutyrate (1.0 equiv., 16.8 mmol, 1.95 g). The material was purified by column chromatography on silica gel (*n*-hexane:EtOAc 90:10) to give the product as a pale yellow liquid (2.1 g, 39% over two steps). Analytical data is consistent with that reported in the literature.[49]

^{1}H NMR (400 MHz, $CDCl_3$) δ 5.12 (dddd, *J* = 7.6, 6.1, 2.9, 1.5 Hz, 1H), 2.30 – 2.18 (m, 2H), 1.71 (d, *J* = 1.3 Hz, 3H), 1.61 (d, *J* = 1.4 Hz, 3H), 1.18 (s, 6H).

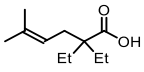

2,2-Diethyl-5-methylhex-4-enoic acid (41c)

Prepared according to the general procedure using ethyl 2-ethylbutanoate (1.0 equiv., 16.8 mmol, 2.40 mL). The material was purified by column chromatography on silica gel (*n*-hexane:EtOAc 88:12) to give the product as a pale yellow liquid (0.6 g, 19% over two steps).[49]

^{1}H NMR (500 MHz, $CDCl_3$) δ 5.04 (dddd, *J* = 7.4, 5.9, 2.9, 1.4 Hz, 1H), 2.28 (dp, *J* = 7.3, 1.0 Hz, 2H), 1.70 (q, *J* = 1.3 Hz, 3H), 1.63 (s, 1H), 1.61 (q, *J* = 7.5 Hz, 6H), 0.83 (t, *J* = 7.5 Hz, 6H).

^{13}C NMR (126 MHz, $CDCl_3$) δ 134.08, 119.12, 31.71, 26.75, 26.06, 17.96, 8.48.

HRMS (ESI) Calculated for $C_{11}H_{19}O_2$ $[M-H]^-$: 183.1391, found: 183.1384.

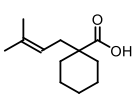

1-(3-Methylbut-2-en-1-yl)cyclohexane-1-carboxylic acid (41d)

Prepared according to the general procedure using ethyl 2-ethylbutanoate (1.0 equiv., 16.8 mmol, 2.78 mL). The material was

purified by column chromatography on silica gel (*n*-hexane:EtOAc 90:10) to give the product as a pale yellow liquid (0.6 g, 18% over two steps). Analytical data is consistent with that reported in the literature.[49]

^{1}H NMR (300 MHz, $CDCl_3$) δ 5.11 (t, *J* = 7.7 Hz, 1H), 2.24 (d, *J* = 7.7 Hz, 2H), 2.05 (d, *J* = 13.1 Hz, 2H), 1.70 (d, *J* = 1.4 Hz, 3H), 1.60 – 1.13 (m, 13H).

The following acids were synthesized using reported procedures different from the general method described above.

5-Methyl-2,2-diphenylhex-4-enoic acid (41a)[39]

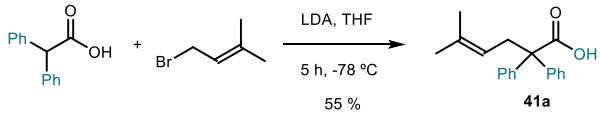

Figure 3.20. Preparation of gem-dimethyl acid **41a.**

A 500 mL round bottom flask was equipped with a magnetic stirrer, fitted with a septum, and purged with nitrogen. To the flask was added freshly distilled diisopropylamine (2.2 equiv., mmol, 5.86 mL) in THF (120 mL). The solution was cooled to 0 °C and a solution of *n*-BuLi (2.5 M in hexanes, 15.3 mL, 2.1 equiv.) was added carefully to the reaction. After 30 minutes, the reaction was cooled to -78 °C and a solution of diphenylacetic acid (4.0 g) in THF was added dropwise. The reaction, which turned cloudy and bright yellow, was allowed to stir for 1 hour at -78 °C before prenyl bromide (3.26 mL) was added dropwise. Upon completion of the addition, the reaction was warmed to ambient temperature and stirred for an additional 3 hours. The reaction was then quenched with saturated ammonium chloride (60 mL) and diluted with ether. The organics were separated, and the aqueous extracted with diethyl ether (3x40 mL). The combined organics were washed with aq. HCl (1M, 100 mL), water (100 mL), and brine (100 mL), then dried over magnesium sulfate, filtered, and concentrated to give a viscous oil. The crude material was purified by column chromatography on silica gel (*n*-hexane:EtOAc 86:14) to give the product as a white crystalline solid (2.91 g, 55%). Analytical data is consistent with that reported in the literature.[39]

^{1}H NMR (400 MHz, $CDCl_3$) δ 7.35 – 7.22 (m, 10H), 5.02 (t, *J* = 7.4, 3.9, 1.4 Hz, 1H), 3.08 (d, *J* = 7.0 Hz, 2H), 1.56 (s, 3H), 1.25 (s, 3H).

5-Methyl-hex-4-enoic acid (41e)[50]

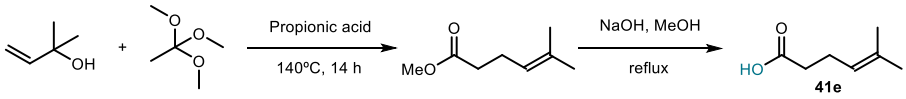

Figure 3.21. Preparation of unsubstituted acid **41e.**

A mixture of 2-methylbut-3-en-2-ol (1.0 equiv., 63.9 mmol, 6.67 mL) and propionic acid (0.063 equiv., 4.02 mmol, 0.3 mL) in 1,1,1-trimethoxyethane (10 equiv., 639 mmol, 81 mL) was heated at 140 °C for 14 hours. Then, the reaction mixture was slowly added into an ice-cooled aq. HCl (1 N, 70 mL) and extracted with diethyl ether (3x). The combined organic layers were washed with saturated $NaHCO_3$ and brine, dried over $MgSO_4$, and concentrated *in vacuo*. The product was purified by column chromatography on silica gel (*n*-hexane:EtOAc 97:3) to give the methyl ester as an oil (2.0 g, 22%). A solution of the synthesized ester and aq. NaOH (3M, 15 mL) in methanol (5 mL) was stirred at reflux for 36 hours. The reaction mixture was cooled to ambient temperature and the methanol evaporated. The mixture was acidified with aq. HCl (2 M) to pH 2 and the product was extracted with diethyl ether (3x). The organic layer was washed with brine and dried over anhydrous Mg_2SO_4. The solvent was removed under reduced pressure to give the acid as a colorless oil that was used without further purification. Analytical data is consistent with that reported in the literature.[50]

^{1}H NMR (300 MHz, $CDCl_3$) δ 5.10 (tp, *J* = 5.6, 1.5 Hz, 1H), 2.44 – 2.24 (m, 4H), 1.69 (d, *J* = 1.4, 3H), 1.62 (d, *J*= 1.4 Hz, 3H).

4-Cyclohexylidenebutanoic acid (41f)[51]

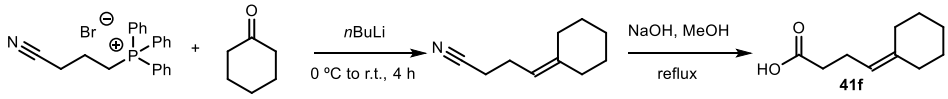

Figure 3.22. Preparation of acid bearing a cyclohexyl on the double bond **41f.**

Synthesis of phosphonium salt

A solution of triphenylphosphine (1.0 equiv., 10 mmol, 2.62 g) and 4-bromobutyronitrile (1.0 equiv., 10 mmol, 1.620 g, 1.09 mL) in anhydrous toluene (85

[50] Mura, S.; Zouhiri, F.; Lerondel, S.; Maksimenko, A.; Mougin, J.; Gueutin, C.; Brambilla, D.; Caron, J.; Sliwinski, E.; LePape, A.; Desmaele, D.; Couvreur, P. "Novel Isoprenoyl Nanoassembled Prodrug for Paclitaxel Delivery" *Bioconjugate Chem.*, **2013**, *24*, 1840.
[51] Zheng, T.; Narayan, R. S.; Schomaker, J. M.; Borhan, B. "One-Pot Regio- and Stereoselective Cyclization of 1,2,*n*-Triols"*J. Am. Chem. Soc.* **2005**, *127*, 6946.

mL) was refluxed under argon for 72 hours. A white precipitate was formed. After the reaction mixture was cooled, the product was collected by filtration, washed with ether, and dried under vacuum. The phosphonium salt was obtained as a white solid (2.9 g, 70% yield).

Synthesis of the nitrile

n-BuLi (2.5 M in hexanes, 2.8 mL, 1.0 equiv.) was added to a solution of the phosphonium salt (2.9 g, 1.0 equiv.) in anhydrous THF (7 mL) at ambient temperature under argon. After 1 hour, the mixture was cooled to 0 °C and cyclohexanone (1.47 mL, 2.0 equiv.) was added and stirred for an additional hour at ambient temperature. The reaction mixture was then heated to 100 °C for 3 hours. The reaction was quenched with 10% aq. HCl and the product extracted from the aqueous phase with diethyl ether (3x). The combined organic layers were washed with saturated $NaHCO_3$ and brine, dried over anhydrous Mg_2SO_4, and concentrated *in vacuo*. The product was purified by column chromatography on silica gel (*n*-hexane:EtOAc 96:4) to give the nitrile (0.6 g, 57%). Analytical data is consistent with that reported in the literature.[51]

^{1}H NMR (400 MHz, $CDCl_3$) δ 5.08 (t, *J* = 5.7 Hz, 1H), 2.43 – 2.25 (m, 4H), 2.11 (dt, *J* = 18.3, 5.1 Hz, 4H), 1.54 (s, 6H).

Synthesis of the carboxylic acid

A solution of the aforementioned nitrile (0.6 g, 1.0 equiv.) and aq. NaOH (6M, 27 mL) in methanol (90 mL) was stirred at reflux for 72 hours. The reaction mixture was cooled to ambient temperature and the methanol evaporated. The mixture was acidified with 2M HCl and the product was extracted with EtOAc (3x). The organic layer was washed with brine and dried over anhydrous Mg_2SO_4. The solvent was removed under reduced pressure to give the crude as a dark oil. The product was purified by column chromatography on silica gel (*n*-hexane:EtOAc 75:25) to give the desired acid as a pale yellow oil (0.27 g, 40%). Analytical data is consistent with that reported in the literature.[51]

^{1}H NMR (300 MHz, $CDCl_3$) δ 5.09 – 5.02 (m, 1H), 2.43 – 2.27 (m, 4H), 2.10 (dt, *J* = 22.5, 5.3 Hz, 5H), 1.51 (tt, *J* = 6.5, 3.9 Hz, 6H).

Synthesis of alcohols 42

Alcohols **42g** and **42h** were synthesized as shown in Figure 3.23 according to reported procedure:[39]

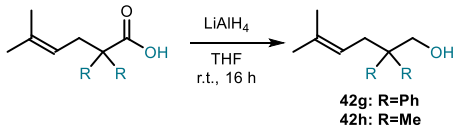

Figure 3.23. Preparation of *gem*-disubstituted alcohol.

A 100 mL round bottom flask purged with argon was charged with $LiAlH_4$ (1.0 equiv.) and dry THF (0.2 M). Subsequently, the acid was added dropwise at 0 °C. After H_2 evolution ceased, the mixture was warmed at ambient temperature. The resulting solution was refluxed for 16 hours and quenched by careful addition of water and aq. NaOH (1.0 M). The resulting suspension was filtered through Celite and eluted with diethyl ether. The eluent was dried over Mg_2SO_4 and concentrated *in vacuo*. The product was purified by column chromatography on silica gel to give the alcohol.

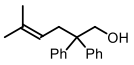

5-Methyl-2,2-diphenylhex-4-en-1-ol (42g)

Prepared according to the procedure described above using $LiAlH_4$ (1.0 equiv., 5.3 mmol, 0.20 g), THF (25 mL), acid **42a** (1.0 equiv., 5.3 mmol, 1.5 g). The material was purified by column chromatography on silica gel (*n*-hexane:EtOAc 90:10) to give the product as a yellow oil (0.9 g, 63%). Analytical data is consistent with that reported in the literature.[39]

^{1}H NMR (300 MHz, $CDCl_3$) δ 7.32 (ddt, *J* = 10.5, 6.8, 3.2 Hz, 4H), 7.29 – 7.18 (m, 6H), 4.88 (ddd, *J* = 7.3, 5.9, 1.4 Hz, 1H), 4.15 (s, 1H), 2.91 (d, *J* = 7.2 Hz, 2H), 1.63 (s, 2H), 1.57 (s, 2H), 1.29 (t, *J* = 7.1 Hz, 1H).

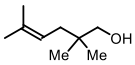

2,2,5-Trimethylhex-4-en-1-ol (42h)

Prepared according to the procedure described above using $LiAlH_4$ (1.0 equiv., 6.9 mmol, 0.26 g), THF (30 mL), acid **42b** (1.0 equiv., 6.9 mmol, 2.0 g). The product was obtained as a pale yellow liquid (0.8 g, 81%) with no need for purification. Analytical data is consistent with that reported in the literature.[52]

^{1}H NMR (300 MHz, $CDCl_3$) δ 5.21 (tdt, *J* = 7.7, 2.8, 1.4 Hz, 1H), 3.33 (s, 2H), 1.96 (d, *J* = 7.7 Hz, 2H), 1.77 – 1.70 (m, 3H), 1.63 (s, 3H), 0.89 (s, 6H).

[52] Hodgson, D. M.; Chung, Y. K.; Nuzzo, I.; Freixas, G.; Kulikiewicz, K. K.; Cleator, E.; Paris, J.-M. "Intramolecular Cyclopropanation of Unsaturated TerminalEpoxides and Chlorohydrins" *J. Am. Chem. Soc.* **2007**, 129, 4456.

Synthesis of enals 42

(*E*)-3-(*p*-Tolyl)acrylaldehyde (**42k**) was purchased from Fluorochem. Enals **42g**, **42h**, **42l** were synthesized according to the reported procedure.[47] Enal **42j** was synthesized according to reported procedure.[34]

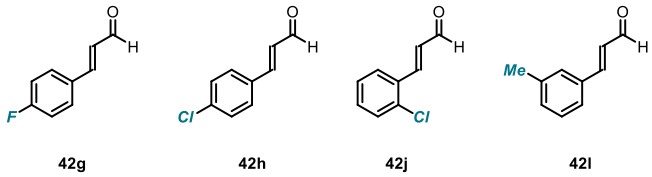

Figure 3.24. Enals used in the reaction scope

General Method

Enals **30i**, **30m**, **30n** were synthesized as shown in Figure 3.25 following reported procedure:[47]

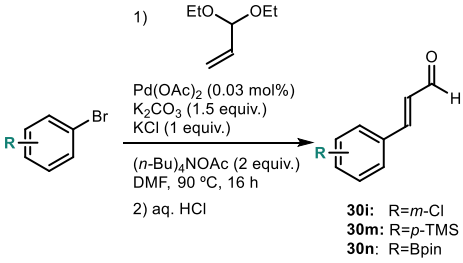

Figure 3.25. Preparation of enals

To an oven-dried, argon purged, two necks round-bottomed flask fitted with a condenser was added an orange, cloudy mixture of 3,3-diethoxyprop-1-ene (3.0 equiv.), $Pd(OAc)_2$ (3 mol%), K_2CO_3 (1.5 equiv.), KCl (1.0 equiv.), $(n\text{-}Bu)_4OAc$ (2.0 equiv.) and aryl bromide (1.0 equiv.) in DMF (20 mL). The reaction mixture was heated to 90 °C. After 18 hours of stirring, the black solution was allowed to cool to ambient temperature. Aq. HCl (2 M, 15 mL) was added dropwise and the mixture was stirred for 15 minutes. Water (100 mL) was added and the mixture extracted with diethyl ether (100 mL). The organic layer was dried over $MgSO_4$ and concentrated to give a brown oil, which was purified by column chromatography to afford the pure enal.

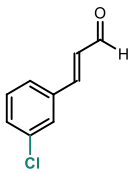

(*E*)-3-(3-Chlorophenyl)acrylaldehyde (30i)

Prepared according to the general procedure using 3,3-diethoxyprop-1-ene (3 equiv., 9.0 mmol, 1.37 mL), $Pd(OAc)_2$ (3 mol%, 90 µmol, 20 mg), K_2CO_3 (1.5 equiv., 4.5 mmol, 620 mg), KCl (1.0 equiv., 3.0 mmol, 220 mg), $(n\text{-}Bu)_4OAc$ (2.0 equiv., 6.0 mmol, 2.0 g) and 1-bromo-3-chlorobenzene

(1.0 equiv., 3.0 mmol, 0.35 mL) in DMF (20 mL). The material was purified by column chromatography on silica gel (*n*-hexane:EtOAc 95:5) to give the product as a pale yellow solid (0.3 g, 60%). Analytical data is consistent with that reported in the literature.[53]

^{1}H NMR (300 MHz, $CDCl_3$) δ 9.72 (d, *J* = 7.5 Hz, 1H), 7.55 (d, *J* = 18 Hz, 1H), 7.48 – 7.33 (m, 4H), 6.71 (dd, *J* = 16.0 Hz, 7.6 Hz, 1H).

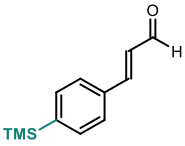

(*E*)-3-(4-(Trimethylsilyl)phenyl)acrylaldehyde (3om)

Prepared according to the general procedure using 3,3-diethoxyprop-1-ene (3.0 equiv., 9.0 mmol, 1.4 mL), $Pd(OAc)_2$ (3 mol%, 90 µmol, 20 mg), K_2CO_3 (1.5 equiv., 4.5 mmol, 620 mg), KCl (1 equiv., 3.0 mmol, 220 mg), $(n\text{-Bu})_4OAc$ (2.0 equiv., 6.0 mmol, 2.0 g) and 1-chloro-2-iodobenzene (1.0 equiv., 3.0 mmol, 0.59 mL) in DMF (20 mL). The material was purified by column chromatography on silica gel (*n*-hexane:EtOAc 95:5) to give the product as a pale yellow solid (0.35 g, 57%). Analytical data is consistent with that reported in the literature.[54]

^{1}H NMR (300 MHz, $CDCl_3$) δ 9.71 (d, *J* = 7.7 Hz, 1H), 7.57 (q, *J* = 8.2 Hz, 4H), 7.48 (d, *J* = 16.0 Hz, 1H), 6.75 (dd, *J* = 15.9, 7.6 Hz, 1H), 0.29 (s, 9H).

^{13}C NMR (101 MHz, $CDCl_3$) δ 193.8, 152.9, 145.2, 134.2, 134.0, 128.7, 127.6, -1.3.

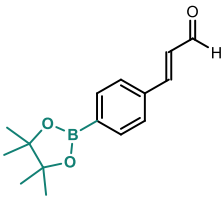

(*E*)-3-(4-(4,4,5,5-Tetramethyl-1,3,2-dioxaborolan-2-yl)phenyl) acrylaldehyde (3on)[48]

To an oven-dried, argon purged, round-bottomed flask fitted with a condenser were added $Pd(dppf)Cl_2$ (0.05 equiv., 240 µmol, 170 mg), bis(pinacolato)diboron (1.1 equiv., 5.2 mmol, 1.3 g), potassium acetate (3.0 equiv., 14 mmol, 1.4 g), and (*E*)-3-(4-bromophenyl)acrylaldehyde (1.0 equiv., 4.5 mmol, 1.0 g) in dry DMF (10 mL). The reaction mixture was heated to 50 °C. After 18 hours of stirring, the black solution was allowed to cool to ambient temperature. Water (50 mL) was added and the mixture extracted with EtOAc (3x50 mL). The organic layer was dried over $MgSO_4$ and concentrated to give a black oil, which was purified by column chromatography on

[53] Jiang, J.-A.; Du, J.-L.; Wang, Z.-G.; Zhang, Z.-N.; Xu, X.; Zheng, G.-L.; Ji, Y.-F. "Practical $Cu(OAc)_2$/TEMPO-catalyzed selective aerobic alcohol oxidation under ambient conditions in aqueous acetonitrile" *Tetrahedron Lett.* **2014**, *55*, 1677.

[54] Liu, J.; Zhu, J.; Jiang, H.; Wang, W.; Li, J. "Pd-catalyzed cascade Heck–Saegusa: direct synthesis of enalsfrom aryl iodides and allyl alcohol" *Chem. Commun.* **2010**, 46, 415.

silica gel (*n*-hexane:EtOAc 85:15) to give the desired acrylate as a pale yellow solid (0.51 g, 42%).

^{1}H NMR (300 MHz, $CDCl_3$) δ 9.72 (d, J = 7.6 Hz, 1H), 7.86 (d, J = 8.1 Hz, 2H), 7.62 – 7.46 (m, 3H), 6.76 (dd, J = 16.0, 7.7 Hz, 1H), 1.36 (s, 12H).

^{13}C NMR (75 MHz, $CDCl_3$) δ 193.66, 152.52, 136.36, 135.37, 129.25, 127.61, 80.14, 24.88.

HRMS (ESI) Calculated for $C_{15}H_{19}NaBO_3$ $[M+Na]^+$: 280.1356, found: 280.1359.

Synthesis of α-difluoroacids 54[55]

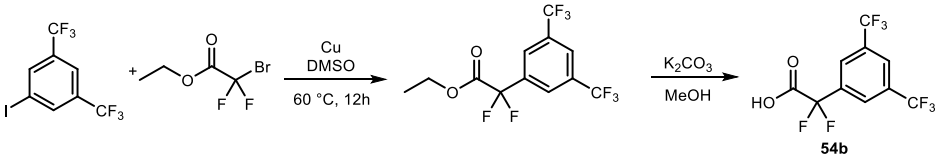

Figure 3.26. Synthesis of difluoroacid **54b**.

In a 50 mL round bottom flask under an atmosphere of argon, 1-iodo-3,5-bis(trifluoromethyl)benzene (0.89 ml, 5.0 mmol) and ethyl 2-bromo-2,2-difluoroacetate (0.64 mL, 5.0 mmol) were added to a suspension of activated copper (0.83 g, 13 mmol) in DMSO (13 ml). The reaction mixture was stirred at 60 °C for 12 hours, after which time it was poured into a mixture of ice and sat. ammonium chloride. The aqueous phase was extracted with diethyl ether (3x50 mL). The combined organic phases were washed with sat. aq. NH_4Cl (2x50 mL) and brine (2x50 mL), then dried over $MgSO_4$, filtered and concentrated. The crude mixture was purified by flash column chromatography to afford ethyl 2-(3,5-bis(trifluoromethyl)phenyl)-2,2-difluoroacetate as a colorless oil (1.21 g, 3.6 mmol, 72% yield).

^{1}H NMR (400 MHz, $CDCl_3$) δ 8.08 (s, 2H), 8.03 (s, 1H), 4.35 (q, *J* = 7.1 Hz, 2H), 1.33 (t, *J* = 7.1 Hz, 3H).

^{13}C NMR (101 MHz, $CDCl_3$) δ 162.9, 135.5, 132.7 (q, *J* = 34.3 Hz), 126.4 (br. s), 125.2 (br. s), 122.86 (q, *J* = 273.0 Hz), 112.1 (t, *J* = 254.2 Hz) 64.1, 13.9.

^{19}F NMR (376 MHz, $CDCl_3$) δ -63.16, -104.22.

Ethyl 2-(3,5-bis(trifluoromethyl)phenyl)-2,2-difluoroacetate (1.20 g, 3.57 mmol) was added to a mixture of MeOH (12.0 mL) and potassium carbonate (3.57 mL, 3.57 mmol)

[55] Khotavivattana, T.; Verhoog, S.; Tredwell, M.; Pfeifer, L.; Calderwood, S.; Wheelhouse, K.; Collier, T. L.; Gouverneur, V. "^{18}F-Labeling of Aryl-SCF_3,-OCF_3 and -$OCHF_2$ with [^{18}F]Fluoride" *Angew. Chem. Int. Ed.*, **2015**, *54*, 9991.

and stirred at ambient temperature for 3 hours before removing methanol *in vacuo*. Ether was then added, and the phases were separated to remove the residual ethyl aryldifluoroacetate. Concentrated hydrochloric acid was added to the aqueous phase until pH = 1, and the aqueous phase was extracted with EtOAc (2x20 mL), washed with brine (10 mL), dried over anhydrous Mg_2SO_4 and concentrated to give 2-(3,5-bis(trifluoromethyl)phenyl)-2,2-difluoroacetic acid as a white hygroscopic solid (782 mg, 2.5 mmol, 71% yield).

^{1}H NMR (400 MHz, CD_3CN) δ 9.45 (s, 1H), 8.24 (s, 1H), 8.20 (s, 2H).

^{13}C NMR (101 MHz, CD_3CN) δ 163.9, 136.3 (t, *J* = 26.5 Hz), 132.9 (q, *J* = 34.2 Hz), 127.6, 126.5, 124.0 (q, *J* = 272.1 Hz).

^{19}F NMR (376 MHz, CD_3CN) δ -63.70, -104.75.

3.8.3. Catalysts Synthesis

The chiral amine catalyst **33** was synthesized as shown in the following scheme according to the reported procedure:[34]

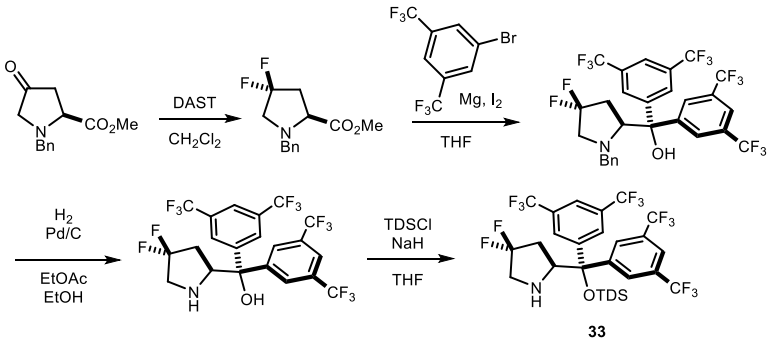

Figure 3.27 Synthetic pathway for preparing the chiral secondary amine catalyst **33;** TDSCl: chloro(dimethyl)thexylsilane.

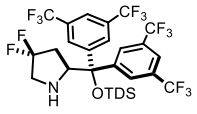

(*S*)-2-(Bis-(3,5-bis-(trifluoromethyl)-phenyl)-(((2,3- dimethyl butan-2-yl)-dimethylsilyl)-oxy)-methyl)-4,4- difluoro pyrrolidine (33)

^{1}H NMR (400 MHz, $CDCl_3$) δ 8.10 (s, 2H, *ortho*), 7.91 (s, 2H, *para* and *para'*), 7.72 (s, 2H, *ortho'*), 4.46 (t, *J* = 8.3 Hz, 1H, C2*H*), 3.15 (td, *J* = 13.9 Hz, 7.2 Hz, 1H, C5*H*H), 2.62 (ddd, *J* = 20.2 Hz, 12.9 Hz, 7.9 Hz, 1H, C5H*H*), 2.31-2.08 (m, 2H, C3*H*H and N*H*), 1.95-1.69 (m, 2H, C3H*H* and SiCC*H*), 0.95 (d, *J* = 3.0 Hz, 3H, SiCCHCH_3), 0.93 (d, *J* = 3.0 Hz, 3H,

SiCCHCH_3'), 0.89 (s, 3H, SiCCH_3), 0.87 (s, 3H, SiCCH_3'), -0.14 (s, 3H, SiCH_3), -0.47 (s, 3H, SiCH_3).

^{13}C NMR (101 MHz, $CDCl_3$) δ 146.6 (*ipso*), 145.0 (*ipso'*), 132.2 (2C, q, J_{CF} = 33.6 Hz, *meta*), 131.4 (2C, q, J_{CF} = 33.5 Hz, *meta'*), 129.7 (dd, J_{CF} = 254.0 Hz, 246.9 Hz, *C4*), 129.5 (2C, q, J_{CF} = 4.1 Hz, *ortho*), 128.8 (2C, q, J_{CF} = 4.1 Hz, *ortho'*), 123.4 (2C, q, J_{CF} = 272.8 Hz, ArCF_3), 123.2 (2C, q, J_{CF} = 272.9 Hz, Ar'CF_3), 122.6 (apparent p, J_{CF} = 3.8 Hz, *para*), 122.4 (apparent p, J_{CF} = 3.8 Hz, *para'*), 82.2 (*C6*), 62.8 (dd, J_{CF} = 6.5 Hz, 1.3 Hz, *C2*), 53.9 (t, J_{CF} = 28.8 Hz, *C3*), 37.6 (t, J_{CF} = 25.0 Hz, *C5*), 33.9 (SiCCH), 26.0 (SiCCH), 20.4 (SiCCH_3), 20.2 (SiCCH_3'), 18.7 (2C, SiCCHCH_3), -0.03 (SiCH_3), -0.80 (SiCH_3').

The chiral amine catalyst **51** was synthesized as shown in the following scheme according to the reported procedure:[34]

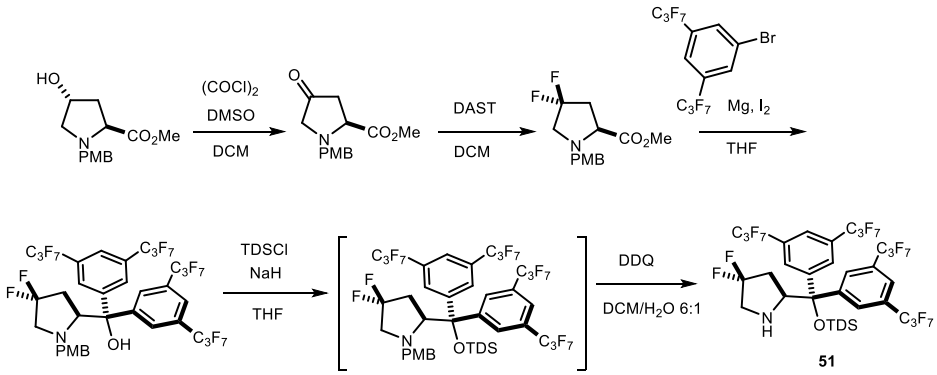

Figure 3.28. Synthetic pathways for preparing catalyst **51.** DDQ = 2,3-dichloro-5,6-dicyano-*p*-benzoquinone; PMB = *p*-methoxybenzyl.

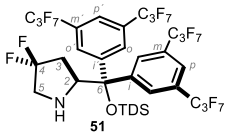

(*S*)-2-(Bis-(3,5-bis-(perfluoropropan-2-yl)-phenyl)-(((2,3-dimethylbutan-2-yl)-dimethylsilyl)-oxy)-methyl)-4,4-difluoro-1-(4-methoxybenzyl)-pyrrolidine (51)

^{1}H NMR (400 MHz, $CDCl_3$): δ 8.06 (s, 2H, *ortho*), 7.88 (s, 1H, *para*), 7.87 (s, 1H, *para'*), 7.70 (s, 2H, *ortho'*), 4.52 (br t, *J* = 7.2 Hz, 1H, C2*H*), 3.11-2.96 (m, 1H, C5*H*H), 2.41-2.21 (m, 2H, C5H*H* and C3*H*H), 2.14 (br s, 1H, N*H*), 1.87 (dtd, *J* = 22.2 Hz, 14.0 Hz, 8.3 Hz, 1H, C3H*H*), 1.75 (sept, *J* = 6.9 Hz, 1H, SiCC*H*),0.92 (d, *J* = 2.4 Hz, 3H, SiCCHCH_3), 0.91 (d, *J* = 2.4 Hz, 3H, SiCCHCH_3'), 0.88 (s, 3H, SiCCH_3), 0.87 (s, 3H, SiCCH_3'), -0.09 (s, 3H, SiCH_3), -0.55 (s, 3H, SiCH_3').

^{13}C NMR (101 MHz, $CDCl_3$): δ 146.7 (*ipso*), 145.0 (*ipso'*), 129.5 (dd, J_{CF} = 254.0 Hz, 245.7 Hz, *C4*), 129.4 (2C, d, J_{CF} = 10.1 Hz, *ortho*), 128.9 (2C, d, J_{CF} = 10.1 Hz, *ortho'*, partially overlaid with *meta*), 128.8 (2C, dd, J_{CF} = 20.9 Hz, 2.1 Hz, *meta*), 127.9 (2C, dd, J_{CF} = 20.7 Hz, 2.3 Hz, *meta'*), 123.5 (t, J_{CF} = 10.8 Hz, *para*), 123.2 (t, J_{CF} = 11.5 Hz, *para'*),

120.6 (4C, qd, J_{CF} = 287.1 Hz, 27.5 Hz, CF_3), 120.3 (4C, qd, J_{CF} = 287.3 Hz, 27.3 Hz, CF_3'), 91.3 (2C, apparent dp, J_{CF} = 204.5 Hz, 33.6 Hz, CF_3CF), 91.2 (2C, apparent dp, J_{CF} = 204.7 Hz, 33.6 Hz, CF_3CF'), 82.7 (*C6*), 62.2 (d, J_{CF} = 6.3 Hz, *C2*), 53.4 (t, J_{CF} = 28.8 Hz, *C5*), 37.3 (t, J_{CF} = 25.1 Hz, *C3*), 33.7 (SiCCH), 25.7 (SiCCH), 20.1 ($SiCCH_3$), 19.9 ($SiCCH_3$'), 18.44 ($SiCCHCH_3$), 18.49 ($SiCCHCH_3$'), -0.3 ($SiCH_3$), -1.5 ($SiCH_3$').

3.8.4. General Procedure for the Photochemical Two-Component Cascade

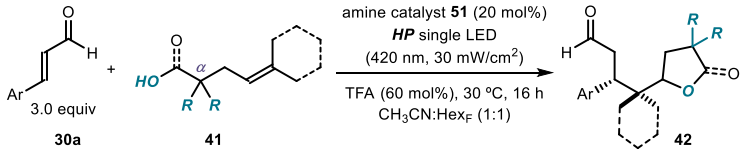

Figure 3.29. General Procedure for the synthesis of products **42.**

General Procedure: To a 5 mL argon-purged glass vial, containing the amine catalyst **51** (22.1 mg, 0.02 mmol, 20 mol%) and the desired acid **41** (0.1 mmol, 1 equiv.), was added enal **30** (0.3 mmol, 3 equiv.) Alternatively, for oily acids, the latter was added to a 5 mL vial and the amine catalyst **51** was added as a stock solution in dichloromethane. Then, the solvent was evaporated under vacuum, and enal **30** was added. At that time, 200 µL of an argon-sparged 0.2 M acetonitrile solution of TFA (4.6 µL, 0.06 mmol, 60 mol%) and tetradecafluorohexane (Hex_F) (200 µL) were added. The vial was sealed with Parafilm, and then placed into an aluminum block on a 3D-printed holder, fitted with a 420 nm high-power single LED. The irradiance was fixed at 30±2 mW/cm², as controlled by an external power supply, and measured using a photodiode light detector at the start of each reaction. This setup secured reliable irradiation while keeping a distance of 1 cm between the reaction vessel and the light source (the setup is detailed in Figure 3.30).

The reaction was stirred for 16 hours. Then the solvent was evaporated, and the crude mixture was purified by column chromatography on silica gel to furnish the product **42**.

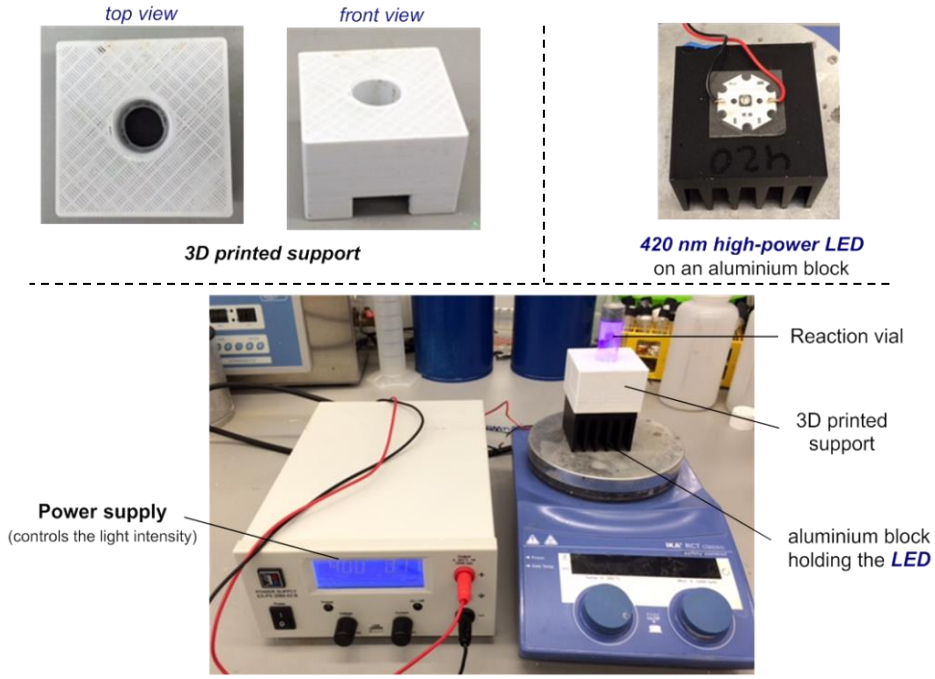

Figure 3.30. Detailed set-up and illumination system. The light source for illuminating the reaction vessel consisted of a single 420 nm high-power LED (OCU-440 UE420-X-T) purchased from OSA OPTO.

3.8.5. General Procedure for the Determination of Enantiomeric Excess

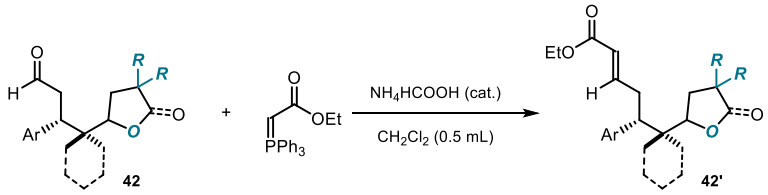

Figure 3.31. General Procedure for the synthesis of enoate **42'**.

The purified aldehyde product **42** was dissolved in CH_2Cl_2 (0.5 mL). Ethyl 2-(triphenyl-λ^5-phosphanylidene)acetate (1.2 eq.) and ammonium formate (4 mg) were added and the resulting mixture was stirred at ambient temperature until completion of the reaction, as inferred by TLC analysis. The crude reaction mixture was evaporated and directly purified by flash column chromatography to afford the enoate derivative **42'**.

3.8.6.Characterization of Products 42 and 52

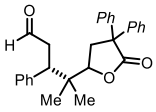

(3*S*)-4-Methyl-4-(5-oxo-4,4-diphenyltetrahydrofuran-2-yl)-3-phenyl pentanal (42a)

Prepared according to the general procedure in section 3.8.3 using 5-methyl-2,2-diphenylhex-4-enoic acid (**2a**). The crude mixture was purified by column chromatography (*n*-hexane:EtOAc 85:15, two consecutive purifications) to give product **42a** as a white solid (22.0 mg, 54%, 1:1 dr, average of two runs, 89% ee_A and 92% ee_B). The enantiomeric excess was determined by HPLC analysis on a Daicel Chiralpak IC-3 column (10:90 ^{i}PrOH:hexane, 1.0 mL/min, 30 ^{o}C, λ = 230 nm). *Diastereosiomer A*: τ_{Major} = 32.0 min, τ_{Minor} = 29.8 min. *Diastereoisomer B*: τ_{Major} = 40.4 min, τ_{Minor} = 35.6 min. $[\alpha]_D^{26}$ = -25.91 (c = 0.25, $CHCl_3$, 1:1 dr, 89% ee_A and 94% ee_B). Absolute configuration determined by anomalous dispersion X-ray crystallographic analysis, see X-ray Crystallographic Data in section 3.8.10.

^{1}H NMR (400 MHz, $CDCl_3$) 1:1 mixture of diastereoisomers δ 9.51 (p, *J* = 1.4 Hz, 2H), 7.34 – 7.27 (m, 17H), 7.25-7.18 (m, 14H), 4.16 (dd, *J* = 11.1, 4.8 Hz, 1H), 4.03 (dd, *J* = 11.1, 5.0 Hz, 1H), 3.50 (dd, *J* = 10.4, 5.0 Hz, 1H), 3.36 (dd, *J* = 11.0, 4.1 Hz, 1H), 3.02 (ddd, *J* = 17.0, 11.0, 2.7 Hz, 1H), 2.96 – 2.81 (m, 4H), 2.73 (ddd, *J* = 13.0, 11.1, 7.4 Hz, 2H), 2.60 (dd, *J* = 12.8, 5.0 Hz, 1H), 1.12 (s, 3H), 1.05 (s, 3H), 0.93 (s, 3H), 0.79 (s, 3H).

^{13}C NMR (101 MHz, $CDCl_3$) 1:1 mixture of diastereoisomers δ 201.59, 201.55, 176.93, 176.85, 142.37, 142.03, 139.86, 139.69, 139.33, 139.16, 129.64, 128.93, 128.85, 128.45, 128.42, 128.36, 128.28, 127.83, 127.77, 127.70, 127.68, 127.29, 127.26, 127.22, 127.18, 80.70, 80.38, 58.06, 57.94, 47.06, 46.44, 44.79, 44.25, 39.30, 38.89, 38.81, 38.63, 21.06, 20.33, 18.99, 18.77.

HRMS (ESI) Calculated for $C_{28}H_{28}NaO_3$ $[M+Na]^+$: 435.1931, found: 435.1941.

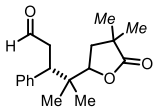

(3*S*)-4-(4,4-Dimethyl-5-oxotetrahydrofuran-2-yl)-4-methyl-3-phenylpentanal (42b)

Prepared according to the general procedure in section 3.8.3 using 2,2,5-trimethylhex-4-enoic acid (**41b**). The crude mixture was purified by column chromatography (*n*-hexane:EtOAc 80:20, three consecutive purifications) to give product **42b** as a yellow oil (21.7 mg, 75%, 1:1 dr, average of two runs). The enantiomeric excess was determined by HPLC analysis of the derivatized product prepared according to the procedure in section 3.8.6.

^{1}H NMR (500 MHz, $CDCl_3$) 1:1 mixture of diastereoisomers δ 9.51 (dd, *J* = 2.6, 1.2 Hz, 1H), 9.49 (dd, *J* = 2.9, 1.5 Hz, 1H), 7.30 (dd, *J* = 8.1, 6.6 Hz, 4H), 7.25 – 7.19 (m, 6H), 4.25 (dd, *J* = 9.2, 7.5 Hz, 1H), 4.07 (dd, *J* = 10.7, 6.1 Hz, 1H), 3.50 (dd, *J* = 10.5, 5.0 Hz, 1H), 3.33 (dd, *J* = 10.9, 4.3 Hz, 1H), 3.04 (ddd, *J* = 17.0, 10.9, 2.6 Hz, 1H), 2.95 – 2.80 (m, 3H), 1.94 – 1.84 (m, 3H), 1.76 (dd, *J* = 12.7, 6.1 Hz, 1H), 1.26 (d, *J* = 3.7 Hz, 7H), 1.21 (s, 3H), 1.15 (s, 3H), 1.02 (s, 3H), 0.94 (s, 3H), 0.85 (s, 3H), 0.73 (s, 3H).

^{13}C NMR (126 MHz, $CDCl_3$) 1:1 mixture of diastereoisomers δ 201.85, 201.73, 181.74, 181.64, 139.89, 139.49, 128.36, 128.33, 127.20, 127.15, 80.16, 80.00, 47.16, 46.30, 44.90, 44.29, 40.25, 40.08, 39.33, 38.84, 38.41, 38.16, 24.85, 24.83, 24.63, 24.60, 21.12, 19.92, 18.51, 18.28.

HRMS (ESI) Calculated for $C_{16}H_{24}NaO_3$ [M+Na]$^+$: 311.1618, found: 311.1616.

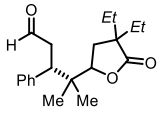

(3*S*)-4-(4,4-Diethyl-5-oxotetrahydrofuran-2-yl)-4-methyl-3-phenylpentanal (42c)

Prepared according to the general procedure in section 3.8.3 using 2,2-diethyl-5-methylhex-4-enoic acid (**41c**). The crude mixture was purified by column chromatography (*n*-hexane:EtOAc 85:15) to give product **42c** as a yellow oil (19.6 mg, 62%, 1:1 dr, average of two runs). The enantiomeric excess was determined by HPLC analysis of the derivatized product prepared according to the procedure in section 3.8.4.

^{1}H NMR (500 MHz, $CDCl_3$) 1:1 mixture of diastereoisomers δ 9.51 (dd, *J* = 2.6, 1.2 Hz, 1H), 9.49 (dd, *J* = 2.9, 1.4 Hz, 1H), 7.33 – 7.27 (m, 4H), 7.25 – 7.19 (m, 6H), 4.18 (dd, *J* = 10.3, 6.7 Hz, 1H), 4.03 (dd, *J* = 10.4, 6.8 Hz, 1H), 3.50 (dd, *J* = 10.6, 5.0 Hz, 1H), 3.32 (dd, *J* = 11.0, 4.2 Hz, 1H), 3.04 (ddd, *J* = 17.0, 10.9, 2.6 Hz, 1H), 2.95 – 2.79 (m, 3H), 2.00 (ddd, *J* = 33.6, 13.0, 10.4 Hz, 2H), 1.83 (dd, *J* = 13.0, 6.7 Hz, 1H), 1.66 (dd, *J* = 13.1, 6.8 Hz, 1H), 1.65 – 1.56 (m, 6H), 1.52 (qd, *J* = 7.5, 1.4 Hz, 2H), 1.02 (s, 3H), 0.96 (s, 3H), 0.93 – 0.87 (m, 9H), 0.87 – 0.82 (m, 6H), 0.74 (s, 3H).

^{13}C NMR (126 MHz, $CDCl_3$) 1:1 mixture of diastereoisomers δ 201.87, 201.77, 180.66, 181.57, 139.87, 139.49, 129.72, 128.31, 127.18, 127.15, 80.34, 80.16, 48.42, 48.32, 47.18, 46.27, 44.84, 44.24, 39.82, 39.38, 32.47, 29.53, 29.49, 28.11, 20.81, 19.93, 18.56, 18.22, 8.78, 8.70.

HRMS (ESI) Calculated for $C_{20}H_{28}NaO_3$ [M+Na]$^+$: 339.1931, found: 339.1936.

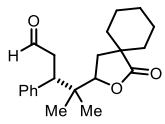

(3*S*)-4-Methyl-4-(1-oxo-2-oxaspiro[4.5]decan-3-yl)-3-phenylpentanal (42d)

Prepared according to the general procedure in section 3.8.3 using 1-(3-methylbut-2-en-1-yl)cyclohexane-1-carboxylic acid (**41d**). The crude mixture was purified by column chromatography (*n*-hexane:EtOAc 85:15, three consecutive purifications) to give product **42d** a as yellow oil (18.1 mg, 55 %, 1:1 dr, average of two runs). The enantiomeric excess was determined by HPLC analysis of the derivatised product according to the procedure in section 3.8.4

^{1}H NMR (400 MHz, $CDCl_3$) 1:1 mixture of diastereoisomers δ 9.51 (dd, *J* = 2.6, 1.2 Hz, 1H), 9.49 (dd, *J* = 2.8, 1.6 Hz, 1H), 7.30 (dd, *J* = 7.9, 6.2 Hz, 4H), 7.25 – 7.19 (m, 6H), 4.22 (dd, *J* = 10.5, 6.3 Hz, 1H), 4.04 (dd, *J* = 10.5, 6.4 Hz, 1H), 3.51 (dd, *J* = 10.0, 5.7 Hz, 1H), 3.35 (dd, *J* = 10.7, 4.4 Hz, 1H), 3.05 (ddd, *J* = 17.0, 10.7, 2.6 Hz, 1H), 2.97 – 2.76 (m, 3H), 2.12 (dd, *J* = 12.9, 6.3 Hz, 1H), 1.97 (dd, *J* = 12.9, 6.5 Hz, 1H), 1.89 – 1.40 (m, 16H), 1.39 – 1.16 (m, 8H), 1.01 (s, 3H), 0.94 (s, 3H), 0.86 (s, 3H), 0.76 (s, 3H).

^{13}C NMR (101 MHz, $CDCl_3$) 1:1 mixture of diastereoisomers δ 201.85, 201.74, 181.32, 181.24, 139.94, 139.53, 129.78, 128.36, 128.31, 127.16, 127.12, 80.47, 80.29, 47.22, 46.28, 44.91, 44.67, 44.51, 44.31, 39.49, 38.96, 34.42, 34.16, 34.11, 31.60, 25.25, 25.15, 21.08, 19.88, 18.53, 18.26.

HRMS (ESI) Calculated for $C_{21}H_{28}NaO_3$ $[M+Na]^+$: 351.1931, found: 351.1924.

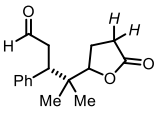

(3*S*)-4-Methyl-4-(5-oxotetrahydrofuran-2-yl)-3-phenylpentanalphenyl pentanal (42e)

Prepared according to the general procedure in section 3.8.3 using 5-methylhex-4-enoic acid (**41e**). The crude mixture was purified by column chromatography (*n*-hexane:EtOAc 60:40, two consecutive purifications) to give product **42e** as yellow oil (14.8 mg, 57%, 1:1 dr, average of two runs). The enantiomeric excess was determined by HPLC analysis of the derivatised product according to the procedure in section 3.8.4

^{1}H NMR (500 MHz, $CDCl_3$) 1:1 mixture of diastereoisomers δ 9.52 (dd, *J* = 2.6, 1.1 Hz, 1H), 9.49 (dd, *J* = 2.9, 1.5 Hz, 1H), 7.30 (t, *J* = 7.1 Hz, 4H), 7.26 – 7.18 (m, 6H), 4.29 (dd, *J* = 8.8, 7.0 Hz, 1H), 4.08 (dd, *J* = 8.8, 7.3 Hz, 1H), 3.52 (dd, *J* = 10.5, 5.0 Hz, 1H), 3.34 (dd, *J* = 10.9, 4.2 Hz, 1H), 3.05 (ddd, *J* = 17.0, 10.9, 2.6 Hz, 1H), 2.95 – 2.89 (m, 1H), 2.86 (dd, *J* = 10.6, 2.9 Hz, 1H), 2.83 (dd, *J* = 5.0, 1.5 Hz, 1H), 2.79 (d, *J* = 5.0 Hz, 1H), 2.54 – 2.44 (m, 3H), 2.16 – 1.92 (m, 4H), 1.04 (s, 3H), 0.96 (s, 3H), 0.87 (s, 3H), 0.79 (s, 3H).

^{13}C NMR (126 MHz, $CDCl_3$) 1:1 mixture of diastereoisomers δ 201.80, 201.72, 176.97 , 176.88, 139.74, 139.42, 129.76, 128.40, 128.36, 127.21, 127.18, 84.09, 83.99, 47.10, 46.09, 44.81, 44.26, 39.88, 39.48, 29.04, 28.85, 23.11, 22.89, 21.01, 19.86, 18.71, 18.14.

HRMS (ESI) Calculated for $C_{16}H_{20}NaO_3$ [M+ Na]$^+$: 283.1305, found: 283.1309.

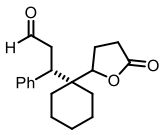

(3*S*)-3-(1-(5-Oxotetrahydrofuran-2-yl)cyclohexyl)-3-phenylpropanal (42f)

Prepared according to the general procedure in section 3.8.3 using 1-(3-methylbut-2-en-1-yl)cyclohexane-1-carboxylic acid (**41f**). The diastereomeric ratio was measured to be 1.24:1 by ^{1}H NMR on the crude mixture. The crude mixture was purified by column chromatography (*n*-hexane:EtOAc 68:32, two consecutive purifications) to give the major diastereoisomer **42f$_{maj}$** as a yellow oil (10 mg, 33%, average of two runs) and the minor diastereoisomer **42f$_{min}$**, with a small amount of the major one, as a yellow oil (8.1 mg, 27%, average of two runs). The enantiomeric excess was determined by HPLC analysis of the derivatised product according to the procedure in section 3.8.4

Major diastereoisomer:

^{1}H NMR (400 MHz, $CDCl_3$) δ 9.56 (dd, *J* = 2.3, 0.7 Hz, 1H), 7.29 (d, *J* = 3.3 Hz, 4H), 7.23 (ddd, *J* = 5.6, 4.4, 2.2 Hz, 1H), 4.38 (dd, *J* = 9.5, 6.8 Hz, 1H), 3.91 (dd, *J* = 11.9, 3.2 Hz, 1H), 3.41 (ddd, *J* = 17.7, 11.9, 2.3 Hz, 1H), 2.83 (dd, *J* = 17.5, 3.1 Hz, 1H), 2.54 – 2.30 (m, 2H), 2.06 (dq, *J* = 12.8, 9.8 Hz, 1H), 1.96 – 1.84 (m, 2H), 1.82 – 1.56 (m, 4H), 1.40 – 1.20 (m, 4H), 1.07 – 0.98 (m, 1H).

^{13}C NMR (101 MHz, $CDCl_3$) δ 202.39, 177.07, 139.71, 129.98, 128.35, 127.00, 83.48, 44.72, 40.68, 40.16, 28.61, 28.34, 26.11, 26.07, 22.83, 20.85, 20.16.

Minor diastereoisomer:

^{1}H NMR (400 MHz, $CDCl_3$) δ 9.51 (dd, *J* = 2.7, 0.8 Hz, 1H), 7.33 – 7.18 (m, 5H), 4.41 (dd, *J* = 10.3, 6.7 Hz, 1H), 3.72 (dd, *J* = 12.1, 3.4 Hz, 1H), 3.08 (ddd, *J* = 16.7, 12.1, 2.8 Hz, 1H), 2.89 – 2.68 (m, 1H), 2.57 – 2.32 (m, 2H), 2.08 (dtd, *J* = 12.1, 6.7, 3.3 Hz, 1H), 1.92 (ddd, *J* = 22.5, 12.6, 10.5 Hz, 1H), 1.76 (dt, *J* = 11.2, 7.0 Hz, 2H), 1.69 – 1.48 (m, 10H).

^{13}C NMR (101 MHz, $CDCl_3$) δ 201.69, 176.51, 139.58, 129.58, 128.45, 127.23, 84.70, 44.49, 42.13, 40.90, 30.42, 29.27, 29.20, 25.60, 23.51, 21.65, 21.02.

HRMS (ESI) Calculated for $C_{19}H_{24}NaO_3$ [M+Na]$^+$: 323.1618, found: 323.1619.

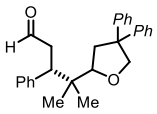

(3*S*)-4-(4,4-Diphenyltetrahydrofuran-2-yl)-4-methyl-3-phenylpentanal (52a)

Prepared according to the general procedure in section 3.8.3 using 5-methyl-2,2-diphenylhex-4-en-1-ol (**41g**) and catalyst A in CH_3CN (0.5 M). The crude mixture was purified by column chromatography (*n*-hexane:EtOAc 96:4, two consecutive purifications) to give product **52a** as colorless oil (16.5 mg, 42%, 1:1 dr, average of two runs). The enantiomeric excess was determined by HPLC analysis of the derivatised product according to the procedure in section 3.8.4

^{1}H NMR (400 MHz, $CDCl_3$) 1:1 mixture of diastereoisomers δ 9.56 – 9.49 (m, 2H), 7.38 – 7.14 (m, 30H), 4.70 (dd, *J* = 12.8, 8.7 Hz, 2H), 4.06 (dd, *J* = 15.0, 8.6 Hz, 2H), 3.88 (dd, *J* = 10.6, 5.5 Hz, 1H), 3.68 (dd, *J* = 10.7, 5.6 Hz, 1H), 3.50 (dd, *J* = 10.2, 5.5 Hz, 1H), 3.37 (dd, *J* = 10.2, 5.2 Hz, 1H), 3.08 – 2.79 (m, 4H), 2.50 (dt, *J* = 18.9, 11.4 Hz, 2H), 2.34 (dd, *J* = 11.9, 5.5 Hz, 1H), 2.18 (dd, *J* = 11.9, 5.5 Hz, 1H), 1.04 (s, 3H), 0.92 (s, 3H), 0.79 (s, 3H), 0.69 (s, 3H).

^{13}C NMR (101 MHz, $CDCl_3$) 1:1 mixture of diastereoisomers δ 203.15, 202.65, 146.46, 146.25, 145.86, 145.83, 140.69, 129.95, 128.46, 128.44, 128.31, 128.18, 127.97, 127.92, 127.22, 127.16, 127.06, 127.00, 126.74, 126.71, 126.52, 126.28, 126.19, 82.86, 82.07, 55.52, 55.44, 47.97, 46.85, 44.99, 44.41, 40.11, 39.84, 39.46, 21.77, 20.62, 19.86, 18.85.

HRMS (ESI) Calculated for $C_{28}H_{30}NaO_2$ [M+ Na]$^+$: 421.2138, found: 421.2122.

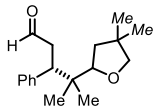

(3*S*)-4-(4,4-Dimethyltetrahydrofuran-2-yl)-4-methyl-3-phenylpentanal (52b)

Prepared according to the general procedure in section 3.8.3 using 2,2,5-trimethylhex-4-en-1-ol (**41h**) and catalyst A in CH_3CN (0.5 M). The crude mixture was purified by column chromatography (*n*-hexane:EtOAc 96:4) to give product **52b** as colorless oil (16.5 mg, 42%, 1:1 dr, average of two runs). The enantiomeric excess was determined by HPLC analysis of the derivatised product according to the procedure in section 3.8.4

^{1}H NMR (500 MHz, $CDCl_3$) 1:1 mixture of diastereoisomers δ 9.51 – 9.42 (m, 2H), 7.28 (d, *J* = 7.9 Hz, 3H), 7.21 (t, *J* = 7.4 Hz, 7H), 3.82 (dd, *J* = 9.6, 7.0 Hz, 1H), 3.66 (dd, *J* = 10.1, 6.7 Hz, 1H), 3.52 – 3.39 (m, 6H), 3.32 (dd, *J* = 9.5, 5.8 Hz, 1H), 2.96 – 2.87 (m, 3H), 2.81 (ddd, *J* = 16.4, 10.8, 3.1 Hz, 1H), 1.56 – 1.47 (m, 2H), 1.44 – 1.38 (m, 1H), 1.09 (s, 3H), 1.07 (d, *J* = 3.9 Hz, 6H), 1.01 (s, 3H), 0.98 (s, 3H), 0.86 (s, 3H), 0.76 (s, 3H), 0.64 (s, 3H).

^{13}C NMR (126 MHz, $CDCl_3$) 1:1 mixture of diastereoisomers δ 203.17, 202.67, 141.05, 140.64, 129.91, 127.96, 127.94, 126.62, 83.72, 83.07, 80.43, 80.32, 47.47, 46.89, 45.04, 44.49, 41.77, 41.56, 39.79, 39.31, 39.18, 39.10, 26.71, 26.59, 26.52, 21.33, 20.41, 19.91, 18.59.

HRMS (ESI) Calculated for $C_{18}H_{26}NaO_3$ [M+ Na]$^+$: 297.1825, found: 297.1821.

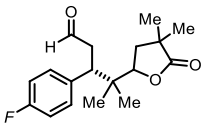

(3*S*)-4-(4,4-Dimethyl-5-oxotetrahydrofuran-2-yl)-3-(4-fluorophenyl)-4-methylpentanal (42g)

Prepared according to the general procedure in section 3.8.3 using 3-(4-fluorophenyl)acrylaldehyde (**6g**), 2,2,5-trimethylhex-4-enoic acid (**41b**). The crude mixture was purified by column chromatography (*n*-hexane:EtOAc 80:20) to give product **42g** as brown oil (17.6 mg, 57%, 1:1 dr, average of two runs). The enantiomeric excess was determined by HPLC analysis of the derivatised product according to the procedure in section 3.8.4

^{1}H NMR (500 MHz, $CDCl_3$) 1:1 mixture of diastereoisomers δ 9.51 (dd, *J* = 2.6, 1.2 Hz, 1H), 9.49 (dd, *J* = 2.9, 1.5 Hz, 1H), 7.30 (dd, *J* = 8.1, 6.6 Hz, 4H), 7.25 – 7.19 (m, 4H), 4.25 (dd, *J* = 9.2, 7.5 Hz, 1H), 4.07 (dd, *J* = 10.7, 6.1 Hz, 1H), 3.50 (dd, *J* = 10.5, 5.0 Hz, 1H), 3.33 (dd, *J* = 10.9, 4.3 Hz, 1H), 3.04 (ddd, *J* = 17.0, 10.9, 2.6 Hz, 1H), 2.95 – 2.80 (m, 3H), 1.94 – 1.84 (m, 3H), 1.76 (dd, *J* = 12.7, 6.1 Hz, 1H), 1.26 (d, *J* = 3.7 Hz, 6H), 1.21 (s, 3H), 1.15 (s, 3H), 1.02 (s, 3H), 0.94 (s, 3H), 0.85 (s, 3H), 0.73 (s, 3H).

^{13}C NMR (126 MHz, $CDCl_3$) 1:1 mixture of diastereoisomers δ 201.85, 201.73, 181.74, 181.64, 139.89, 139.49, 128.36, 128.33, 127.20, 127.15, 80.16, 80.00, 47.16, 46.30, 44.90, 44.29, 40.25, 40.08, 39.33, 38.84, 38.41, 38.16, 24.85, 24.83, 24.63, 24.60, 21.12, 19.92, 18.51, 18.28.

^{19}F NMR (376 MHz, $CDCl_3$) 1:1 mixture of diastereoisomers δ -115.36, -115.51.

HRMS (ESI) Calculated for $C_{18}H_{23}FNaO_3$ $[M+Na]^+$: 329.1523, found: 329.1524.

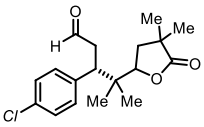

(3*S*)-3-(4-Chlorophenyl)-4-(4,4-dimethyl-5-oxotetrahydro furan-2-yl)-4-methylpentanal (42h)

Prepared according to the general procedure in section 3.8.3 using 3-(4-chlorophenyl)acrylaldehyde (**6h**), 2,2,5-trimethylhex-4-enoic acid (**41b**). The crude mixture was purified by column chromatography (*n*-hexane:EtOAc 78:22) to give product **42h** as brown oil (20.3 mg, 63%, 1:1 dr, average of two runs). The enantiomeric excess was determined by HPLC analysis of the derivatised product according to the procedure in section 3.8.4

^{1}H NMR (400 MHz, $CDCl_3$) 1:1 mixture of diastereoisomers δ 9.53 (dd, *J* = 2.4, 1.0 Hz, 1H), 9.50 (t, *J* = 2.0 Hz, 1H), 7.28 (d, *J* = 8.6 Hz, 4H), 7.20 – 7.13 (m, 4H), 4.22 (dd, *J* = 9.9, 6.9 Hz, 1H), 4.01 (dd, *J* = 10.6, 6.2 Hz, 1H), 3.50 (dd, *J* = 8.8, 6.7 Hz, 1H), 3.33 (dd, *J* = 10.5, 4.5 Hz, 1H), 3.03 (ddd, *J* = 17.3, 10.6, 2.4 Hz, 1H), 2.94 (ddd, *J* = 17.2, 4.5, 1.0 Hz, 1H), 2.87 – 2.83 (m, 2H), 1.88 (ddd, *J* = 12.7, 10.3, 4.1 Hz, 3H), 1.77 (dd, *J* = 12.7, 6.2 Hz, 1H), 1.26 (d, *J* = 3.7 Hz, 6H), 1.22 (s, 3H), 1.16 (s, 3H), 1.00 (s, 3H), 0.93 (s, 3H), 0.82 (s, 3H), 0.72 (s, 3H).

^{13}C NMR (101 MHz, $CDCl_3$) 1:1 mixture of diastereoisomers δ 201.21, 201.01, 181.56, 181.45, 138.47, 138.09, 133.07, 132.99, 130.98, 128.53, 128.48, 79.96, 79.65, 46.68, 45.64, 44.95, 44.31, 40.21, 40.02, 39.32, 38.73, 38.40, 38.15, 24.84, 24.82, 24.68, 24.61, 21.21, 19.85, 18.33, 18.25.

HRMS (ESI) Calculated for $C_{18}H_{23}ClNaO_3$ $[M+Na]^+$: 345.1228, found: 345.1227.

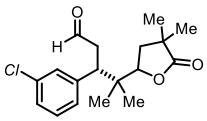

(3*S*)-3-(3-Chlorophenyl)-4-(4,4-dimethyl-5-oxotetrahydrofuran-2-yl)-4-methylpentanal (42i)

Prepared according to the general procedure in section 3.8.3 using 3-(3-chlorophenyl)acrylaldehyde (**6i**), 2,2,5-trimethylhex-4-enoic acid (**41b**). The crude mixture was purified by column chromatography (*n*-hexane:EtOAc 75:25, two consecutive purifications) to give product **42i** as brown oil (20.3 mg, 63%, 1:1 dr, average of two runs). The enantiomeric excess was determined by HPLC analysis of the derivatised product according to the procedure in section 3.8.4

^{1}H NMR (300 MHz, $CDCl_3$) 1:1 mixture of diastereoisomers δ 9.55 (dd, *J* = 2.2, 1.2 Hz, 1H), 9.53 (t, *J* = 1.9 Hz, 1H), 7.26 – 7.18 (m, 7H), 7.18 – 7.06 (m, 3H), 4.24 (dd, *J* = 9.1, 7.5 Hz, 1H), 4.05 (dd, *J* = 10.4, 6.3 Hz, 1H), 3.49 (dd, *J* = 8.5, 6.8 Hz, 1H), 3.34 (dd, *J* = 10.2, 4.7 Hz, 1H), 3.12 – 2.90 (m, 2H), 2.91 – 2.82 (m, 2H), 1.96 – 1.73 (m, 3H), 1.26 (t, *J* = 3.3 Hz, 3H), 1.23 (s, 3H), 1.17 (s, 3H), 1.01 (s, 3H), 0.93 (s, 3H), 0.84 (s, 3H), 0.74 (s, 3H).

^{13}C NMR (75 MHz, $CDCl_3$) 1:1 mixture of diastereoisomers δ 201.09, 200.88, 181.55, 181.44, 142.23, 141.93, 134.29, 129.58, 129.54, 127.45, 127.37, 80.11, 79.70, 46.85, 46.01, 44.88, 44.35, 40.21, 40.06, 39.36, 38.77, 38.40, 38.18, 24.83, 24.81, 24.65, 24.60, 21.18, 19.92, 18.50, 18.34.

HRMS (ESI) Calculated for $C_{18}H_{23}ClNaO_3$ $[M+Na]^+$: 345.1228, found: 345.1230.

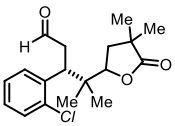

(3*R*)-3-(2-Chlorophenyl)-4-(4,4-dimethyl-5-oxotetrahydrofuran-2-yl)-4-methylpentanal (42j)

Prepared according to the general procedure in section 3.8.3 using 3-(2-chlorophenyl)acrylaldehyde (**6j**), 2,2,5-trimethylhex-4-enoic acid (**41b**). The crude mixture was purified by column chromatography (*n*-hexane:EtOAc 70:30) to give product 3j as brown oil (24.2 mg, 75%, 1:1 dr, average of two runs, 91% ee_A and 93% ee_B). The enantiomeric excess was determined by HPLC analysis of the derivatised product according to the procedure in section 3.8.4

^{1}H NMR (400 MHz, $CDCl_3$) 1:1 mixture of diastereoisomers δ 9.50 (dd, *J* = 2.6, 1.0 Hz, 1H), 9.48 (t, *J* = 1.9 Hz, 1H), 7.39 (ddd, *J* = 7.9, 2.7, 1.3 Hz, 2H), 7.30 – 7.21 (m, 3H), 7.20 – 7.13 (m, 2H),

4.42 – 4.34 (m, 2H), 4.20 – 4.04 (m, 2H), 3.05 – 2.83 (m, 4H), 2.01 – 1.85 (m, 4H), 1.27 (dd, *J* = 10.9, 5.4 Hz, 16H), 1.06 (s, 3H), 0.94 (s, 3H), 0.90 (s, 3H), 0.72 (s, 3H).

^{13}C NMR (101 MHz, $CDCl_3$) 1:1 mixture of diastereoisomers δ 201.32, 200.78, 181.66, 181.46, 138.23, 138.19, 135.78, 135.71, 130.10, 129.97, 129.72, 129.48, 128.18, 128.12, 126.82, 126.76, 82.42, 80.07, 45.93, 45.46, 41.40, 41.02, 40.20, 40.15, 40.01, 39.69, 38.72, 38.54, 24.88, 24.79, 24.58, 24.42, 21.23, 19.69, 19.32, 18.43.

HRMS (ESI) Calculated for $C_{18}H_{23}ClNaO_3$ [M+Na]$^+$: 345.1228, found: 345.1230.

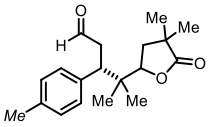

(3*S*)-4-(4,4-Dimethyl-5-oxotetrahydrofuran-2-yl)-4-methyl-3-(p-tolyl)pentanal (42k)

Prepared according to the general procedure in section 3.8.3 using 3-(*p*-tolyl)acrylaldehyde (**6k**), 2,2,5-trimethylhex-4-enoic acid (**41b**). The crude mixture was purified by column chromatography (*n*-hexane:EtOAc 70:30, two consecutive purifications) to give product **42k** as pale yellow oil (19.7 mg, 66%, 1:1 dr, average of two runs). The enantiomeric excess was determined by HPLC analysis of the derivatised product according to the procedure in section 3.8.4

^{1}H NMR (400 MHz, $CDCl_3$) 1:1 mixture of diastereoisomers δ 9.50 (dd, *J* = 2.7, 1.2 Hz, 1H), 9.47 (dd, *J* = 3.0, 1.5 Hz, 1H), 7.11 – 7.08 (m, 8H), 4.28 – 4.22 (m, 1H), 4.10 (dd, *J* = 10.7, 6.1 Hz, 1H), 3.46 (dd, *J* = 10.6, 5.1 Hz, 1H), 3.28 (dd, *J* = 11.0, 4.3 Hz, 1H), 3.02 (ddd, *J* = 16.8, 11.0, 2.7 Hz, 1H), 2.92 – 2.76 (m, 3H), 2.31 (s, 6H), 1.93 – 1.82 (m, 3H), 1.76 (dd, *J* = 12.7, 6.2 Hz, 1H), 1.26 (d, *J* = 2.3 Hz, 6H), 1.21 (s, 3H), 1.16 (s, 3H), 1.01 (s, 3H), 0.94 (s, 3H), 0.84 (s, 3H), 0.72 (s, 3H).

^{13}C NMR (101 MHz, $CDCl_3$) 1:1 mixture of diastereoisomers δ 202.00, 201.91, 181.74, 181.65, 136.78, 136.75, 136.66, 136.22, 129.59, 129.04, 129.02, 80.14, 80.05, 46.82, 45.91, 44.86, 44.22, 40.26, 40.07, 39.28, 38.83, 38.42, 38.15, 24.85, 24.67, 24.61, 21.09, 20.99, 20.97, 19.90, 18.53, 18.21.

HRMS (ESI) Calculated for $C_{19}H_{26}NaO_3$ [M+Na]$^+$: 325.1774, found: 325.1775.

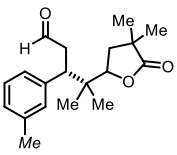

(3*S*)-4-(4,4-Dimethyl-5-oxotetrahydrofuran-2-yl)-4-methyl-3-(m-tolyl)pentanal (42l)

Prepared according to the general procedure in section 3.8.3 using 3-(*m*-tolyl)acrylaldehyde (**6l**), 2,2,5-trimethylhex-4-enoic acid (**41b**). The crude mixture was purified by column chromatography (*n*-hexane:EtOAc 80:20) to give product **42l** as brown oil (22.7 mg, 75%, 1:1 dr, average of two runs). The

enantiomeric excess was determined by HPLC analysis of the derivatised product according to the procedure in section 3.8.4

^{1}H NMR (400 MHz, $CDCl_3$) 1:1 mixture of diastereoisomers δ 9.51 (dd, *J* = 2.5, 1.2 Hz, 1H), 9.48 (dd, *J* = 2.9, 1.5 Hz, 1H), 7.18 (t, *J* = 7.8 Hz, 2H), 7.03 (dd, *J* = 11.9, 6.1 Hz, 6H), 4.26 (t, *J* = 8.4 Hz, 1H), 4.11 (dd, *J* = 10.6, 6.2 Hz, 1H), 3.45 (dd, *J* = 10.5, 5.1 Hz, 1H), 3.29 (dd, *J* = 10.9, 4.3 Hz, 1H), 3.02 (ddd, *J* = 16.9, 10.9, 2.6 Hz, 1H), 2.93 – 2.76 (m, 3H), 2.32 (s, 6H), 1.93 – 1.83 (m, 3H), 1.76 (dd, *J* = 12.7, 6.2 Hz, 1H), 1.26 (s, 6H), 1.21 (s, 3H), 1.16 (s, 3H), 1.01 (s, 3H), 0.94 (s, 3H), 0.85 (s, 3H), 0.73 (s, 3H).

^{13}C NMR (101 MHz, $CDCl_3$) 1:1 mixture of diastereoisomers δ 201.98, 201.88, 181.71, 181.63, 139.79, 139.39, 137.89, 137.86, 130.55, 128.18, 128.16, 127.92, 127.87, 126.70, 80.23, 80.09, 47.05, 46.26, 44.83, 44.25, 40.26, 40.08, 39.27, 38.80, 38.42, 38.16, 24.82, 24.64, 24.58, 21.52, 21.16, 19.92, 18.57, 18.36.

HRMS (ESI) Calculated for $C_{19}H_{26}NaO_3$ $[M+Na]^+$: 325.1774, found: 325.1767.

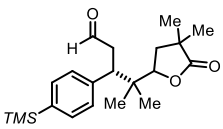

(3*S*)-4-(4,4-Dimethyl-5-oxotetrahydrofuran-2-yl)-4-methyl-3-(4-trimethylsilyl)phenyl)pentanal (42m)

Prepared according to the general procedure in section 3.8.3 using 3-(4-(trimethylsilyl)phenyl)acrylaldehyde (**6m**), 2,2,5-trimethylhex-4-enoic acid (**41b**). The crude mixture was purified by column chromatography (*n*-hexane:EtOAc 85:15) to give product **42m** as pale yellow oil (21.9 mg, 61%, 1:1 dr, average of two runs). The enantiomeric excess was determined by HPLC analysis of the derivatised product according to the procedure in section 3.8.4

^{1}H NMR (500 MHz, $CDCl_3$) 1:1 mixture of diastereoisomers δ 9.51 (dd, *J* = 2.6, 1.2 Hz, 1H), 9.48 (dd, *J* = 2.8, 1.5 Hz, 1H), 7.43 (d, *J* = 8.1 Hz, 4H), 7.19 (dd, *J* = 11.6, 8.0 Hz, 4H), 4.27 (t, *J* = 8.3 Hz, 1H), 4.11 (dd, *J* = 10.7, 6.2 Hz, 1H), 3.49 (dd, *J* = 10.5, 5.0 Hz, 1H), 3.32 (dd, *J* = 10.8, 4.3 Hz, 1H), 3.04 (ddd, *J* = 17.0, 10.7, 2.6 Hz, 1H), 2.95 – 2.77 (m, 3H), 1.88 (dd, *J* = 21.8, 9.4 Hz, 3H), 1.78 (dd, *J* = 12.7, 6.2 Hz, 1H), 1.26 (s, 6H), 1.23 (s, 3H), 1.17 (s, 3H), 1.01 (s, 3H), 0.95 (s, 3H), 0.85 (s, 3H), 0.73 (s, 3H), 0.25 (s, 18H).

^{13}C NMR (126 MHz, $CDCl_3$) 1:1 mixture of diastereoisomers δ 202.28, 202.17, 182.09, 181.98, 140.70, 140.28, 139.56, 139.51, 133.66, 133.68, 129.48, 80.56, 80.39, 47.42, 46.62, 45.20, 44.61, 40.60, 40.43, 39.74, 39.26, 38.77, 38.50, 25.22, 25.06, 25.01, 21.50, 20.29, 18.85, 18.73, -0.76.

HRMS (ESI) Calculated for $C_{21}H_{32}NaO_3Si$ $[M+Na]^+$: 383.2013, found: 383.2002.

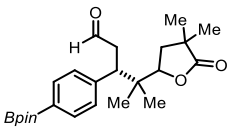

(3*S*)-4-(4,4-Dimethyl-5-oxotetrahydrofuran-2-yl)-4-methyl-3-(4-(4,4,5,5-tetramethyl-1,3,2-dioxaborolan-2-yl)phenyl)pentanal (42n)

Prepared according to the general procedure in section 3.8.3 using (*E*)-3-(4-(4,4,5,5-tetramethyl-1,3,2-dioxaborolan-2-yl)phenyl)acrylaldehyde (**6n**), 2,2,5-trimethylhex-4-enoic acid (**41b**). The crude mixture was purified by column chromatography (*n*-hexane:EtOAc 75:25, two consecutive purifications) to give product **42m** as colorless oil (14.2 mg, 34%, 1:1 dr, average of two runs). The enantiomeric excess was determined by HPLC analysis of the derivatised product according to the procedure in section 3.8.4

^{1}H NMR (500 MHz, $CDCl_3$) 1:1 mixture of diastereoisomers δ 9.51 (dd, *J* = 2.4, 1.2 Hz, 1H), 9.48 (dd, *J* = 2.8, 1.5 Hz, 1H), 7.74 (dd, *J* = 8.2, 1.1 Hz, 4H), 7.23 (dd, *J* = 10.9, 8.1 Hz, 4H), 4.23 (dd, *J* = 9.9, 6.8 Hz, 1H), 4.07 (dd, *J* = 10.7, 6.1 Hz, 1H), 3.52 (dd, *J* = 10.7, 4.9 Hz, 1H), 3.33 (dd, *J* = 10.9, 4.2 Hz, 1H), 3.07 (ddd, *J* = 17.1, 10.9, 2.4 Hz, 1H), 2.96 – 2.80 (m, 3H), 1.92 – 1.81 (m, 3H), 1.74 (dd, *J* = 12.7, 6.1 Hz, 1H), 1.33 (s, 24H), 1.26 (d, *J* = 5.2 Hz, 7H), 1.20 (s, 3H), 1.15 (s, 3H), 1.01 (s, 3H), 0.94 (s, 3H), 0.83 (s, 3H), 0.72 (s, 3H).

^{13}C NMR (126 MHz, $CDCl_3$) 1:1 mixture of diastereoisomers δ 201.98, 201.87, 182.04, 181.93, 143.53, 143.14, 135.11, 135.10, 84.22, 80.46, 80.28, 47.76, 46.80, 45.19, 44.54, 40.60, 40.41, 39.74, 39.22, 38.77, 38.53, 30.06, 25.26, 25.23, 25.21, 25.18, 25.01, 24.96, 21.51, 20.33, 18.86, 18.63.

HRMS (ESI) Calculated for $C_{25}H_{39}NaO_6B$ $[M+MeOH+Na]^+$: 468.2768, found: 468.2770.

3.8.7. Characterization of Enoate Derivatives

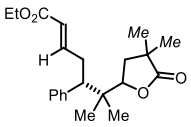

Ethyl (5*S*,*E*)-6-(4,4-dimethyl-5-oxotetrahydrofuran-2-yl)-6-methyl-5-phenylhept-2-enoate (42b')

Prepared according to the general procedure discussed in section 3.8.4 using **42b** (1.0 equiv., 0.072 mmol, 21 mg), ethyl 2-(triphenyl-λ^5-phosphanylidene)acetate (1.2 equiv., 0.086 mmol, 29 mg) and ammonium formate (4 mg). The crude mixture was purified by column chromatography (*n*-hexane:EtOAc 80:20) to give product **42b'**as a yellow oil (18.3 mg, 71%, 1:1 dr, average of two runs, 89% ee_A and 92% ee_B). The enantiomeric excess was determined by HPLC analysis on a Daicel Chiralpak IC-3 column (5:95 ^{i}PrOH:*n*-hexane, 1.0 mL/min, 30 ^{o}C, λ = 230 nm). *Diastereosiomer A*: τ_{Major} = 87.0 min, τ_{Minor} = 71.5 min. *Diastereoisomer B*: τ_{Major} = 82.2 min, τ_{Minor} = 76.0 min. $[\alpha]_D^{26}$ = -12.37 (c = 0.26, $CHCl_3$, 1:1 dr, 89% ee_A and 92% ee_B). Absolute configuration determined in comparison to compound **42a**.

^{1}H NMR (400 MHz, $CDCl_3$) 1:1 mixture of diastereoisomers δ 7.28 (t, *J* = 7.3 Hz, 4H), 7.24 – 7.12 (m, 6H), 6.67 – 6.56 (m, 2H), 5.73 – 5.65 (m, 2H), 4.31 – 4.23 (m, 1H), 4.07 (qd, *J* = 7.1, 2.7 Hz, 5H), 2.94 (dd, *J* = 8.8, 6.6 Hz, 1H), 2.70 – 2.63 (m, 5H), 2.14 – 1.87 (m, 4H), 1.25 (d, *J* = 2.1 Hz, 6H), 1.23 – 1.17 (m, 9H), 1.13 (s, 3H), 1.05 (s, 3H), 0.94 (s, 3H), 0.87 (s, 3H), 0.73 (s, 3H).

^{13}C NMR (101 MHz, $CDCl_3$) 1:1 mixture of diastereoisomers δ 177.02, 176.92, 166.30, 166.24, 147.67, 147.50, 139.66, 139.49, 129.72, 128.22, 128.19, 126.96, 126.89, 122.50, 122.46, 84.45, 84.33, 60.08, 60.05, 52.49, 51.27, 40.18, 39.97, 32.73, 32.36, 29.08, 28.93, 20.82, 20.00, 19.25, 17.81, 14.17.

HRMS (ESI) Calculated for $C_{22}H_{30}NaO_4$ $[M+Na]^+$: 381.2036, found: 381.2018.

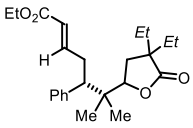

Ethyl (5*S*,*E*)-6-(4,4-diethyl-5-oxotetrahydrofuran-2-yl)-6-methyl-5-phenyl hept-2-enoate (42c')

Prepared according to the general procedure in section 3.8.4 using **42c** (1.0 equiv., 0.059 mmol, 18.7 mg), ethyl 2-(triphenyl- λ^5-phosphanylidene)acetate (1.2 equiv., 0.071 mmol, 24.7 mg) and ammonium formate (4 mg). The crude mixture was purified by column chromatography (*n*hexane:EtOAc 84:16) to give product **42c'** as a yellow oil (20.0 mg, 88%, 1:1 dr, average of two runs, 94% ee_A and 95% ee_B). The enantiomeric excess was determined by HPLC analysis on a Daicel Chiralpak IC-3 column (10:90 ^{i}PrOH:*n*-hexane, 1.0 mL/min, 30 °C, λ = 230 nm). *Diastereosiomer A*: τ_{Major} = 34.2 min, τ_{Minor} = 26.7 min. *Diastereoisomer B*: τ_{Major} = 30.6 min, τ_{Minor} = 29.0 min. $[\alpha]_D^{26}$ = -11.51 (c = 0.18, $CHCl_3$, 1:1 dr, 94% ee_A and 95% ee_B). Absolute configuration determined in comparison to compound **42a**.

^{1}H NMR (400 MHz, $CDCl_3$) 1:1 mixture of diastereoisomers δ 7.29 (ddd, *J* = 8.3, 4.8, 2.9 Hz, 4H), 7.25 – 7.13 (m, 6H), 6.68 – 6.56 (m, 2H), 5.74 – 5.65 (m, 2H), 4.18 (dd, *J* = 10.3, 6.7 Hz, 1H), 4.11 – 3.98 (m, 5H), 2.93 (q, *J* = 7.9 Hz, 1H), 2.78 – 2.62 (m, 5H), 1.99 (ddd, *J* = 21.2, 13.0, 10.4 Hz, 2H), 1.81 (dd, *J* = 13.0, 6.7 Hz, 1H), 1.67 – 1.46 (m, 10H), 1.20 (td, *J* = 7.1, 1.9 Hz, 6H), 1.06 (s, 3H), 0.96 (s, 3H), 0.93 – 0.86 (m, 12H), 0.84 (t, *J* = 7.5 Hz, 3H), 0.74 (s, 3H).

^{13}C NMR (101 MHz, $CDCl_3$) 1:1 mixture of diastereoisomers δ 180.78, 180.68, 166.35, 166.29, 147.85, 147.66, 139.83, 139.52, 128.31, 128.18, 128.12, 126.94, 126.88, 122.46, 122.41, 80.70, 80.54, 60.10, 60.06, 52.55, 51.34, 48.46, 48.38, 40.12, 39.86, 32.81, 32.57, 32.36, 32.29, 29.55, 29.51, 28.15, 28.01, 20.67, 20.14, 19.19, 17.88, 14.18, 8.79, 8.71.

HRMS (ESI) Calculated for $C_{24}H_{34}NaO_4$ $[M+Na]^+$: 409.2349, found: 409.2340.

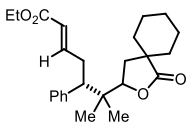

Ethyl (5*S*,*E*)-6-methyl-6-(1-oxo-2-oxaspiro[4.5]decan-3-yl)-5-phenylhept-2-enoate (42d')

Prepared according to the general procedure in in section 3.8.4 using **42d** (1.0 equiv., 0.031 mmol, 10.2 mg), ethyl 2-(triphenyl- λ^5-phosphanylidene)acetate (1.2 equiv., 0.037 mmol, 24.7 mg) and ammonium formate (4 mg). The crude mixture was purified by column chromatography (*n*-hexane:EtOAc 85:15) to give product **42d'** as a yellow oil (6.0 mg, 15%, 1:1 dr, average of two runs, 95% ee_A and 94% ee_B). The enantiomeric excess was determined by HPLC analysis on a Daicel Chiralpak IC-3 column (7:93 ^{i}PrOH:*n*-hexane, 1.0 mL/min, 30 ^{o}C, λ = 215 nm). *Diastereosiomer A*: τ_{Major} = 74.0 min, τ_{Minor} = 55.7 min. *Diastereoisomer B*: τ_{Major} = 66.4 min, τ_{Minor} = 59.4 min. $[\alpha]_D^{26}$ = -15.13 (c = 0.10, $CHCl_3$, 1:1 dr, 95% ee_A and 94% ee_B). Absolute configuration determined in comparison to compound **42a**.

^{1}H NMR (400 MHz, $CDCl_3$) 1:1 mixture of diastereoisomers δ 7.33 – 7.26 (m, 4H), 7.25 – 7.11 (m, 6H), 6.67 – 6.56 (m, 2H), 5.74 – 5.64 (m, 2H), 4.24 (dd, *J* = 10.5, 6.4 Hz, 1H), 4.07 (qd, *J* = 7.1, 3.0 Hz, 4H), 4.02 (dd, *J* = 10.5, 6.5 Hz, 1H), 2.96 (dd, *J* = 9.0, 6.3 Hz, 1H), 2.82 – 2.63 (m, 5H), 2.11 (dd, *J* = 12.9, 6.4 Hz, 1H), 1.93 (dd, *J* = 12.9, 6.5 Hz, 1H), 1.87 – 1.24 (m, 23H), 1.20 (td, *J* = 7.1, 2.4 Hz, 6H), 1.05 (s, 3H), 0.94 (s, 3H), 0.88 (s, 3H), 0.76 (s, 3H).

^{13}C NMR (101 MHz, $CDCl_3$) 1:1 mixture of diastereoisomers δ 181.44, 181.35, 166.33, 166.27, 147.84, 147.62, 139.86, 129.77, 128.18, 126.91, 126.86, 122.47, 122.40, 80.80, 80.60, 60.08, 60.03, 52.64, 51.36, 44.70, 44.58, 39.78, 39.42, 34.37, 34.15, 34.11, 34.03, 32.80, 32.37, 31.61, 31.59, 25.29, 25.26, 22.16, 22.13, 22.09, 20.92, 20.05, 19.13, 17.89, 14.18.

HRMS (ESI) Calculated for $C_{25}H_{34}NaO_4$ $[M+Na]^+$: 421.2349, found: 421.2338.

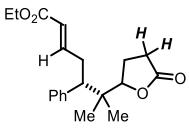

Ethyl (5*S*,*E*)-6-methyl-6-(5-oxotetrahydrofuran-2-yl)-5-phenylhept-2-enoate (42e')

Prepared according to the general procedure in section 3.8.4 using **42e** (1.0 equiv., 0.055 mmol, 14.5 mg), ethyl 2-(triphenyl- λ^5-phosphanylidene)acetate (1.2 equiv., 0.066 mmol, 22.5 mg) and ammonium formate (4 mg). The crude mixture was purified by column chromatography (*n*-hexane:EtOAc 62:38) to give product **42e'**as a yellow oil (5.0 mg, 28%, 1:1 dr, average of two runs, 95% ee_A and 95% ee_B). The enantiomeric excess was determined by HPLC analysis on a Daicel Chiralpak ID-3 column (25:75 ^{i}PrOH:*n*-hexane 1.2 mL/min, 30 ^{o}C, λ = 230 nm). *Diastereosiomer A*: τ_{Major} = 13.4 min, τ_{Minor} = 11.7 min. *Diastereoisomer B*: τ_{Major} = 39.6 min, τ_{Minor} = 15.6 min. $[\alpha]_D^{26}$ = -49.5 (c = 0.10, $CHCl_3$, 1:1 dr, 95% ee_A and 95% ee_B). Absolute configuration determined in comparison to compound **42a**.

^{1}H NMR (400 MHz, $CDCl_3$) 1:1 mixture of diastereoisomers δ 7.34 – 7.26 (m, 4H), 7.25 – 7.07 (m, 6H), 6.61 (dq, *J* = 14.4, 7.3 Hz, 2H), 5.69 (dd, *J* = 15.6, 3.6 Hz, 2H), 4.30 (dd, *J* = 8.7, 7.0 Hz, 1H), 4.07 (qd, *J* = 7.1, 2.4 Hz, 5H), 2.96 (dd, *J* = 9.3, 6.0 Hz, 1H), 2.80 – 2.62 (m, 5H), 2.55 – 2.42 (m, 4H), 2.15 – 1.87 (m, 4H), 1.20 (td, *J* = 7.1, 1.7 Hz, 6H), 1.07 (s, 3H), 0.96 (s, 3H), 0.90 (s, 3H), 0.79 (s, 3H).

^{13}C NMR (101 MHz, $CDCl_3$) 1:1 mixture of diastereoisomers δ 177.03, 176.93, 166.31, 166.24, 147.68, 147.51, 139.66, 139.49, 128.22, 128.20, 126.96, 126.89, 122.50, 122.46, 84.46, 84.33, 60.08, 60.05, 52.48, 51.27, 40.18, 39.97, 32.73, 32.36, 29.08, 28.93, 23.04, 22.79, 20.82, 20.00, 19.24, 17.80, 14.17.

HRMS (ESI) Calculated for $C_{20}H_{26}NaO_4$ $[M+Na]^+$: 353.1723, found: 353.1719.

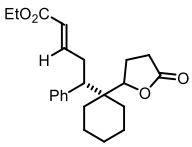

Ethyl (5*S*,*E*)-6-methyl-6-(5-oxotetrahydrofuran-2-yl)-5-phenylhept-2-enoate (42f')

Major diastereoisomer: Prepared according to the general procedure in section 3.8.4 using **42f$_{maj}$** (1.0 equiv., 0.027 mmol, 8.0 mg), ethyl 2-(triphenyl-λ^5-phosphanylidene)acetate (1.2 equiv., 0.037 mmol, 24.7 mg) and ammonium formate (4 mg). The crude mixture was purified by column chromatography (*n*-hexane:EtOAc 70:30) to give product **42f$_{maj}$'** as a yellow oil (8.9 mg, 89%, 1:1 dr, average of two runs, 90% ee). The enantiomeric excess was determined by HPLC analysis on a Daicel Chiralpak ID-3 column (10:90 ^{i}PrOH:*n*-hexane 1.0 mL/min, 30 ^{o}C, λ = 215 nm). τ_{Major} = 59.7 min, τ_{Minor} = 43.4 min. $[\alpha]_D^{26}$ = -100.7 (c = 0.03, $CHCl_3$, 90% ee). Absolute configuration determined in comparison to compound **42a**.

^{1}H NMR (500 MHz, $CDCl_3$) 1:1 mixture of diastereoisomers δ 7.31 (t, *J* = 7.4 Hz, 2H), 7.24 (t, *J* = 7.3 Hz, 3H), 7.18 (d, *J* = 7.2 Hz, 1H), 6.64 (dt, *J* = 15.4, 7.1 Hz, 1H), 5.72 (d, *J* = 15.6 Hz, 1H), 4.43 (dd, *J* = 10.0, 6.7 Hz, 1H), 4.11 (q, *J* = 7.1 Hz, 2H), 3.19 (dd, *J* = 8.8, 6.6 Hz, 1H), 2.75 – 2.69 (m, 2H), 2.57 – 2.40 (m, 2H), 2.16 (dddd, *J* = 12.4, 9.4, 6.7, 2.8 Hz, 1H), 2.12 – 1.98 (m, 1H), 1.78 – 1.68 (m, 2H), 1.68 – 1.37 (m, 8H), 1.23 (t, *J* = 7.2 Hz, 3H).

^{13}C NMR (126 MHz, $CDCl_3$) 1:1 mixture of diastereoisomers δ 176.56, 166.29, 147.85, 139.42, 128.29, 126.99, 122.45, 84.80, 60.14, 47.16, 41.45, 32.69, 30.42, 29.28, 28.64, 25.67, 23.64, 21.65, 21.03, 14.18.

HRMS (ESI) Calculated for $C_{23}H_{30}NaO_4$ $[M+Na]^+$: 393.2036, found: 393.2045.

Minor diastereoisomer: Prepared according to the general procedure in section 3.8.4 using **42f$_{min}$** (1.0 equiv., 0.020 mmol, 6 mg), ethyl 2-(triphenyl-λ^5-phosphanylidene)acetate (1.2 equiv., 0.037 mmol, 24.7 mg) and ammonium formate (4 mg) The crude mixture was purified by column chromatography (*n*-hexane:EtOAc

70:30) to give product **42f$_{min}$'** as a yellow oil (6.6 mg, 89%, 1:1 dr, average of two runs, 97% ee). The enantiomeric excess was determined by HPLC analysis on a Daicel Chiralpak ID-3 column (10:90 ^{i}PrOH:*n*-hexane 1.0 mL/min, 30 °C, λ = 215 nm). τ_{Major} = 44.9 min, τ_{Minor} = 37.2 min. $[\alpha]_D^{24}$ = -17.5 (c = 0.01, $CHCl_3$, 97% ee). Absolute configuration determined in comparison to compound **42a**.

^{1}H NMR (400 MHz, $CDCl_3$) 1:1 mixture of diastereoisomers δ 7.29 (d, *J* = 7.0 Hz, 2H), 7.25 – 7.19 (m, 1H), 7.18 – 7.14 (m, 1H), 6.61 (dt, *J* = 15.6, 7.0 Hz, 1H), 5.69 (d, *J* = 15.6 Hz, 1H), 4.40 (dd, *J* = 10.0, 6.7 Hz, 1H), 4.08 (q, *J* = 7.1 Hz, 2H), 3.17 (p, *J* = 7.9 Hz, 1H), 2.75 – 2.66 (m, 2H), 2.56 – 2.33 (m, 2H), 2.14 (dddd, *J* = 12.5, 9.5, 6.8, 3.0 Hz, 1H), 1.72 (dd, *J* = 9.7, 3.6 Hz, 2H), 1.64 – 1.49 (m, 10H), 1.21 (t, *J* = 7.1 Hz, 3H).

^{13}C NMR (101 MHz, $CDCl_3$) 1:1 mixture of diastereoisomers δ 166.30, 147.87, 128.30, 126.99, 122.45, 84.80, 60.15, 41.45, 32.68, 30.42, 29.29, 28.62, 25.67, 23.63, 21.02, 14.18.

HRMS (ESI) Calculated for $C_{23}H_{30}NaO_4$ $[M+Na]^+$: 393.2036, found: 393.2045.

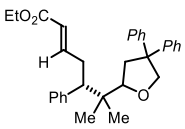

Ethyl (5*S*,*E*)-6-(4,4-diphenyltetrahydrofuran-2-yl)-6-methyl-5-phenylhept-2-enoate (52a')

Prepared according to the general procedure in section 3.8.4 using **52a** (1.0 equiv., 0.030 mmol, 12.0 mg), ethyl 2-(triphenyl- λ^5-phosphanylidene)acetate (1.2 equiv., 0.036 mmol, 12.6 mg) and ammonium formate (4 mg). The crude mixture was purified by column chromatography (*n*-hexane:ethyl acetate 92:8) to give product **52a'** as a yellow oil (5.6 mg, 40%, 1:1 dr, average of two runs, 93% ee_A and 91% ee_B). The enantiomeric excess was determined by UPC² analysis on a Daicel Chiralpak AMY1 column (gradient ^{i}PrOH:CO_2 from 100%CO_2 to 40%^{i}PrOH over 9 minutes, curve 6, 2.0 mL/min, λ = 220 nm). *Diastereosiomer A*: τ_{Major} = 3.93 min, τ_{Minor} = 4.23 min. *Diastereoisomer B*: τ_{Major} = 4.00 min, τ_{Minor} = 4.57 min. $[\alpha]_D^{26}$ = -3.84 (c = 0.23, $CHCl_3$, 1:1 dr, 93% ee_A and 91% ee_B). Absolute configuration determined in comparison to compound **42a**.

^{1}H NMR (500 MHz, $CDCl_3$) 1:1 mixture of diastereoisomers δ 7.31 – 7.25 (m, 7H), 7.24 – 7.09 (m, 23H), 6.64 (dtd, *J* = 15.8, 7.1, 2.3 Hz, 2H), 5.66 (dd, *J* = 15.6, 5.5 Hz, 2H), 4.64 (dd, *J* = 23.5, 8.5 Hz, 2H), 4.06 (dd, *J* = 7.1, 5.2 Hz, 4H), 4.01 (dd, *J* = 24.5, 8.6 Hz, 2H), 3.89 (dd, *J* = 10.6, 5.5 Hz, 1H), 3.63 (dd, *J* = 10.7, 5.6 Hz, 1H), 2.91 (dd, *J* = 11.6, 3.8 Hz, 1H), 2.82 (dd, *J* = 11.7, 3.4 Hz, 1H), 2.78 – 2.55 (m, 4H), 2.44 (dt, *J* = 22.4, 11.4 Hz, 2H), 2.32 (dd, *J* = 12.1, 5.1 Hz, 1H), 2.12 (dd, *J* = 11.6, 5.4 Hz, 1H), 1.19 (td, *J* = 7.1, 0.8 Hz, 6H), 1.03 (s, 3H), 0.85 (s, 3H), 0.77 (s, 3H), 0.65 (s, 3H).

^{13}C NMR (101 MHz, $CDCl_3$) 1:1 mixture of diastereoisomers δ 166.53, 166.46, 149.00, 148.58, 146.52, 146.34, 145.94, 140.88, 140.33, 128.43, 128.40, 128.27, 128.15, 127.78, 127.72, 127.21, 127.16, 127.05, 127.02, 126.46, 126.40, 126.20, 126.12, 122.05, 121.90, 83.06, 82.40, 60.00, 55.57, 55.51, 52.83, 51.92, 40.44, 39.95, 39.77, 39.43, 32.97, 32.32, 21.44, 20.87, 19.58, 19.43, 14.19.

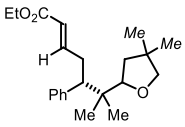

Ethyl (5*S*,*E*)-6-(4,4-dimethyltetrahydrofuran-2-yl)-6-methyl-5-phenyl hept-2-enoate (52b')

Prepared according to the general procedure in section 3.8.4 using **52b** (1.0 equiv., 0.030 mmol, 8.1 mg), ethyl 2-(triphenyl- λ^5-phosphanylidene)acetate (1.2 equiv., 0.036 mmol, 12.3 mg) and ammonium formate (4 mg). The crude mixture was purified by column chromatography (*n*-hexane:EtOAc 90:10) to give product **52b'**as a yellow oil (5.0 mg, 40%, 1:1 dr, average of two runs, 95% ee_A and 94% ee_B). The enantiomeric excess was determined by HPLC analysis on a Daicel Chiralpak IC-3 column (2:98 ^{i}PrOH:*n*-hexane 1.0 mL/min, 30 ^{o}C, λ = 215 nm). *Diastereosiomer A*: τ_{Major} = 19.9 min, τ_{Minor} = 14.3 min. *Diastereoisomer B*: τ_{Major} = 17.1 min, τ_{Minor} = 25.7 min. $[\alpha]_D^{23}$ = -6.46 (c = 0.01, $CHCl_3$, 95% ee_A and 94% ee_B ee). Absolute configuration determined in comparison to compound **42a**.

^{1}H NMR (500 MHz, $CDCl_3$) 1:1 mixture of diastereoisomers δ 7.28 – 7.23 (m, 5H), 7.22 – 7.10 (m, 5H), 6.71 – 6.55 (m, 2H), 5.74 – 5.62 (m, 2H), 4.06 (qd, *J* = 7.2, 1.8 Hz, 4H), 3.85 (dd, *J* = 9.1, 7.5 Hz, 1H), 3.67 (dd, *J* = 10.1, 6.6 Hz, 1H), 3.53 – 3.35 (m, 4H), 2.88 – 2.57 (m, 5H), 1.55 – 1.46 (m, 4H), 1.40 (dd, *J* = 12.2, 6.7 Hz, 1H), 1.20 (td, *J* = 7.1, 1.5 Hz, 5H), 1.09 – 1.04 (m, 8H), 1.02 (d, *J* = 5.0 Hz, 6H), 0.84 (s, 3H), 0.80 (s, 3H), 0.63 (s, 3H).

^{13}C NMR (126 MHz, $CDCl_3$) 1:1 mixture of diastereoisomers δ 166.53, 166.46, 149.05, 148.67, 141.09, 140.60, 129.85, 127.79, 127.72, 126.33, 121.99, 121.84, 83.94, 83.49, 80.42, 80.25, 59.98, 59.93, 52.58, 51.89, 41.73, 41.41, 40.12, 39.78, 39.25, 39.15, 32.97, 32.39, 26.63, 26.53 (d, *J* = 3.6 Hz), 21.23, 20.73, 19.42 (d, *J* = 4.5 Hz), 14.18.

HRMS (ESI) Calculated for $C_{22}H_{32}NaO_3$ $[M+Na]^+$: 367.2244, found: 367.2233.

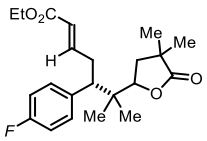

Ethyl (5*S*,*E*)-6-(4,4-dimethyl-5-oxotetrahydrofuran-2-yl)-5-(4-fluoro phenyl)-6-methylhept-2-enoate (42g')

Prepared according to the general procedure in section 3.8.4 using **42g** (1.0 equiv., 0.039 mmol, 12 mg), ethyl 2-(triphenyl- λ^5-phosphanylidene)acetate (1.2 equiv., 0.047 mmol, 16.4 mg) and ammonium formate (4 mg). The crude mixture was purified by column chromatography (*n*-hexane:EtOAc

80:20) to give product **42g'**as a yellow oil (8.8 mg, 62%, 1:1 dr, average of two runs, 93% ee_A and 94% ee_B). The enantiomeric excess was determined by UPC² analysis on a Daicel Chiralpak IG column (5:95 MeOH:CO_2, 2.0 mL/min, 3 λ = 220 nm). *Diastereosiomer A*: τ_{Major} = 4.93 min, τ_{Minor} = 8.52 min. *Diastereoisomer B*: τ_{Major} = 6.65 min, τ_{Minor} = 5.45 min. $[\alpha]_D^{26}$ = -8.22 (c = 0.14, $CHCl_3$, 1:1 dr, 93% ee_A and 94% ee_B). Absolute configuration determined in comparison to compound **42a**.

^{1}H NMR (500 MHz, $CDCl_3$) 1:1 mixture of diastereoisomers δ 7.20 – 7.09 (m, 4H), 6.99 (td, *J* = 8.7, 1.3 Hz, 4H), 6.66 – 6.51 (m, 2H), 5.68 (ddt, *J* = 15.6, 6.4, 1.4 Hz, 2H), 4.26 (dd, *J* = 9.0, 7.7 Hz, 1H), 4.08 (qd, *J* = 7.1, 3.7 Hz, 4H), 3.99 (dd, *J* = 10.7, 6.1 Hz, 1H), 2.95 (dd, *J* = 11.9, 3.6 Hz, 1H), 2.79 (dd, *J* = 12.0, 3.4 Hz, 1H), 2.77 – 2.53 (m, 4H), 1.90 – 1.81 (m, 3H), 1.74 (dd, *J* = 12.7, 6.1 Hz, 1H), 1.26 (d, *J* = 4.1 Hz, 6H), 1.24 – 1.18 (m, 9H), 1.14 (s, 3H), 1.04 (s, 3H), 0.91 (s, 3H), 0.85 (s, 3H), 0.73 (s, 3H).

^{13}C NMR (126 MHz, $CDCl_3$) 1:1 mixture of diastereoisomers δ 181.72, 181.61, 166.25, 166.18, 162.73, 160.78, 147.42, 147.18, 135.47, 135.14, 122.70, 122.63, 115.17, 115.01, 80.28, 80.00, 60.16, 60.12, 51.93, 50.71, 40.25, 40.11, 39.62, 39.25, 38.42, 38.04, 32.81, 32.38, 24.89, 24.84, 24.68, 24.64, 20.85, 19.97, 18.97, 17.77, 14.17.

^{19}F NMR (376 MHz, $CDCl_3$) 1:1 mixture of diastereoisomers δ -115.93, -115.94.

HRMS (ESI) Calculated for $C_{22}H_{29}FO_4Na$ $[M+Na]^+$: 399.1942, found: 399.1945.

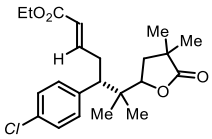

Ethyl (5*S*,*E*)-5-(4-chlorophenyl)-6-(4,4-dimethyl-5-oxotetrahydrofuran-2-yl)-6-methylhept-2-enoate (42h')

Prepared according to the general procedure in section 3.8.4 using **42h** (1.0 equiv., 0.053 mmol, 17 mg), ethyl 2-(triphenyl- λ⁵-phosphanylidene)acetate (1.2 equiv., 0.064 mmol, 22.0 mg) and ammonium formate (4 mg). The crude mixture was purified by column chromatography (*n*-hexane:EtOAc 78:22) to give product **42h'** as a brown oil (14.4 mg, 69%, 1:1 dr, average of two runs, 93% ee_A and 94% ee_B). The enantiomeric excess was determined by HPLC analysis on a Daicel Chiralpak ID-3 column (3:97 ^{i}PrOH:hexane, 1.0 mL/min, 30 °C, λ = 215 nm). *Diastereosiomer A*: τ_{Major} = 48.4 min, τ_{Minor} = 64.9 min. *Diastereoisomer B*: τ_{Major} = 73.7 min, τ_{Minor} = 70.2 min. $[\alpha]_D^{26}$ = -49.47 (c = 0.20, $CHCl_3$, 1:1 dr, 93% ee_A and 94% ee_B). Absolute configuration determined in comparison to compound **42a**.

^{1}H NMR (500 MHz, $CDCl_3$) 1:1 mixture of diastereoisomers δ 7.30 – 7.24 (m, 4H), 7.11 (dd, *J* = 18.3, 8.4 Hz, 4H), 6.58 (td, *J* = 15.6, 7.1 Hz, 2H), 5.68 (dd, *J* = 15.6, 5.9 Hz, 2H), 4.26 (dd, *J* = 9.1, 7.6 Hz, 1H), 4.08 (qd, *J* = 7.2, 3.7 Hz, 4H), 3.98 (dd, *J* = 10.7, 6.2 Hz, 1H), 2.95 (dd, *J* = 11.8, 3.6 Hz, 1H), 2.83 – 2.54 (m, 5H), 1.89 – 1.83 (m, 3H), 1.74 (dd, *J* = 12.7, 6.2 Hz, 1H),

1.26 (d, *J* = 4.2 Hz, 6H), 1.23 – 1.19 (m, 9H), 1.15 (s, 3H), 1.04 (s, 3H), 0.91 (s, 3H), 0.84 (s, 3H), 0.72 (s, 3H).

^{13}C NMR (126 MHz, $CDCl_3$) 1:1 mixture of diastereoisomers δ 181.68, 181.58, 166.21, 166.14, 147.22, 146.98, 138.35, 138.03, 132.74, 128.41, 122.81, 122.74, 80.21, 79.88, 60.18, 60.15, 52.15, 50.85, 40.24, 40.10, 39.62, 39.23, 38.42, 38.02, 32.63, 32.20, 24.89, 24.84, 24.73, 24.66, 20.86, 19.98, 18.94, 17.78.

HRMS (ESI) Calculated for $C_{22}H_{29}ClO_4Na$ $[M+Na]^+$: 415.1647, found: 415.1632.

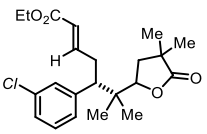

Ethyl (5*S*,*E*)-5-(3-chlorophenyl)-6-(4,4-dimethyl-5-oxotetrahydrofuran-2-yl)-6-methylhept-2-enoate (42i')

Prepared according to the general procedure in section 3.8.4 using **42i** (1.0 equiv., 0.046 mmol, 15 mg), ethyl 2-(triphenyl-λ^5-phosphanylidene)acetate (1.2 equiv., 0.055 mmol, 19.4 mg) and ammonium formate (4 mg). The crude mixture was purified by column chromatography (*n*-hexane:EtOAc 70:30) to give product **42i'**as a brown oil (13.0 mg, 72%, 1:1 dr, average of two runs, 91% ee_A and 93% ee_B). The enantiomeric excess was determined by HPLC analysis on a Daicel Chiralpak ID-3 column (3:97 ^{i}PrOH:*n*-hexane, 1.0 mL/min, 30 °C, λ = 230 nm). *Diastereosiomer A*: τ_{Major} = 41.5 min, τ_{Minor} = 57.2 min. *Diastereoisomer B*: τ_{Major} = 61.0 min, τ_{Minor} = 64.4 min. $[\alpha]_D^{26}$ = -26.27 (c = 0.08, $CHCl_3$, 1:1 d.r, 91% ee_A and 93% ee_B). Absolute configuration determined in comparison to compound **42a**.

^{1}H NMR (400 MHz, $CDCl_3$) 1:1 mixture of diastereoisomers δ 7.27 – 7.18 (m, 4H), 7.16 (d, *J* = 8.9 Hz, 2H), 7.12 – 7.01 (m, 2H), 6.59 (dtd, *J* = 15.6, 7.0, 5.7 Hz, 2H), 5.71 (ddt, *J* = 15.6, 4.2, 1.4 Hz, 2H), 4.29 (t, *J* = 8.3 Hz, 1H), 4.09 (qd, *J* = 7.1, 2.8 Hz, 4H), 4.02 (dd, *J* = 10.6, 6.2 Hz, 1H), 2.93 (dd, *J* = 11.5, 3.8 Hz, 1H), 2.82 – 2.53 (m, 5H), 1.93 – 1.83 (m, 3H), 1.76 (dd, *J* = 12.7, 6.2 Hz, 1H), 1.26 (d, *J* = 3.2 Hz, 6H), 1.24 – 1.20 (m, 9H), 1.16 (s, 3H), 1.05 (s, 3H), 0.91 (s, 3H), 0.86 (s, 3H), 0.74 (s, 3H).

^{13}C NMR (101 MHz, $CDCl_3$) 1:1 mixture of diastereoisomers δ 181.62, 181.52, 166.20, 166.15, 147.06, 146.84, 142.11, 141.82, 134.15, 129.46, 127.26, 127.24, 122.86, 122.82, 80.29, 79.90, 60.19, 60.15, 52.36, 51.29, 40.25, 40.13, 39.68, 39.29, 38.42, 38.05, 32.59, 32.23, 24.87, 24.82, 24.69, 24.63, 20.78, 20.02, 19.02, 17.97, 14.17.

HRMS (ESI) Calculated for $C_{22}H_{29}ClO_4Na$ $[M+Na]^+$: 415.1647, found: 415.1640.

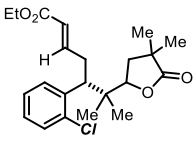

Ethyl (5*S*,*E*)-5-(2-chlorophenyl)-6-(4,4-dimethyl-5-oxotetrahydrofuran-2-yl)-6-methylhept-2-enoate (42j')

Prepared according to the general procedure in section 3.8.4 using **42j** (1.0 equiv., 0.068 mmol, 22 mg), ethyl 2-(triphenyl-λ⁵-phosphanylidene)acetate (1.2 equiv., 0.082 mmol, 28.5 mg) and ammonium formate (4 mg) The crude mixture was purified by column chromatography (*n*-hexane:EtOAc 75:25) to give product **42j'** as a yellow oil (10.2 mg, 38%, 1:1 dr, average of two runs, 91% ee_A and 93% ee_B). The enantiomeric excess was determined by HPLC analysis on a Daicel Chiralpak IC-3 column (5:95 ^{i}PrOH:*n*-hexane, 1.0 mL/min, 30 °C, λ = 230 nm). *Diastereosiomer A*: τ_{Major} = 75.2 min, τ_{Minor} = 83.1 min. *Diastereoisomer B*: τ_{Major} = 100.9 min, τ_{Minor} = 126.4 min. $[\alpha]_D^{24}$ = -26.3 (c = 0.08, $CHCl_3$, 1:1 d.r, 91% ee_A and 93% ee_B). Absolute configuration determined in comparison to compound **42a**.

^{1}H NMR (400 MHz, $CDCl_3$) 1:1 mixture of diastereoisomers δ 7.37 (dd, *J* = 7.9, 1.4 Hz, 2H), 7.32 (dd, *J* = 7.9, 1.7 Hz, 1H), 7.28 (dd, *J* = 7.9, 1.9 Hz, 1H), 7.26 (d, *J* = 1.4 Hz, 1H), 7.23 (dd, *J* = 7.8, 1.3 Hz, 1H), 7.21 – 7.11 (m, 2H), 6.71 – 6.36 (m, 2H), 5.84 – 5.49 (m, 2H), 4.41 (ddd, *J* = 15.1, 10.2, 6.5 Hz, 2H), 4.08 (qd, *J* = 7.1, 4.1 Hz, 4H), 3.66 (dd, *J* = 11.9, 3.5 Hz, 1H), 3.55 (dd, *J* = 11.8, 3.7 Hz, 1H), 2.86 – 2.54 (m, 4H), 2.04 – 1.81 (m, 4H), 1.28 (s, 6H), 1.27 (s, 3H), 1.24 (s, 3H), 1.21 (td, *J* = 7.2, 2.2 Hz, 6H), 1.11 (s, 3H), 0.95 (s, 3H), 0.91 (s, 3H), 0.69 (s, 3H).

^{13}C NMR (101 MHz, $CDCl_3$) 1:1 mixture of diastereoisomers δ 181.74, 181.52, 166.25, 166.13, 146.97, 146.42, 138.22, 137.95, 135.98, 135.95, 129.99, 129.88, 129.41, 129.23, 127.98, 127.89, 126.68, 126.61, 122.83, 122.63, 82.39, 80.33, 60.16, 60.05, 46.39, 45.27, 40.49, 40.32, 40.06, 38.59, 38.55, 33.70, 33.07, 24.94, 24.84, 24.61, 24.55, 21.09, 19.95, 19.52, 18.73, 14.17.

HRMS (ESI) Calculated for $C_{22}H_{29}ClO_4Na$ $[M+Na]^+$: 415.1647, found: 415.1632.

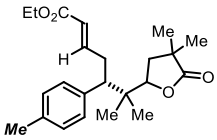

Ethyl (5*S*,*E*)-6-(4,4-dimethyl-5-oxotetrahydrofuran-2-yl)-6-methyl-5-(*p*-tolyl)hept-2-enoate (42k')

Prepared according to the general procedure in in section 3.8.4 using **42k** (1.0 equiv., 0.050 mmol, 15.0 mg), ethyl 2-(triphenyl- λ⁵-phosphanylidene)acetate (1.2 equiv., 0.060 mmol, 20.7 mg) and ammonium formate (4 mg) The crude mixture was purified by column chromatography (*n*-hexane:EtOAc 80:20) to give product **42k'** as a brown oil (14.1 mg, 76%, 1:1 dr, average of two runs, 89% ee_A and 91% ee_B). The enantiomeric excess was determined by HPLC analysis on a Daicel Chiralpak ID-3 column (6:94 ^{i}PrOH:*n*-hexane, 1.0 mL/min, 30 °C, λ = 215 nm). *Diastereosiomer A*: τ_{Major} = 21.5 min, τ_{Minor} = 25.6 min. *Diastereoisomer B*: τ_{Major} =

29.2 min, τ_{Minor} = 28.2 min. $[\alpha]_D^{26}$ = -6.41 (c = 0.07, $CHCl_3$, 89% ee_A and 91% ee_B). Absolute configuration determined in comparison to compound **42a**.

^{1}H NMR (400 MHz, $CDCl_3$) 1:1 mixture of diastereoisomers δ 7.11 – 7.01 (m, 8H), 6.67 – 6.56 (m, 2H), 5.74 – 5.65 (m, 2H), 4.26 (dd, *J* = 8.9, 7.7 Hz, 1H), 4.08 (qd, *J* = 7.1, 2.5 Hz, 5H), 2.90 (dd, *J* = 8.9, 6.4 Hz, 1H), 2.71 (d, *J* = 4.2 Hz, 3H), 2.64 (td, *J* = 7.0, 1.6 Hz, 2H), 2.31 (s, 6H), 1.96 – 1.80 (m, 3H), 1.73 (dd, *J* = 12.7, 6.2 Hz, 1H), 1.25 (d, *J* = 1.4 Hz, 6H), 1.21 (td, *J* = 7.1, 2.0 Hz, 9H), 1.14 (s, 3H), 1.04 (s, 3H), 0.94 (s, 3H), 0.86 (s, 3H), 0.72 (s, 3H).

^{13}C NMR (101 MHz, $CDCl_3$) 1:1 mixture of diastereoisomers δ 181.89, 181.78, 166.40, 166.33, 148.07, 147.84, 136.61, 136.42, 136.36, 136.30, 128.91, 128.87, 122.36, 122.28, 80.51, 80.38, 60.07, 60.04, 52.21, 50.93, 40.29, 40.13, 39.58, 39.29, 38.40, 38.06, 32.85, 32.33, 24.89, 24.86, 24.70, 24.64, 21.02, 21.00, 20.07, 19.12, 17.88, 14.19.

HRMS (ESI) Calculated for $C_{23}H_{32}NaO_4$ $[M+Na]^+$: 395.2193, found: 395.2178.

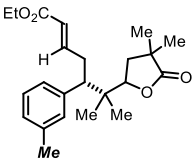

Ethyl (5*S*,*E*)-6-(4,4-dimethyl-5-oxotetrahydrofuran-2-yl)-6-methyl-5-(*m*-tolyl)hept-2-enoate (42l')

Prepared according to the general procedure in in section 3.8.4 using **42l** (1.0 equiv., 0.075 mmol, 22.7 mg), ethyl 2-(triphenyl- λ^5-phosphanylidene)acetate (1.2 equiv., 0.090 mmol, 31.9 mg) and ammonium formate (4 mg) The crude mixture was purified by column chromatography (*n*-hexane:EtOAc 80:20) to give product **42l'**as a brown oil (20.1 mg, 72%, 1:1 dr, average of two runs, 94% ee_A and 94% ee_B). The enantiomeric excess was determined by HPLC analysis on a Daicel Chiralpak ID-3 column (7:93 ^{i}PrOH:*n*-hexane, 1.0 mL/min, 30 °C, λ = 215 nm). *Diastereosiomer A*: τ_{Major} = 17.4 min, τ_{Minor} = 21.6 min. *Diastereoisomer B*: τ_{Major} = 23.6 min, τ_{Minor} = 22.7 min. $[\alpha]_D^{26}$ = -10.07 (c = 0.08, $CHCl_3$, 1:1 dr, 94% ee_A and 94% ee_B). Absolute configuration determined in comparison to compound **42a**.

^{1}H NMR (400 MHz, $CDCl_3$) 1:1 mixture of diastereoisomers δ 7.16 (t, *J* = 7.4 Hz, 2H), 7.03 (d, *J* = 7.4 Hz, 2H), 7.00 – 6.87 (m, 4H), 6.70 – 6.55 (m, 2H), 5.77 – 5.62 (m, 2H), 4.27 (dd, *J* = 9.4, 7.3 Hz, 1H), 4.08 (qd, *J* = 7.1, 2.6 Hz, 5H), 2.87 (q, *J* = 7.6 Hz, 1H), 2.72 (d, *J* = 4.0 Hz, 3H), 2.67 – 2.61 (m, 2H), 2.32 (s, 6H), 1.91 – 1.79 (m, 3H), 1.73 (dd, *J* = 12.7, 6.1 Hz, 1H), 1.25 (s, 6H), 1.24 – 1.18 (m, 9H), 1.14 (s, 3H), 1.05 (s, 3H), 0.94 (s, 3H), 0.87 (s, 3H), 0.72 (s, 3H).

^{13}C NMR (101 MHz, $CDCl_3$) 1:1 mixture of diastereoisomers δ 181.84, 181.73, 166.40, 166.33, 148.02, 147.81, 139.75, 139.44, 137.63, 137.58, 128.02, 127.97, 127.68, 127.65, 122.36, 122.29, 80.58, 80.40, 60.07, 60.04, 52.47, 51.32, 40.29, 40.14, 39.57, 39.26, 38.42, 38.08, 32.85, 32.37, 24.86, 24.84, 24.68, 24.61, 21.56, 21.06, 20.09, 19.20, 18.02, 14.18.

HRMS (ESI) Calculated for $C_{23}H_{32}NaO_4$ $[M+Na]^+$: 395.2193, found: 395.2199.

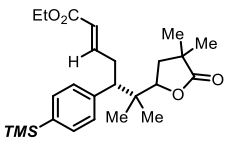

Ethyl (5*S*,*E*)-6-(4,4-dimethyl-5-oxotetrahydrofuran-2-yl)-6-methyl-5-(4-(trimethylsilyl)phenyl) hept-2-enoate (42m')

Prepared according to the general procedure in in section 3.8.4 using **42m** (1.0 equiv., 0.055 mmol, 20.0 mg), ethyl 2-(triphenyl-λ^5-phosphanylidene)acetate (1.2 equiv., 0.066 mmol, 23.2 mg) and ammonium formate (4 mg). The crude mixture was purified by column chromatography (*n*-hexane:EtOAc 80:20) to give product **42m'** as a colorless oil (18.2 mg, 80%, 1:1 dr, average of two runs, 90% ee_A and 90% ee_B). The enantiomeric excess was determined by HPLC analysis on a Daicel Chiralpak IG column (30:70 CH_2Cl_2:Heptane, 2.0 mL/min, 20 °C, λ = 230 nm). *Diastereosiomer A*: τ_{Major} = 8.7 min, τ_{Minor} = 11.4 min. *Diastereoisomer B*: τ_{Major} = 13.3 min, τ_{Minor} = 16.5 min. $[\alpha]_D^{24}$ = -92.5 (c = 0.06, $CHCl_3$, 90% ee_A and 90% ee_B). Absolute configuration determined in comparison to compound **42a**.

^{1}H NMR (400 MHz, $CDCl_3$) 1:1 mixture of diastereoisomers δ 7.42 (d, *J* = 7.9 Hz, 4H), 7.14 (dd, *J* = 12.9, 7.8 Hz, 4H), 6.68 – 6.54 (m, 2H), 5.75 – 5.63 (m, 2H), 4.28 (dd, *J* = 9.7, 6.9 Hz, 1H), 4.08 (qd, *J* = 7.2, 2.6 Hz, 5H), 2.91 (dd, *J* = 8.4, 6.8 Hz, 1H), 2.73 (dd, *J* = 5.0, 1.1 Hz, 3H), 2.66 (td, *J* = 7.7, 6.9, 1.6 Hz, 2H), 1.94 – 1.82 (m, 3H), 1.75 (dd, *J* = 12.7, 6.2 Hz, 1H), 1.25 (d, *J* = 1.3 Hz, 6H), 1.23 – 1.18 (m, 9H), 1.15 (s, 3H), 1.05 (s, 3H), 0.94 (s, 3H), 0.87 (s, 3H), 0.73 (s, 3H), 0.25 (s, 18H).

^{13}C NMR (101 MHz, $CDCl_3$) 1:1 mixture of diastereoisomers δ 181.85, 181.73, 166.40, 166.33, 147.96, 147.75, 140.31, 140.00, 138.81, 138.74, 133.19, 133.15, 129.13, 122.41, 122.33, 80.54, 80.35, 60.07, 60.04, 52.54, 51.41, 40.28, 40.12, 39.70, 39.37, 38.40, 38.05, 32.80, 32.34, 29.70, 24.88, 24.72, 24.67, 21.03, 20.10, 19.16, 18.01.

HRMS (ESI) Calculated for $C_{25}H_{38}NaO_4Si$ $[M+Na]^+$: 453.2432, found: 453.2426.

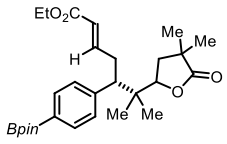

Ethyl (5*S*,*E*)-6-(4,4-dimethyl-5-oxotetrahydrofuran-2-yl)-6-methyl-5-(4-(4,4,5,5-tetramethyl-1,3,2-dioxaborolan-2-yl)phenyl)hept-2-enoate (42n')

Prepared according to the general procedure in in section 3.8.4 using **42n** (1.0 equiv., 0.037 mmol, 15.3 mg), ethyl 2-(triphenyl-λ^5-phosphanylidene)acetate (1.2 equiv., 0.044 mmol, 15.3 mg) and ammonium formate (4 mg) The crude mixture was purified by column chromatography (*n*-hexane:EtOAc 75:25) to give product **42n'**as a colorless oil (6.0 mg, 33%, 1:1 dr, average of two runs, 91 ee_A and 94% ee_B). The enantiomeric excess was determined by HPLC analysis on a Daicel Chiralpak ID3 column (11:89 ^{i}PrOH:*n*-hexane, 0.4 mL/min, 30 °C, λ = 215 nm). *Diastereosiomer A*: τ_{Major} = 31.9 min, τ_{Minor} = 34.6 min. *Diastereoisomer B*: τ_{Major} =

39.1 min, τ_{Minor} = 33.6 min. $[\alpha]_D^{26}$ = -7.91 (c = 0.09, $CHCl_3$, 1:1 dr, 91 ee_A and 94% ee_B). Absolute configuration determined in comparison to compound **42a**.

^{1}H NMR (400 MHz, $CDCl_3$) 1:1 mixture of diastereoisomers δ 7.73 (dd, *J* = 8.1, 1.4 Hz, 4H), 7.19 (dd, *J* = 13.0, 8.0 Hz, 4H), 6.60 (dt, *J* = 15.6, 7.0 Hz, 2H), 5.68 (dd, *J* = 15.5, 5.2 Hz, 2H), 4.25 (t, *J* = 8.3 Hz, 1H), 4.07 (qd, *J* = 7.1, 2.4 Hz, 5H), 3.01 – 2.92 (m, 1H), 2.82 – 2.64 (m, 5H), 1.92 – 1.81 (m, 3H), 1.71 (dd, *J* = 12.7, 6.1 Hz, 1H), 1.35 (s, 24H), 1.25 (d, *J* = 3.7 Hz, 6H), 1.20 (td, *J* = 7.1, 2.0 Hz, 9H), 1.13 (s, 3H), 1.05 (s, 3H), 0.94 (s, 3H), 0.85 (s, 3H), 0.72 (s, 3H).

^{13}C NMR (101 MHz, $CDCl_3$) 1:1 mixture of diastereoisomers δ 181.80, 181.67, 166.27, 166.17, 147.72, 147.58, 147.34, 143.14, 142.88, 134.62, 134.57, 122.59, 122.52, 83.82, 80.40, 80.19, 60.08, 60.04, 52.85, 51.51, 40.27, 40.12, 39.67, 39.34, 38.40, 32.67, 32.17, 24.94, 24.92, 24.88, 24.87, 24.84, 20.95, 20.12, 19.11, 17.90, 14.17.

HRMS (ESI) Calculated for $C_{28}H_{41}NaBO_6$ $[M+Na]^+$: 506.2925, found: 506.2321.

3.8.8. General Procedure for the Photochemical Three-Component Cascade

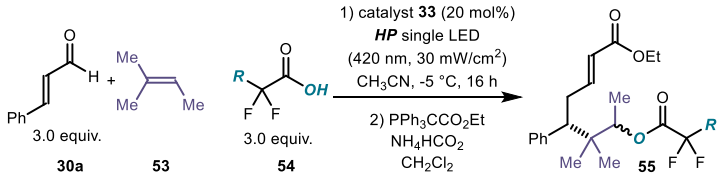

Figure 3.32. General Procedure for the synthesis of products **55.**

General Procedure: To a 5 mL argon-purged glass vial, containing the amine catalyst **33** (14.1 mg, 0.02 mmol, 20 mol%) and the desired acid **54** (0.3 mmol, 3.0 equiv.), was added enal **30a** (0.3 mmol, 3.0 equiv.). Then acetonitrile (200 µL, argon sparged, 0.1 M) and amylene **53** (0.1 mmol, 1.0 equiv.) were added. The vial was sealed with Parafilm and then placed into an aluminum block on a 3D-printed holder, fitted with a 420 nm high-power single LED. The irradiance was fixed at 30±2 mW/cm², as controlled by an external power supply, and measured using a photodiode light detector at the start of each reaction. This setup secured reliable irradiation while keeping a distance of 1 cm between the reaction vessel and the light source. The internal temperature was kept at -5 °C with a chiller connected to the irradiation plate (the setup is detailed in Figure 3.33). The reaction was stirred for 16 hours, then the reaction was quenched with $NaHCO_3$ (5.0 mL), extracted with CH_2Cl_2 (2 x 5.0 mL). The combined organics were dried over $MgSO_4$, filtered and evaporated. The aldehyde was then dissolved in CH_2Cl_2 (0.5 mL). Ethyl 2-(triphenyl-l5-phosphanylidene)acetate (1.2 equiv.) and ammonium

formate (1.0 equiv.) were added and the resulting mixture was stirred at ambient temperature until completion (TLC analysis). The crude reaction mixture was evaporated and directly purified by flash column chromatography to afford the enoate product **55**.

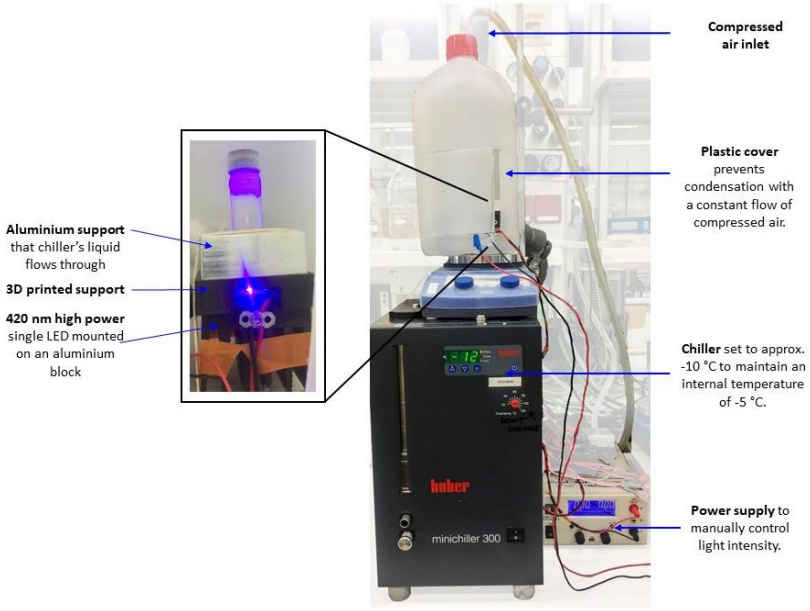

Figure 3.33. Reaction set up for chilled photochemical reactions. The light source for illuminating the reaction vessel consisted of a single 420 nm high-power LED (OCU-440 UE420-X-T) purchased from OSA OPTO.

3.8.9.Characterization of Products 55

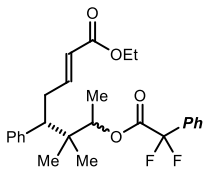

Ethyl (5S,E)-7-(2,2-difluoro-2-phenylacetoxy)-6,6-dimethyl-5-phenyloct-2-enoate (55a).

Prepared according to the general procedure described in section 3.8.7 using 2,2- acid **54a** (51.5 mg, 0.3 mmol). The crude material was purified by flash column chromatography (20:1 *n*-hexane:EtOAc, SiO_2 gel) to give the product **55a** as a colorless oil (17.5 mg, 39.5%, over two steps, 1:1 dr, 71% ee and 70% ee, average of two runs). The enantiomeric excess was determined by HPLC analysis on a Daicel Chiralpak IC-3 column (5:95 ^{i}PrOH:hexane, 1.0 mL/min, 20 °C, λ = 215 nm) τ_{major} = 10.5 min, τ_{minor} = 11.2 min τ_{major} = 14.3 min, τ_{minor} = 25.2 min. $[\alpha]_D^{26}$ = +3.9 (c = 0.34, CH_2Cl_2, 1:1.3 dr, 71% ee and 70% ee).

^{1}H NMR (400 MHz, $CDCl_3$) mixture of two diastereoisomers δ 7.64 (ddt, *J* = 9.5, 6.7, 2.2 Hz, 5H), 7.54 – 7.42 (m, 7H), 7.25 – 7.13 (m, 6H), 6.91 (d, *J* = 7.2 Hz, 2H), 6.76 (s, 2H), 6.55 – 6.48 (m, 1H), 6.34 (dt, *J* = 15.6, 6.7 Hz, 1H), 5.66 – 5.59 (m, 1H), 5.57 – 5.49 (m, 1H), 5.00 (q, *J* = 6.4 Hz, 1H), 4.54 (q, *J* = 6.3 Hz, 1H), 4.11 (q, *J* = 7.1 Hz, 2H), 4.10 (q, *J* = 7.0 Hz, 2H), 2.55 (s, 1H), 2.53 (s, 1H), 2.50 – 2.35 (m, 2H), 1.21 – 1.27 (m, 9H), 1.12 (d, *J* = 6.4 Hz, 3H), 0.98 (s, 3H), 0.86 (s, 3H), 0.78 (s, 3H), 0.67 (s, 3H).

^{13}C NMR (126 MHz, $CDCl_3$, 298K) mixture of two diastereoisomers δ 166.4, 163.21 (dd, *J* = 35.1, 33.1 Hz), 163.65 (t, *J* = 35.9, 34.0 Hz), 147.7, 147.5, 139.8, 139.5, 133.11 (t, *J* = 25.7 Hz), 133.09 (t, *J* = 25.6 Hz), 131.33 – 131.14 (m), 129.6 (br. s), 129.4 (br. s), 128.9, 128.8, 128.3, 128.2, 127.1, 127.0, 125.62 (t, *J* = 6.2 Hz), 125.50 (t, *J* = 6.1 Hz) 122.5, 113.58 (t, *J* = 252.6 Hz), 113.53 (t, *J* = 252.0 Hz), 78.6, 78.3, 60.24, 60.17, 50.9, 50.4, 40.7, 40.6, 32.7, 32.2, 21.1, 20.1, 20.1, 19.7, 14.9, 14.4.

^{19}F NMR (376 MHz, $CDCl_3$) mixture of two diastereoisomers δ -103.08 (d, *J* = 251.2 Hz), -104.33 (d, *J* = 249.5 Hz), -106.12 (d, *J* = 249.5 Hz), -106.78 (d, *J* = 250.9 Hz).

HRMS (ESI) Calculated for $C_{26}H_{30}F_2NaO_4$ $[M+Na]^+$: 467.2004, found: 467.2017.

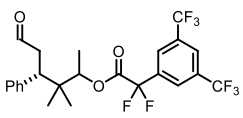

(4S)-3,3-Dimethyl-6-oxo-4-phenylhexan-2-yl 2-(3,5-bis(trifluoro methyl)phenyl)-2,2-difluoroacetate (55b')

Prepared according to the general procedure described in section 3.8.7 using 2-(3,5-bis(trifluoromethyl)phenyl)-2,2-difluoroacetic acid **54b** (92.0 mg, 0.3 mmol). The crude material was purified by flash column chromatography (20:1 *n*-hexane:EtOAc, SiO_2 gel) to give **55b'** as a colorless oil (16 mg, 29% yield, 1:1 dr, average of two runs).

^{1}H NMR (500 MHz, $CDCl_3$) mixture of two diastereoisomers δ 9.44 (d, *J* = 1.7 Hz, 2H), 9.39 (d, *J* = 1.6 Hz, 1H), 8.12 (s, 2H), 8.10 (s, 2H), 8.06 (s, 2H), 7.30 – 7.20 (m, 7H), 7.05 (d, *J* = 7.2 Hz, 2H), 6.91 (d, *J* = 7.3 Hz, 2H), 4.88 (q, *J* = 6.4 Hz, 1H), 4.61 (q, *J* = 6.4 Hz, 1H), 3.13 (td, *J* = 12.9, 12.2, 3.7 Hz, 2H), 2.85 (dtd, *J* = 16.6, 11.3, 2.6 Hz, 2H), 2.69 (dt, *J* = 16.6, 2.8 Hz, 2H), 1.27 (d, *J* = 6.4 Hz, 3H), 1.15 (d, *J* = 6.4 Hz, 3H), 0.98 (s, 3H), 0.91 (s, 3H), 0.83 (s, 3H), 0.76 (s, 3H);

^{13}C NMR (126 MHz, $CDCl_3$) mixture of two diastereoisomers δ 200.9, 200.7, 162.1 (t, *J* = 34.3 Hz), 161.9 (t, *J* = 34.2 Hz), 139.4, 139.2, 135.4 (t, *J* = 26.8 Hz), 135.3 (t, *J* = 26.8 Hz), 132.6 (q, *J* = 34.3 Hz), 132.6 (q, *J* = 34.3 Hz), 129.5 (br. s), 129.2 (br. s), 128.5, 128.4, 127.4, 127.3, 127.3 (br. s), 126.2 (br. s), 122.7 (q, *J* = 273.1 Hz), 112.0 (t, *J* = 254.6 Hz), 79.6, 79.30, 45.4, 45.0, 44.4, 44.3, 40.2, 40.1, 20.7, 20.4, 19.9, 19.7, 14.7, 14.0;

^{19}F NMR (376 MHz, $CDCl_3$) mixture of two diastereoisomers δ -63.13, -104.41 (dd, *J* = 528.2, 261.2 Hz), -104.68 (dd, *J* = 459.2, 258.8 Hz).

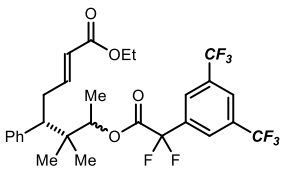

Ethyl (5*S*,*E*)-7-(2-(3,5-bis(trifluoromethyl)phenyl)-2,2-difluoro acetoxy)-6,6-dimethyl-5-phenyloct-2-enoate (55b)

Prepared according to the general procedure described in section 3.8.7 from **55b'**. The crude reaction mixture was purified by flash column chromatography (*n*-hexane:EtOAc 20:1, SiO_2 gel) to afford **55b** as a colourless oil (10.5 mg, 19% isolated over two steps, 66% ee_A and 68% ee_B). The enantiomeric excess was determined by HPLC analysis on a Daicel Chiralpak IC-3 column (2:98 ^{i}PrOH:*n*-hexane, 1.0 mL/min, 20 °C, λ = 215 nm) τ_A = 8.76 min, τ_A = 9.34 min; τ_B = 9.99 min, τ_B = 11.29 min. $[\alpha]_D^{26}$ = +15.7 (c = 0.18, $CHCl_3$, 1:1.3 dr, 66% ee_A and 68% ee_B).

^{1}H NMR (400 MHz, $CDCl_3$) mixture of two diastereoisomers δ 8.10 (s, 2H), 8.08 (s, 2H), 8.05 (s, 2H), 7.29 – 7.18 (m, 6H), 7.01 (br. d, *J* = 7.0 Hz, 2H), 6.87 (br. d, *J* = 4.4 Hz, 2H), 6.56 – 6.48 (m, 1H), 6.44 (dtd, *J* = 15.6, 6.7, 5.3, 1.0 Hz, 1H), 5.63 (d, *J* = 15.5 Hz, 1H), 5.58 (d, *J* = 15.6 Hz, 1H), 4.93 (q, *J* = 6.4 Hz, 1H), 4.64 (q, *J* = 6.4 Hz, 1H), 4.08 (q, *J* = 7.1 Hz, 2H), 4.07 (q, *J* = 7.1 Hz, 2H), 2.61 – 2.46 (m, 6H), 1.23 (d, *J* = 6.4 Hz, 3H), 1.22 (t, *J* = 7.1 Hz, 3H), 1.20 (t, *J* = 7.2 Hz, 3H), 1.14 (d, *J* = 6.4 Hz, 3H), 0.98 (s, 3H), 0.92 (s, 3H), 0.82 (s, 3H), 0.74 (s, 3H).

^{13}C NMR (101 MHz, $CDCl_3$) mixture of two diastereoisomers δ 166.29, 166.26, 162.35 (t, *J* = 34.2 Hz), 161.98 (t, *J* = 34.1 Hz), 147.11, 147.05, 139.43, 139.35, 135.64 (t, *J* = 27.0 Hz), 135.60 (t, *J* = 26.9 Hz), 132.75 (q, *J* = 34.1 Hz), 129.66 (br. s) 129.44 (br. s.), 128.45, 128.39, 127.3, 127.21, 126.56 – 125.98, 125.64 – 124.90, 122.82 (q, *J* = 272.8 Hz), 122.76, 122.71, 112.14 (t, *J* = 254.5 Hz), 79.99, 79.87, 60.26, 60.23, 51.31, 50.99, 40.69, 40.65, 32.77, 32.50, 20.96, 20.49, 20.17, 19.74, 14.81, 14.28, 14.16. *The two* p-*CH coupling to two* CF_3 *groups were not observed.*

^{19}F NMR (376 MHz, $CDCl_3$) mixture of two diastereoisomers δ -63.13, -63.14, -103.98 (dd, *J* = 260.2, 127.9 Hz), -105.20 (dd, *J* = 259.8, 74.6 Hz).

HRMS (ESI) Calculated for $C_{28}H_{28}F_8NaO_4$ $[M+Na]^+$: 603.1752, found: 603.1753.

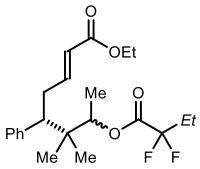

Ethyl (5*S*,*E*)-7-((2,2-difluorobutanoyl)oxy)-6,6-dimethyl-5-phenyloct-2-enoate (55c)

Prepared according to the general procedure described in section 3.8.7 using 2,2-difluorobutanoic acid **54c** (30.5 µL, 0.3 mmol). The crude material was purified by flash column chromatography (10:1 *n*-hexane:EtOAc, SiO_2 gel) to afford **55c** as a colourless oil (11.0 mg, 32% 1:1 dr, 85% ee_A and 79% ee_B, isolated yield over two steps, average of two runs). The enantiomeric excess was determined by HPLC analysis on Daicel Chiralpak IC-3 column (5:95 ^{i}PrOH:*n*-hexane, 1 mL/min, 20 °C, λ = 215 nm) *Diastereosiomer A*: τ_{Minor} = 10.8 min, τ_{Major} = 11.5 min; *Diastereoisomer B*: τ_{Major} = 13.1 min, τ_{Minor} = 31.5 min. $[\alpha]_D^{24}$ = +6.7 (c = 0.34, $CHCl_3$, 1:1.5 dr, 85% ee_A and 79% ee_B).

^{1}H NMR (400 MHz, $CDCl_3$) mixture of two diastereoisomers δ 7.32 – 7.18 (m, 6H), 7.12 (dd, *J* = 6.9, 1.8 Hz, 2H), 7.06 (d, *J* = 6.9 Hz, 2H), 6.60 (dt, *J* = 15.0, 7.4 Hz, 1H), 6.56 (dt, *J* = 15.0, 7.0 Hz, 1H), 5.69 (dt, *J* = 15.0, 1.4 Hz, 1H), 5.67 (dt, *J* = 15.0, 1.4 Hz, 1H), 4.97 (q, *J* = 6.4 Hz, 1H), 4.68 (q, *J* = 6.4 Hz, 1H), 4.08 (q, *J* = 7.1 Hz, 2H), 4.07 (q, *J* = 7.1 Hz, 2H), 2.81 – 2.54 (m, 6H), 2.18 – 2.00 (m, 4H), 1.28 (d, *J* = 6.4 Hz, 3H), 1.23 (t, *J* = 7.1 Hz, 3H), 1.23 (d, *J* = 6.4 Hz, 3H), 1.22 (t, *J* = 7.1 Hz, 3H), 1.09 (s, 3H) 1.08 (t, *J* = 7.5 Hz, 3H), 1.08 (t, *J* = 7.5 Hz, 3H), 1.00 (s, 3H), 0.85 (s, 3H), 0.83 (s, 3H).

^{13}C NMR (126 MHz, $CDCl_3$) mixture of two diastereoisomers δ 166.45, 166.43, 163.88 (t, *J* = 32.9 Hz), 163.72 (t, *J* = 32.9 Hz), 147.63, 139.87, 139.66, 129.77, 128.38, 128.32, 127.15, 127.07, 122.62, 116.83(t, *J* = 250.1 Hz), 116.80 (t, *J* = 251.0 Hz), 78.40, 78.36, 60.26, 60.20, 51.07, 50.81, 40.61, 40.52, 32.80, 32.54, 28.11 (t, *J* = 24.0 Hz), 28.08 (t, *J* = 24.0 Hz), 21.41, 20.55, 20.27, 19.92, 14.93, 14.31, 14.29, 5.96 (*app.* q, *J* = 5.7 Hz).

^{19}F NMR (376 MHz, $CDCl_3$) mixture of two diastereoisomers δ -107.25 (dd, *J* = 258.3, 19.9 Hz), -108.07 (dd, *J* = 258.3, 4.1 Hz).

HRMS (ESI) Calculated for $C_{22}H_{30}F_2NaO_4$ $[M+Na]^+$: 419.2004, found: 419.2008.

3.8.10. Cyclic Voltammetry of the Radical Precursors

The substrates **41a-h** were electrochemically characterized.

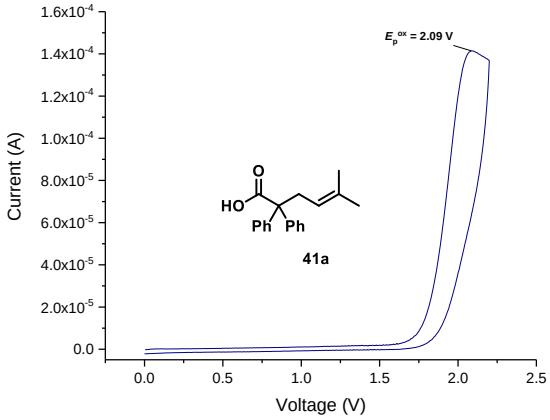

Figure 3.34. Cyclic voltammogram of **41a** [5 mM] in [0.1 M] $TBAPF_6$ in CH_3CN. Sweep rate: 100 mV/s. Glassy carbon electrode working electrode, Ag/AgCl (NaCl sat.) reference electrode, Pt wire auxiliary electrode. Irreversible oxidation. $E_p^A = E_p^{ox}$(**41a**$^{\bullet+}$/**41a**) = +2.09 V; E_p^A is the anodic peak potential, while E_p^{ox} value describes the electrochemical properties of **41a**.

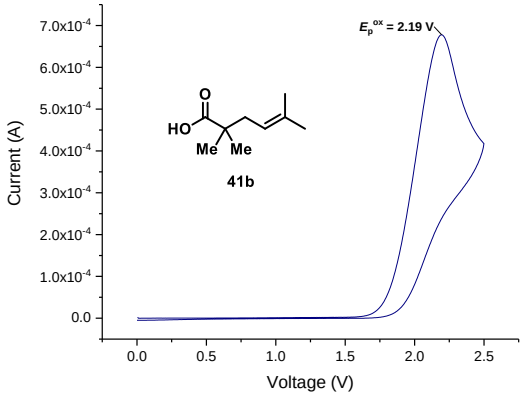

Figure 3.35. Cyclic voltammogram of **41b** [20 mM] in [0.1 M] $TBAPF_6$ in CH_3CN. Sweep rate: 100 mV/s. Glassy carbon electrode working electrode, Ag/AgCl (NaCl sat.) reference electrode, Pt wire auxiliary electrode. Irreversible oxidation. $E_p^A = E_p^{ox}$(**41b**$^{\bullet+}$/**41b**) = +2.19 V; E_p^A is the anodic peak potential, while E_p^{ox} value describes the electrochemical properties of **41b**.

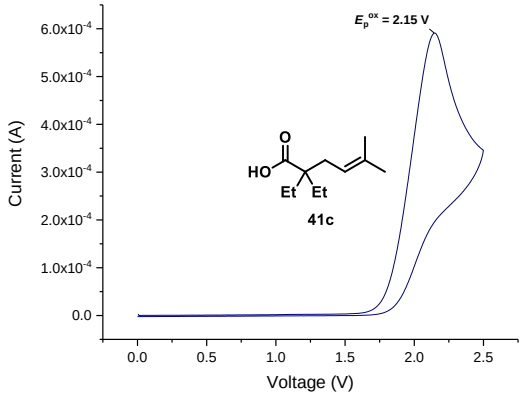

Figure 3.36. Cyclic voltammogram of **41c** [20 mM] in [0.1 M] $TBAPF_6$ in CH_3CN. Sweep rate: 100 mV/s. Glassy carbon electrode working electrode, Ag/AgCl (NaCl sat.) reference electrode, Pt wire auxiliary electrode. Irreversible oxidation. $E_P^A = E_p^{ox}$ (**41c**$^{\bullet+}$/**41c**) = +2.15 V; E_p^A is the anodic peak potential, while E_p^{ox} value describes the electrochemical properties of **41c**.

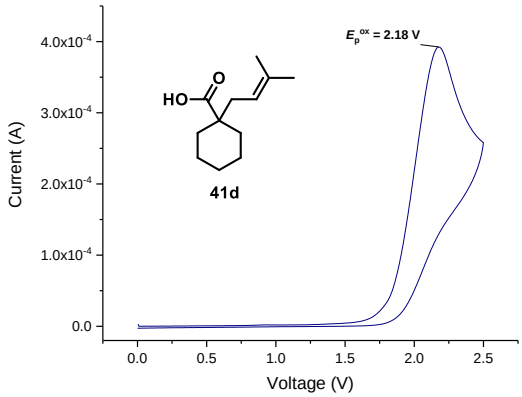

Figure 3.37. Cyclic voltammogram of **41d** [20 mM] in [0.1 M] $TBAPF_6$ in CH_3CN. Sweep rate: 100 mV/s. Glassy carbon electrode working electrode, Ag/AgCl (NaCl sat.) reference electrode, Pt wire auxiliary electrode. Irreversible oxidation. $E_P^A = E_p^{ox}$ (**41d**$^{\bullet+}$/**41d**) = +2.18 V; E_p^A is the anodic peak potential, while E_p^{ox} value describes the electrochemical properties of **41d**.

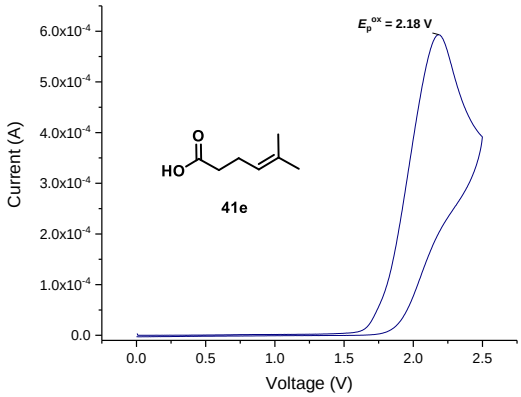

Figure 3.38. Cyclic voltammogram of **41e** [20 mM] in [0.1 M] $TBAPF_6$ in CH_3CN. Sweep rate: 100 mV/s. Glassy carbon electrode working electrode, Ag/AgCl (NaCl sat.) reference electrode, Pt wire auxiliary electrode. Irreversible oxidation. $E_P^A = E_p^{ox}$ (**41e**$^{\bullet+}$/**41e**) = +2.18 V; E_p^A is the anodic peak potential, while E_p^{ox} value describes the electrochemical properties of **41e**.

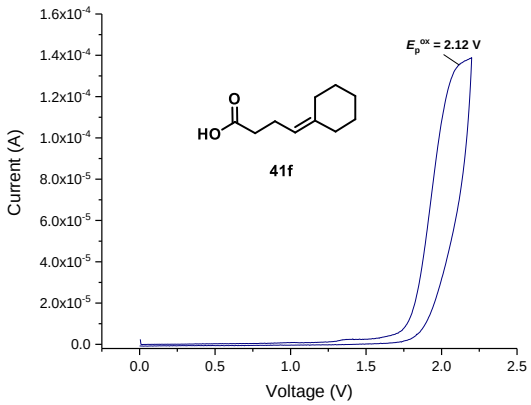

Figure 3.39. Cyclic voltammogram of **41f** [5 mM] in [0.1 M] $TBAPF_6$ in CH_3CN. Sweep rate: 100 mV/s. Glassy carbon electrode working electrode, Ag/AgCl (NaCl sat.) reference electrode, Pt wire auxiliary electrode. Irreversible oxidation. $E_P^A = E_p^{ox}$ (**41f**$^{\bullet+}$/**41f**) = +2.12 V; E_p^A is the anodic peak potential, while E_p^{ox} value describes the electrochemical properties of **41f**.

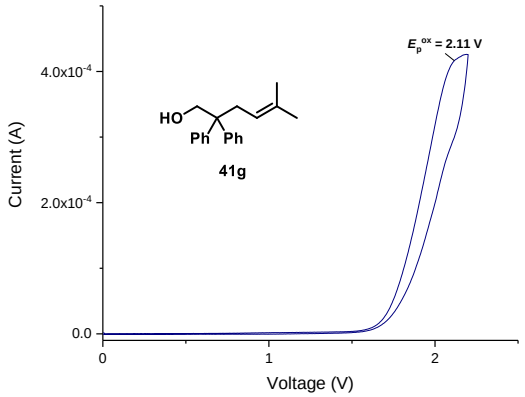

Figure 3.40. Cyclic voltammogram of **41g** [5 mM] in [0.1 M] $TBAPF_6$ in CH_3CN. Sweep rate: 50 mV/s. Glassy carbon electrode working electrode, Ag/AgCl (NaCl sat.) reference electrode, Pt wire auxiliary electrode. Irreversible oxidation. $E_P^A = E_p^{ox}$ (**41g**$^{\bullet+}$/**41g**) = +2.11 V; E_p^A is the anodic peak potential, while E_p^{ox} value describes the electrochemical properties of **41g**.

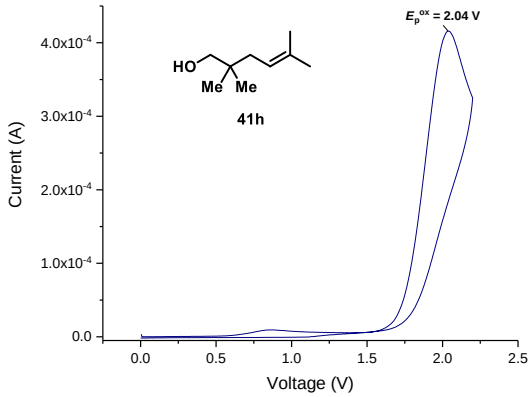

Figure 3.41. Cyclic voltammogram of **41h** [5 mM] in [0.1 M] $TBAPF_6$ in CH_3CN. Sweep rate: 100 mV/s. Glassy carbon electrode working electrode, Ag/AgCl (NaCl sat.) reference electrode, Pt wire auxiliary electrode. Irreversible oxidation. $E_P^A = E_p^{ox}$ (**41h**$^{\bullet+}$/41**h**) = +2.04 V; E_p^A is the anodic peak potential, while E_p^{ox} value describes the electrochemical properties of **41h**.

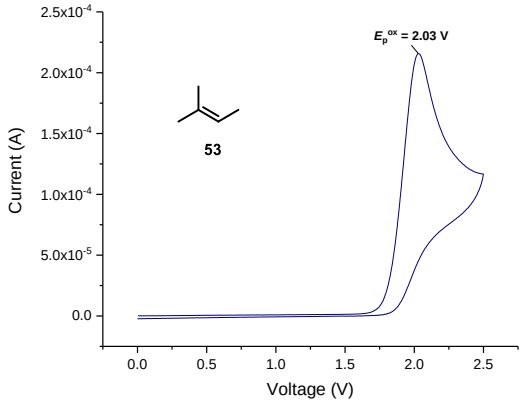

Figure 3.42. Cyclic voltammogram of **53** [20 mM] in [0.1 M] $TBAPF_6$ in CH_3CN. Sweep rate: 100 mV/s. Glassy carbon electrode working electrode, Ag/AgCl (NaCl sat.) reference electrode, Pt wire auxiliary electrode. Irreversible oxidation. $E_P^A = E_p^{ox}$ (**53**$^{\bullet+}$/**53**) = +2.03 V; E_P^A is the anodic peak potential, while E_p^{ox} value describes the electrochemical properties of **53**.

3.8.11. X-ray Crystallographic Data

Single Crystal X-ray Diffraction Data for compound 42a

Crystals of the compound **42a** were obtained by slow evaporation of a diethyl ether solution. *Data Collection.* Measurements were made on a Bruker-Nonius diffractometer equipped with an APPEX 2 4K CCD area detector, a FR591 rotating anode with MoKα radiation. Montel mirrors and a Cryostream Plus low-temperature device (T = 100K). Full-sphere data collection was used with ω and ϕ scans.

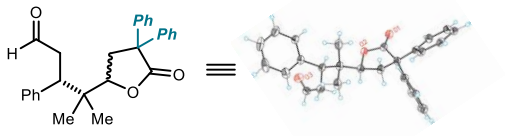

42a CCDC 1854258

Table 3.2. Crystal data and structure refinement for **42a**. ***CCDC1854258***

Empirical formula	$C_{28}H_{28}O_3$	
Formula weight	412.50	
Temperature	100(2) K	
Wavelength	1.54178 Å	
Crystal system	Orthorhombic	
Space group	P2(1)2(1)2	
Unit cell dimensions	a = 11.5127(4)Å	α= 90°.

	b = 22.3170(8)Å	β= 90°.
	c = 8.4981(3)Å	γ= 90°.
Volume	2183.41(13) Å^3	
Z	4	
Density (calculated)	1.255 Mg/m^3	
Absorption coefficient	0.632 mm^{-1}	
F(000)	880	
Crystal size	0.30 x 0.20 x 0.15 mm^3	
Theta range for data collection	4.321 to 68.115°.	
Index ranges	-7<=h<=13,-26<=k<=26,-9<=l<=8	
Reflections collected	15393	
Independent reflections	3821[R(int) = 0.0240]	
Completeness to theta =68.115°	96.8%	
Absorption correction	Multi-scan	
Max. and min. transmission	0.911 and 0.701	
Refinement method	Full-matrix least-squares on F^2	
Data / restraints / parameters	3821/ 111/ 310	
Goodness-of-fit on F^2	1.083	
Final R indices [I>2sigma(I)]	R1 = 0.0306, wR2 = 0.0802	
R indices (all data)	R1 = 0.0309, wR2 = 0.0804	
Flack parameter	x =0.03(5)	
Largest diff. peak and hole	0.215 and -0.141 e.Å^{-3}	

Chapter IV

Photochemical Organocatalytic Enantioselective Radical Cascade Enabled by Single-Electron Transfer Activation of Allenes

Target

Developing a visible-light-driven organocatalytic strategy to trigger a stereocontrolled radical cascade reaction upon activation of allenes.

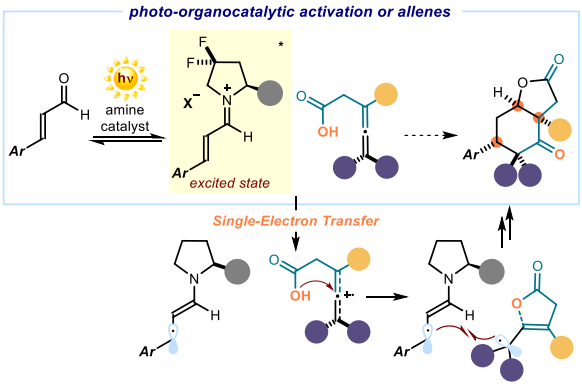

Tool

Using the excited-state reactivity of chiral iminium ions to activate allenes by single-electron transfer (SET) oxidation. The ensuing allene cation radicals participate in cascade reactions to deliver chiral polycyclic products with good enantioselectivity and high diastereoselectivity.[1]

4.1. Introduction

We have previously established that the photochemical activity of chiral iminium ions **I*** can be used to activate unactivated olefins **1** and trigger an enantioselective radical cascade process (Figure 4.1).[2] The single-electron transfer (SET) oxidation of **1** from the excited iminium ion **I*** formed concomitantly the alkene radical cation **II** and the chiral 5π-electron intermediate **IV**. The nucleophilic moiety within **II** first triggered a cyclization, exploiting the simultaneous polar and radical nature of such radical cation intermediate. The more stable tertiary radical **III** then underwent a stereocontrolled

[1] The project discussed in this chapter has been conducted in collaboration with Dr. Luca A. Perego, who was involved in the discovery and optimization of the process, performed part of the reaction scope and carried out DFT calculations. I investigated the scope of the cascade processes. This work has been published: Perego, L. A.; Bonilla, P.; Melchiorre, P. "Photo-Organocatalytic Enantioselective Radical Cascade Enabled by Single-Electron Transfer Activation of Allenes" *Adv. Synth. Catal.*, **2020**, *362*, 302. The work was part of a Dedicated Issue to Professor Eric Jacobsen on the occasion of his 60th birthday.

[2] Bonilla, P.; Rey, Y. P.; Holden, C. M.; Melchiorre, P. "Photo-Organocatalytic Enantioselective Radical Cascade Reactions of Unactivated Olefins" *Angew. Chem. Int. Ed.*, **2018**, *57*, 12819.

radical coupling with **IV** to deliver the chiral cascade product **2** with high enantioselectivity. The overall process converted alkenes **1** and α,β-unsaturated aldehydes into chiral adducts **2** in a single step through two sequential radical-based bond-forming events.

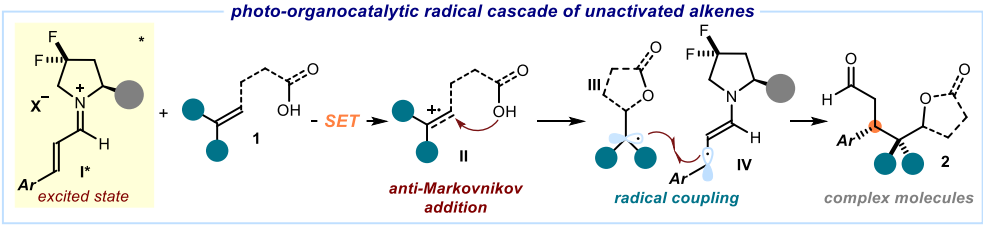

Figure 4.1 Radical cascade of unactivated alkenes triggered by excited iminium ions. SET: single-electron transfer.

To further explore the synthetic potential of asymmetric radical cascade processes, we wondered if this photochemical organocatalytic activation mode could be applied to the design of other radical cascades leading to the one-step stereoselective synthesis of complex chiral scaffolds. Hence, we aimed at activating other unsaturated functionalities *via* SET oxidation from the excited iminium ion. Specifically, we questioned if our system could successfully activate allenes to trigger a similar radical cascade process with high stereoselectivity. To better contextualize the background of this project, the following section will briefly discuss the chemistry of allenes and the few previous reports that involve the reactivity of allene radical cations.

4.2. The Reactivity of Allenes

Allenes are compounds with two cumulated C=C bonds in which two π-bonds are orthogonal to each other with an ideal C–C–C angle of 180º (Figure 4.2). The first synthesis of allenes dates back to 1884.[3] However, the study of their reactivity was delayed for a long period since their unique structure rendered them highly unstable compounds.[4] Recently, there has been an increasing interest in allene chemistry. Once seen as exotic and hard to access, allenes are now recognized as suitable substrates for many synthetically useful transformations.[5] One of the main features in the chemistry

[3] Burton, B. S.; Pechman, H. V "Ueber die Einwirkung von Chlorphosphor auf Acetondicarbonsäureäther" *Chem. Ber.*, **1887**, *20*, 145.

[4] Ma, S. "Electrophilic Addition and Cyclization Reactions of Allenes" *Acc. Chem. Res.*, **2009**, *42*, 1679.

[5] Ma, S. "Some Typical Advances in the Synthetic Applications of Allenes" *Chem. Rev.*, **2005**, *105*, 2829.

of allenes arises from their easily tuned reactivity and selectivity, which can be modulated by electronic or steric effects of their substituents.[6] Allenes have been successfully used in cycloaddition reactions,[7] radical processes,[8] and metal-catalyzed transformations. [9] Allene chemistry has also been applied in natural product synthesis,[5,10] while enantioselective catalytic variants have been developed applying both metal-based strategies[11] and organocatalysis.[12] The activation of allenes by single-electron transfer (SET) oxidation may offer new reactivity patterns to further expand the synthetic potential of these substrates. However, while photo-induced SET oxidation strategies have been extensively used to activate simple alkenes, the activation of allenes has remained scarcely explored and has found a limited synthetic utility to date.[13]

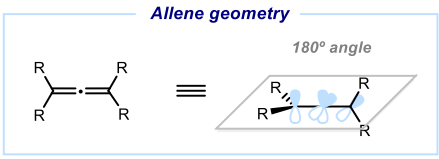

Figure 4.2. Allene structure and orbital geometry.

[6] Soriano, E.; Fernandez, I. "Allenes and computational chemistry: from bonding situations to reaction mechanisms" *Chem. Soc. Rev.*, **2015**, *43*, 3041.

[7] For reviews on cycloadditions see: a) Lopez, F.; Mascareñas, J. L. "[4+2] and [4+3] catalytic cycloadditions of allenes" *Chem. Soc. Rev.*, **2014**, *43*, 2904; For a review on [2+2] cycloadditions: b) Alcaide, B.; Almendros, P.; Aragoncillo, C. "Exploiting [2+2] cycloaddition chemistry: achievements with allenes" *Chem. Soc. Rev.*, **2010**, *39*, 783; c) Kitagaki, S.; Inagaki, F.; Mukai, C. "[2+2+1] Cyclization of allenes" *Chem. Soc. Rev.*, **2014**, *43*, 2956.

[8] Qiu, G.; Zhang, J.; Zhou, K.; Wu, J., "Recent advances in the functionalization of allenes via radical process" *Tetrahedron*, **2018**, *74*, 7290.

[9] a) Ma, S. "Transition Metal-Catalyzed/ Mediated Reaction of Allenes with a Nucleophilic Functionality Connected to the α-Carbon Atom" *Acc. Chem. Res.*, **2003**, *36*, 701; b) Widenhoefer, R. A. "Transition Metal-Catalyzed Hydroarylation of Allenes in Catalytic Hydroarylation of Carbon-Carbon Multiple Bonds" in Ackermann, L. (ed.) Catalytic Hydroarylation of Carbon-Carbon Multiple Bonds, Wiley-VCH, **2018**.

[10] Ma, S.; Yu, S. "Allenes in Catalytic Asymmetric Synthesis and Natural Product Syntheses" *Angew. Chem. Int. Ed.*, **2012**, *51*, 3074.

[11] Holmes, M.; Schwartz, L. A.; Krische, M. J. "Intermolecular Metal-Catalyzed Reductive Coupling of Dienes, Allenes, and Enynes with Carbonyl Compounds and Imines" *Chem. Rev.*, **2018**, *118*, 6026; b) Koschker, P.; Breit, B. "Branching Out: Rhodium-Catalyzed Allylation with Alkynes and Allenes" *Acc. Chem. Res.*, **2016**, *49*, 1524.

[12] Elsner, P.; Bernardi, L.; Dela Salla, G.; Overgaard, J.; Jørgensen, K. A. "Organocatalytic Asymmetric Conjugate Addition to Allenic Esters and Ketones" *J. Am. Chem. Soc.*, **2008**, *130*, 4897; b) Hölzl-Hobmeier, A.; Bauer, A.; Vieira Silva, A.; Huber, S. M.; Bannwarth, C.; Bach, T. "Catalytic deracemization of chiral allenes by sensitized excitation with visible light" *Nature*, **2018**, *564*, 240.

[13] For a review on SET oxidation of alkenes, see: a) Margrey, K. A.; Nicewicz, D. A. "A General Approach to Catalytic Alkene Anti-Markovnikov Hydrofunctionalization Reactions via Acridinium Photoredox Catalysis" *Acc. Chem. Res.*, **2016**, *49*, 1997.

4.2.1. SET Activation of Allenes

The first synthetically relevant example based on the SET oxidation of allenic derivatives (**3a**-**3b**) relied upon electrochemical methods (Figure 4.3). [14] This transformation was highly unselective and delivered complex mixtures (**4**-**9**) due to further oxidation of the products followed by the addition of the solvents or the salts present in the electrochemical cells.

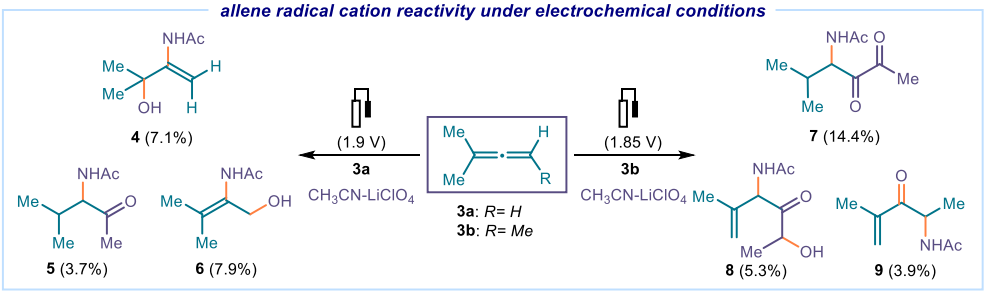

Figure 4.3. Reactivity of allenes activated by electrochemical methods.

It was then devised that overoxidation could be avoided by UV-light irradiation of symmetric tetraphenylallene **10b** (Figure 4.4).

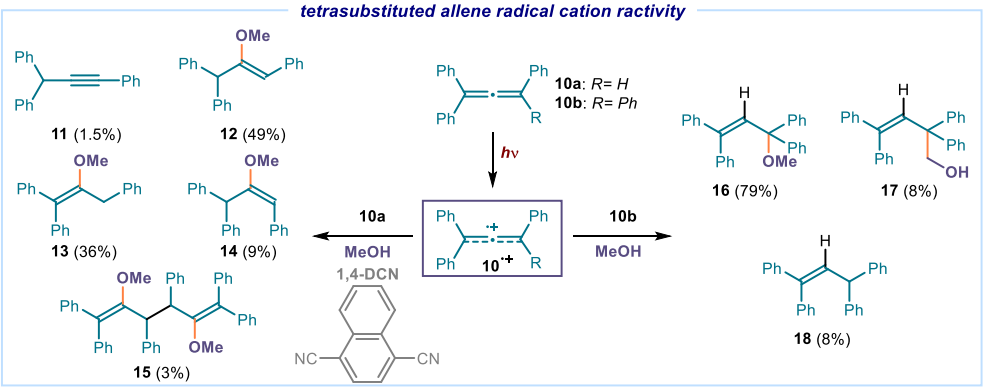

Figure 4.4. UV-light-irradiation of allenes leading to a mixture of products. DCN: dicyanonaphthalene.

This milder allene activation strategy effectively generated the allene radical cation **10**$^{\bullet+}$. The highly reactive intermediate **10**$^{\bullet+}$ then reacted with the solvent (methanol) to

[14] Becker, J. Y.; Zinger, B. "Electrochemical Oxidation of Alkylsubstituted Allenes in Methanol" *Tetrahedron*, **1982**, *38*, 1677; b) Becker, J. Y.; Zinger, B. "Electrochemical Oxidation of Allenic Hydrocarbons in Acetonitrile" *J. Chem. Soc. Perkin Trans.* 2, **1982**, 395; c) Schlegel, G.; Schäfer, H. J. "Elektrochemische Reduktion und Oxidation von Allenen" *Chem. Ber.*, **1983**, *116*, 960.

deliver a mixture of products (**16**:**17**:**18**) with a 10:1:1 ratio.[15] Substituting one of the phenyl groups for hydrogen within the substrate **10** required the addition of a 1,4-dicyanonaphthalene (1,4-DCN) as a photosensitizer and afforded an even more complex mixture of products, including regioisomers (**11-14**) and the dimeric species **15** (right part of Figure 4.4).[16] Similar regioisomeric mixtures were obtained by Arnold when performing the transformation with di- and tetra-cyanoaromatic compounds as electron acceptors.[17]

Mariano reported that also excited iminium ion salts (**19***) could activate allenic derivatives (**20**, **3a**)[18] via SET oxidation (Figure 4.5).[19] Upon excitation and SET from 1,2-propadiene (**20**) to **19***, the ensuing allene radical cation afforded three different products (**21-23**). Variations on the allene substitution (**3a**) resulted in substantial changes in the product distributions (**24-28**).

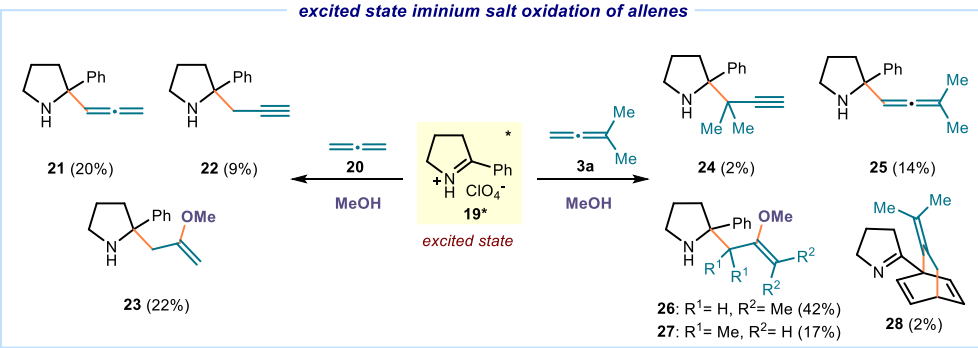

Figure 4.5. Excite-state photochemistry of iminium ion salts with allenes.

[15] Klett, M. W.; Johnson, R. P. "Cumulene Photochemistry: Photoaddition of Neutral Methanol to Phenylallenes" *Tetrahedron Lett.*, **1983**, 24, 1107.

[16] Klett, M. W.; Johnson, R. P. "Photogeneration of Triphenyl C3 Radical Cations: Deprotonation and Nucleophilic Addition as Competitive Pathways" *J. Am. Chem. Soc.*, **1985**, *107*, 6615.

[17] Arnold, D. R. J.; McManus, K. A.; Chan, M. S. W. "Photochemical nucleophile-olefin combination, aromatic substitution (photo-NOCAS) reaction, Part 13. The scope and limitations of the reaction with cyanide anion as the nucleophile" *Can. J. Chem.*, **1997**, 75, 1055; b) Mangion, D.; Arnold, D. R. J.; Cameron, T. S.; Robertson, K. N. "The electron transfer photochemistry of allenes with cyanoarenes. Photochemical nucleophile–olefin combination, aromatic substitution (photo-NOCAS) and related reactions" *Chem. Soc. Perk.Trans.* 2, **2001**, 48.

[18] a) Somekawa, K.; Haddaway, K.; Mariano, P. S. "Electron-Transfer Photochemistry of Allene-Iminium Salt Systems. Probes of Allene Cation Radical Structure by Theoretical and Chemical Techniques" *J. Am. Chem. Soc.*, **1984**, *106*, 3060; b) Haddaway, K.; Somekawa, K.; Fleming, P.; Tossell, J. A.; Mariano, P. S. "The Chemistry of Allene Cation Radicals Probed by the Use of Theoretical and Electron-Transfer Photochemical Methods" *J. Org. Chem.*, **1987**, 52, 4239.

[19] Stavinoha, J. L.; Mariano, P. S. "Novel Photochemical Addition Reactions of Iminium Salts. Electron Transfer Initiated Additions of Olefins to 2-Phenyl-l-pyrrolinium Perchlorate" *J. Am. Chem. Soc.*, **1978**, *100*, 1978; b) Stavinoha, J. L.; Mariano, P. S. "Electron-Transfer Photochemistry of Iminium Salts. Olefin Photoadditions to 2-Phenyl-1-pyrrolinium Perchlorate" *J. Am. Chem. Soc.*, **1981**, *103*, 3136.

The few reported examples based on the SET oxidation of allenes all suffered from regioselectivity issues and considerable limitations in scope. These restrictions mainly originated from the unique reactivity of allene cation radicals **29**$^{\bullet+}$, which are generated upon SET oxidation of allenes **29** (Figure 4.6). These highly reactive intermediates **29**$^{\bullet+}$ are distonic radical cations, where the positive charge mainly resides on the central allene carbon, while the spin density is located on the other two carbon atoms.[18] One of the main reactivity paths exploits the propensity of **29**$^{\bullet+}$ to undergo nucleophilic additions.[17,18] As expected from the charge distribution, this process generally takes place at the central allene carbon and delivers a more stable substituted allyl-type radical **V** (path *i* in Figure 4.6). The ensuing radical trap can then take place at both C-termini of **V**, potentially creating a problem of regioselectivity.

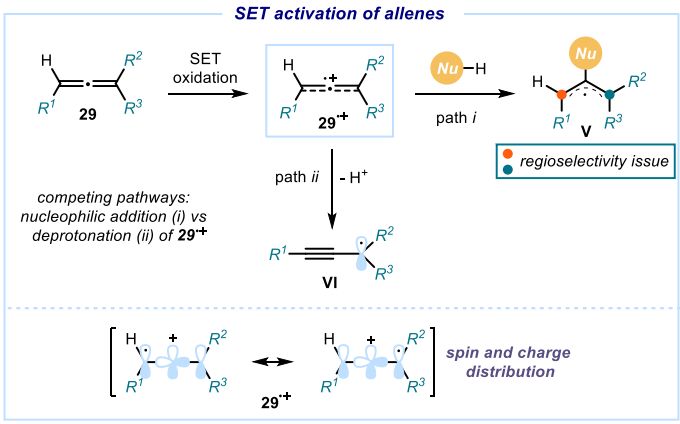

Figure 4.6. Accessing allene cation radicals **29**$^{\bullet+}$ by single-electron transfer (SET) oxidation of allenes, and the competing reaction pathways available to these reactive intermediates.

A competing pathway available to the allene cation radical **29**$^{\bullet+}$ is the deprotonation at the terminal carbon, which leads to a reactive propargyl radical **VI** (path *ii* in Figure 4.6). The multiple reactive manifolds available to **29**$^{\bullet+}$ highlight the difficulty of taming their reactivity, which is why complex mixtures of products are generally obtained.[14,18]

4.3. Targets of the Project

A study of the literature revealed that, while controlling the reactivity of allene radical cations is far from easy, engaging them in enantioselective transformations is unprecedented. To achieve this target, we set out to use the photochemistry of iminium ions to activate allenes **31** by SET oxidation and obtain reactive allene cation radicals **31**$^{\bullet+}$ (Figure 4.7). To address the reactivity challenges connected with the chemistry of allene radical-cations, we planned the use of an allene substrate **31**

adorned with a suitable oxygen-centered nucleophilic handle. This substrate **31** should selectively trigger an intramolecular nucleophilic addition into the central allene carbon of **31**$^{\bullet+}$, thus preventing undesired pathways. This step would produce a substituted double-bond moiety within intermediate **VII** capable of triggering a cascade process, leading to complex cyclic scaffolds.

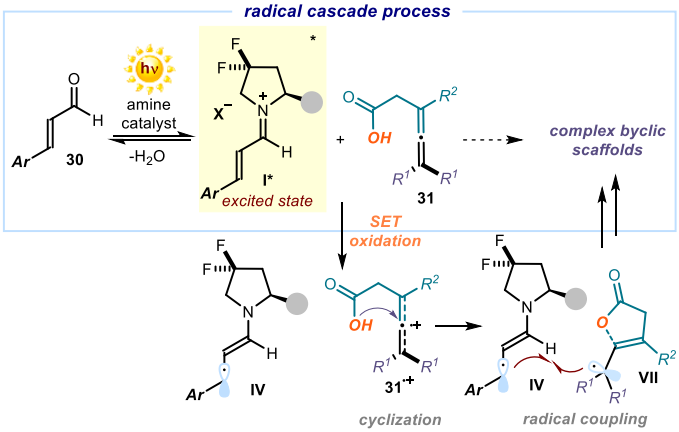

Figure 4.7. Our strategy to for the photo-organocatalytic activation of allenes by SET oxidation to deliver complex polycyclic compounds.

Figure 4.8 shows a more detailed picture of our proposed strategy to develop an enantioselective radical cascade enabled by SET activation of allenes. We envisioned a catalytic cycle where the condensation of a chiral amine catalyst with enal **30** would form the colored iminium ion intermediate **I***. Selective excitation with a single high-power light-emitting diode (LED) turns **I** into a strong oxidant **I*** (estimated reduction potential (E_{red}*(**I***/ **IV**) ≈ +2.40 V,[20] vs Ag/Ag$^+$ in CH_3CN)).[21]

The photo-excited iminium ion **I*** can oxidize the allene substrate **31** bearing a nucleophilic acid moiety. The feasibility of this SET was corroborated by cyclic voltammetry studies (see the experimental section for details), which established that substrates of type **31** have an oxidation potential ranging from +1.76 to +2.28 V (vs. Ag/Ag$^+$ in CH_3CN). The SET activation of allene **31** would consequently form the chiral 5π-electron intermediate **IV** and the allene cation radical **31**$^{\bullet+}$. The acidic moiety within **31**$^{\bullet+}$ would then trigger a polar-radical-crossover nucleophilic addition onto the central carbon of the allene radical cation to afford the tertiary radical **VII**. A stereocontrolled

[20] The redox potential was estimated using the Rehm-Weller approximation. Rehm, D.; Weller, A. "Kinetics of Fluorescence Quenching by Electron and H-Atom Transfer" *Isr. J. Chem.*, **1970**, *8*, 259.

[21] Silvi, M.; Verrier, C.; Rey, Y. P.; Buzzetti, L; Melchiorre, P. "Visible-light Excitation of Iminium Ions Enables the Enantioselective Catalytic β-Alkylation of Enals" *Nat. Chem.*, **2017**, 9, 868.

radical coupling with **IV** would afford intermediate **VIII**. This species contains a reactive β,γ-unsaturated lactone moiety that, acting as an enolate equivalent, could trigger an aldol-type cyclization to afford **IX**. A final acyl migration step would then afford the final product of the cascade, namely the complex bicyclic lactone **32**.

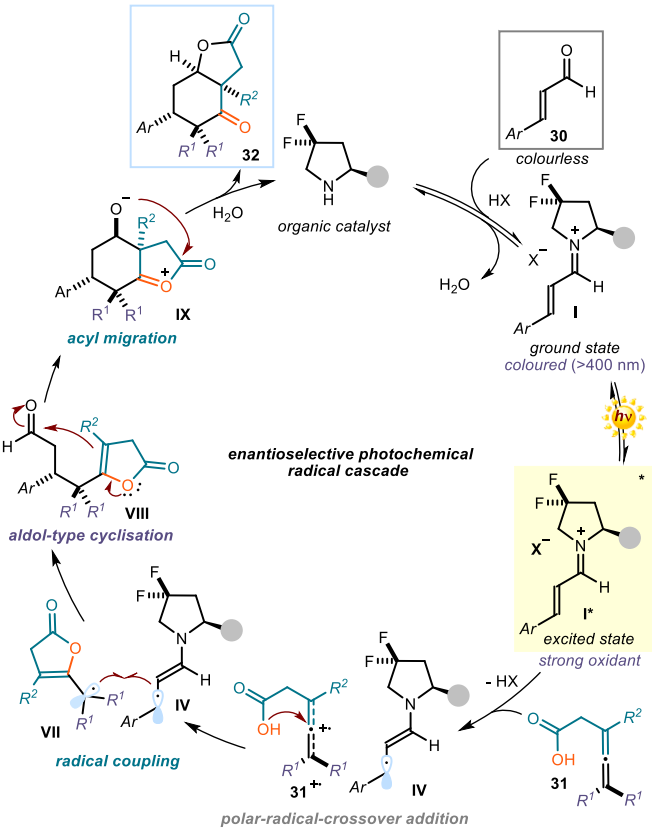

Figure 4.8. Mechanistic proposal for the photo-organocatalytic enantioselective radical cascade triggered by the SET activation of allenic acids **31**.

4.4. Results and Discussion

4.4.1. Optimization

The feasibility of this photochemical plan was evaluated by exploring the reaction of cinnamaldehyde **30a** catalyzed by the *gem*-difluorinated diarylprolinol silylether **33a**, which secured the formation of the chiral iminium ion (Table 4.1). The experiments were conducted in acetonitrile (CH_3CN), under irradiation by a single high-power (HP)

LED (λ_{max} = 420 nm) with an irradiance of 90 mW/cm², as controlled by an external power supply.[22]

Table 4.1. Optimization studies. [a]

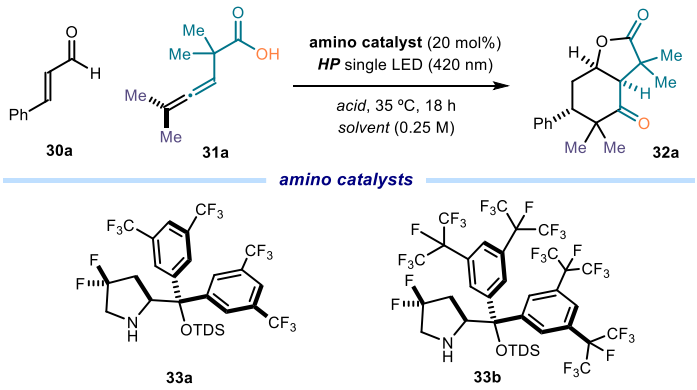

Entry	Catalyst	Acid [mol%]	Solvent	Yield [%][b]	*ee* [%][c]
1	**33a**	TFA (25)	CH_3CN	44	54
2	**33a**	$Zn(OTf)_2$ (25)	CH_3CN	56	60
3	**33a**	$Sc(OTf)_2$ (25)	CH_3CN	0	--
4	**33a**	$Zn(OTf)_2$ (50)	CH_3CN	45	54
5	**33a**	$Zn(OTf)_2$ (50)	CH_2Cl_2	33	54
6	**33a**	$Zn(OTf)_2$ (50)	Benzene	32	48
7	**33b**	$Zn(OTf)_2$ (25)	CH_3CN	29	42
8[d]	**33a**	$Zn(OTf)_2$ (50)	CH_3CN	0	--
9	**33a**	none	CH_3CN	0	--
10	none	$Zn(OTf)_2$ (50)	CH_3CN	0	--

[a] Reactions performed on a 0.1 mmol scale at 35 °C for 18 h using 0.4 mL of solvent under illumination by a single high-power (HP) LED (λ_{max}=420 nm) with an irradiance of 90 mWcm^{-2}; **32a** formed as a single diastereoisomer (dr > 19:1; the diastereoisomeric ratio (dr) was inferred by ^{1}H NMR analysis of the crude mixture. [b] Yield of isolated product **32a** after purification by flash chromatography. [c] Enantiomeric excess determined by HPLC analysis on a chiral stationary phase. [d] No light. TFA: trifluoroacetic acid; TDS: thexyldimethylsilyl.

[22] The vial was placed into an aluminum block on a 3D-printed holder, fitted with a 420 nm high-power single LED. This setup secured a reliable irradiation while keeping a distance of 1 cm between the reaction vessel and the light source. The temperature inside the vial was 35 °C. Details of the experimental set-up, including irradiation and temperature control, are available in the experimental section 4.6.

Allenic acid **31a** was selected as the model substrate because of its oxidation potential (E_p (**31a**$^{\bullet+}$/**31a**) = +2.28 V vs Ag/Ag$^+$ in CH_3CN), which makes it prone to SET activation from the excited iminium ion. Gratifyingly, we observed that TFA (25 mol%), which served the dual role of facilitating iminium ion formation and triggering the aldol-type cyclization of intermediate **VIII** into **IX** (see Figure 4.7), successfully enabled the overall cascade process (entry 1). The complex bicyclic product **32a** was formed with moderate chemical yield and enantioselectivity, but with full control over the relative stereochemistry (dr >19:1, as inferred by ^{1}H-NMR analysis of the crude mixture).

We reasoned that Lewis acids could provide an additional means to assist iminium ion formation while promoting the overall radical cascade. Accordingly, the use of zinc(II) triflate (25 mol%) provided product **32a** with improved efficiency (entry 2, 56% yield, 60% ee, full diastereocontrol). Triflates of trivalent metals, such as $Sc(OTf)_3$, were completely ineffective (entry 3). Increasing the amount of $Zn(OTf)_2$ (entry 4) or using reaction media other than CH_3CN did not improve the efficiency of the cascade process (entries 5 and 6). To further increase the stereocontrol, we used the more encumbered amine catalyst **33b**, which however afforded largely inferior results (entry 7). Control experiments indicated that the Lewis acid co-catalyst, the organic catalyst **33a**, and visible light irradiation were all essential for the reaction to proceed (entries 8-10).

4.4.2. Substrate Scope

Adopting the optimized conditions described in Table 4.1, entry 2, we evaluated the generality of the photochemical radical cascade process (Figure 4.9).

As for the scope of the allenic acid substrates **31**, we observed an increase in enantioselectivity when bulkier ethyl (**32b**), cyclohexyl (**32c**), and cyclododecyl (**32d**) substituents were installed onto the allene moiety. Changing the steric profile of the substituents at the alpha position of the acid moiety within **31** did not significantly affect the reactivity and stereoselectivity of the cascade (products **32e**-**f**). The tetracyclic adduct **32g** bearing two spirocycles could also be successfully synthesized. Regarding the scope of the enal substrate **30**, moderately electron-withdrawing (**32h, 32j**) and electron-donating groups (**32i**) on the aromatic ring were tolerated well.

As a limitation of the system, and in consonance with our previous studies,[2,21] **Error! Bookmark not defined.** aliphatic enals were not suitable substrates as the reactivity was completely inhibited. Remarkably, products **32** were all obtained as single diastereoisomers, since no minor isomers could be detected by ^{1}H NMR analysis of the crude reaction mixtures.

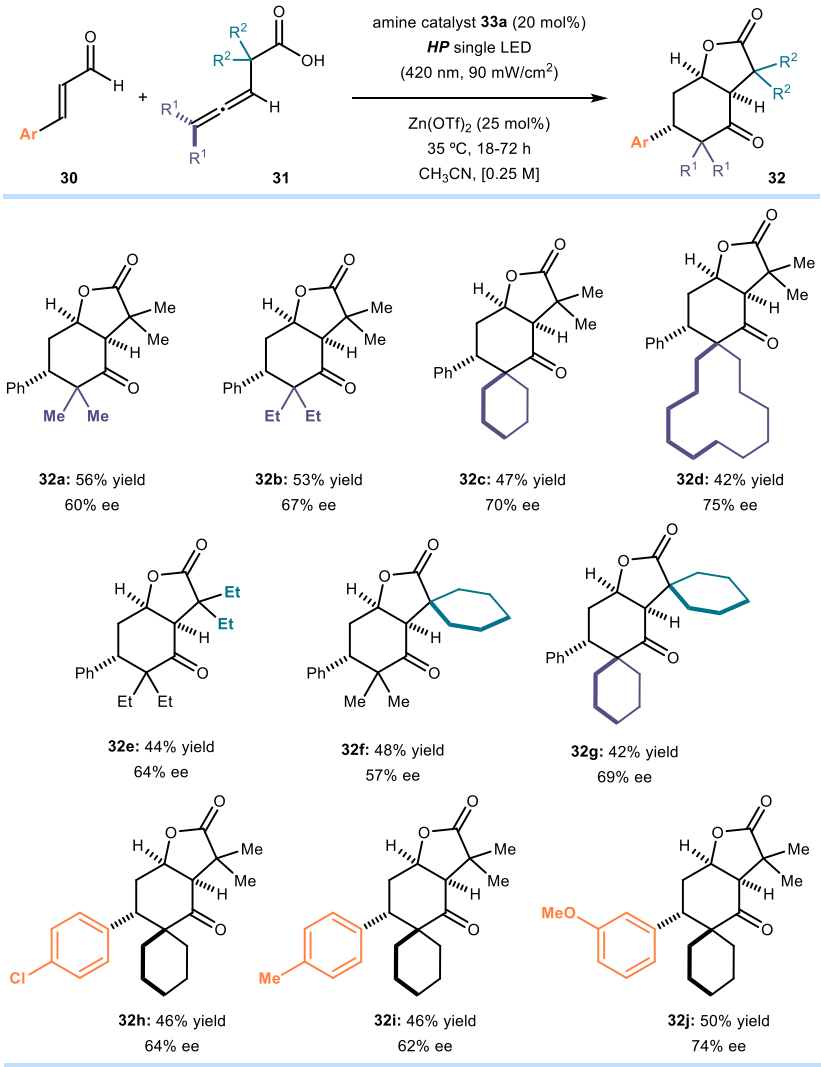

Figure 4.9. Survey of the allenic acids **31** and enals **30** that can participate in the photochemical asymmetric radical cascade process. Reactions performed on 0.1 mmol scale using 3 equiv. of **30**. Yields and enantiomeric excesses of the isolated products **32** are indicated below each entry (average of two runs per substrate). All products were formed as single diastereoisomers (d.r.>19:1); the diastereoisomeric ratio (d.r.) was inferred by ^{1}H NMR analysis of the crude mixture.

We then explored the tendency of substrates with a tetrasubstituted allene moiety (**34**) to participate in the cascade process (Figure 4.10). While the light-mediated radical manifold was still operative, the presence of a fourth substituent on the allene moiety greatly lowered the nucleophilicity of intermediate **35** (which corresponds to **VIII** in the overall mechanistic picture in Figure 4.7). Indeed, **35** could not cyclize further, thus interrupting the cascade. Nevertheless, the treatment of the isolable intermediates **35**

with 2.5 equiv. of a Lewis acid (BF_3•OEt_2) in the presence of 2,6-lutidine (20 mol%) smoothly delivered the complex products **36** containing a quaternary stereocenter α to the carbonyl function. The role of 2,6-lutidine is presumably to neutralize small amounts of HBF_4 generated upon hydrolysis of BF_3•OEt_2 by adventitious moisture.

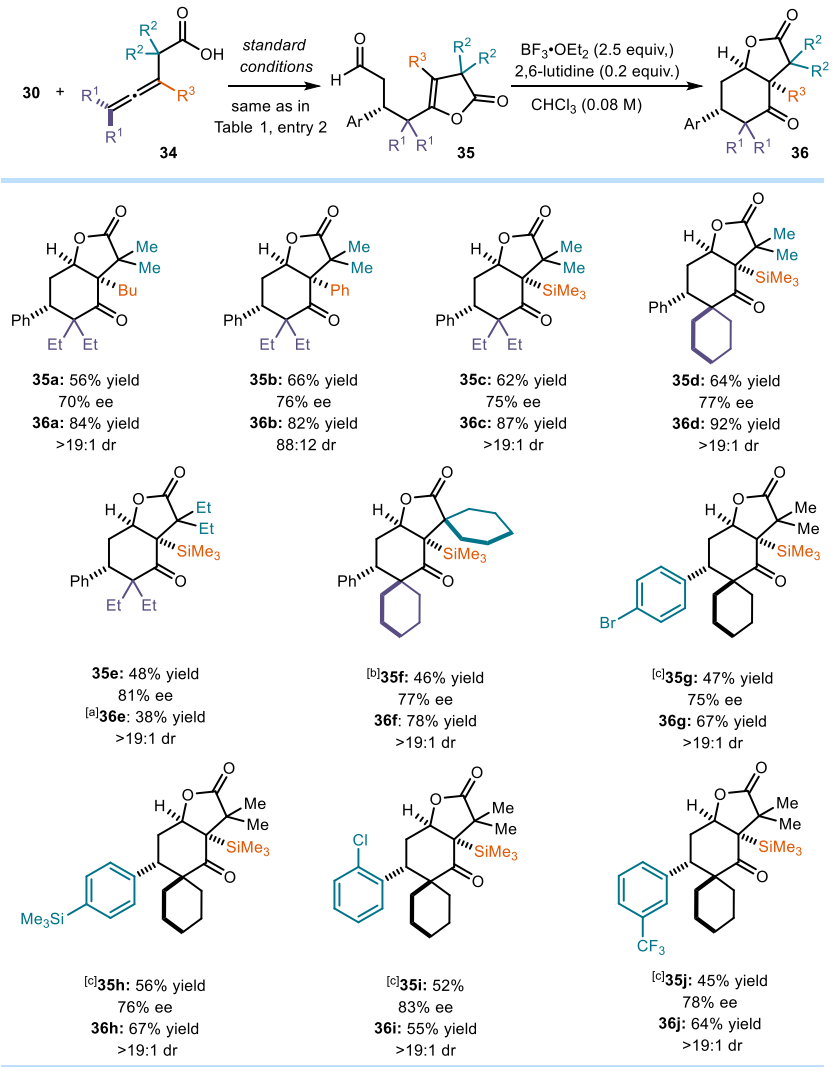

Figure 4.10. Survey of tetrasubstituted allenic acids **34**. *Standard conditions* are those reported in Table 4.1, entry 2. Reactions performed on 0.1 mmol scale using 3 equiv. of **30**. The second cyclization step was performed on the isolated pure adducts **35**. Yields and enantiomeric excesses of the isolated products **35** and **36** are indicated below each entry (average of two runs per substrate). Diastereomeric ratio (dr) was inferred from ^{1}H NMR analysis of the crude mixture. [a]Reaction performed using 5 equiv. of $BF_3 \bullet OEt_2$. [b] Reaction performed using PrCN as the solvent. [c] Reaction performed with TFA (60 mol%) instead of $Zn(OTf)_2$ and using CH_3CN [0.5 M] as the solvent.

The effect of the substituents on allenic acids **34** mirrors the trends observed for substrates **31** since larger groups modestly improved yields and enantioselectivities. Alkyl (product **36a**), aryl (**36b**), and trimethylsilyl (**36c**) groups are tolerated at the R^3 position within substrates **34**. Concerning the enal substrates **30**, strongly electron-withdrawing groups were tolerated on the aromatic ring (**36j**). Notably, synthetically useful groups, which can undergo further functionalization, were also tolerated. These included halogens (**36g, 36i**) and trimethylsilyl (**36h**). The diastereoselectivity of the ring closure was generally excellent (>19:1 dr), except for product **36b** (88:12 dr).

To our surprise, when carrying out the reaction with substrate **34e**, we observed a substantial decrease in the yield of the second cyclization step. Analyzing the outcome of the reaction involving **34e** and BF_3•OEt_2, we identified product **36e'** (31% yield) in addition to **36e** (38% yield) (Figure 4.11). We hypothesized that the unexpected product **36e'** might arise from a Lewis-acid mediated ring-opening of **36e**, which leads to the formation of a stabilized carbocation **X**, due to the β-silicon effect (Figure 4.11.a). Intermediate **X** can then undergo a cationic rearrangement driven by the excess of BF_3•OEt_2 and by the formation of an α,β-unsaturated ketone within **36e'**. Interestingly, adduct **35d** was also prone to the BF_3-catalyzed cyclization shown in Figure 4.10. This implies that the use of a more vigorous Lewis acid ($Me_3Si(OTf)$) can enable a divergent cyclisation path leading to structurally different chiral adducts from the same intermediate. The rearranged product (isolated as the methyl ester **37** after treatment with Me_3SiCHN_2) could then be efficiently obtained in a 60% overall yield (Figure 4.11.b).

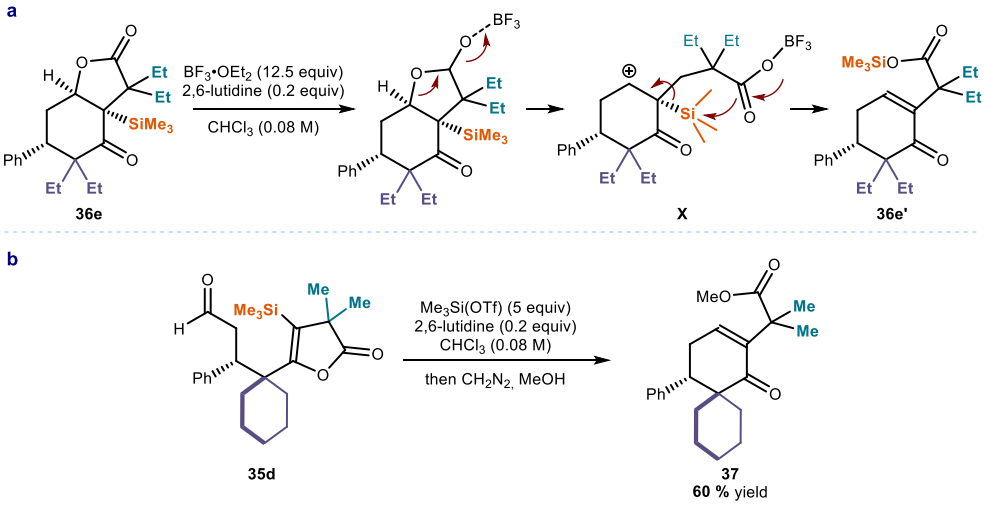

Figure 4.11. a) A plausible mechanism for the formation of **36e'** when using an excess of BF_3•OEt_2. b) Optimized conditions for the manipulation of product **35d**. Reactions performed on 0.08 mmol scale.

Crystals of compound **36f** were suitable for X-ray crystallographic analysis (Figure 4.12), [23] which secured the absolute configuration and confirmed the relative configuration of the products previously assigned by NOESY experiments.

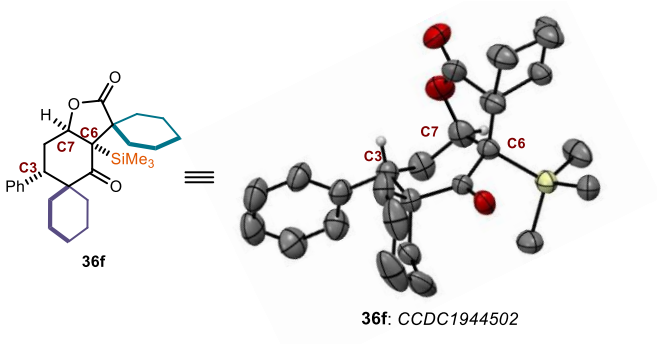

Figure 4.12. ORTEP representation of the X-ray crystal of **36f**.

4.4.3. Computational Studies[24]

The second part of the cascade process involves the aldol cyclization leading to products **32** from intermediates of type **VIII** (see Figure 4.8) and products **36** from intermediates **35**. Mukaiyama[25] already described the intermolecular aldol reaction of enol esters with aldehydes promoted by Lewis acids. However, its diastereoselectivity in the intramolecular variant has never been examined. Thus, it is mechanistically interesting, especially when considering the full diastereoselectivity observed. We resorted to DFT calculations to gain more insight into the origin of the relative stereocontrol and the role of Zn as a catalyst (Figure 4.13).[26]

---

[23] Crystallographic data for compound **36f** has been deposited with the Cambridge Crystallographic Data Centre,

accession number CCDC 1944502.

[24] Computational studies were carried out by Dr. Luca A. Perego.

[25] a) Mukaiyama, T.; Izawa, T.; Saigo, K. "Reaction of Enol Acetate with Acetal and Carbonyl Compound in the Presence of Lewis Acid" *Chem. Lett.*, **1974**, 323; b) Yanagisawa, M.; Shimamura, T.; Iida, D.; Matsuo, J.; Mukaiyama, T. "Aldol Reaction of Enol Esters Catalyzed by Cationic Species Paired with Tetrakis(pentafluorophenyl)borate" *Chem. Pharm. Bull.*, **2000**, *48*, 1838; c) Masuyama, Y.; Sakai, T.; Kurusu, T. "Palladium-Catalyzed Aldol-Type Condensation by Enol Esters with $SnCl_2$" *Tetrahedron Lett.*, **1993**, 34, 653; d) Yanagisawa, A.; Kushihara, N.; Yoshida, K. "Catalytic Enantioselective Synthesis of Chiral γ-Butyrolactones" *Org. Lett.*, **2011**, *13*, 1576.

[26] Level of theory for geometry optimization and frequency calculations: B3LYP/6-31+G(d) (for C, H, N, O), LANL2TZ/LANL2 (for Zn), IEF-PCM (CH_3CN); for single-point electronic energies: B3LYP-D3BJ/6-311+G(2d,2p) (for C, H, N, O), LANL08+/LANL2 (for Zn), IEF-PCM (CH_3CN). See the experimental section for full computational details.

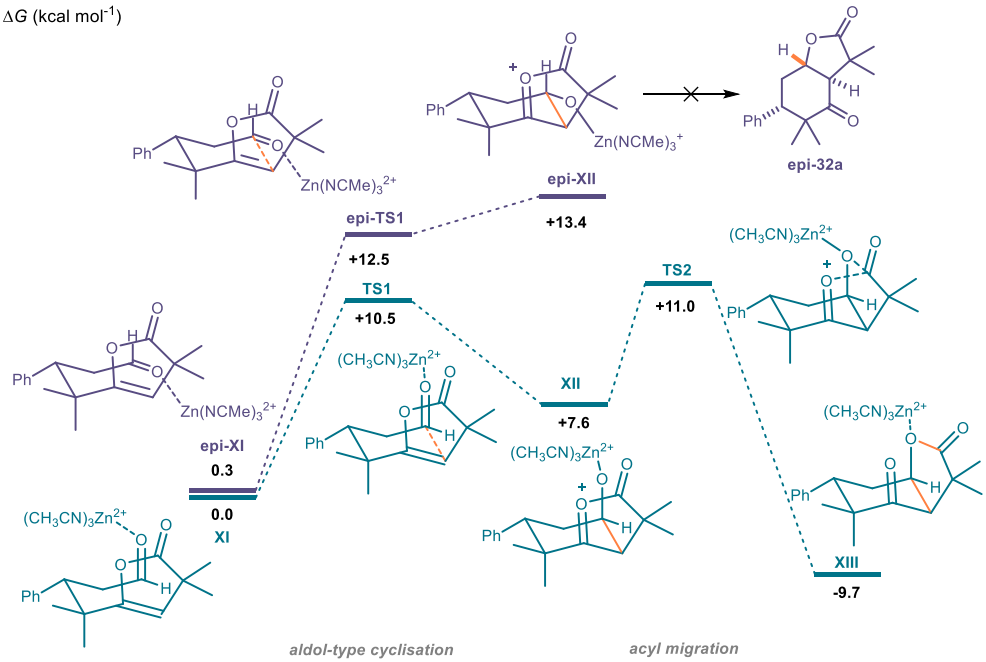

Figure 4.13. In green: Computed Gibbs-energy profile of the Zn^{2+} catalyzed aldol-type cyclization of the aldehyde intermediate **XI** deriving from the photochemical coupling of the allene carboxylic acid **32a** and cinnamaldehyde. In purple: Hypothetical pathway for the Zn-catalysed formation of **epi-32a** from intermediate **epi-XI**, as studied by DFT computations. Relative Gibbs energies at 298 K are reported in kcal mol^{-1}.

$Zn((NCCH_3)_3)^{2+}$, acting as a Lewis acid,[27] coordinates the aldehyde oxygen, thereby enhancing the electrophilicity of the carbonylic carbon. In the reactive conformation of this Lewis acid-substrate adduct (**XI**), the forming cyclohexane ring is in a chair-like conformation where the aldehyde oxygen and the oxygen of the enol ether are in pseudo-axial positions while the phenyl ring occupies an equatorial site. The aldol-type addition is predicted to be a stepwise process: first, an acyloxonium intermediate **XII** is formed through transition state **TS1** ($\Delta G^{\ddagger}$ = 10.5 kcal mol^{-1}). This reaction is endergonic (ΔG = +7.6 kcal mol^{-1}), but the acyl transfer via **TS2** is exergonic and it provides the thermodynamic driving force for the overall process (total ΔG = −9.7 kcal mol^{-1} from **XI** to **XIII**). For the crucial acyl transfer process to take place, both oxygen

[27] $Zn(OTf)_2$ is almost completely dissociated in CH_3CN solutions, as evinced by an association constant as low as $K_a = 3 \cdot 10^{-2}$ M^{-1}, which was measured by electroanalytical studies, see: Fujinaga, T.; Sakamoto, I. "Electrochemical studies of sulfonates in non-aqueous solvents. Journal of Electroanalytical Chemistry and Interfacial Electrochemistry" *J. Electroanal. Chem.*, **1976**, *73*, 235. Therefore, solvent-coordinated Zn^{2+} was considered as the Lewis acid in the theoretical calculations. As for the solvent, an electrostatic model (IEF-PCM) has been employed to reproduce bulk solvation effects.

atoms (origin and terminus of the migration) must be in close proximity, which is only possible if they are in a 1,3-diaxial-like relationship. This stereochemical requirement determines the experimentally observed diastereoselectivity for the *cis*-fused bicyclic system.

The Zn-catalyzed pathway expected to lead to the diastereomer **epi-32a**, which is not formed under experimental conditions, was also examined (Figure 4.13 in purple). A transition state **epi-TS1** corresponding to this reaction could be located only 2.0 kcal mol⁻¹ higher in free energy than **TS1** (Figure 4.13 in green). However, the acyloxonium **epi-XII** was predicted to be slightly higher in free energy ($\Delta G^{\ddagger}$ = 13.4 kcal mol⁻¹) than **epi-TS1** itself. More importantly, there is no possibility for acyl migration proceeding from this species to **epi-32a**. This hypothetical pathway is thus not relevant for the reaction under study.

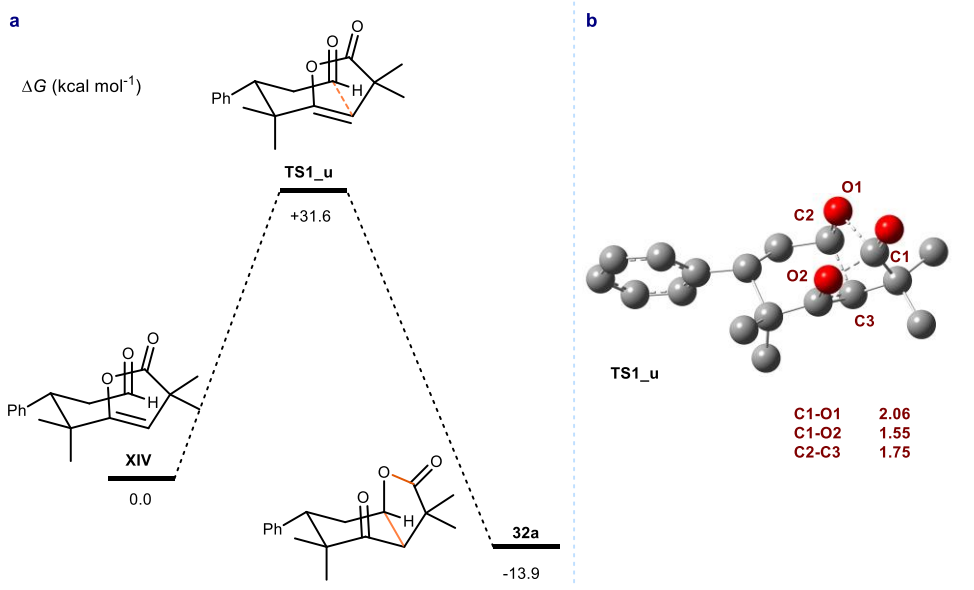

Figure 4.14 a) Uncatalyzed pathway for the aldol-type cyclization of intermediate **XIV**, as studied by DFT computations; b) A ball-and-stick model of **TS1_u** (hydrogen atoms removed for clarity) with selected bond lengths (in Å) is reported, showing that the C2-C3 bond forms at the same time as the migration of the acyl group from O2 to O1. Relative Gibbs energies (Δ*G*) at 298 K are reported in kcal mol⁻¹.

Finally, we also examined computationally the possibility for the cascade process to take place in an uncatalyzed fashion. Calculations revealed that, in the absence of Zn catalysis, the conversion of **XIV** to **32a** would take place in one step without a stable acyloxonium intermediate similar to **XII** (Figure 4.13). Indeed, cyclization and acyl migration would take place in a concerted fashion through transition state **TS1_u** (Figure 4.14), in which C–C bond formation and acyl migration take place at the same

time. However, the computed activation energy of this process ($\Delta G^{\ddagger}$ = +31.6 kcal mol^{-1}) suggested that this pathway is not accessible at the temperature at which the reaction is carried out (25–35 °C) and catalysis by Zn^{2+} is actually required for the reaction to take place.

4.5. Conclusions

In summary, we have exploited the photochemical activity of chiral iminium ions to activate allenes by SET oxidation. The propensity of allene radical cations to undergo the addition of nucleophiles was crucial to design a cascade process leading to complex, chiral polysubstituted bicyclic lactones with high stereocontrol. DFT calculations aided us in establishing the crucial role of Zn as a Lewis acid catalyst to achieve excellent diastereoselectivities. This report offers the first example of the use of allene radical cations in asymmetric transformations and we expect that this activation strategy may offer fresh opportunities to further expand the synthetic potential of allenes.

4.6. Experimental

4.6.1. General Information

The ^{1}H NMR, ^{19}F NMR, ^{13}C NMR spectra, and HPLC or UPC2 traces are available in the literature**Error! Bookmark not defined.** and are not reported in the present dissertation.

The NMR spectra were recorded at 300 MHz, 400 MHz, and 500 MHz for ^{1}H or at 75 MHz, 101 MHz, and 126 MHz for ^{13}C, 376 MHz for ^{19}F, respectively. The chemical shifts (δ) for ^{1}H and ^{13}C{^{1}H} are given in ppm relative to residual signals of the solvents ($CHCl_3$ @ 7.26 ppm ^{1}H NMR, 77.00 ppm ^{13}C NMR). Coupling constants are given in Hz. The following abbreviations are used to indicate the multiplicity: s, singlet; d, doublet; t, triplet; q, quartet; m, multiplet; br s, broad signal.

High-resolution mass spectra (HRMS) were obtained from the ICIQ High-Resolution Mass Spectrometry Unit on MicroTOF Focus and Maxis Impact (Bruker Daltonics) with electrospray ionization. X-ray data were obtained from the ICIQ X-Ray Unit using an Apex DUO diffractometer equipped with a Kappa 4-axis goniometer, an APEX II 4K CCD area detector, a Microfocus Source E025 IuS using MoKα radiation, Quazar MX multilayer Optics as monochromator and an Oxford Cryosystems low-temperature device Cryostream 700 plus (T = -173 °C). Optical rotations were measured on a

Polarimeter Jasco P-1030 and are reported as follows: $[\alpha]_D$ ambient temperature (c in g per 100 mL, solvent). Melting points are reported as a range and were determined using a Mettler Toledo MP70 melting point apparatus. Cyclic voltammetry studies were carried out on a Princeton Applied Research PARSTAT 2273 potentiostat offering compliance voltage up to ± 100 V (available at the counter electrode), ± 10 V scan range and ± 2 A current range.

The authors are indebted to the team of the Research Support Area at ICIQ.

General Procedures. All reactions were set up under an argon atmosphere in oven-dried glassware using standard Schlenk techniques unless otherwise stated. Synthesis grade solvents were used as purchased. Anhydrous solvents were taken from a commercial SPS solvent dispenser. Chromatographic purification of products was accomplished using flash column chromatography (FC) on silica gel (35-70 mesh). For thin-layer chromatography (TLC) analysis throughout this work, Merck precoated TLC plates (silica gel 60 GF_{254}, 0.25 mm) were used, using UV light as the visualizing agent and either phosphomolybdic acid in EtOH, *p*-anisaldehyde or basic aqueous potassium permanganate ($KMnO_4$) and heat as developing agents. Organic solutions were concentrated under reduced pressure on a Büchi rotary evaporator (*in vacuo* at 40 °C, ~5 mbar).

Determination of Diastereomeric Ratio. The diastereomeric ratio was determined by ^{1}H NMR analysis of the crude reaction mixture through integration of diagnostic signals.

Determination of Enantiomeric Purity: HPLC analysis on a chiral stationary phase was performed on an Agilent 1200 series HPLC, using Daicel Chiralpak IC-3 and ID-3 columns with ^{i}PrOH:*n*-hexane as the eluent. UPC^2 analysis on a chiral stationary phase was performed on a Waters Acquity instrument using IC-3, IE-3, ID-3, IA, CEL-1, and AMY1 chiral columns. The exact conditions for the analyses are specified within the characterization section. HPLC and UPC^2 traces were compared to racemic samples prepared by running the reaction in the presence of a catalytic amount (20 mol%) of an approximately 1:1 mixture of (2*R*, 5*R*)- and (2*S*, 5*S*)-2-*tert*-butyl-3-methyl-5-benzyl-4-imidazolidinone, which are commercially available from Sigma Aldrich.

Materials: Commercial grade reagents and solvents were purchased at the highest commercial quality from Sigma Aldrich, Fluka, Acros Organics, Fluorochem, or Alfa Aesar and used as received unless otherwise stated. Chiral secondary amine catalysts **33a** and **33b** were prepared according to the reported literature.[21] Cinnamaldehyde **30a**, 4-chlorocinnamaldehyde, and 4-bromocinnamaldehyde are commercially available.

Cinnamaldehyde **30a** was distilled prior to use. The rest of the enals were prepared according to a literature procedure.[28]

4.6.2. Substrate Synthesis

Synthesis of allenic acids 31a and 34

The synthetic plan adopted for the preparation of most of the allenic acid substrates is summarized in Figure 4.15. According to the General Procedure A, propargylic esters (**38**) were obtained by addition of alkynyllithium compound to ketones and reaction of the so formed tertiary lithium alcolates with acyl chlorides. These esters (**38**) were subjected to the conditions of the Ireland-Claisen rearrangement (General Procedure B), *i.e.* the corresponding silyl ketene acetals were formed by enolization with LDA and quenching with Me_3SiCl. The silyl ketene acetals underwent a spontaneous [3,3]-sigmatropic rearrangement below room temperature, which delivered silyl esters. *In situ* hydrolysis finally delivered the required allenic acids (**34**).

For trisubstituted allenic acids **31**, the sequence was performed starting from ethynyltrimethylsilane ($R^1 = Me_3Si$, Figure 3.19). The allenic acid can be protodesilylated efficiently with KF in DMSO at high temperatures (General Procedure C). Some substrates have been prepared by different procedures, which are detailed in the following for each compound.

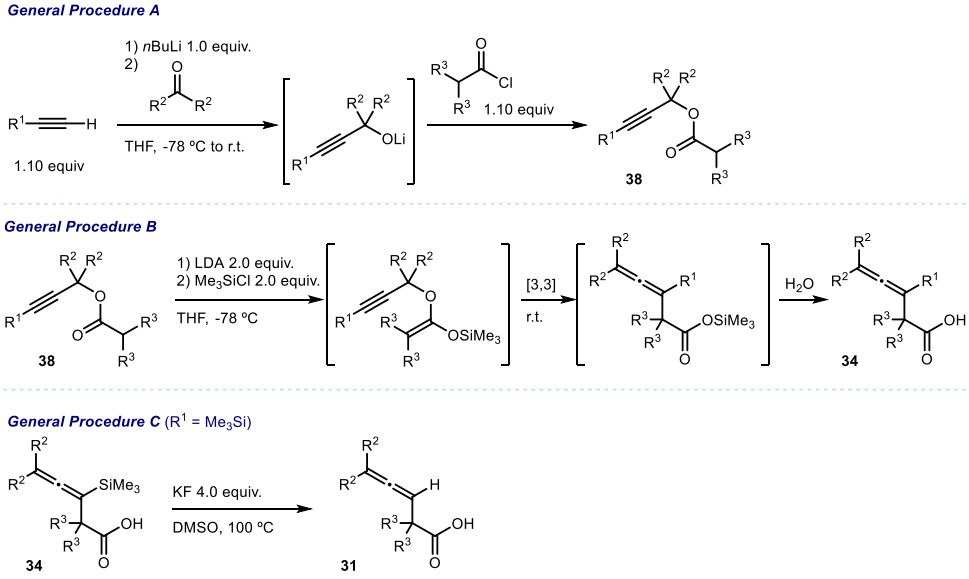

Figure 4.15. Synthesis of allenic acids.

[28] Battistuzzi, G.; Cacchi, S.; Fabrizi, G. "An Efficient Palladium-Catalyzed Synthesis of Cinnamaldehydes from Acrolein Diethyl Acetal and Aryl Iodides and Bromides" *Org. Lett.* **2003**, *5*, 777.

General Procedure A – Synthesis of Propargylic Esters 38

A round-bottom flask of appropriate size equipped with a magnetic stirrer and an argon inlet tube was conditioned with argon. Dry THF (3.0 mL per mmol of substrate) and the appropriate 1-alkyne (1.1 equiv.) were introduced by syringe. The solution was cooled to –78 °C with a dry ice/acetone bath, then *n*BuLi (dispensed as a 2.5 M solution in hexanes, 0.40 mL per mmol of substrate, 1.0 equiv.) was added dropwise. After stirring for 15 minutes at –78 °C, the appropriate ketone was added. The cold bath was then removed and the mixture was allowed to warm up to room temperature.

The solution was again cooled to –78 °C, and an acyl chloride (1.1 equiv.) was added by syringe. The bath was removed and the mixture was left stirring overnight at room temperature.

Saturated aqueous NH_4Cl solution (0.20 mL per mmol of substrate) was added and most of the THF was evaporated under reduced pressure. The residue was diluted with Et_2O (5 mL per mmol of substrate) and extracted with water (3 x 1 mL per mmol of substrate), then with brine. The organic layer was dried over Na_2SO_4 and concentrated *in vacuo*. The organic extract was then filtered through a short pad of silica gel. Concentration under reduced pressure and purification as described for each compound yielded the required propargyl ester.

General Procedure B – Ireland-Claisen-Saucy-Marbet Rearrangement of Propargylic Esters 38

According to a procedure adapted from the literature,[29] a round-bottom flask of appropriate size equipped with a magnetic stirrer and an argon inlet tube was conditioned under argon. Dry THF (2.5 mL per mmol of substrate) and *i*Pr_2NH (282 µL per mmol of substrate, 2.0 equiv.) were introduced by syringe. After cooling to –78 °C, LDA was prepared *in situ* by adding *n*BuLi (2.5 M solution in hexanes, 0.80 mL per mmol of substrate, 2.0 equiv.). The appropriate propargylic ester substrate dissolved in THF (0.4 mL per mmol of substrate) was then added dropwise by syringe. The resulting solution was stirred at –78 °C for 30 minutes, then chlorotrimethylsilane (254 µL per mmol of substrate, 2.0 equiv.) was added. The bath was removed and the mixture was stirred overnight at room temperature.

Saturated aqueous NH_4Cl solution (200 µL per mmol of substrate) was added and most of the THF was evaporated under reduced pressure. The residue was diluted with Et_2O (10 mL per mmol of substrate) and extracted with HCl (1 M in water, 3 x 2 mL per mmol

[29] Baldwin, J. E.; Bennett, P. A. R.; Forrest, A. K. "Preparation and decarboxylation of allenyl acetic acids: a route to substituted buta-1,3-dienes" *J. Chem. Soc., Chem. Commun.*, **1987**, 250.

of substrate), then with brine. The organic layer was dried over Na_2SO_4 and concentrated *in vacuo*. The residue was purified as described in detail for each compound.

General Procedure C – Protodesilylation of Trimethylsilyl-Substituted Allenic Acids 34

According to a procedure adapted from the literature,[30] a mixture of the appropriate trimehylsilyl-substituted allenic acid and KF (4.0 equiv.) in dry DMSO (2.5 mL per mmol of substrate) was stirred at 100 °C overnight. The crude reaction mixture was diluted tenfold with water and extracted with EtOAc (13 volumes of the original mixture, subdivided into 4 portions). The organic extracts were back-extracted with water (2.5 times the volume of the original mixture, 4 times) to remove DMSO, dried over Na_2SO_4, and concentrated under reduced pressure. The residue was dissolved in CH_2Cl_2 and filtered through a short plug of silica gel. Concentration under reduced pressure afforded the required product **31**.

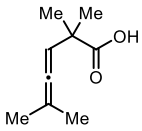

2,2,5-Trimethylhexa-3,4-dienoic acid (31a)

The title compound was prepared by the Cannizzaro reaction of 2,2,5-trimethylhexa-3,4-dienal, which was in turn obtained from isobutyraldehyde and 2-methylbut-3-yn-2-ol according to a literature procedure.[31] A solution of NaOH (1.8 g, 45 mmol, 3 equiv.) in water (1.8 mL) was added to a solution of 2,2,5-trimethylhexa-3,4-dienal (2.07 g, 15 mmol) in MeOH (7.5 mL). The resulting mixture was heated at 60 °C overnight.

The mixture was diluted with water (10 mL) and brine (10 mL) and extracted with Et_2O (4 x 12.5 mL). The aqueous phase was acidified with concentrated HCl and extracted with Et_2O (4 x 12.5 mL). The latter organic extracts were pooled, dried over Na_2SO_4, and concentrated under reduced pressure. The residue was purified by low-temperature crystallization from hexanes. The crude material was dissolved in the required amount of hexanes at room temperature and cooled to –78 °C in a dry ice/acetone bath. The solid was collected by filtration at reduced pressure and washed with a small amount of cold (–78 °C) hexanes. The title compound was thus obtained in the form of a white solid (402 mg, 17% yield). The spectroscopic characterization

[30] Chan, T. H.; Mychajlowskij, W. "Cleavage of the silicon-vinyl carbon bond by fluoride ion: An unexpected β-hydroxy effect" *Tetrahedron Lett.*, **1974,** *39*, 3479.

[31] Diaf, I.; Joffrin, A.; Lemière, G.; Duñach, E. "Synthesis and odour evaluation of allenic derivatives" *Flavour Frag. J.*, **2015,** *30*, 478.

matched with data reported in the literature.[32] If desired, 2,2,5-trimethylhexa-3,4-dien-1-ol can be obtained from the first Et_2O extract.

^{1}H NMR (400 MHz, $CDCl_3$) δ 5.20 (sept, *J* = 2.8 Hz, 1H), 1.71 (s, 3H), 1.70 (s, 3H), 1.29 (s, 6H).

^{13}C NMR (101 MHz, $CDCl_3$) δ 200.5, 183.7, 99.1, 95.3, 42.8, 25.3, 20.6.

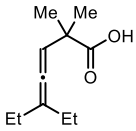

5-Ethyl-2,2-dimethylhepta-3,4-dienoic acid (31b)

The reaction of 5-ethyl-2,2-dimethyl-3-(trimethylsilyl)hepta-3,4-dienoic acid (**34b**, 382 mg, 1.5 mmol) according to general procedure C yielded the title compound in the form of a colorless oil (249 mg, 91% yield).

^{1}H NMR (300 MHz, $CDCl_3$) δ 5.41 (p, *J* = 3.2 Hz, 1H), 1.98 (qd, *J* = 7.4, 3.2 Hz, 4H), 1.29 (s, 6H), 0.99 (t, *J* = 7.4 Hz, 6H).

^{13}C NMR (75 MHz, $CDCl_3$) δ 198.8, 183.5, 112.2, 99.4, 42.8, 25.8, 25.4, 12.4.

HRMS (ESI) *m*/*z* Calculated for $C_{11}H_{17}O_2^-$ [M–H]$^-$: 181.1234, found 181.1233.

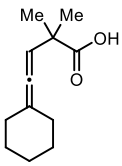

4-Cyclohexylidene-2,2-dimethylbut-3-enoic acid (31c)

The reaction of 4-cyclohexylidene-2,2-dimethyl-3-(trimethylsilyl)but-3-enoic acid (**34c**, 1.0 g, 3.75 mmol) according to general procedure C yielded the title compound in the form of a white solid (649 mg, 89% yield).

^{1}H NMR (300 MHz, $CDCl_3$) δ 5.20 (td, *J* = 2.5, 1.2 Hz, 1H), 2.23 – 2.01 (m, 4H), 1.72 – 1.39 (m, 6H), 1.29 (s, 6H).

^{13}C NMR (101 MHz, $CDCl_3$) δ 197.1, 183.7, 106.5, 95.2, 42.8, 31.6, 27.7, 26.2, 25.4.

HRMS (ESI) *m*/*z* Calculated for $C_{12}H_{17}O_2^-$ [M–H]$^-$: 193.1234, found 193.1235.
m.p. = 50 – 54 °C

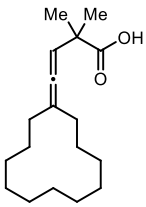

4-Cyclododecylidene-2,2-dimethylbut-3-enoic acid (31d)

The reaction of 4-cyclododecylidene-2,2-dimethyl-3-(trimethylsilyl)but-3-enoic acid (**34d**, 351 mg, 1.0 mmol) according to general procedure C yielded the title compound in the form of a colorless foam (255 mg, 92% yield).

^{1}H NMR (400 MHz, $CDCl_3$) δ 5.35 (p, *J* = 2.7 Hz, 1H), 2.06 (ddt, *J* = 7.4, 5.0, 2.5 Hz, 4H), 1.56 – 1.45 (m, 4H), 1.42 – 1.29 (m, 20H).

[32] Naapuri, J.; Rolfes, J. D.; Keil, J.; Manzuna Sapu, C.; Deska, J. "Enzymatic halocyclization of allenic alcohols and carboxylates: a biocatalytic entry to functionalized O-heterocycles" *Green Chem.*, **2017**, *19*, 447.

^{13}C NMR (101 MHz, $CDCl_3$) δ 200.8, 183.7, 106.0, 97.4, 43.0, 29.8, 25.6, 24.7, 24.4, 24.3, 23.6, 22.7.

HRMS (ESI) *m/z* Calculated for $C_{18}H_{29}O_2^-$ $[M-H]^-$: 277.2173, found 277.2171.

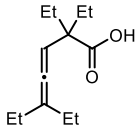

2,2,5-Triethylhepta-3,4-dienoic acid (31e)

The reaction of 2,2,5-triethyl-3-(trimethylsilyl)hepta-3,4-dienoic acid (**34e**, 200 mg, 0.71 mmol) according to general procedure C yielded the title compound in the form of a colorless oil (145 mg, 98% yield).

^{1}H NMR (300 MHz, $CDCl_3$) δ 5.79 (s, 1H), 5.32 (p, *J* = 3.2 Hz, 1H), 2.07 – 1.91 (m, 4H), 1.68 (q, *J* = 7.4 Hz, 4H), 0.99 (t, *J* = 7.4 Hz, 6H), 0.84 (t, *J* = 7.4 Hz, 6H).

^{13}C NMR (75 MHz, $CDCl_3$) δ 199.9, 174.5, 111.3, 95.8, 51.5, 28.7, 25.8, 12.5, 9.0.

HRMS (ESI) *m/z* Calculated for $C_{13}H_{22}O_2^-$ $[M-H]^-$: 209.1547, found 209.1551.

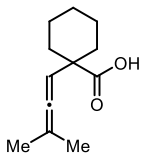

1-(3-Methylbuta-1,2-dien-1-yl)cyclohexane-1-carboxylic acid (31f)

The title compound was prepared by the oxidation of 1-(3-methylbuta-1,2-dien-1-yl)cyclohexane-1-carbaldehyde (950 mg, 5.3 mmol, prepared from 2-methylbut-3-yn-2-ol and cyclohexanecarbaldehyde as described in the literature[31]) with freshly prepared Ag_2O according to a reported protocol.[33] Purification by flash chromatography on silica gel (eluent: hexanes:EtOAc 90:10) afforded the title compound in the form of an off-white solid (380 mg, 37% yield).

^{1}H NMR (300 MHz, $CDCl_3$) δ 4.99 (p, *J* = 2.9 Hz, 1H), 2.03 – 1.88 (m, 2H), 1.70 (s, 6H), 1.64 – 1.25 (m, 8H).

^{13}C NMR (75 MHz, $CDCl_3$) δ 201.8, 182.1, 99.0, 94.3, 47.3, 33.6, 25.8, 23.1, 20.4.

HRMS (ESI) *m/z* Calculated for $C_{12}H_{17}O_2^-$ $[M-H]^-$: 193.1234, found 193.1236.

m.p. = 101 – 105 °C

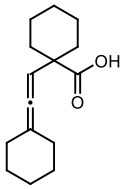

1-(2-Cyclohexylidenevinyl)cyclohexane-1-carboxylic acid (31g)

The reaction of 1-(2-cyclohexylidene-1-(trimethylsilyl)vinyl)cyclohexane-1-carboxylic acid (**34g**, 200 mg, 0.65 mmol) according to general procedure C yielded the title compound in the form of white solid (110 mg, 72% yield).

^{1}H NMR (300 MHz, $CDCl_3$) δ 4.99 (p, *J* = 2.2 Hz, 1H), 2.23 – 1.89 (m, 6H), 1.71 – 1.25 (m, 14H).

^{13}C NMR (75 MHz, $CDCl_3$) δ 198.3, 182.1, 106.3, 94.1, 47.4, 33.7, 31.5, 27.7, 26.2, 25.8, 23.1.

[33] Campaigne, E.; LeSuer, W. M. "Alloxantin Dihydrate" *Organic Syntheses*, **1953**, 33, 94.

HRMS (ESI) *m/z* Calculated for $C_{15}H_{21}O_2^-$ $[M-H]^-$: 233.1547, found 233.1552.

m.p. = 99 – 101 °C

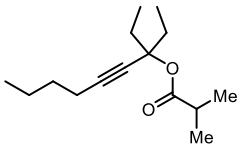

3-Ethylnon-4-yn-3-yl isobutyrate (38a)

The reaction of pentan-3-one (861 mg 10 mmol), 1-hexyne (1.25 mL, 11 mmol), and isobutyryl chloride (1.15 mL, 11 mmol) according to General Procedure A (purified by flash chromatography on silica gel, eluent: hexanes) gave the title compound in the form of a colorless oil.

^{1}H NMR (500 MHz, $CDCl_3$) δ 2.49 (hept, *J* = 7.0 Hz, 1H), 2.22 (t, *J* = 7.0 Hz, 2H), 2.02 (dq, *J* = 13.7, 7.4 Hz, 2H), 1.86 (dq, *J* = 13.7, 7.4 Hz, 2H), 1.53 – 1.45 (m, 2H), 1.45 – 1.36 (m, 2H), 1.14 (d, *J* = 6.9 Hz, 6H), 0.95 (t, *J* = 7.4 Hz, 6H), 0.90 (t, *J* = 7.3 Hz, 3H).

^{13}C NMR (101 MHz, $CDCl_3$) δ 175.5, 86.3, 80.3, 79.8, 35.0, 31.2, 31.0, 22.0, 19.2, 18.6, 13.7, 8.5.

HRMS (ESI) *m/z* Calculated for $C_{15}H_{26}NaO_2$ $[M+Na]^+$: 261.1825, found 261.1824.

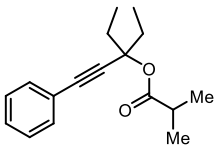

3-Ethyl-1-phenylpent-1-yn-3-yl isobutyrate (38b)

The esterification of the known 3-ethyl-1-phenylpent-1-yn-3-ol[34] (565 mg, 3.0 mmol) with isobutyril chloride (377 µl, 3.6 mmol, 1.2 equiv.) and triethylamine (836 µL, 6.0 mmol, 2.0 equiv.) in CH_2Cl_2 (10 mL) yielded the title compound in quantitative yield (770 mg, 76% yield).

^{1}H NMR (300 MHz, $CDCl_3$) δ 7.48 – 7.40 (m, 2H), 7.32 – 7.26 (m, 3H), 2.54 (hept, *J* = 7.0 Hz, 1H), 2.21 – 2.07 (m, 2H), 2.06 – 1.93 (m, 2H), 1.18 (d, *J* = 7.0 Hz, 6H), 1.04 (t, *J* = 7.4 Hz, 6H).

^{13}C NMR (75 MHz, $CDCl_3$) δ 175.4, 132.0, 128.3, 128.3, 123.1, 88.9, 85.8, 80.0, 34.9, 31.1, 19.2, 8.6.

HRMS (ESI) *m/z* Calculated for $C_{17}H_{22}NaO_2^+$ $[M+Na]^+$: 281.1512, found 281.1511.

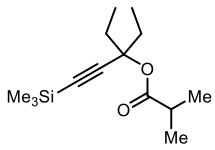

3-Ethyl-1-(trimethylsilyl)pent-1-yn-3-yl isobutyrate (38c)

The reaction of pentan-3-one (861 mg, 10 mmol), ethynyltrimethylsilane (1.52 mL, 11 mmol), and isobutyryl chloride (1.15 mL, 11 mmol) according to General Procedure A

[34] Dai, L.-Z.; Qi, M.-J.; Shi, Y.-L.; Liu, X.-G.; Shi, M. "Gold(I)-Catalyzed Cascade Cyclization Reaction: Highly Regio- and Diastereoselective Intermolecular Addition of Water and Alcohols to Epoxy Alkynes" *Org.Lett.*, **2007**, *9*, 3191.

(purified by flash chromatography on silica gel, eluent: hexanes) gave the title compound in the form of a colorless oil (1.95 g, 77% yield).

^{1}H NMR (300 MHz, $CDCl_3$) δ 2.50 (hept, *J* = 7.0 Hz, 1H), 2.11 – 1.96 (m, 2H), 1.95 – 1.79 (m, 2H), 1.14 (d, *J* = 7.0 Hz, 6H), 0.96 (t, *J* = 7.4 Hz, 6H), 0.16 (s, 9H).

^{13}C NMR (101 MHz, $CDCl_3$) δ 175.2, 105.1, 90.2, 80.1, 34.9, 31.0, 19.2, 8.5, 0.1.

HRMS (ESI) *m/z* Calculated for $C_{14}H_{26}NaO_2Si$ $[M+Na]^+$: 277.1594, found 277.1596.

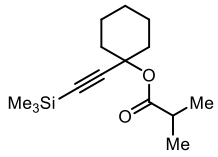

1-((Trimethylsilyl)ethynyl)cyclohexyl isobutyrate (38d)

The reaction of cyclohexanone (2.07 mL, 20 mmol), ethynyltrimethylsilane (3.04 mL, 22 mmol), and isobutyryl chloride (2.30 mL, 22 mmol) according to General Procedure A (purified by flash chromatography on silica gel, eluent: hexanes:EtOAc gradient from 100:0 to 96:4) gave the title compound in the form of a colorless oil (2.52 g, 47% yield).

^{1}H NMR (500 MHz, $CDCl_3$) δ 2.49 (hept, *J* = 7.0 Hz, 1H), 2.05 (dt, *J* = 12.1, 5.6 Hz, 2H), 1.88 (dt, *J* = 12.8, 6.5 Hz, 2H), 1.59 (p, *J* = 6.2 Hz, 4H), 1.53 – 1.44 (m, 1H), 1.38 – 1.29 (m, 1H), 1.15 (d, *J* = 7.0 Hz, 6H), 0.16 (s, 9H).

^{13}C NMR (126 MHz, $CDCl_3$) 175.0, 105.9, 90.4, 75.3, 37.1, 34.8, 25.4, 22.7, 19.1, 0.1.

HRMS (ESI) *m/z* Calculated for $C_{15}H_{26}NaO_2Si$ $[M+Na]^+$: 289.1594, found 289.1595.

1-((Trimethylsilyl)ethynyl)cyclododecyl isobutyrate (38e)

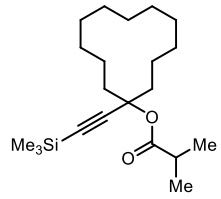

The reaction of cyclododecanone (1.82 g, 10 mmol), ethynyltrimethylsilane (1.52 mL, 11 mmol), and isobutyryl chloride (1.15 mL, 11 mmol) according to General Procedure A (purified by flash chromatography on silica gel, eluent: hexanes) gave the title compound in the form of a colorless viscous oil (1.00 g, 29%).

^{1}H NMR (500 MHz, $CDCl_3$) δ 2.47 (hept, *J* = 7.0 Hz, 1H), 2.12 (ddd, *J* = 13.7, 11.6, 4.7 Hz, 2H), 1.77 (ddd, *J* = 13.7, 11.5, 4.5 Hz, 2H), 1.55 – 1.45 (m, 2H), 1.40 – 1.23 (m, 16H), 1.14 (d, *J* = 7.0 Hz, 6H), 0.15 (s, 9H).

^{13}C NMR (101 MHz, $CDCl_3$) 174.9, 106.1, 89.9, 77.8, 34.8, 33.0, 26.2, 26.0, 22.4, 22.2, 19.3, 19.1, 0.1.

HRMS (ESI) *m/z* Calculated for $C_{21}H_{38}NaO_2Si$ $[M+Na]^+$: 373.2533, found 373.2532.

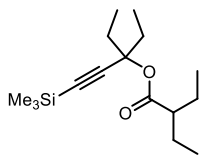

3-Ethyl-1-(trimethylsilyl)pent-1-yn-3-yl 2-ethylbutanoate (38f)

The reaction of pentan-3-one (0.861 g, 10 mmol), ethynyltrimethylsilane (1.54 mL, 11 mmol), and 2-ethylbutanoyl chloride (1.51 mL, 11 mmol) according to General Procedure A gave the title compound that was used crude for the next reaction.

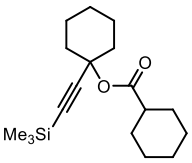

1-((Trimethylsilyl)ethynyl)cyclohexyl cyclohexanecarboxylate (38g)

The reaction of cyclohexanone (0.491 g, 5 mmol), ethynyltrimethylsilane (0.76 mL, 5.5 mmol), and cyclohexanecarbonyl chloride (0.74 mL, 5.5 mmol) according to General Procedure A (eluent: hexanes:EtOAc 98:2) gave the title compound in the form of a colorless viscous oil (0.982 g, 64% yield).

^{1}H NMR (500 MHz, $CDCl_3$) δ 2.25 (tt, *J* = 11.1, 3.7 Hz, 1H), 2.04 (m, 2H), 1.88 (m, 4H), 1.78 – 1.69 (m, 2H), 1.65 – 1.54 (m, 5H), 1.45 (m, 3H), 1.39 – 1.18 (m, 4H), 0.15 (s, 9H).

^{13}C NMR (126 MHz, $CDCl_3$) δ 174.18, 106.26, 90.52, 75.41, 44.11, 37.38, 29.35, 26.22, 25.80, 25.60, 22.90, 0.35.

HRMS (ESI) *m/z* Calculated for $C_{18}H_{30}NaO_2Si$ $[M+Na]^+$: 329.1907, found 329.1895.

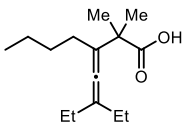

3-Butyl-5-ethyl-2,2-dimethylhepta-3,4-dienoic acid (34a)

The reaction of 3-ethylnon-4-yn-3-yl isobutyrate (**38a**, 477 mg, 2.0 mmol) according to General Procedure B (purified by flash chromatography on silica gel, eluent: hexanes:EtOAc 90:10) gave the title compound in the form of a colorless oil (450 mg, 94% yield).

^{1}H NMR (400 MHz, $CDCl_3$) δ 1.98 (q, *J* = 7.4 Hz, 4H), 1.95 – 1.90 (m, 2H), 1.37 – 1.30 (m, 4H), 1.29 (s, 6H), 0.98 (t, *J* = 7.4 Hz, 6H), 0.91 – 0.85 (m, 3H).

^{13}C NMR (101 MHz, $CDCl_3$) δ 196.9, 183.5, 112.5, 111.1, 45.9, 30.7, 28.3, 26.2, 25.1, 22.8, 14.2, 12.5.

HRMS (ESI) *m/z* Calculated for $C_{15}H_{22}O_2^-$ $[M-H]^-$: 237.1860, found 237.1855.

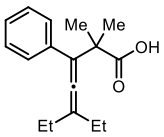

5-Ethyl-2,2-dimethyl-3-phenylhepta-3,4-dienoic acid (34b)

The reaction of 3-ethyl-1-phenylpent-1-yn-3-yl isobutyrate (**38b**, 300 mg, 1.16 mmol) according to General Procedure B (purified by flash chromatography on silica gel, eluent: hexanes:EtOAc 95:5) gave the title compound in the form of a white solid (241 mg, 80% yield).

^{1}H NMR (300 MHz, $CDCl_3$) δ 7.35 – 7.18 (m, 5H), 2.11 (q, *J* = 7.4 Hz, 4H), 1.44 (s, 6H), 1.10 (t, *J* = 7.4 Hz, 6H).

^{13}C NMR (75 MHz, $CDCl_3$) δ 200.2, 183.7, 137.3, 128.2, 127.8, 126.6, 113.0, 112.7, 45.1, 26.3, 26.2, 12.3.

HRMS (ESI) *m/z* Calculated for $C_{17}H_{21}O_2^-$ $[M-H]^-$: 257.1547, found 257.1551.

m.p. = 50 – 51 °C

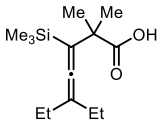

5-Ethyl-2,2-dimethyl-3-(trimethylsilyl)hepta-3,4-dienoic acid (34c)

The reaction of 3-ethyl-1-(trimethylsilyl)pent-1-yn-3-yl isobutyrate (**38c**, 1.27 g, 5.0 mmol) according to General Procedure B (purified by flash chromatography on silica gel, eluent: hexanes:EtOAc 95:5) gave the title compound in the form of a colorless oil (1.20 g, 94% yield).

^{1}H NMR (300 MHz, $CDCl_3$) δ 2.01 – 1.88 (m, 4H), 1.33 (s, 6H), 0.99 (t, *J* = 7.4 Hz, 6H), 0.11 (s, 9H).

^{13}C NMR (75 MHz, $CDCl_3$) δ 203.9, 183.5, 106.2, 105.0, 45.3, 26.8, 25.4, 12.5, 0.8.

HRMS (ESI) *m/z* Calculated for $C_{14}H_{25}O_2Si^-$ $[M-H]^-$: 253.1629, found 253.1635.

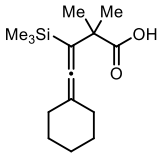

1-(3-Ethyl-1-(trimethylsilyl)penta-1,2-dien-1-yl)cyclohexane-1-carboxylic acid (34d)

The reaction of 1-((trimethylsilyl)ethynyl)cyclohexyl isobutyrate (**38d**, 2.13 g, 8.0 mol) according to General Procedure B (purification by flash chromatography on silica gel, eluent: hexanes:EtOAc 90:10) gave the title compound in the form of a white solid (1.62 g, 76% yield).

For preparation on a larger scale, a different purification procedure was devised to avoid column chromatography. After the aqueous workup described in General Procedure B, the crude material was suspended in a small amount of saturated aqueous NH_4Cl solution (approx. 2 mL per gram of crude material) and concentrated aqueous ammonia solution was added until a strongly alkaline pH was reached while stirring vigorously. A white solid (the ammonium salt of acid **34d**) precipitated together with non-polar impurities. The solid was collected by filtration, washed with a half-saturated aqueous NH_4Cl, and then re-suspended and washed thoroughly with hexanes to remove impurities (repeated three times). The dried solid was then dissolved in water and the solution was brought to acid pH. Extraction with CH_2Cl_2 and evaporation afforded the product **34d** in a pure state.

^{1}H NMR (300 MHz, $CDCl_3$) δ 2.15 – 2.05 (m, 4H), 1.65 – 1.45 (m, 6H), 1.32 (s, 6H), 0.11 (s, 9H).

^{13}C NMR (75 MHz, $CDCl_3$) δ 202.1, 184.4, 101.3, 100.2, 45.3, 31.0, 27.7, 26.7, 26.4, 0.8.

HRMS (ESI) *m/z* Calculated for $C_{15}H_{25}O_2Si^-$ $[M-H]^-$: 265.1629, found 265.1617.

m.p. = 45 – 49 °C

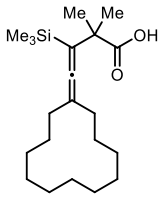

1-(3-Ethyl-1-(trimethylsilyl)penta-1,2-dien-1-yl)cyclododecane-1-carboxylic acid (34e)

The reaction of 1-((trimethylsilyl)ethynyl)cyclododecyl isobutyrate (**38e**, 701 mg, 2.0 mmol) according to General Procedure B (purification by flash chromatography on silica gel, eluent: hexanes:EtOAc 90:10) gave the title compound in the form of a white solid (604 mg, 86% yield).

^{1}H NMR (300 MHz, $CDCl_3$) δ 2.06 – 1.97 (m, 4H), 1.59 – 1.11 (m, 24H), 0.10 (s, 9H).

^{13}C NMR (101 MHz, $CDCl_3$) δ 205.1, 183.7, 102.6, 101.1, 45.6, 29.4, 27.1, 24.7, 24.6, 24.5, 24.2, 23.3, 0.9.

HRMS (ESI) *m/z* Calculated for $C_{21}H_{37}O_2Si^-$ $[M-H]^-$: 349.2568, found 349.2558.

m.p. = 76 – 80 °C

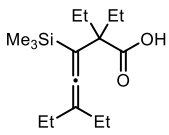

2,2,5-Triethyl-3-(trimethylsilyl)hepta-3,4-dienoic acid (34f)

The reaction of 3-ethyl-1-(trimethylsilyl)pent-1-yn-3-yl 2-ethylbutanoate (**38f**, 1.08 mg, 3.82 mmol) according to General Procedure B (purified by flash chromatography on silica gel, eluent: hexanes:EtOAc 95:5) gave the title compound in the form of a white solid (454 mg, 42% yield).

^{1}H NMR (500 MHz, $CDCl_3$) δ 1.98 (qd, *J* = 7.5, 3.9 Hz, 4H), 1.82 (dq, *J* = 14.9, 7.4 Hz, 2H), 1.66 (dq, *J* = 14.9, 7.5 Hz, 2H), 1.02 (t, *J* = 7.4 Hz, 6H), 0.80 (t, *J* = 7.5 Hz, 6H), 0.09 (s, 9H).

^{13}C NMR (101 MHz, $CDCl_3$) δ 205.96, 182.19, 105.70, 102.41, 53.32, 26.58, 25.75, 12.87, 8.86, 0.96.

HRMS (ESI) *m/z* Calculated for $C_{16}H_{29}O_2Si^-$ $[M-H]^-$: 281.1942, found 281.1941.

m.p. = 60 – 62 °C

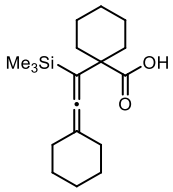

4-Cyclododecylidene-2,2-dimethyl-3-(trimethylsilyl)but-3-enoic acid (34g)

The reaction of 1-((trimethylsilyl)ethynyl)cyclohexyl cyclohexanecarboxylate (**38g**, 980 mg, 1.16 mmol) according to General Procedure B (purified by flash chromatography on silica gel, eluent: hexanes:EtOAc 95:5) gave the title compound in the form of a white solid (545 mg, 56% yield).

^{1}H NMR (400 MHz, $CDCl_3$) δ 2.12 (m, *J* = 7.6 Hz, 6H), 1.68 – 1.38 (m, 14H), 1.36 – 1.24 (m, 1H), 0.13 (s, 9H).

^{13}C NMR (101 MHz, $CDCl_3$) δ 203.67, 182.72, 99.38, 50.22, 34.52, 30.64, 27.40, 26.24, 25.75, 23.40, 3.06, 1.00.

HRMS (ESI) *m/z* Calculated for $C_{18}H_{30}O_2Si$ [M+]: 329.1907, found 329.1911.

m.p. = 79 – 83 °C

4.6.3. General Procedure for the Asymmetric Organocatalytic Cascade Reaction of Trisubstituted Allenic Acids

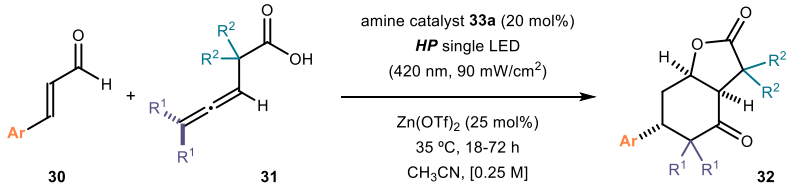

Figure 4.16. General Procedure for the synthesis of products **32.**

General Procedure: A Schlenk flask (approximate diameter: 15 mm) was charged with the appropriate allenic acid **31** (0.1 mmol), the amine catalyst **33a** (14.1 mg, 0.02 mmol, 0.20 equiv.), the enal **30** (0.30 mmol, 3.0 equiv.), $Zn(OTf)_2$ (9.1 mg, 0.025 mmol, 0.25 equiv.) and acetonitrile (400 µL). The mixture was degassed by three freeze-pump-thaw cycles and conditioned under an atmosphere of argon. The Schlenk flask was placed into an aluminum block on a 3D-printed holder, fitted with a 420 nm high-power single LED. The irradiance was fixed at 90±2 mW/cm², as controlled by an external power supply, and measured using a photodiode light detector at the start of each reaction. This setup secured reliable irradiation while keeping a distance of 1 cm between the reaction vessel and the light source (the setup is detailed in Figure 4.17). This illumination set-up generated a temperature within the reaction vessel of 35 °C,

as measured by a thermometer. The reaction was stirred for the indicated reaction time.

The reaction mixture was then passed through a silica plug and flushed with Et_2O. Then, added to silica gel (approx. 1 g), volatiles were removed under reduced pressure and the resulting solids were directly loaded on a flash chromatography column (silica gel). Elution with the specified solvent system gave the required products. In some cases, the separation of the product **32** from the enal starting material posed difficulties, in these cases the enal was removed by heating at 50 °C under high vacuum.

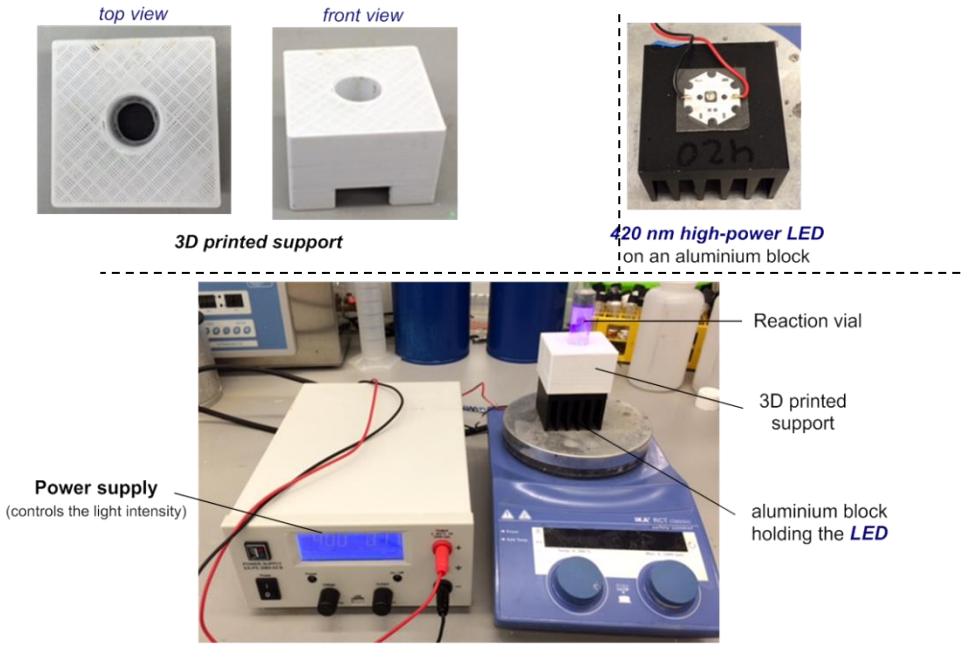

Figure 4.17. Detailed set-up and illumination system. The light source for illuminating the reaction vessel consisted of a single 420 nm high-power LED (OCU-440 UE420-X-T) purchased from OSA OPTO.

4.6.4. Characterization of Products 32

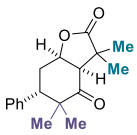

(3a*R*,6*S*,7a*R*)-3,3,5,5-Tetramethyl-6-phenylhexahydrobenzofuran-2,4- dione (32a)

The reaction of 2,2,5-trimethylhexa-3,4-dienoic acid (**31a**) with cinnamaldehyde according to the general procedure detailed in section 4.6.3 (reaction time: 18 h, flash chromatography eluent: hexanes:EtOAc 90:10) gave the title product in the form of an off-white solid (16.0 mg, 56%, average of two runs, 60% ee, >19:1 dr). The enantiomeric excess was determined by UPC² analysis on a chiral stationary phase (Daicel Chiralpak IC-3, gradient: CO_2:MeOH from 100:0 to 60:40 over

4.0 minutes, flow rate: 3.0 mL/min, λ = 207 nm, τ_{major} = 2.45 min, τ_{minor} = 2.55 min). $[\alpha]_D^{26}$ = +4.2 (*c* = 0.13, $CHCl_3$, 60% ee).

^{1}H NMR (300 MHz, $CDCl_3$) δ 7.36 – 7.26 (m, 3H), 7.17 – 7.10 (m, 2H), 5.13 (dt, *J* = 7.2, 3.3 Hz, 1H), 3.14 (dd, *J* = 12.6, 3.3 Hz, 1H), 2.97 (d, *J* = 7.2 Hz, 1H), 2.47 (ddd, *J* = 15.0, 12.6, 3.3 Hz, 1H), 2.35 (dt, *J* = 15.0, 3.3 Hz, 1H), 1.45 (s, 3H), 1.30 (s, 3H), 1.02 (s, 3H), 0.95 (s, 3H).

^{13}C NMR (126 MHz, $CDCl_3$) δ 213.4, 180.9, 139.4, 129.4, 128.2, 127.2, 74.7, 55.4, 48.6, 45.0, 43.5, 29.9, 28.2, 24.7, 23.0, 21.3.

HRMS (ESI) *m*/*z* Calculated for $C_{18}H_{22}NaO_3^+$ $[M+Na]^+$: 309.1461, found 309.1468.

m.p. = 146 – 152 °C

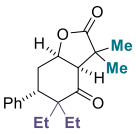

(3a*R*,6*S*,7a*R*)-5,5-Diethyl-3,3-dimethyl-6-phenylhexahydrobenzofuran-2,4-dione (32b)

The reaction of 5-ethyl-2,2-dimethylhepta-3,4-dienoic acid (**31b**) with cinnamaldehyde according to the general procedure detailed in section 4.6.3 (reaction time: 72 h, flash chromatography eluent: hexanes:EtOAc gradient from 90:10 to 85:15) gave the title product in the form of a pale yellow oil (16.5 mg, 53%, average of two runs, 67% ee, >19:1 dr). The enantiomeric excess was determined by UPC² analysis on a chiral stationary phase (Daicel Chiralpak CEL1, gradient: CO_2:CH_3CN from 100:0 to 60:40 over 4.0 minutes, flow rate: 3.0 mL/min, λ = 207 nm, τ_{major} = 3.44 min, τ_{minor} = 4.10 min). $[\alpha]_D^{26}$ = +3.7 (*c* = 0.115, $CHCl_3$, 67% ee).

^{1}H NMR (500 MHz, $CDCl_3$) δ 7.34 – 7.24 (m, 3H), 7.23 – 7.17 (m, 2H), 5.05 (dt, *J* = 6.8, 3.8 Hz, 1H), 3.54 (dd, *J* = 12.2, 3.8 Hz, 1H), 2.73 (d, *J* = 6.8 Hz, 1H), 2.63 (ddd, *J* = 15.1, 12.2, 3.8 Hz, 1H), 2.36 (dt, *J* = 15.1, 3.8 Hz, 1H), 1.92 (dq, *J* = 14.6, 7.4 Hz, 1H), 1.71 (dq, *J* = 14.8, 7.4 Hz, 1H), 1.43 (s, 3H), 1.40 (s, 3H), 1.37 (dq, *J* = 14.8, 7.4 Hz, 1H), 1.08 (dq, *J* = 14.8, 7.4 Hz, 1H), 0.82 (t, *J* = 7.4 Hz, 3H), 0.69 (t, *J* = 7.4 Hz, 3H).

^{13}C NMR (101 MHz, $CDCl_3$) δ 210.8, 180.8, 139.9, 129.2, 128.3, 127.2, 75.0, 55.6, 55.4, 45.0, 39.6, 29.7, 27.4, 25.8, 25.1, 22.4, 9.2, 8.6.

HRMS (ESI) *m*/*z* Calculated for $C_{20}H_{26}NaO_3^+$ $[M+Na]^+$: 337.1774, found 337.1771.

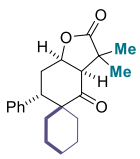

(3a*R*,6*S*,7a*R*)-3,3-Dimethyl-6-phenyltetrahydro-4*H*-spiro[benzofuran-5,1'-cyclohexane]-2,4(3*H*)-dione (32c)

The reaction of 4-cyclohexylidene-2,2-dimethylbut-3-enoic acid (**31c**) with cinnamaldehyde according to the general procedure detailed in section 4.6.3 (reaction time: 18 h, flash chromatography eluent: hexanes:EtOAc

gradient from 90:10 to 85:15) gave the title product in the form of an off-white solid (15.3 mg, 47%, average of two runs, 70% ee, >19:1 dr). The enantiomeric excess was determined by UPC² analysis on a chiral stationary phase (Daicel Chiralpak IA, gradient: CO_2:MeOH from 100:0 to 60:40 over 4.0 minutes, flow rate: 3.0 mL/min, λ = 215 nm, τ_{major} = 3.85 min, τ_{minor} = 4.43 min). $[\alpha]_D^{26}$ = +6.2 (*c* = 0.115, $CHCl_3$, 70% ee).

^{1}H NMR (500 MHz, $CDCl_3$) δ 7.35 – 7.25 (m, 3H), 7.12 (d, *J* = 7.3 Hz, 2H), 5.13 – 5.08 (m, 1H), 3.21 (d, *J* = 6.4 Hz, 1H), 3.08 (dd, *J* = 11.7, 4.3 Hz, 1H), 2.60 (ddd, *J* = 15.8, 11.7, 5.0 Hz, 1H), 2.24 (dt, *J* = 15.8, 4.3 Hz, 1H), 2.17 (br d, *J* = 13.6 Hz, 1H), 1.80 (br d, *J* = 12.9 Hz, 1H), 1.60 – 1.40 (m, 4H), 1.53 (s, 3H), 1.39 (s, 3H), 1.37 – 0.82 (m, 4H).

^{13}C NMR (126 MHz, $CDCl_3$) δ 212.5, 180.3, 139.0, 129.4, 128.4, 127.4, 77.1 (overlaps with the peak of $CDCl_3$, detected by HSQC), 55.7, 53.4, 49.2, 43.3, 32.0, 29.7, 28.4, 25.8, 25.7, 23.1, 22.3, 21.8.

HRMS (ESI) *m*/*z* Calculated for $C_{21}H_{26}NaO_3^+$ $[M+Na]^+$: 349.1774, found 349.1785.

m.p. = 187 – 191 °C

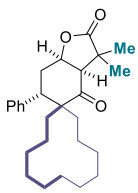

(3a*R*,6*S*,7a*R*)-3,3-Dimethyl-6-phenyltetrahydro-4*H*-spiro[benzofuran-5,1'-cyclododecane]-2,4(3*H*)-dione (32d)

The reaction of 4-cyclododecylidene-2,2-dimethylbut-3-enoic acid (**31d**) with cinnamaldehyde according to the general procedure detailed in section 4.6.3 (reaction time: 18 h, flash chromatography eluent: toluene:EtOAc gradient from 99:1 to 97:3) gave the title product in the form of an off-white solid (17.3 mg, 42%, average of two runs, 75% ee, >19:1 dr). The enantiomeric excess was determined by UPC² analysis on a chiral stationary phase (Daicel Chiralpak IE-3, gradient: CO_2:EtOH from 100:0 to 60:40 over 4.0 minutes, flow rate: 3.0 mL/min, λ = 210 nm, τ_{major} = 4.49 min, τ_{minor} = 4.70 min). $[\alpha]_D^{26}$ = −47.7 (*c* = 0.105, $CHCl_3$, 75% ee).

^{1}H NMR (500 MHz, $CDCl_3$) δ 7.34 – 7.22 (m, 2H), 7.07 – 7.03 (m, 2H), 4.79 (td, *J* = 8.9, 6.2 Hz, 1H), 3.19 (d, *J* = 8.8 Hz, 1H), 3.10 (dd, *J* = 6.2, 4.0 Hz, 1H), 2.40 (dt, *J* = 14.2, 6.2 Hz, 1H), 2.26 (ddd, *J* = 14.2, 8.9, 4.0 Hz, 1H), 1.98 (ddd, *J* = 14.8, 11.8, 3.2 Hz, 1H), 1.88 – 1.79 (m, 1H), 1.60 – 0.75 (m, 20H), 1.48 (s, 3H), 1.34 (s, 3H).

^{13}C NMR (126 MHz, $CDCl_3$) δ 212.6, 180.6, 140.8, 128.7 (4C), 127.1, 74.6, 56.2, 52.9, 47.5, 43.9, 32.2, 31.9, 28.1, 28.0, 27.1, 27.0, 26.3, 23.4, 23.3, 23.0 (2C), 22.8, 19.8, 18.4.

HRMS (ESI) *m*/*z* Calculated for $C_{27}H_{38}NaO_3^+$ $[M+Na]^+$: 433.2713, found 433.2713.

m.p. = 172 – 177 °C

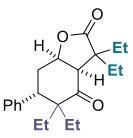

(3a*R*,6*S*,7a*R*)-3,3,5,5-Tetraethyl-6-phenylhexahydrobenzofuran-2,4-dione (32e)

The reaction of 2,2,5-triethylhepta-3,4-dienoic acid (**31e**) with cinnamaldehyde according to the general procedure detailed in section 4.6.3 (reaction time: 18 h, flash chromatography eluent: hexanes:EtOAc gradient from 100:0 to 85:15) gave the title product in the form of an off-white solid (15.0 mg, 44%, average of two runs, 64% ee). The enantiomeric excess was determined by UPC² analysis on a chiral stationary phase (Daicel Chiralpak AMY1, gradient: CO_2:*i*PrOH from 100:0 to 60:40 over 4.0 minutes, flow rate: 3.0 mL/min, λ = 215 nm, τ_{major} = 3.88 min, τ_{minor} = 4.07 min). $[\alpha]_D^{26}$ = +2.6 (*c* = 0.105, $CHCl_3$, 64% ee, >19:1 dr).

^{1}H NMR (400 MHz, $CDCl_3$) δ 7.35 – 7.27 (m, 3H), 7.24 – 7.19 (m, 2H), 5.03 (dt, *J* = 6.9, 4.0 Hz, 1H), 3.48 (dd, *J* = 12.2, 4.0 Hz, 1H), 2.83 (d, *J* = 6.9 Hz, 1H), 2.62 (ddd, *J* = 15.2, 12.1, 4.0 Hz, 1H), 2.32 (dt, *J* = 15.2, 4.0 Hz, 1H), 1.99 – 1.69 (m, 6H), 1.41 (dq, *J* = 14.7, 7.4 Hz, 1H), 1.15 (dq, *J* = 14.5, 7.3 Hz, 1H), 1.04 (t, *J* = 7.3 Hz, 3H), 0.99 (t, *J* = 7.4 Hz, 3H), 0.77 (t, *J* = 7.3 Hz, 3H), 0.70 (t, *J* = 7.4 Hz, 3H).

^{13}C NMR (101 MHz, $CDCl_3$) δ = 210.8, 179.0, 140.2, 129.2, 128.4, 127.2, 75.1, 55.8, 53.4, 52.6, 40.9, 30.3, 27.3, 25.8, 24.8, 23.9, 9.1, 9.0, 8.7, 8.5.

HRMS (ESI) *m*/*z* Calculated for $C_{22}H_{30}NaO_3^+$ $[M+Na]^+$: 365.2087, found 365.2089.

m.p. = 114 – 119 °C

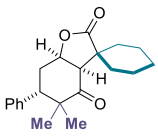

(3a*R*,6*S*,7a*R*)-5,5-Dimethyl-6-phenyltetrahydro-2*H*-spiro[benzofuran-3,1'-cyclohexane]-2,4(3a*H*)-dione (32f)

The reaction of 1-(3-Methylbuta-1,2-dien-1-yl)cyclohexane-1-carboxylic acid (**31f**) with cinnamaldehyde according to the general procedure detailed in section 4.6.3 (reaction time: 18 h, flash chromatography eluent: hexanes:EtOAc gradient from 90:10 to 85:15) gave the title product in the form of an off-white solid (15.8 mg, 48%, average of two runs, 57% ee, >19:1 dr). The enantiomeric excess was determined by UPC² analysis on a chiral stationary phase (Daicel Chiralpak AMY1, gradient: CO_2:*i*PrOH from 100:0 to 60:40 over 4.0 minutes, flow rate: 3.0 mL/min, λ = 210 nm, τ_{major} = 4.53 min, τ_{minor} = 4.84 min). $[\alpha]_D^{26}$ = +25.0 (*c* = 0.145, $CHCl_3$, 57% ee).

^{1}H NMR (500 MHz, $CDCl_3$) δ 7.35 – 7.23 (m, 3H), 7.17 – 7.12 (m, 2H), 5.08 (dt, *J* = 6.6, 3.0 Hz, 1H), 3.18 (dd, *J* = 13.2, 3.0 Hz, 1H), 3.07 (d, *J* = 6.6 Hz, 1H), 2.45 (ddd, *J* = 15.0, 13.2, 3.0 Hz, 1H), 2.35 (dt, *J* = 15.0, 3.0 Hz, 1H), 1.96 – 1.20 (m, 10H), 1.00 (s, 3H), 0.96 (s, 3H).

^{13}C NMR (126 MHz, $CDCl_3$) δ 213.5, 180.1, 139.8, 129.6, 128.4, 127.4, 75.1, 53.9, 49.44, 49.39, 43.7, 35.2, 30.7, 30.1, 25.6, 24.9, 22.7, 22.0, 21.5.

HRMS (ESI) *m/z* Calculated for $C_{21}H_{26}NaO_3^+$ $[M+Na]^+$: 349.1774, found 349.1761.

m.p. = 166 – 170 °C

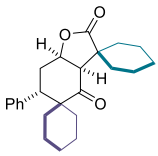

(3a'*R*,6'*S*,7a'*R*)-6'-Phenyltetrahydro-2'*H*,4'*H*-dispiro[cyclohexane-1,3'-benzofuran-5',1''-cyclohexane]-2',4'-dione (32g)

The reaction of 1-(2-cyclohexylidenevinyl)cyclohexane-1-carboxylic acid (**31g**) with cinnamaldehyde according to the general procedure detailed in section 4.6.3 (reaction time: 18 h, flash chromatography eluent: hexanes:EtOAc 80:20) gave the title product in the form of an off-white solid (15.7 mg, 42%, average of two runs, 69% ee, >19:1 dr). The enantiomeric excess was determined by UPC² analysis on a chiral stationary phase (Daicel Chiralpak IC-3, gradient: CO_2:*i*PrOH from 100:0 to 60:40 over 4.0 minutes, flow rate: 3.0 mL/min, λ = 215 nm, τ_{major} = 5.23 min, τ_{minor} = 4.88 min). $[\alpha]_D^{26}$ = +33.0 (*c* = 0.140, $CHCl_3$, 69% ee).

^{1}H NMR (500 MHz, $CDCl_3$) δ = 7.33 – 7.25 (m, 3H), 7.15 – 7.11 (m, 2H), 5.12 (td, *J* = 5.3, 2.1 Hz, 1H), 3.42 (d, *J* = 5.3 Hz, 1H), 3.00 (dd, *J* = 13.5, 4.4 Hz, 1H), 2.74 (br d, *J* = 13.5 Hz, 1H), 2.63 (ddd, *J* = 15.8, 13.5, 4.4 Hz, 1H), 2.26 (dddd, *J* = 17.9, 15.7, 4.4, 2.2 Hz, 2H), 1.95 – 1.38 (m, 13H), 1.32 – 1.14 (m, 2H), 1.06 – 0.80 (m, 2H), 0.70 – 0.61 (m, 1H).

^{13}C NMR (126 MHz, $CDCl_3$) δ = 212.6, 179.4, 138.9, 129.4, 128.3, 127.5, 78.2, 54.7, 51.2, 50.8, 48.1, 31.8, 31.7, 28.9, 28.8, 28.1, 26.0, 25.7, 24.0, 22.9, 22.8, 22.6.

HRMS (ESI) *m/z* Calculated for $C_{24}H_{30}NaO_3^+$ $[M+Na]^+$: 389.2087, found 389.2098.

m.p. = 167 – 173 °C

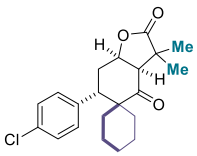

(3a*R*,6*S*,7a*R*)-6-(4-Chlorophenyl)-3,3-dimethyltetrahydro-4*H*-spiro[benzofuran-5,1'-cyclohexane]-2,4(3*H*)-dione (32h)

The reaction of 4-cyclohexylidene-2,2-dimethylbut-3-enoic acid (**31c**) with 4-chlorocinnamaldehyde according to the general procedure detailed in section 4.6.3 (reaction time: 18 h, flash chromatography eluent: hexanes:EtOAc gradient from 100:0 to 85:15) gave the title product in the form of an off-white solid (16.1 mg, 46%, average of two runs, 64% ee, >19:1 dr). The enantiomeric excess was determined by UPC² analysis on a chiral stationary phase (Daicel Chiralpak

IE-3, gradient: CO_2:EtOH from 100:0 to 60:40 over 4.0 minutes, flow rate: 3.0 mL/min, λ = 223 nm, τ_{major} = 6.67 min, τ_{minor} = 6.24 min). $[\alpha]_D^{26}$ = +3.1 (*c* = 0.140, $CHCl_3$, 64% ee).

^{1}H NMR (500 MHz, $CDCl_3$) δ = 7.30 (d, *J* = 8.5 Hz, 2H), 7.06 (d, *J* = 8.5 Hz, 2H), 5.11 (ddd, *J* = 6.3, 4.6, 3.7 Hz, 1H), 3.18 (d, *J* = 6.3 Hz, 1H), 3.04 (dd, *J* = 12.1, 4.6 Hz, 1H), 2.56 (ddd, *J* = 15.4, 12.1, 4.6 Hz, 1H), 2.23 (dt, *J* = 15.4, 3.97Hz, 1H), 2.16 (br d, *J* = 14.1 Hz, 1H), 1.80 (br d, *J* = 13.2 Hz, 1H), 1.62 – 1.35 (m, 3H), 1.54 (s, 3H), 1.38 (s, 3H), 1.11 – 0.95 (m, 3H), 0.91 – 0.77 (m, 2H).f

^{13}C NMR (126 MHz, $CDCl_3$) δ = 212.0, 180.1, 137.4, 133.3, 130.6, 128.6, 77.1, 55.6, 53.4, 48.9, 43.3, 31.8, 29.4, 28.2, 25.8, 25.5, 23.2, 22.3, 21.6.

HRMS (ESI) *m*/*z* Calculated for $C_{21}H_{25}ClNaO_3^+$ $[M+Na]^+$: 383.1384, found 383.1383.

m.p. = 210 – 216 °C

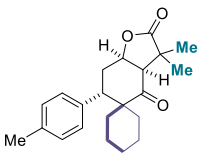

(3a*R*,6*S*,7a*R*)-3,3-Dimethyl-6-(p-tolyl)tetrahydro-4*H*-spiro [benzo furan-5,1'-cyclohexane]-2,4(3*H*)-dione (32i)

The reaction of 4-cyclohexylidene-2,2-dimethylbut-3-enoic acid (**31c**) with 4-methylcinnamaldehyde according to the general procedure detailed in section 4.6.3 (reaction time: 18 h, flash chromatography eluent: hexanes:EtOAc gradient from 100:0 to 85:15) gave the title product in the form of an off-white solid (15.7 mg, 46%, average of two runs, 62% ee, >19:1 dr). The enantiomeric excess was determined by UPC² analysis on a chiral stationary phase (Daicel Chiralpak IE-3, gradient: CO_2:*i*PrOH from 100:0 to 60:40 over 4.0 minutes, flow rate: 3.0 mL/min, λ = 221 nm, τ_{major} = 7.72 min, τ_{minor} = 6.68 min). $[\alpha]_D^{26}$ = +9.9 (*c* = 0.100, $CHCl_3$, 62% ee).

^{1}H NMR (500 MHz, $CDCl_3$) δ 7.14 – 7.07 (m, 2H), 7.03 – 6.98 (m, 2H), 5.09 (dt, *J* = 4.8 Hz, 1H), 3.20 (d, *J* = 6.4 Hz, 1H), 3.05 (dd, *J* = 11.6, 4.3 Hz, 1H), 2.57 (ddd, *J* = 15.5, 11.6, 5.1 Hz, 1H), 2.34 (s, 3H), 2.22 (dt, *J* = 15.4, 4.2 Hz, 1H), 2.14 (br d, *J* = 12.4 Hz, 1H), 1.78 (d, *J* = 13.1 Hz, 1H), 1.53 (s, 3H), 1.52 – 1.42 (m, 2H), 1.39 (s, 3H), 1.29 – 1.21 (m, 2H), 1.12 – 0.99 (m, 2H), 0.97 – 0.81 (m, 2H).

^{13}C NMR (126 MHz, $CDCl_3$) δ 212.6, 180.3, 137.1, 136.0, 129.3, 129.1, 77.2, 55.6, 53.4, 48.8, 43.3, 31.9, 29.8, 28.5, 25.8, 25.7, 23.1, 22.3, 21.8, 21.2.

HRMS (ESI) *m*/*z* Calculated for $C_{22}H_{28}NaO_3^+$ $[M+Na]^+$: 363.1931, found 363.1926.

m.p. = 230 – 237 °C

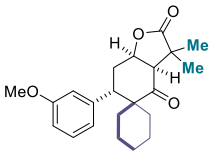

(3a*R*,6*S*,7a*R*)-6-(3-Methoxyphenyl)-3,3-dimethyltetrahydro-4*H*-spiro[benzofuran-5,1'-cyclohexane]-2,4(3*H*)-dione (32j)

The reaction of 4-cyclohexylidene-2,2-dimethylbut-3-enoic acid (**31c**) with 3-methoxycinnamaldehyde according to the general procedure detailed in section 4.6.3 (reaction time: 72 h, flash chromatography eluent: hexanes:EtOAc gradient from 100:0 to 85:15) gave the title product in the form of an off-white solid (17.8 mg, 50%, average of two runs, 74% ee, >19:1 dr). The enantiomeric excess was determined by UPC² analysis on a chiral stationary phase (Daicel Chiralpak IA, gradient: CO_2:MeOH from 100:0 to 60:40 over 4.0 minutes, flow rate: 3.0 mL/min, λ = 273 nm, τ_{major} = 5.53 min, τ_{minor} = 5.97 min). $[\alpha]_D^{26}$ = +13.8 (*c* = 0.180, $CHCl_3$, 74% ee).

^{1}H NMR (500 MHz, $CDCl_3$) δ 7.23 (t, *J* = 7.9 Hz, 1H), 6.82 (ddd, *J* = 8.2, 2.6, 0.9 Hz, 1H), 6.70 (dt, *J* = 7.7, 1.2 Hz, 1H), 6.67 (t, *J* = 2.1 Hz, 1H), 5.10 (dt, *J* = 6.2, 4.3 Hz, 1H), 3.81 (s, 3H), 3.20 (d, *J* = 6.3 Hz, 1H), 3.04 (dd, *J* = 11.7, 4.3 Hz, 1H), 2.57 (ddd, *J* = 15.4, 11.7, 5.1 Hz, 1H), 2.24 (dt, *J* = 15.4, 4.2 Hz, 1H), 2.18 – 2.12 (m, 1H), 1.79 (br d, *J* = 13.3 Hz, 1H), 1.60 – 1.43 (m, 2H), 1.53 (s, 3H), 1.38 (s, 3H), 1.27 – 1.21 (m, 2H), 1.12 – 1.01 (m, 2H), 0.97 – 0.81 (m, 2H).

^{13}C NMR (126 MHz, $CDCl_3$) δ 212.4, 180.3, 159.5, 140.7, 129.3, 121.8, 115.9, 112.0, 77.2, 55.6, 55.4, 53.4, 49.2, 43.3, 32.0, 29.7, 28.5, 25.8, 25.6, 23.2, 22.3, 21.8.

HRMS (ESI) *m*/*z* Calculated for $C_{22}H_{28}NaO_3^+$ $[M+Na]^+$: 379.1880, found 379.1885.

m.p. = 155 – 157 °C

4.6.5. General Procedure for the Asymmetric Organocatalytic Cascade Reaction of Tetrasubstituted Allenic Acids

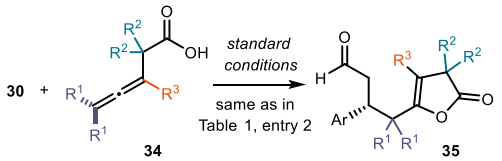

Figure 4.18. General Procedure for the synthesis of products **35**.

General Procedure A: A Schlenk tube (approximate diameter: 15 mm) was charged with the appropriate allenic acid **34** (0.1 mmol), the amine catalyst **33a** (14.1 mg, 0.02 mmol, 0.20 equiv.), the enal **30** (0.30 mmol, 3.0 equiv.), $Zn(OTf)_2$ (9.1 mg, 0.025 mmol, 0.25 equiv.) and acetonitrile (400 µL). The mixture was degassed by three freeze-pump-thaw cycles and conditioned under an atmosphere of Ar. The Schlenk flask was placed into an aluminum block on a 3D-printed holder, fitted with a 420 nm high-power single LED. The irradiance was fixed at 90±2 mW/cm², as controlled by an external power supply, and measured using a photodiode light detector at the start of each reaction. This setup secured reliable irradiation while keeping a distance of 1 cm between the reaction vessel and the light source (the setup is detailed in Figure 4.17). This illumination set-up generated a temperature within the reaction vessel of 35 °C, as measured by a thermometer. The reaction was stirred for the indicated reaction time.

The reaction mixture was then passed through a silica plug and flushed with Et_2O. Then, added to silica gel (approx. 1 g), volatiles were removed under reduced pressure and the resulting solids were directly loaded on a flash chromatography column (silica gel). Elution with the specified solvent system gave the required products. In some cases, the separation of the product from the enal starting material posed difficulties, in these cases the enal was removed by heating at 50 °C under high vacuum.

General Procedure B: A Schlenk flask (approximate diameter: 15 mm) was charged with the appropriate allenic acid **35** (0.1 mmol), the amine catalyst **33a** (14.1 mg, 0.02 mmol, 0.20 equiv.), the enal **30** (0.30 mmol, 3.0 equiv.), TFA (4,59 µL, 0.06 mmol, 0.60 equiv.) and acetonitrile (200 µL). The mixture was degassed by three freeze-pump-thaw cycles and conditioned under an atmosphere of Ar. The Schlenk flask was placed into an aluminum block on a 3D-printed holder, fitted with a 420 nm high-power single LED. The irradiance was fixed at 90±2 mW/cm², as controlled by an external power supply, and measured using a photodiode light detector at the start of each reaction. This setup secured reliable irradiation while keeping a distance of 1 cm between the reaction vessel and the light source (the setup is detailed in Figure 4.17). The reaction was stirred for the prescribed reaction time.

The reaction mixture was then passed through a silica plug and flushed with Et_2O. Then, added to silica gel (approx. 1 g), volatiles were removed under reduced pressure and the resulting solids were directly loaded on a flash chromatography column (silica gel). Elution with the specified solvent system gave the required products.

4.6.6. Characterization of Products 35

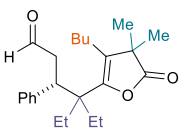

(*S*)-4-(3-Butyl-4,4-dimethyl-5-oxo-4,5-dihydrofuran-2-yl)-4-ethyl-3-phenylhexanal (35a)

The reaction of 3-butyl-5-ethyl-2,2-dimethylhepta-3,4-dienoic acid (**34a**) with cinnamaldehyde according to the general procedure **A** detailed in section 4.6.5 (reaction time: 18 h, flash chromatography eluent: hexanes:EtOAc 95:5) gave the title product in the form of a pale yellow oil (20.7 mg, 56%, average of two runs). The enantiomeric excess was determined by analysis of the corresponding cyclized product **36a**.

^{1}H NMR (500 MHz, $CDCl_3$) δ 9.54 (dd, *J* = 2.2, 1.2 Hz, 1H), 7.26 – 7.14 (m, 3H), 7.11 – 7.07 (m, 2H), 3.52 (dd, *J* = 10.1, 4.9 Hz, 1H), 3.16 – 3.04 (m, 2H), 1.96 (dq, *J* = 14.6, 7.5 Hz, 1H), 1.75 – 1.67 (m, 2H), 1.63 – 1.46 (m, 4H), 1.21 (s, 3H), 1.11-1.01 (m, 2H), 1.21 (s, 4H), 0.98 (t, *J* = 7.3 Hz, 3H), 0.85 (t, *J* = 7.4 Hz, 4H), 0.72 (t, *J* = 7.4 Hz, 3H), 0.59 – 0.47 (m, 1H).

^{13}C NMR (126 MHz, $CDCl_3$) δ 202.2, 182.3, 148.6, 140.9, 129.5, 128.2, 127.2, 126.2, 48.4, 47.3, 45.4, 44.4, 32.8, 24.6, 24.3, 23.8, 23.4, 23.2, 23.0, 13.7, 9.0, 8.1.

HRMS (ESI) *m/z* Calculated for $C_{24}H_{34}NaO_3^+$ $[M+Na]^+$: 393.2400, found 393.2406.

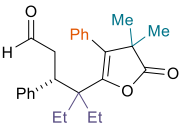

(*S*)-4-(4,4-Dimethyl-5-oxo-3-phenyl-4,5-dihydrofuran-2-yl)-4-ethyl-3-phenylhexanal (35b)

The reaction of 5-ethyl-2,2-dimethyl-3-phenylhepta-3,4-dienoic acid (**34b**) with cinnamaldehyde according to the general procedure **A** detailed in section 4.6.5 (reaction time: 18 h, flash chromatography eluent: toluene:EtOAc 98:2) gave the title product in the form of a colorless foam (25.9 mg, 66%, average of two runs). The enantiomeric excess was determined by analysis of the corresponding cyclized product **36b**.

^{1}H NMR (400 MHz, $CDCl_3$) δ 9.57 (dd, *J* = 2.3, 1.1 Hz, 1H), 7.34 – 7.29 (m, 3H), 7.20 – 6.93 (m, 5H), 6.67 (br s, 1H), 5.71 (br s, 1H), 3.53 (dd, *J* = 10.4, 4.7 Hz, 1H), 3.24 (ddd, *J* = 17.4, 10.4, 2.3 Hz, 1H), 3.12 (ddd, *J* = 17.4, 4.7, 1.1 Hz, 1H), 1.93 – 1.74 (m, 1H), 1.38 – 1.24 (m, 1H), 1.16 (s, 3H), 1.11 (dt, *J* = 14.6, 6.9 Hz, 1H), 1.05 (s, 3H), 1.01 – 0.86 (m, 1H), 0.81 (t, *J* = 7.4 Hz, 3H), 0.75 (t, *J* = 7.3 Hz, 3H).

^{13}C NMR (101 MHz, $CDCl_3$) δ 202.1, 181.8, 149.5, 141.2, 132.2, 130.0 (broad), 129.6, 128.3, 127.54, 127.52, 127.3, 127.1, 48.2, 47.4, 45.2, 43.9, 24.1, 24.0, 23.5, 22.3, 9.0, 7.9.

HRMS (ESI) *m/z* Calculated for $C_{26}H_{30}NaO_3^+$ $[M+Na]^+$: 413.2087, found 413.2099.

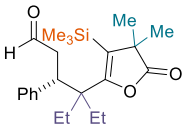

(*S*)-4-(4,4-Dimethyl-5-oxo-3-(trimethylsilyl)-4,5-dihydrofuran-2-yl)-4-ethyl-3-phenylhexanal (35c)

The reaction of 5-ethyl-2,2-dimethyl-3-(trimethylsilyl)hepta-3,4-dienoic acid (**34c**) with cinnamaldehyde according to the general procedure **A** detailed in section 4.6.5 (reaction time: 18 h, flash chromatography eluent: toluene:EtOAc gradient from 100:0 to 95:5) gave the title product in the form of a pale yellow oil (24.1 mg, 62%, average of three runs). The enantiomeric excess was determined by analysis of the corresponding cyclized product **36c.**

^{1}H NMR (400 MHz, $CDCl_3$) δ 9.54 (dd, *J* = 2.1, 1.1 Hz, 1H), 7.24 – 7.14 (m, 3H), 7.12 – 7.04 (m, 2H), 3.55 (dd, *J* = 10.0, 4.8 Hz, 1H), 3.21 – 3.06 (m, 2H), 2.03 – 1.92 (m, 1H), 1.72 – 1.58 (m, 1H), 1.59 – 1.40 (m, 2H), 1.31 (s, 3H), 1.30 (s, 3H), 0.95 (t, *J* = 7.3 Hz, 3H), 0.80 (t, *J* = 7.4 Hz, 3H), -0.05 (s, 9H). ^{13}C NMR (101 MHz, $CDCl_3$) δ 202.2, 184.1, 161.9, 140.8, 129.4, 128.2, 127.3, 121.9, 49.7, 48.6, 45.7, 44.3, 25.0, 24.6, 24.0, 23.0, 9.0, 7.5, 3.7.

HRMS (ESI) *m/z* Calculated for $C_{26}H_{34}NaO_3Si^+$ $[M+Na]^+$: 409.2169, found 409.2169.

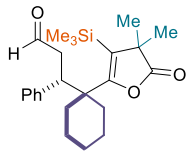

(*S*)-3-(1-(4,4-Dimethyl-5-oxo-3-(trimethylsilyl)-4,5-dihydrofuran-2-yl)cyclohexyl)-3-phenylpropanal (35c)

The reaction of 1-(3-ethyl-1-(trimethylsilyl)penta-1,2-dien-1-yl)cyclohexane-1-carboxylic acid (**34c**) with cinnamaldehyde according to the general procedure **A** detailed in section 4.6.5 (reaction time: 18 h, flash chromatography eluent: hexanes:EtOAc gradient from 100:0 to 90:10) gave the title product in the form of a pale yellow oil (25.6 mg, 64%, average of two runs). The enantiomeric excess was determined by analysis of the corresponding cyclized product **36d.**

^{1}H NMR (500 MHz, $CDCl_3$) δ 9.49 (dd, *J* = 2.3, 1.3 Hz, 1H), 7.29 – 7.18 (m, 3H), 7.18 – 7.14 (m, 2H), 3.55 (dd, *J* = 11.0, 3.9 Hz, 1H), 3.08 (ddd, *J* = 17.0, 11.0, 2.4 Hz, 1H), 2.71 (dd, *J* = 17.0, 3.9 Hz, 1H), 2.17 – 1.97 (m, 2H), 1.69 – 1.42 (m, 4H), 1.34 (s, 3H), 1.32 (s, 3H), 1.39 – 1.22 (m, 2H), 1.09 – 0.96 (m, 1H), 0.91 – 0.79 (m, 1H), 0.34 (s, 9H).

^{13}C NMR (126 MHz, $CDCl_3$) δ 201.3, 184.0, 163.9, 139.6, 130.2, 128.2, 127.4, 119.2, 50.1, 48.5, 46.0, 44.7, 33.2, 30.6, 25.6, 25.2, 24.7, 23.9, 23.8, 3.2. Some resonances in the ^{13}C NMR spectrum are broadened due to conformational equilibria.

HRMS (ESI) *m/z* Calculated for $C_{24}H_{34}NaO_3Si^+$ $[M+Na]^+$: 421.2169, found 421.2189.

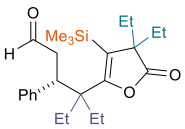

(*S*)-4-(4,4-Diethyl-5-oxo-3-(trimethylsilyl)-4,5-dihydrofuran-2-yl)-4-ethyl-3-phenylhexanal (35e)

The reaction of 2,2,5-triethyl-3-(trimethylsilyl)hepta-3,4-dienoic acid (**34e**) with cinnamaldehyde according to the general procedure **A** detailed in section 4.6.5 (reaction time: 18 h, flash chromatography eluent hexanes:EtOAc 96:4) gave the title product as a yellow oil (19.9 mg, 48%, average of two runs). The enantiomeric excess was determined by analysis of the corresponding cyclized product **36e.**

^{1}H NMR (400 MHz, $CDCl_3$) δ 9.53 (d, *J* = 1.7 Hz, 1H), 7.28 – 7.17 (m, 5H), 3.58 (dd, *J* = 11.3, 3.7 Hz, 1H), 3.18 (ddd, *J* = 17.2, 11.3, 2.5 Hz, 1H), 3.02 (dd, *J* = 16.9, 3.3 Hz, 1H), 2.04 (dq, *J* = 14.6, 7.4 Hz, 1H), 1.80 (m, 5H), 1.60 (m, 2H), 0.91 (t, *J* = 7.3 Hz, 3H), 0.87 – 0.78 (m, 9H), 0.11 (s, 9H).

^{13}C NMR (101 MHz, $CDCl_3$) δ 201.93, 182.36, 163.24, 140.20, 129.77, 127.12, 117.47, 60.64, 45.76, 45.02, 30.63, 30.53, 25.85, 23.10, 10.37, 10.05, 8.68, 7.88, 3.59.

HRMS (ESI) Calculated for $C_{25}H_{38}NaO_3Si$ $[M+Na]^+$: 437.2482, found: 437.2478.

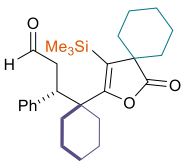

(*S*)-3-(1-(1-Oxo-4-(trimethylsilyl)-2-oxaspiro[4.5]dec-3-en-3-yl)cyclohexyl)-3-phenylpropanal (35f)

The reaction of 1-(2-cyclohexylidene-1-(trimethylsilyl)vinyl)cyclohexane-1-carboxylic acid (**34e**) with cinnamaldehyde according to modified general procedure **A** detailed in section 4.6.5 using propionitrile (400 µL) as solvent (reaction time: 18 h, flash chromatography eluent hexanes:EtOAc 97:3, rest of cinnamaldehyde remove at 50 °C, 0.01 mbar) gave the title product as a yellow oil (20.1 mg, 46%, average of two runs). The enantiomeric excess was determined by analysis of the corresponding cyclized product **36e.**

^{1}H NMR (400 MHz, $CDCl_3$) δ 9.50 (dd, *J* = 2.3, 1.2 Hz, 1H), 7.32 – 7.27 (m, 1H), 7.25 – 7.11 (m, 3H), 3.57 (dd, *J* = 11.3, 3.7 Hz, 1H), 3.11 (ddd, *J* = 17.0, 11.3, 2.4 Hz, 1H), 2.70 (dd, *J* = 17.0, 3.0 Hz, 1H), 2.19 – 1.99 (m, 5H), 1.92 (ddd, *J* = 18.1, 8.8, 4.4 Hz, 2H), 1.77 (d, *J* = 13.2 Hz, 1H), 1.70 – 1.45 (m, 7H), 1.45 – 1.12 (m, 7H), 1.05 – 0.92 (m, 0H), 0.39 (s, 6H).

^{13}C NMR (101 MHz, $CDCl_3$) δ 201.36, 181.00, 163.90, 139.32, 130.17, 128.00, 127.19, 118.74, 52.22, 48.40, 45.89, 44.59, 33.13, 31.15, 31.04, 30.18, 25.48, 24.58, 23.88, 23.71, 20.28, 20.03, 3.87.

HRMS (ESI) Calculated for $C_{27}H_{38}NaO_3Si$ $[M+Na]^+$: 461.2482, found: 461.2483.

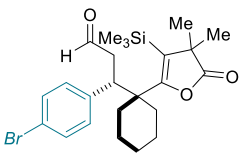

(*S*)-3-(4-Bromophenyl)-3-(1-(4,4-dimethyl-5-oxo-3-(trimethylsilyl)-4,5-dihydrofuran-2-yl)cyclohexyl)propanal (35g)

The reaction of 4-cyclohexylidene-2,2-dimethyl-3-(trimethylsilyl)but-3-enoic acid (**34d**) with (*E*)-3-(4-bromophenyl)acrylaldehyde according to the general procedure **B** detailed in section 4.6.5 (reaction time: 18 h, flash chromatography eluent: hexanes:EtOAc 96:4) gave the title product in the form of a yellow foam (22.3 mg, 47%, average of two runs). The enantiomeric excess was determined by analysis of the corresponding cyclized product **36g.**

^{1}H NMR (400 MHz, $CDCl_3$) δ 9.52 (dd, *J* = 2.0, 1.0 Hz, 1H), 7.40 (d, *J* = 8.4 Hz, 2H), 7.05 (d, *J* = 8.4 Hz, 2H), 3.55 (dd, *J* = 10.9, 3.7 Hz, 1H), 3.06 (ddd, *J* = 17.3, 11.0, 2.1 Hz, 1H), 2.78 – 2.64 (m, 1H), 2.06 (dd, *J* = 37.8, 11.2 Hz, 2H), 1.76 – 1.59 (m, 1H), 1.57 – 1.45 (m, 2H), 1.36 (s, 3H), 1.33 (s, 3H), 1.30 – 1.17 (m, 4H), 1.10 – 0.98 (m, 1H), 0.35 (s, 9H).

^{13}C NMR (101 MHz, $CDCl_3$) δ 200.51, 183.74, 163.43, 138.59, 131.62, 131.16, 121.20, 119.32, 49.99, 47.60, 45.69, 44.61, 33.08, 30.33, 25.42, 25.08, 24.55, 23.66, 23.54, 3.01.

HRMS (ESI) *m/z* Calculated for $C_{24}H_{33}NaO_3Si^+$ $[M+Na]^+$: 499.1275, found: 499.1274

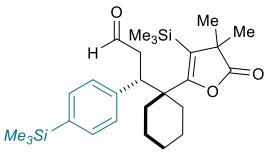

(*S*)-3-(1-(4,4-Dimethyl-5-oxo-3-(trimethylsilyl)-4,5-dihydrofuran-2-yl)cyclohexyl)-3-(4-(trimethylsilyl)phenyl) propanal (35h)

The reaction of 4-cyclohexylidene-2,2-dimethyl-3-(trimethylsilyl)but-3-enoic acid (**34d**) with (*E*)-3-(4-(trimethylsilyl)phenyl)acrylaldehyde according to the general procedure **B** detailed in section 4.6.5 (reaction time: 18 h, flash chromatography eluent: hexanes:EtOAc 97:3) gave the title product in the form of a yellow oil (26.2 mg, 56%, average of two runs). The enantiomeric excess was determined by analysis of the corresponding cyclized product **36h.**

^{1}H NMR (400 MHz, $CDCl_3$) δ 9.50 (dd, *J* = 2.2, 1.2 Hz, 1H), 7.41 (d, *J* = 8.0 Hz, 2H), 7.15 (d, *J* = 7.9 Hz, 2H), 3.56 (dd, *J* = 10.9, 3.8 Hz, 1H), 3.10 (ddd, *J* = 17.0, 10.9, 2.3 Hz, 1H), 2.72 (dd, *J* = 17.1, 3.1 Hz, 1H), 2.08 (dd, *J* = 30.8, 9.9 Hz, 2H), 1.72 – 1.58 (m, 1H), 1.58 – 1.42 (m, 2H), 1.40 – 1.20 (dd, *J* = 11.3, 3.7 Hz, 4H), 1.36 (s, 3H), 1.33 (s, 3H), 1.16 – 0.98 (m, 1H), 0.33 (s, 9H), 0.24 (s, 9H).

^{13}C NMR (101 MHz, $CDCl_3$) δ 201.28, 183.90, 163.73, 139.91, 139.24, 133.00, 129.43, 119.06, 49.98, 48.19, 45.90, 44.58, 33.19, 30.40, 25.46, 25.08, 24.54, 23.69, 23.56, 3.04, -1.14.

HRMS (ESI) *m/z* Calculated for $C_{27}H_{42}NaO_3Si_2^+$ $[M+Na]^+$: 493.2565, found: 493.2555.

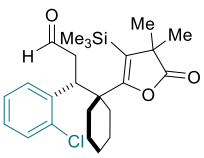

(*R*)-3-(2-Chlorophenyl)-3-(1-(4,4-dimethyl-5-oxo-3-(trimethylsilyl)-4,5-dihydrofuran-2-yl)cyclohexyl)propanal (35i)

The reaction of 4-cyclohexylidene-2,2-dimethyl-3-(trimethylsilyl)but-3-enoic acid (**34d**) with (*E*)-3-(2-chlorophenyl)acrylaldehyde according to the general procedure **B** detailed in section 4.6.5 (reaction time: 18 h, flash chromatography eluent: hexanes:EtOAc 97:3) gave the title product in the form of a yellowish oil (22.6 mg, 52%, average of two runs). The enantiomeric excess was determined by analysis of the corresponding cyclized product **36i.**

^{1}H NMR (400 MHz, $CDCl_3$) δ 9.46 (d, *J* = 1.5 Hz, 1H), 7.39 (d, *J* = 6.9 Hz, 1H), 7.25 – 7.14 (m, 3H), 4.19 (dd, *J* = 11.0, 4.5 Hz, 1H), 3.03 (ddd, *J* = 16.9, 11.1, 2.7 Hz, 1H), 2.84 (dd, *J* = 17.0, 4.0 Hz, 1H), 2.31 – 2.07 (m, 2H), 1.80 – 1.68 (m, 1H), 1.53 (ddd, *J* = 18.8, 9.1, 4.6 Hz, 3H), 1.39 (s, 3H), 1.38 (s, 3H), 1.58 – 1.28 (m, 4H), 0.31 (s, 9H).

^{13}C NMR (126 MHz, $CDCl_3$) δ 201.10, 184.18, 162.52, 137.91, 135.88, 131.56, 130.31, 128.70, 126.69, 120.82, 50.48, 47.13, 46.21, 36.31, 33.63, 32.01, 30.06, 25.93, 25.18, 25.12, 3.47.

HRMS (ESI) *m*/*z* Calculated for $C_{25}H_{37}ClNaO_4Si^+$ $[M+MeOH+Na]^+$: 487.2042, found: 487.2043.

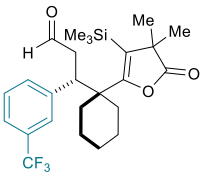

(*S*)-3-(1-(4,4-Dimethyl-5-oxo-3-(trimethylsilyl)-4,5-dihydrofuran-2-yl) cyclohexyl)-3-(3-(trifluoromethyl)phenyl)propanal (35j)

The reaction of 4-cyclohexylidene-2,2-dimethyl-3-(trimethylsilyl)but-3-enoic acid (**34d**) with (*E*)-3-(3-(trifluoromethyl)phenyl)acrylaldehyde according to the general procedure **B** detailed in section 4.6.5 (reaction time: 18 h, flash chromatography eluent: hexanes:EtOAc 96:4) gave the title product in the form of a yellow oil (20.9 mg, 45%, average of two runs). The enantiomeric excess was determined by analysis of the corresponding cyclized product **36j.** ^{1}H NMR (400 MHz, $CDCl_3$) δ 9.77 – 9.03 (m, 1H), 7.50 (d, *J* = 7.1 Hz, 1H), 7.40 (d, *J* = 7.2 Hz, 3H), 3.69 (dd, *J* = 10.7, 3.7 Hz, 1H), 3.13 (ddd, *J* = 17.6, 10.7, 1.8 Hz, 1H), 2.85 (dd, *J* = 17.6, 3.3 Hz, 1H), 2.06 (dd, *J* = 35.9, 11.0 Hz, 2H), 1.69 (dd, *J* = 9.1, 4.1 Hz, 1H), 1.59 – 1.46 (m, 2H), 1.46 – 1.36 (m, 2H), 1.34 (s, 3H), 1.33 (s, 3H), 1.32 – 1.22 (m, 2H), 1.19 – 1.04 (m, 1H), 0.32 (s, 9H).

^{13}C NMR (101 MHz, $CDCl_3$) δ 200.21, 183.66, 163.08, 140.89, 133.29, 130.38 (q, *J* = 31.9 Hz), 128.53, 126.32, 124.17 (q, *J* = 3.6 Hz), 124.02 (q, *J* = 272.0 Hz), 119.58, 49.96, 47.33, 45.67, 44.75, 32.94, 30.77, 29.71, 25.42, 25.07, 24.49, 23.48, 23.41, 3.00.

^{19}F NMR (376 MHz, $CDCl_3$) δ -62.17.

HRMS (ESI) *m/z* Calculated for $C_{25}H_{32}F_3O_3Si_2^-$ $[M-H]^-$: 465.2078, found: 465.2098

4.6.7. General Procedure for the Cyclisation Leading to Products 36

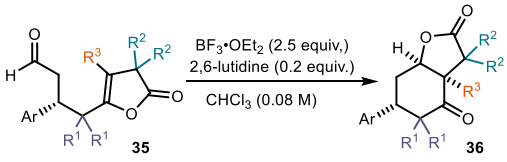

Figure 4.19. General Procedure for the synthesis of products **36**.

General Procedure: A vial was charged with the appropriate aldehyde product **6**, chloroform (0.08 M), and 2,6-lutidine (0.5 equiv.). BF_3•OEt_2 (2.5 equiv.) was added to the mixture and the reaction was stirred until complete disappearance of aldehyde **35**. The reaction mixture was then added to silica gel (approx. 1 g), volatiles were removed under reduced pressure and the resulting solids were directly loaded on a flash chromatography column (silica gel). Elution with the specified solvent system gave the required products.

4.6.8. Characterization of the Cyclisation of products 36

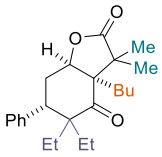

(3a*R*,6*S*,7a*R*)-3a-Butyl-5,5-diethyl-3,3-dimethyl-6-phenyl hexahydro benzo furan-2,4-dione (36a)

The reaction of compound **35a** (20.3 mg, 0.055 mmol) according to the General Procedure detailed in section 4.6.7 (flash chromatography eluent: hexanes:EtOAc 98:2) gave the title compound in the form of a pale yellow oil (17.0 mg, 84%, >19:1 dr). The enantiomeric excess was determined by UPC² analysis on a chiral stationary phase (Daicel Chiralpak CEL1, gradient: CO_2:CH_3CN from 100:0 to 60:40 over 9.0 minutes, flow rate: 3.0 mL/min, λ = 215 nm, τ_{major} = 3.24 min, τ_{minor} = 3.44 min). $[\alpha]_D^{26}$ = +34.0 (*c* = 0.175, $CHCl_3$, 70% ee).

^{1}H NMR (500 MHz, $CDCl_3$) δ 7.30 (dd, *J* = 8.2, 6.7 Hz, 2H), 7.27 – 7.19 (m, 3H), 4.67 (dd, *J* = 4.0, 2.2 Hz, 1H), 3.79 (dd, *J* = 14.2, 3.2 Hz, 1H), 2.76 – 2.62 (m, 1H), 2.35 (dt, *J* = 14.20, 3.2 Hz, 1H), 2.09 (dq, *J* = 12.5, 6.5, 5.8 Hz, 1H), 1.77 – 1.67 (m, 2H), 1.39 (s, 3H), 1.29 (s, 3H), 1.45 – 1.21 (m, 4H), 1.12 (dt, *J* = 14.7, 7.4 Hz, 1H), 0.95 – 0.83 (m, 8H), 0.62 (t, *J* = 7.4 Hz, 3H).

^{13}C NMR (126 MHz, $CDCl_3$) δ 212.1, 180.9, 140.0, 129.6, 128.1, 127.0, 81.2, 58.0, 56.6, 47.4, 37.2, 33.5, 27.2, 27.1, 26.2, 25.9, 23.4, 22.7, 22.0, 13.9, 9.6, 8.2.

HRMS (ESI) *m/z* Calculated for $C_{24}H_{34}NaO_3^+$ $[M+Na]^+$: 393.2400, found 393.2399.

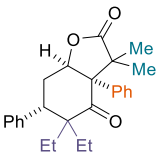

(3a*R*,6*S*,7a*R*)-5,5-diethyl-3,3-dimethyl-3a,6-diphenylhexahydrobenzofuran-2,4-dione (36b)

The reaction of compound **35b** (21.0 mg, 0.054 mmol) according to the General Procedure detailed in section 4.6.7 (flash chromatography eluent: hexanes:EtOAc gradient from 98:2 to 97:3) gave the title compound in the form of a pale yellow oil (17.2 mg, 82%, mixture of two unseparable diasteroisomer in 88:12 ratio, 76% ee). The enantiomeric excess was determined by UPC² analysis on a chiral stationary phase (Daicel Chiralpak CEL1, gradient: CO_2:CH_3CN from 100:0 to 60:40 over 9.0 minutes, flow rate: 3.0 mL/min, λ = 215 nm, major diasteroisomer τ_{major} = 3.71 min, τ_{minor} = 3.82 min, min diasteroisomer τ_{major} = 3.98 min, τ_{minor} = 4.27 min). $[\alpha]_D^{26}$ = +125.5 (*c* = 0.200, $CHCl_3$, 76% ee, mixture of diasteroisomers).

Major diastereoisomer. ^{1}H NMR (500 MHz, $CDCl_3$) δ 7.50 (s, 2H), 7.42 – 7.39 (m, 2H), 7.37 – 7.33 (m, 1H), 7.31 – 7.28 (m, 2H), 7.27 – 7.23 (m, 4H), 3.89 (dd, *J* = 13.7, 3.3 Hz, 1H), 3.04 (ddd, *J* = 14.8, 13.7, 2.3 Hz, 1H), 2.54 (dt, *J* = 14.9, 3.6 Hz, 1H), 2.04 – 1.95 (m, 1H), 1.67 (s, 3H), 1.22 – 1.12 (m, 1H), 1.04 – 0.97 (m, 1H), 0.91 (t, *J* = 7.2 Hz, 3H), 0.04 (t, *J* = 7.4 Hz, 3H).

^{13}C NMR (126 MHz, $CDCl_3$) δ 209.3, 180.0, 139.7, 133.9, 129.7, 129.1, 128.2, 128.1, 127.2 (br), 127.1, 77.8, 62.0, 58.3, 49.6, 37.7, 26.8, 25.7, 24.6, 22.9, 22.6, 9.4, 7.1.

Minor diastereoisomer. ^{1}H NMR (500 MHz, $CDCl_3$) δ *(only signals resolved from those of the major diastereoisomer are given)* 7.16 – 7.13 (m, 2H), 5.51 (dd, *J* = 7.9, 5.6 Hz, 1H), 3.24 (dd, *J* = 13.2, 4.9 Hz, 1H), 2.82 (ddd, *J* = 15.0, 13.1, 5.6 Hz, 1H), 2.68 (ddd, *J* = 15.0, 7.9, 4.8 Hz, 1H), 1.94 – 1.81 (m, 2H), 1.58 (s, 3H), 0.81 (s, 3H), 0.68 (d, *J* = 7.3 Hz, 4H), 0.44 (t, *J* = 7.3 Hz, 3H).

^{13}C NMR (126 MHz, $CDCl_3$) δ 210.8, 179.8, 139.9, 133.9, 129.2, 129.2, 128.3, 128.2, 127.3, 127.0, 79.1, 63.2, 56.8, 41.7, 34.8, 25.4, 24.7, 24.2, 23.1, 22.8, 8.8, 8.5.

HRMS (ESI) *m/z* Calculated for $C_{26}H_{30}NaO_3^+$ $[M+Na]^+$: 413.2087, found 413.2091.

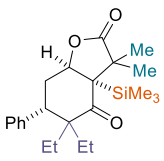

(3a*S*,6*S*,7a*R*)-5,5-Diethyl-3,3-dimethyl-6-phenyl-3a-(trimethylsilyl)hexa hydro benzofuran-2,4-dione (36c)

The reaction of compound **35c** (16.5 mg, 0.043 mmol) according to the General Procedure detailed in section 4.6.7 (flash chromatography eluent: hexanes:EtOAc gradient from 98:2 to 97:3) gave the title compound in the form of a pale yellow oil (14.3 mg, 87%, 75% ee, >19:1 dr). The enantiomeric excess was determined by UPC² analysis on a chiral stationary phase (Daicel Chiralpak IE3, gradient: CO_2:EtOH from 100:0 to 60:40 over 9.0 minutes, flow rate: 3.0 mL/min, λ = 210 nm, τ_{major} = 4.49 min, τ_{minor} = 4.70 min). $[\alpha]_D^{26}$ = +76.4 (*c* = 0.130, $CHCl_3$, 75% ee).

^{1}H NMR (500 MHz, $CDCl_3$) δ 7.32 – 7.27 (m, 2H), 7.26 – 7.22 (m, 1H), 7.20 – 7.16 (m, 2H), 5.16 – 5.14 (m, 1H), 3.87 (dd, *J* = 11.9, 4.3 Hz, 1H), 2.49 – 2.38 (m, 2H), 2.14 – 2.03 (m, 1H), 1.63 – 1.55 (m, 1H), 1.44 (s, 3H), 1.33 (s, 3H), 1.20 – 1.10 (m, 1H), 1.09 – 1.00 (m, 1H), 0.89 (t, *J* = 7.4 Hz, 3H), 0.54 (t, *J* = 7.3 Hz, 3H), 0.29 (s, 9H).

^{13}C NMR (126 MHz, $CDCl_3$) δ 216.0, 181.3, 140.7, 129.5, 128.1, 126.9, 77.9, 57.6, 56.4, 49.4, 37.0, 29.7, 27.6, 26.8, 25.9, 22.3, 9.9, 8.5, 1.0.

HRMS (ESI) *m*/*z* Calculated for $C_{23}H_{34}NaO_3Si^+$ $[M+Na]^+$: 409.2169, found 409.2153.

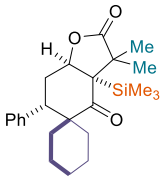

(3a*S*,6*S*,7a*R*)-3,3-Dimethyl-6-phenyl-3a-(trimethylsilyl)tetra hydro-4*H*-spiro [benzofuran-5,1'-cyclohexane]-2,4(3*H*)-dione (36d)

The reaction of compound **35d** (14.4 mg, 0.0365 mmol) according to the General Procedure detailed in section 4.6.7 (flash chromatography eluent: hexanes:EtOAc 95:5) gave the title compound in the form of a pale yellow oil (13.2 mg, 92%, 77% ee, >19:1 dr). The enantiomeric excess was determined by UPC² analysis on a chiral stationary phase (Daicel Chiralpak IA, gradient: CO_2:*i*PrOH from 100:0 to 60:40 over 9.0 minutes, flow rate: 3.0 mL/min, λ = 215 nm, τ_{major} = 3.46 min, τ_{minor} = 3.63 min). $[\alpha]_D^{26}$ = +26.8 (*c* = 0.150, $CHCl_3$, 77% ee).

^{1}H NMR (500 MHz, $CDCl_3$) δ 7.33 – 7.28 (m, 2H), 7.27 – 7.23 (m, 1H), 7.18 – 7.15 (m, 2H), 5.10 (dd, *J* = 3.8, 2.6 Hz, 1H), 3.28 (dd, *J* = 11.0, 5.7 Hz, 1H), 2.37 – 2.27 (m, 2H), 1.85 – 1.59 (m, 3H), 1.47 (s, 3H), 1.46 – 1.37 (m, 4H), 1.22 (s, 3H), 1.09 – 0.98 (m, 2H), 0.95 – 0.83 (m, 1H), 0.29 (s, 9H).

^{13}C NMR (126 MHz, $CDCl_3$) δ 216.4, 181.7, 141.1, 130.2, 128.1, 127.0, 77.5, 57.6, 50.5, 49.1, 44.7, 34.8, 31.8, 29.3, 25.4, 25.0, 24.1, 21.7, 21.1, 1.0.

HRMS (ESI) *m*/*z* Calculated for $C_{24}H_{34}NaO_3Si^+$ $[M+Na]^+$: 421.2169, found 421.2158.

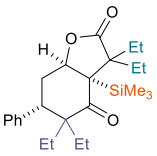

(3a*S*,6*S*,7a*R*)-3,3,5,5-Tetraethyl-6-phenyl-3a-(trimethylsilyl) hexahydro benzofuran-2,4-dione (36e)

The reaction of compound **35g** (19.5 mg, 0.047 mmol) according to the General Procedure detailed in section 4.6.7 (flash chromatography eluent: hexanes:EtOAc 97:3) gave the title compound in the form of a pale yellow oil (7.3 mg, 38%, 81% ee, >19:1 dr). The enantiomeric excess was determined by UPC² Daicel Chiralpak IE3 column (gradient CO_2:*i*PrOH from 100:0 to 60:40 over 9 minutes, 3.0 mL/min, λ = 220 nm, τ_{major} = 5.12 min, τ_{minor} = 5.24 min). $[\alpha]_D^{25}$ = +182.3 (*c* = 0.09, $CHCl_3$, 81% ee).

^{1}H NMR (300 MHz, $CDCl_3$) δ 7.35 – 7.24 (m, 2H), 7.25 – 7.16 (m, 3H), 5.12 (dd, *J* = 4.0, 2.1 Hz, 1H), 3.71 (dd, *J* = 12.4, 3.9 Hz, 1H), 2.53 – 2.31 (m, 2H), 2.16 – 1.87 (m, 3H), 1.73 (dq, *J* = 14.1, 7.1 Hz, 1H), 1.66 (dq, *J* = 14.8, 7.4 Hz, 1H), 1.45 (dq, *J* = 14.9, 7.3 Hz, 1H), 1.28 – 1.13 (m, 2H), 1.10 (t, *J* = 7.4 Hz, 3H), 0.96 (t, *J* = 7.4 Hz, 3H), 0.89 (t, *J* = 7.4 Hz, 3H), 0.45 (t, *J* = 7.4 Hz, 3H), 0.30 (s, 9H).

^{13}C NMR (101 MHz, $CDCl_3$) δ 215.96, 178.68, 140.66, 129.37, 128.01, 126.76, 76.85, 59.81, 56.82, 56.12, 38.38, 30.33, 28.05, 26.31, 26.16, 24.29, 9.71, 8.93 (2C), 8.47, 2.41.

HRMS (ESI) Calculated for $C_{25}H_{38}NaO_3Si$ $[M+Na]^+$: 437.2482, found: 437.2480.

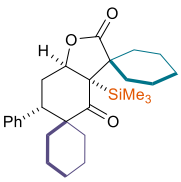

(3a'*S*,6'*S*,7a'*R*)-6'-Phenyl-3a'-(trimethylsilyl)tetrahydro-2'H,4'H-dispiro [cyclohexane-1,3'-benzofuran-5',1''-cyclohexane]-2',4'-dione (36f)

The reaction of compound **35g** (19.8 mg, 0.045 mmol) according to the General Procedure detailed in section 4.6.7 (flash chromatography eluent: hexanes:EtOAc 97:3) gave the title compound in the form of a white solid (15.5 mg, 78%, 77% ee, >19:1 dr). The enantiomeric excess was determined by UPC² Daicel Chiralpak IE3 column (gradient CO_2:EtOH from 100:0 to 60:40 over 9 minutes, 3.0 mL/min, λ = 220 nm, τ_{major} = 5.26 min, τ_{minor} = 5.15 min). $[\alpha]_D^{26}$ = +17.90 (*c* = 0.10, $CHCl_3$,78% ee). The absolute configuration was determined by anomalous dispersion X-ray crystallographic analysis, see X-ray Crystallographic Data in section 4.6.10.

^{1}H NMR (500 MHz, $CDCl_3$) δ 7.28 (t, *J* = 7.3 Hz, 2H), 7.25 – 7.20 (m, 1H), 7.16 (d, *J* = 7.1 Hz, 2H), 5.08 (dd, *J* = 3.9, 2.2 Hz, 1H), 3.33 (dd, *J* = 12.6, 4.2 Hz, 1H), 2.35 – 2.10 (m, 3H), 1.99 (d, *J* = 13.1 Hz, 1H), 1.80 (td, *J* = 12.8, 4.7 Hz, 1H), 1.76 – 1.56 (m, 8H), 1.51 – 1.21 (m, 5H), 1.15 (qt, *J* = 13.2, 4.3 Hz, 1H), 1.02 – 0.93 (m, 2H), 0.92 – 0.80 (m, 1H), 0.28 (s, 6H).

^{13}C NMR (126 MHz, $CDCl_3$) δ 216.36, 179.44, 141.65, 130.39, 128.34, 127.14, 76.78, 59.99, 51.73, 50.75, 44.92, 35.03, 33.67, 32.51, 31.47, 29.93, 25.46, 25.27, 22.70, 22.08, 21.82, 21.51, 1.65.

HRMS (ESI) Calculated for $C_{27}H_{38}NaO_3Si$ $[M+Na]^+$: 461.2482, found: 461.2473.

m.p. = 78 – 84 °C

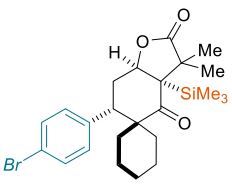

(3a*S*,6*S*,7a*R*)-6-(4-Bromophenyl)-3,3-dimethyl-3a-(trimethylsilyl) tetrahydro-4H-spiro[benzofuran-5,1'-cyclohexane]-2,4(3H)-dione (36g)

The reaction of compound **35d** (19.2 mg, 0.040 mmol) according to the General Procedure detailed in section 4.6.7 (flash chromatography eluent: hexanes:EtOAc 96:4) gave the title compound in the form of a pale yellow solid (12.9 mg, 67%, 75% ee, >19:1 dr). The enantiomeric excess was determined by UPC² Daicel Chiralpak IC3 column (gradient CO_2: EtOH from 100:0 to 60:40 over 9 minutes, 3.0 mL/min, λ = 220 nm, τ_{major} = 3.61 min, τ_{minor} = 3.38 min). $[\alpha]_D^{25}$ = –3.806 (*c* = 0.072, $CHCl_3$, 75% ee).

^{1}H NMR (400 MHz, $CDCl_3$) δ 7.66 – 7.30 (m, 2H), 7.11 – 6.56 (m, 2H), 5.43 – 4.62 (m, 1H), 3.24 (dd, *J* = 11.3, 5.3 Hz, 1H), 2.35 – 2.19 (m, 2H), 1.87 – 1.60 (m, 3H), 1.60 – 1.48 (m, 2H), 1.46 (s, 3H), 1.43 – 1.32 (m, 2H), 1.32 – 1.23 (m, 1H), 1.21 (s, 3H), 1.09 (m, 1H), 1.01 – 0.83 (m, 1H), 0.28 (s, 9H).

^{13}C NMR (101 MHz, $CDCl_3$) δ 215.82, 181.37, 139.89, 131.68, 131.13, 120.84, 77.16, 57.52, 50.11, 48.95, 44.15, 34.55, 31.53, 29.09, 25.31, 24.87, 23.89, 21.47, 20.93, 0.86.

HRMS (ESI) Calculated for $C_{24}H_{33}BrNaO_3Si$ $[M+Na]^+$: 499.1275, found: 499.1271.

m.p. = 166 – 170 °C

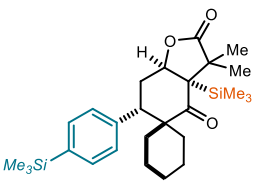

(3a*S*,6*S*,7a*R*)-3,3-Dimethyl-3a-(trimethylsilyl)-6-(4-(trimethyl silyl)phenyl)tetrahydro-4H-spiro[benzofuran-5,1'-cyclohexane]-2,4(3H)-dione (36h)

The reaction of compound **35d** (27.0 mg, 0.057 mmol) according to the General Procedure detailed in section 4.6.7 (flash chromatography eluent: hexanes:EtOAc 97:3) gave the title compound in the form of a pale yellow oil (18.2 mg, 67%, 76% ee, >19:1 dr). The enantiomeric excess was determined by HPLC Daicel Chiralpak IC-3 column (5:95 ^{i}PrOH:*n*hexane 1.0 mL/min,

20 ºC, λ = 254 nm, τ_{major} = 11.58 min, τ_{minor} = 8.78 min). $[\alpha]_D^{25}$ = –13.59 (*c* = 0.10, $CHCl_3$, 76% ee).

^{1}H NMR (400 MHz, $CDCl_3$) δ 7.44 (d, *J* = 8.0 Hz, 2H), 7.14 (d, *J* = 8.0 Hz, 2H), 5.09 (t, *J* = 3.2 Hz, 1H), 3.24 (q, *J* = 7.7, 7.2 Hz, 1H), 2.37 – 2.27 (m, 2H), 1.86 – 1.59 (m, 3H), 1.46 (s, 3H), 1.58 – 1.35 (m, 3H), 1.34 – 1.23 (m, 1H), 1.22 (s, 3H), 1.14 – 0.87 (m, 3H), 0.29 (s, 9H), 0.27 (s, 9H).

^{13}C NMR (101 MHz, $CDCl_3$) δ 216.29, 181.51, 141.33, 138.78, 132.99, 129.48, 77.42, 57.46, 50.29, 48.94, 44.59, 34.53, 31.53, 29.11, 25.32, 24.89, 23.97, 21.56, 20.97, 0.86, -1.08.

HRMS (ESI) Calculated for $C_{27}H_{42}NaO_3Si_2$ $[M+Na]^+$: 493.2565, found: 493.2577.

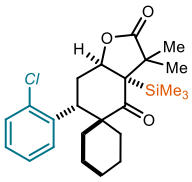

(3a*S*,6*R*,7a*R*)-6-(2-Chlorophenyl)-3,3-dimethyl-3a-(trimethylsilyl) tetrahydro-4H-spiro[benzofuran-5,1'-cyclohexane]-2,4(3H)-dione (36i)

The reaction of compound **35d** (22.0 mg, 0.051 mmol) according to the General Procedure detailed in section 4.6.7 (flash chromatography eluent: hexanes:EtOAc 96:4) gave the title compound in the form of a pale yellow oil (12.1 mg, 55%, 83% ee, >19:1 dr). The enantiomeric excess was determined by UPC² Daicel Chiralpak IB column (gradient CO_2: CH_3CN from 100:0 to 60:40 over 9 minutes, curve 6, 3.0 mL/min, λ = 220 nm, τ_{major} = 3.24 min, τ_{minor} = 3.35 min). $[\alpha]_D^{26}$ = +8.786 (*c* = 0.095, $CHCl_3$, 78% ee).

^{1}H NMR (500 MHz, $CDCl_3$) δ 7.52 – 7.28 (m, 1H), 7.25 – 7.15 (m, 3H), 5.03 (t, *J* = 3.3 Hz, 1H), 4.03 (dd, *J* = 13.5, 3.3 Hz, 1H), 2.33 (ddd, *J* = 14.8, 13.5, 3.3 Hz, 1H), 2.20 (dt, *J* = 14.9, 3.4 Hz, 1H), 1.93 – 1.79 (m, 2H), 1.72 (d, *J* = 14.1 Hz, 1H), 1.62 – 1.50 (m, 2H), 1.49 (s, 3H), 1.40 (dt, *J* = 13.2, 4.3 Hz, 2H), 1.28 (s, 3H), 1.27 – 1.20 (m, 1H), 1.21 – 1.14 (m, 1H), 0.99 – 0.86 (m, 1H), 0.28 (s, 9H).

^{13}C NMR (126 MHz, $CDCl_3$) δ 216.10, 181.49, 138.87, 135.85, 131.18, 130.35, 128.34, 126.60, 77.34, 57.01, 51.73, 49.03, 39.62, 34.53, 32.67, 28.97, 26.03, 25.66, 25.42, 22.36, 21.65, 0.98.

HRMS (ESI) Calculated for $C_{24}H_{33}ClNaO_3Si$ $[M+Na]^+$: 455.1780, found: 455.1784.

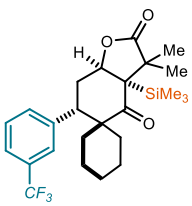

(3a*S*,6*S*,7a*R*)-3,3-Dimethyl-6-(3-(trifluoromethyl)phenyl)-3a-(trimethyl silyl)tetrahydro-4H-spiro[benzofuran-5,1'-cyclohexane]-2,4(3H)-dione (36j)

The reaction of compound **35d** (17.9 mg, 0.038 mmol) according to the General Procedure detailed in section 4.6.7 (flash

chromatography eluent: hexanes:EtOAc 96:4) gave the title compound in the form of a pale yellow oil (11.4 mg, 64%, 78% ee, >19:1 dr). The enantiomeric excess was determined by HPLC Daicel Chiralpak ID-3 column (5:95 ^{i}PrOH:hexane 1.0 mL/min, 20 ºC, λ = 254, nm, τ_{major} = 6.54 min, τ_{minor} = 5.96 min). $[\alpha]_D^{26}$ = +48.60 (*c* = 0.10, $CHCl_3$, 83% ee).

^{1}H NMR (400 MHz, $CDCl_3$) δ 7.53 (d, *J* = 7.7 Hz, 1H), 7.44 (t, *J* = 7.7 Hz, 1H), 7.40 (s, 1H), 7.36 (d, *J* = 7.9 Hz, 1H), 5.11 (t, *J* = 3.1 Hz, 1H), 3.34 (p, *J* = 7.3 Hz, 1H), 2.39 – 2.27 (m, 2H), 1.90 – 1.61 (m, 3H), 1.57 – 1.48 (m, 2H), 1.47 (s, 3H), 1.43 – 1.31 (m, 2H), 1.22 (s, 3H), 1.08 (dp, *J* = 13.1, 4.9, 4.2 Hz, 1H), 0.96 – 0.80 (m, 2H), 0.30 (s, 9H).

^{13}C NMR (101 MHz, $CDCl_3$) δ 215.56, 181.31, 141.84, 133.51, 130.45 (q, *J* = 32.1 Hz), 128.46, 126.47 (q, *J* = 3.7 Hz), 124.09 (q, *J* = 272.6 Hz), 123.86 (q, *J* = 3.5 Hz), 77.05, 57.57, 50.10, 48.97, 44.61, 34.53, 31.51, 29.08, 25.34, 24.83, 23.91, 21.43, 20.83, 0.87.

^{19}F NMR (376 MHz, $CDCl_3$) δ -62.20.

HRMS (ESI) Calculated for $C_{25}H_{33}F_3NaO_3Si$ $[M+Na]^+$: 489.2043, found: 489.2056.

4.6.9. Cyclic Voltammetry Studies

For the cyclic voltammetry measurements, a glassy carbon disk electrode (diameter: 3 mm) was used as a working electrode. A silver wire coated with AgCl immersed in a 3 M aqueous solution of NaCl and separated from the analyte by a fritted glass disk was employed as the reference electrode. A Pt wire counter-electrode completed the electrochemical setup.

All samples have been measured as a 5 mM solution in CH_3CN with $Bu_4N(PF_6)$ (0.1 M) as supporting electrolyte. A scan rate of 500 mV/s was used for all CV experiments.

A set of representative allenic acid substrates (**31a**, **31c**, **34a, 34d**) were characterized by cyclic voltammetry (Figures 4.20-4.23) in CH_3CN. All substrates featured irreversible oxidations under the described conditions. The corresponding anodic half-peak potentials ($E_{p/2}$) and peak potentials (E_p) vs. Ag/AgCl (3 M NaCl) are reported in Table S1. The $E_{p/2}$ of the acids analyzed fall in the range +1.63 to +2.12 V. Substitution at the β position ($R^2 \neq H$) makes the allenic acids easier to oxidize: for example, the fully substituted allenic acids **34a** and **34d** are oxidized at less positive potentials than **31a** and **31c**. The Me_3Si substituent has a comparatively strong effect, as attested by the fact that compound **34d** is reduced at a potential which is 0.44 V less anodic than that of **31c**.

Table 4.2 – Anodic half-peak potentials ($E_{p/2}$) and peak potentials (E_p) of selected allenic acids. Conditions: 5 mM solutions in CH_3CN with $Bu_4N(PF_6)$ (0.1 M) as supporting electrolyte, Ag/AgCl (3 M NaCl) reference electrode.

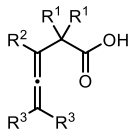

Compound	R1	R2	R3	E_p (V)	$E_{p/2}$ (V)
31a	Me	H	Me	+2.28	+2.12
31c	Me	H	-$(CH_2)_5$-	+2.36	+2.07
34a	Me	Bu	Et	+2.15	+1.95
34d	Me	Me_3Si	-$(CH_2)_5$-	+1.76	+1.63

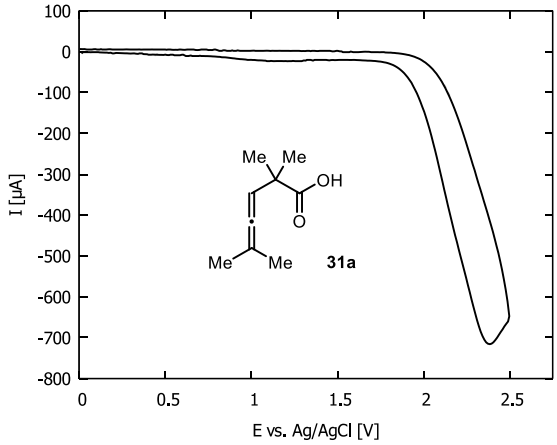

Figure 4.20. Cyclic voltammogram of **31a**. Irreversible oxidation, $E_{p/2}$ (**31a** /**31a**$^{\bullet+}$) = +2.12 V.

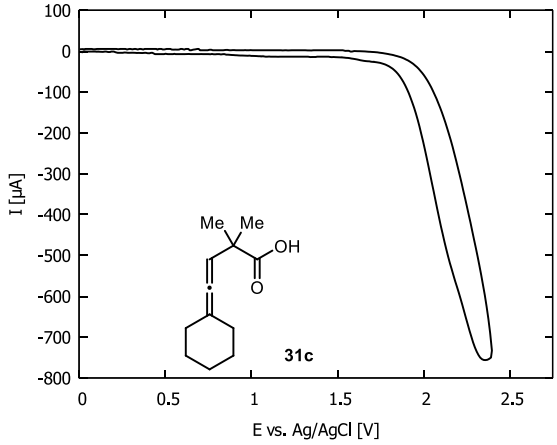

Figure 4.21. Cyclic voltammogram of **31c**. Irreversible oxidation, $E_{p/2}$ (**31c** /**31c**$^{\bullet+}$) = +2.07 V.

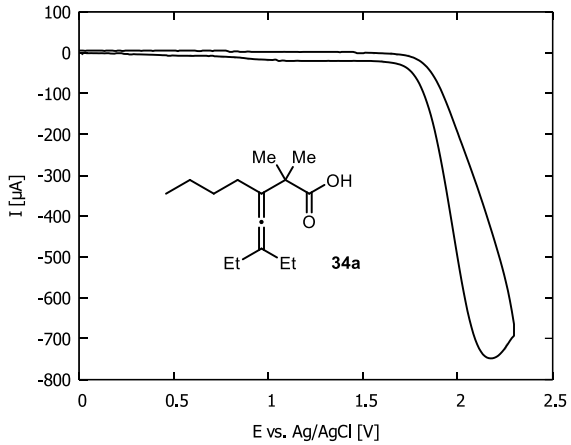

Figure 4.22. Cyclic voltammogram of **34a**. Irreversible oxidation, $E_{p/2}$ (**34a**/**34a**$^{\bullet+}$) = +1.95 V.

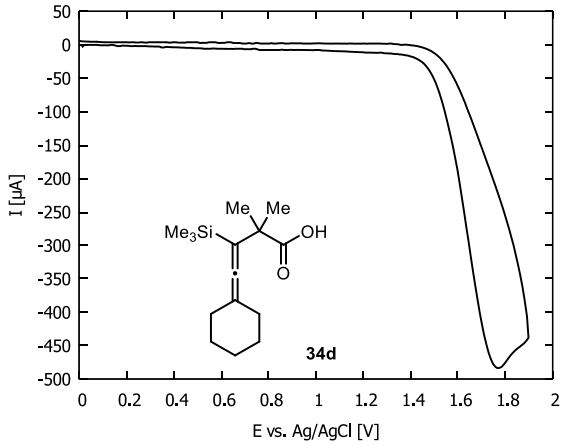

Figure 4.23. Cyclic voltammogram of **34d**. Irreversible oxidation, $E_{p/2}$ (**34d**/**34d**$^{\bullet+}$) = +1.63 V.

4.6.10. X-ray Crystallographic Data

Single Crystal X-ray Diffraction Data for compound 36f

Crystals of the compound **36f** were obtained by slow evaporation of a diethyl ether solution. Measurements were carried out using an Apex DUO diffractometer equipped with a Kappa 4-axis goniometer, an APEX II 4K CCD area detector, a Microfocus Source E025 IuS using MoKα radiation, Quazar MX multilayer Optics as monochromator and an Oxford Cryosystems low-temperature device Cryostream 700 plus (T = -173 °C). Full-sphere data collection was used with ω and ϕ scans. *Programs used:* Data collection APEX-2 (1), data reduction Bruker Saint V/.60A (2), and absorption correction SADABS (3).

(1) Data collection with APEX II version v2013.4-1. Bruker (2007). Bruker AXS Inc., Madison, Wisconsin, USA.

(2) Data reduction with Bruker SAINT version V8.30c. Bruker (2007). Bruker AXS Inc., Madison, Wisconsin, USA.

(3) SADABS: V2012/1 Bruker (2001). Bruker AXS Inc., Madison, Wisconsin, USA. Blessing, Acta Cryst. (1995) A51 33-38.

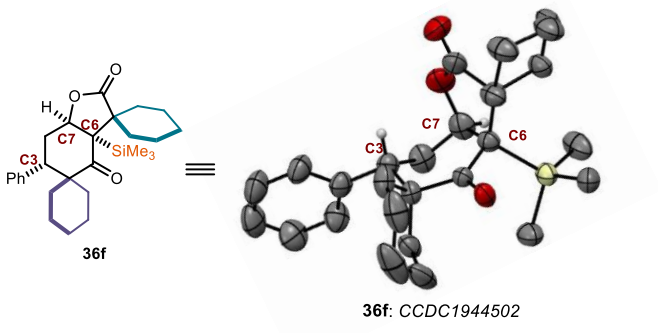

Table 4.3. Crystal data and structure refinement for **36f**. ***CCDC1944502***

Empirical formula	$C_{27}H_{38}O_3Si$
Formula weight	438.66
Temperature	296(2) K
Wavelength	0.71073 Å
Crystal system	Orthorhombic
Space group	P2(1)2(1)2(1)
Unit cell dimensions	a = 10.1731(3)Å, α= 90°. b = 14.6291(4)Å, β = 90°. c = 16.5938(5)Å, γ = 90°.
Volume	2469.54(12) $Å^3$
Z	4
Density (calculated)	1.180 mg/m^3
Absorption coefficient	0.120 mm^{-1}
F(000)	952
Crystal size	0.30 x 0.30 x 0.20 mm^3
Theta range for data collection	1.856 to 27.485°.
Index ranges	-12<=h<=13,-18<=k<=17,-21<=l<=16
Reflections collected	19222
Independent reflections	5652[R(int) = 0.0256]
Completeness to theta =27.485°	99.9%
Absorption correction	Multi-scan
Max. and min. transmission	0.976 and 0.891
Refinement method	Full-matrix least-squares on F^2
Data / restraints / parameters	5652/ 0/ 283
Goodness-of-fit on F^2	1.034
Final R indices [I>2sigma(I)]	R1 = 0.0477, wR2 = 0.1260

R indices (all data)	R1 = 0.0608, wR2 = 0.1359
Flack parameter	x =-0.07(4)
Largest diff. peak and hole	0.412 and -0.178 e.Å^{-3}

4.6.11. Computational Details

All DFT calculations were performed with the Gaussian09 suite of programs (Rev. A.01).[35] The structures of all the studied species were fully optimized without any symmetry constraint using the B3LYP functional[36] in conjunction with the split-valence 6-31+G(d) basis set for C, H, N, and O atoms, and the LANL2TZ triple-zeta quality basis set[37] with the associated LANL2 effective core potential.[38] All stationary points were characterized as minima or as first-order transition states by harmonic frequency calculations. Intrinsic Reaction Coordinate (IRC) calculations were performed to confirm that the transition states link the proper minima. Computed harmonic frequencies were used to calculate the thermal contribution to Gibbs free energy with the usual rigid rotor/harmonic oscillator approximations. Temperature and pressure were fixed at 298 K and 1 atm, respectively. To obtain more accurate electronic energies, single-point calculations were performed with the same functional

[35] **Gaussian 09**, Revision A.01, M. J. Frisch, G. W. Trucks, H. B. Schlegel, G. E. Scuseria, M. A. Robb, J. R. Cheeseman, G. Scalmani, V. Barone, B. Mennucci, G. A. Petersson, H. Nakatsuji, M. Caricato, X. Li, H. P. Hratchian, A. F. Izmaylov, J. Bloino, G. Zheng, J. L. Sonnenberg, M. Hada, M. Ehara, K. Toyota, R. Fukuda, J. Hasegawa, M. Ishida, T. Nakajima, Y. Honda, O. Kitao, H. Nakai, T. Vreven, J. Jr. Montgomery, J. E. Peralta, F. Ogliaro, M. Bearpark, J. J. Heyd, E. Brothers, K. N. Kudin, V. N. Staroverov, R. Kobayashi, J. Normand, K. Raghavachari, A. Rendell, J. C. Burant, S. S. Iyengar, J. Tomasi, M. Cossi, N. Rega, N. J. Millam, M. Klene, J. E. Knox, J. B. Cross, V. Bakken, V. Adamo, J. Jaramillo, R. Gomperts, R. E. Stratmann, O. Yazyev, A. J. Austin, R. Cammi, C. Pomelli, J. W. Ochterski, R. L. Martin, K. Morokuma, V. G. Zakrzewski, G. A. Voth, P. Salvador, J. J. Dannenberg, S. Dapprich, A. D. Daniels, Ö. Farkas, J. B. Foresman, J. V. Ortiz, J. Cioslowski, D. J. Fox, Gaussian Inc., Wallingford, CT., **2009**.

[36] Stephens, P. J.; Devlin, F. J.; Chabalowski, C. F.; Frisch, M. J. "Ab Initio Calculation of Vibrational Absorption and Circular Dichroism Spectra Using Density Functional Force Fields" *J. Phys. Chem.* **1994**, *98*, 11623.

[37] Roy, L. E.; Hay, P. J.; Martin, R. L. "Revised Basis Sets for the LANL Effective Core Potentials" *J. Chem. Theory Comput.* **2008**, *4*, 1029.

[38] a) Hay, P. J.; Wadt, W. R. "Ab initio effective core potentials for molecular calculations. Potentials for the transition metal atoms Sc to Hg" *J. Chem. Phys.* **1985**, *82*, 270–283; b) P Hay, P. J.; Wadt, W. R. "Ab initio effective core potentials for molecular calculations. Potentials for main group elements Na to Bi" *J. Chem. Phys.* **1985**, *82*, 284–298; c) Hay, P. J.; Wadt, W. R. "Ab initio effective core potentials for molecular calculations. Potentials for K to Au including the outermost core orbitals" *J. Chem. Phys.* **1985**, *82*, 299–310.

together with Grimme's D3 empirical correction for dispersion[39] as formulated with the Becke-Johnson damping function[40] [B3LYP-D3(BJ), the empirical correction being requested with the internal option IOp(3/124)=40 in Gaussian09 Rev. A.01] with the larger 6-311+G(2d,2p) basis set for C, H, N and O atoms, and the completely uncontracted LANL08+ basis set[41] for Zn associated to the LANL2 effective core potential.[42] For both optimizations and single-point energy calculations, bulk solvent effects were accounted for by the Polarizable Continuum Model in its Integral Equation Formalism variant (IEF-PCM), as implemented in Gaussian09.[43] The default parameters for acetonitrile were used.

[39] Grimme, S.; Antony, J.; Ehrlich, S.; Krieg, H. "A consistent and accurate ab initio parametrization of density functional dispersion correction (DFT-D) for the 94 elements H-Pu" *J. Chem. Phys.* **2010**, *132*, 154104.

[40] Grimme, S.; Ehrlich, S.; Goerigk, L. "Effect of the damping function in dispersion corrected density functional theory" *J. Comput. Chem.* **2011**, *32*, 1456.

[41] Roy, L. E.; Hay, P. J.; Martin, R. L. "Revised Basis Sets for the LANL Effective Core Potentials" *J. Chem. Theory Comput.*, **2008**, *4*, 1029.

[42] a) Hay, P. J.; Wadt, W. R. "Ab initio effective core potentials for molecular calculations. Potentials for the transition metal atoms Sc to Hg" *J. Chem. Phys.* **1985**, *82*, 270; b) Hay, P. J.; Wadt, W. R. "Ab initio effective core potentials for molecular calculations. Potentials for main group elements Na to Bi" *J. Chem. Phys.* **1985**, *82*, 284; c) Hay, P. J.; Wadt, W. R. "Ab initio effective core potentials for molecular calculations. Potentials for K to Au including the outermost core orbitals" *J. Chem. Phys.* **1985**, *82*, 299.

[43] a) Tomasi, J.; Mennucci, B.; Cammi, R. "Quantum Mechanical Continuum Solvation Models" *Chem. Rev.* **2005**, *105*, 2999; b) Cossi, M.; Scalmani, G.; Rega, N.; Barone, V. "New developments in the polarizable continuum model for quantum mechanical and classical calculations on molecules in solution" *J. Chem. Phys.* **2002**, *117*, 43.

Chapter V

A General Organocatalytic System for Asymmetric Radical Conjugate Additions to Enals

Target

Developing an iminium-ion-based catalytic system for the enantioselective radical conjugate addition to β-substituted aliphatic and aromatic enals.

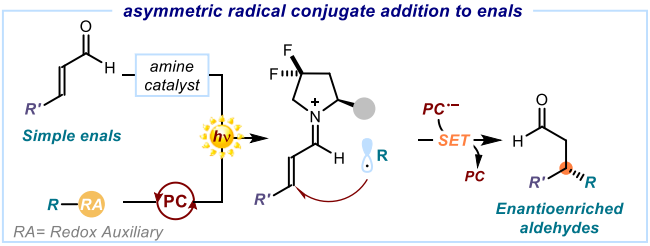

Tool

Combining a photoredox catalyst, which promotes the generation of radicals from stable precursors, and the highly electrophilic nature of ground-state chiral iminium ions, which can effectively trap the open-shell intermediates with high enantioselectivity.[1]

5.1. Introduction and Aim of This Study

Our previous studies on the photochemistry of chiral iminium ions established the possibility to generate radicals upon single-electron transfer (SET) oxidation of stable non-nucleophilic precursors and trap them with high stereocontrol (Figure 5.1.a). This chemistry was proposed to proceed via a radical coupling event between the persistent chiral enaminyl radical **III**, arising from the iminium ion, and the open-shell intermediate **II** generated upon SET oxidation of a stable radical precursor **2**. The overall process offered β-disubstituted chiral aldehydes **3**. The main limitation of this approach was the need for an aromatic substituent at the β position of the enal substrate **1** since the presence of an aliphatic group did shut down the excited-state

[1] The project discussed in this chapter has been conducted in collaboration with Dr. Catherine M. Holden, who was involved in the discovery and optimization of the process, Emilien Le Saux and Dr. Danilo M. Lustosa, who were in charge of investigating part of the reaction scope. I investigated the generality of the catalytic system and carried out mechanistic investigations.

reactivity of the chiral iminium ion. We surmised that a useful strategy to overcome this limitation could rely on independently generating the radical **V**, which would then add onto a ground-state chiral electrophilic iminium ion **IV** (Figure 5.1.b). In this case, the iminium ion would not need to reach the excited-state and, therefore, the presence of aliphatic substituents on the enals **6** should be tolerated.

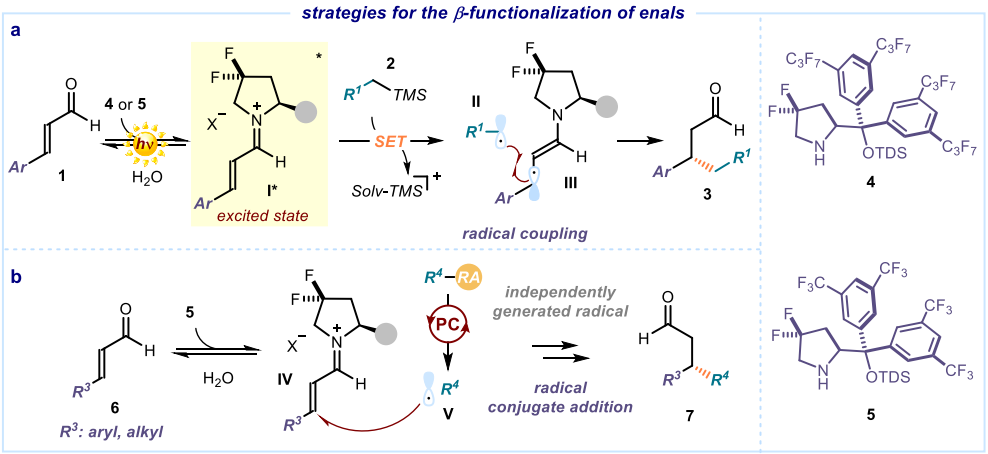

Figure 5.1. a) Excited-state iminium ion reactivity of aromatic enals; b) Our proposed strategy to overcome the limitations of the previous system regarding the need for aromatic enals. SET: Single-electron-transfer, TDS: *tert*-hexyldimethylsilyl.

Overall, the idea behind the design of this catalytic system is to decouple the radical generation strategy and the stereodetermining event. The net reaction would be a radical conjugate addition to linear *aliphatic and aromatic* enals via ground-state iminium ion-mediated catalysis affording β-disubstituted chiral aldehydes **7**.

Recent preliminary studies carried out in our laboratories showcased the feasibility of this approach. Specifically, we found that the difluorinated secondary aminocatalyst **3**, which was purposely designed to promote the excited-state reactivity of iminium ions,[2] had the potential to drive a stereocontrolled conjugate addition of acyl radicals via ground-state iminium ion reactivity (Figure 5.2).[3] In this transformation, the radical generation strategy was based on the direct light irradiation of 4-acyl-dihydropyridines (DHP) **8**, which upon excitation generated nucleophilic acyl radicals **VI**. The acyl-DHP substrate **8** could absorb light at 460 nm, allowing for its selective excitation against

[2] Silvi, M.; Verrier, C.; Rey, Y. P.; Buzzetti, L.; Melchiorre, P. "Visible-light excitation of iminium ions enables the enantioselective catalytic β-alkylation of enals" *Nat. Chem.* **2017**, *9*, 868.

[3] Goti, G.; Bieszczad, B.; Vega-Peñaloza, A.; Melchiorre, P. "Stereocontrolled Synthesis of 1,4-Dicarbonyl Compounds by Photochemical Organocatalytic Acyl Radical Addition to Enals" *Angew. Chem. Int. Ed.* **2019**, *58*, 1213.

the iminium ion. The ensuing open-shell intermediate **VI** was then stereoselectively intercepted by the electrophilic ground-state chiral iminium ion **IV**, formed upon condensation of aminocatalyst **5** with an enal. A variety of substituted acyl radicals underwent the radical conjugate addition with good yields but moderate enantioselectivity (**9a-9b**). Importantly, aliphatic enals (**9c-9e**) also afforded the corresponding 1,4-dicarbonyl products with similar levels of enantiocontrol.

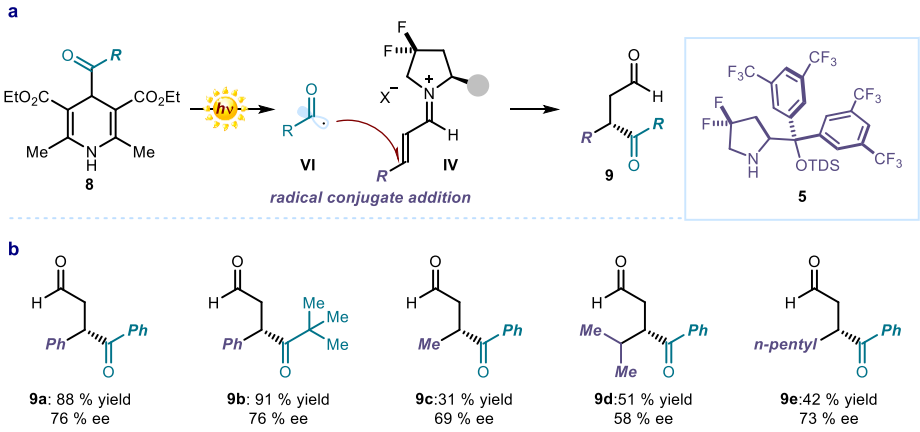

Figure 5.2. a) Stereocontrolled conjugate addition of acyl radicals **VI** mediated by ground-state iminium ion reactivity. Radicals generated upon direct excitation of 4-acyl-1,4-dihydropyridines **8**, at 460 nm; b) Examples from the reaction scope; aliphatic substituents on the enals are also tolerated.

This example prompted us to believe that decoupling the radical generation strategy from the stereo-determining radical trapping step could lead to a general enantioselective iminium ion-based strategy for the radical β-functionalization of simple enals. If successful, this would allow us to expand the radical β-functionalization to aliphatic enals.

5.2. Background

5.2.1. Catalytic Asymmetric Radical Conjugate Additions with Chiral Lewis Acids

Radicals have a strong tendency to react with electron-deficient olefins.[4] Their conjugate addition to α,β-unsaturated carbonyl substrates represents a prominent C-C bond-forming process. However, developing a catalytic enantioselective variant is

[4] a) Giese, B. "The Stereoselectivity of Intermolecular Free Radical Reactions" *Angew. Chem., Int. Ed.*, **1989**, *28*, 969; b) Srikanth, G. S. C.; Castle, S. L. "Advances in radical conjugate additions" *Tetrahedron*, **2005**, *61*, 10377.

difficult because of the intrinsic high reactivity of radicals and their tendency to attack electron-poor olefins without the need for catalyst activation. The main problem to overcome for achieving stereocontrol is, therefore, the presence of a racemic background process. Over the past three decades, some solutions have been found using chiral Lewis acids as catalysts .[5] In 1996, Sibi and Porter reported the first catalytic enantioselective radical 1,4-addition.[6] They devised that a chiral Lewis acid, generated upon coordination of chiral ligand **13a** with MgI_2 or $Zn(OTf)_2$, could activate acyclic enoates **10**, blocking one of the enantiotopic faces of the alkene (Figure 5.3). Stereocontrolled radical addition to the β-position delivered product **12** with moderate to good enantioselectivity. The main drawbacks of this system were the need for very low temperatures (-78 °C) and the significant decrease in enantioselectivity when lowering the amount of Lewis acid. Both aspects are dependent on the need to minimize the rate of a strong background racemic process. Substituting the flexible chiral ligand **13** for a more rigid scaffold **17** increased substantially the enantioselectivity and allowed the use of a lower amount of Lewis acid (10 mol% at -78 °C), and the use of ambient temperature (30 mol% of the chiral Lewis acid).[7]

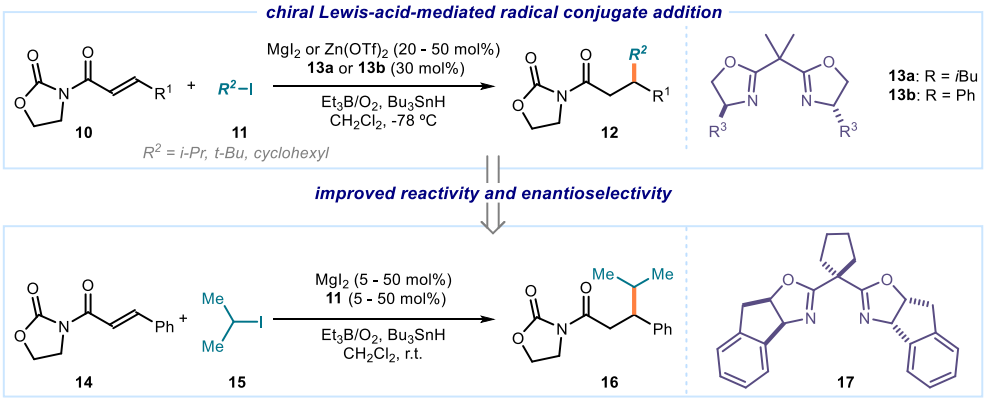

Figure 5.3. Top: The first catalytic enantioselective chiral Lewis acid-mediated radical conjugate addition. Bottom: an improved protocol enabled by ligand design.

[5] Renaud, P.; Gerster, M. "Use of Lewis Acids in Free Radical Reactions" *Angew. Chem. Int. Ed.*, **1998**, *37*, 2562.

[6] Sibi, M. P.; Ji, J.; Wu, J. H.; Gürtler, S.; Porter, N. A. "Chiral Lewis Acid Catalysis in Radical Reactions: Enantioselective Conjugate Radical Additions" *J. Am. Chem. Soc.*, **1996**, *118*, 9200.

[7] Sibi, M. P.; Ji, J. "Practical and Efficient Enantioselective Conjugate Radical Additions" *J. Org. Chem.*, **1997**, *62*, 3800.

Later on, Sibi expanded this Lewis acid-based catalytic system to a variety of conjugated carbonyl substrates, including β-acyloxy acrylates,[8] imides,[9] acyloxy pyrones,[10] and α′-phosphoric enones.[11] Despite the excellent levels of enantioselectivity generally achieved, there are two main disadvantages associated with this strategy: (i) the substrates need to be judiciously prepared since they require a preinstalled moiety acting as an anchoring point to facilitate coordination and geometry control from the chiral Lewis acid; (ii) the radical generation path is promoted by stoichiometric undesirable tin and BEt_3 reagents.

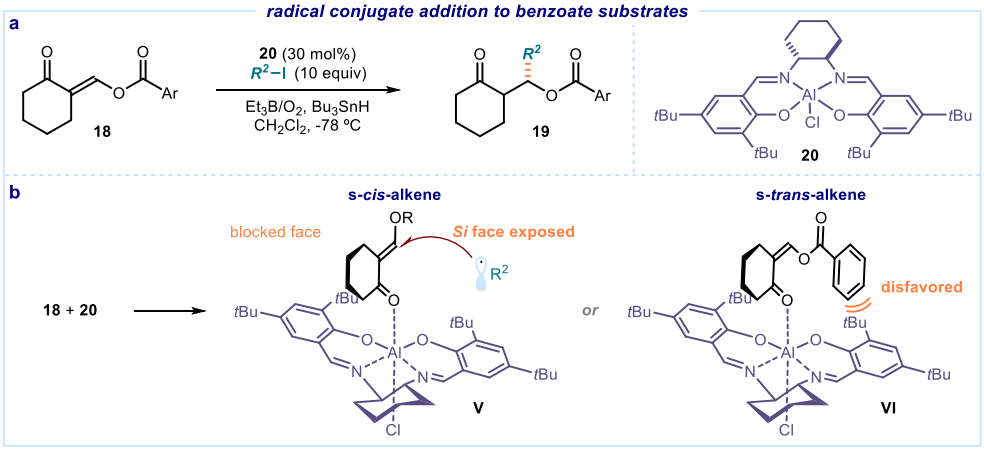

Figure 5.4. a) Radical conjugate addition to cyclic ketones bearing an exocyclic alkene and a benzoate ester group; b) Two of the possible transition states that determine the stereochemical outcome of the reaction.

The Sibi group also reported a radical conjugate addition to a benzoate derivative **18**. Despite being an enone (formal single-point binding substrate), the *exo* double bond and the benzoate moiety of the substrate were both essential to fix the geometry and achieve high stereoselectivity (Figure 5.4.a).[12]

In this particular case, the lone pair of electrons on the oxygen of substrate **18** coordinated with the chiral aluminum Lewis acid **20**. The steric bulk of the OR group

[8] Sibi, M. P.; Zimmerman, J.; Rheault, T. "Enantioselective Conjugate Radical Addition to β-Acyloxy Acrylate Acceptors: An Approach to Acetate Aldol-Type Products" *Angew. Chem. Int. Ed.*, **2003**, *42*, 4521.

[9] Sibi, M. P.; Petrovic, G.; Zimmerman, J. "Enantioselective Radical Addition/Trapping Reactions with α,β-Disubstituted Unsaturated Imides. Synthesis of anti-Propionate Aldols" *J. Am. Chem. Soc.*, **2005**, *127*, 2390.

[10] Sibi, M. P.; Zimmerman, J. "Pyrones to Pyrans: Enantioselective Radical Additions to Acyloxy Pyrones" *J. Am. Chem. Soc.*, **2006**, *128*, 13346.

[11] Lee, S.; Kim, S. "Enantioselective Radical Conjugate Addition to α′-Phosphoric Enones" *Org. Lett.*, **2008**, *10*, 4255.

[12] Sibi, M. P.; Nad, S. "Enantioselective Radical Reactions: Stereoselective Aldol Synthesis from Cyclic Ketones" *Angew. Chem. Int. Ed.*, **2007**, *46*, 9231.

on the ester fixed the alkene conformation in the most stable s-*cis*-geometry and, additionally, it oriented away from the axial groups of the cyclohexane ring of the chiral ligand (Figure 5.4.b). Hence, the most stable transition state **V** left the *si*-face of the alkene more exposed to the radical addition, delivering the enantioenriched chiral product **19**. Also, this approach was limited to specific substrates that rely on a bulky benzoate group to fix the alkene conformation.

With the advent of photoredox catalysis,[13] some of the problems associated with Sibi's strategy could be avoided, since a photoredox catalyst could be used to generate radicals under milder reaction conditions. Recently, the Yoon laboratory employed a Ru(II) photoredox catalysis to generate α-aminoradicals (**VII**) from α-silylamines (**23**, Figure 5.5).[14] A scandium catalyst, coordinated by a chiral PyBox ligand (**25**), could bind and activate a crotonate substrate bearing a pyrazolidinone moiety (**22**) to generate an electrophilic chiral intermediate **VII**. The radical **VIII**, generated upon oxidation of **23** and fragmentation of the trimethylsilyl group, underwent a radical conjugate addition to **VII** to deliver the enantioenriched β-functionalized crotonate **24**. This process established the feasibility of chiral Lewis acids to control the reactivity of photogenerated radicals.

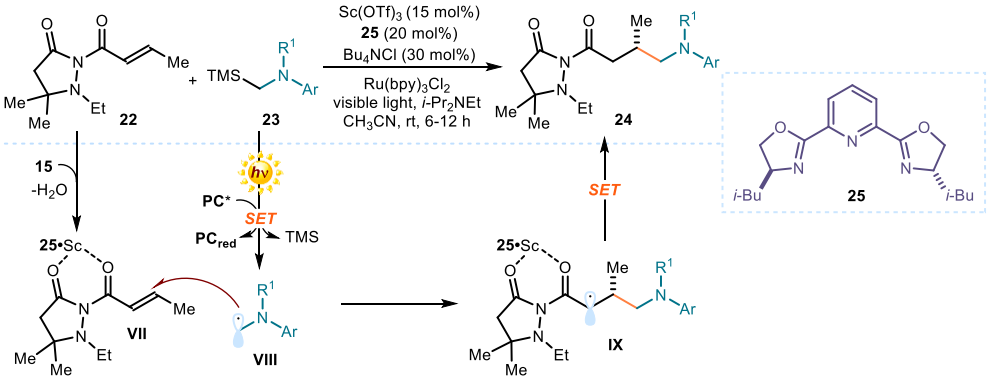

Figure 5.5. Photochemical generation of α-amino radicals for asymmetric conjugate additions.

Meggers expanded this dual strategy, where a chiral Lewis acid works in concert with a photoredox catalyst, to include other types of radicals using an octahedral chiral-at-metal Lewis acid catalyst (Figure 5.6).[15]

[13] MacMillan, D. W. "The Advent and Development of Organocatalysis" *Nature*, **2008**, *455*, 304.

[14] Ruiz Espelt, L.; McPherson, I. S.; Wiensch, E. M.; Yoon, T. P. "Enantioselective Conjugate Additions of α-Amino Radicals via Cooperative Photoredox and Lewis Acid Catalysis" *J. Am. Chem. Soc.*, **2015**, *137*, 2452.

[15] Huo, H.; Harms, K.; Meggers, E. "Catalytic, Enantioselective Addition of Alkyl Radicals to Alkenes via Visible-Light-Activated Photoredox Catalysis with a Chiral Rhodium Complex" *J. Am. Chem. Soc.*, **2016**, *138*, 6936.

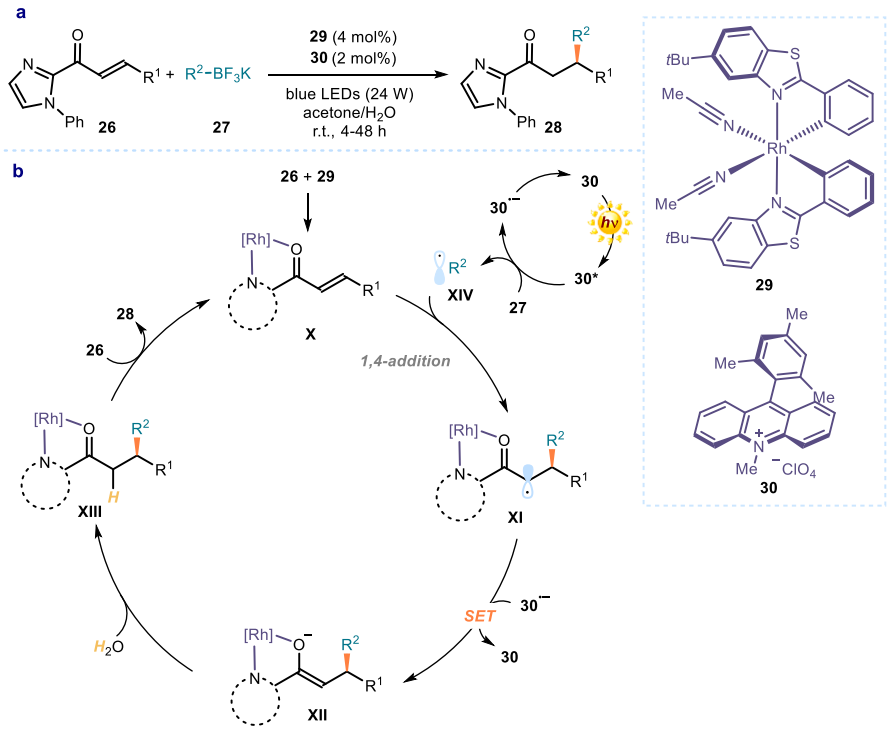

Figure 5.6. Radical conjugate addition reaction using BF_3K salts **27** as radical precursors, a chiral-at-metal rhodium catalyst **29,** and an organophotoredox catalyst **30.**

The C2-symmetrical Rh(III) catalyst **29** coordinated the substrate **26**, which carried an imidazole moiety serving as a template for the coordination of the Lewis acid. Oxidation of potassium trifluoroborate salt **27** by the organic photocatalyst **30** delivered a radical **XIV** (benzylic, α-oxo, or alkyl). Subsequent enantiocontrolled radical addition to **X** formed intermediate **XI**. Final SET reduction of **XI** from the reduced form of the photocatalyst (**30**$^{\bullet-}$), hydrolysis of **XIII**, and ligand exchange delivered product **28** with high yield and enantioselectivity while restarting both catalytic cycles. This system's versatility is demonstrated by the use of different radical precursors, such as dihydropyridines (DHPs)[16] and *N*-(acyloxy)phthalimides,[17] which reacted smoothly to afford β-functionalized products **28**.

[16] de Assis, F. F.; Huang, X.; Akiyama, M.; Pilli, R. A.; Meggers, E. "Visible-Light-Activated Catalytic Enantioselective β-Alkylation of α,β-Unsaturated 2-Acyl Imidazoles Using Hantzsch Esters as Radical Reservoirs" *J. Org. Chem.,* **2018**, *83*, 10922.

[17] Ma, J.; Lin, J.; Zhao, L.; Harms, K.; Marsch, M.; Xie, X.; Meggers, E. "Synthesis of β-Substituted γ-Aminobutyric Acid Derivatives through Enantioselective Photoredox Catalysis" *Angew. Chem. Int. Ed.,* **2018**, 57, 11193.

A different strategy was recently reported based on the use of a chiral Nickel(II) complex (Ni•**34**), generated upon coordination of a nickel salt with a dibenzofurandiyl-2,2′-bis(4-phenyloxazoline) chiral ligand **34** (Figure 5.7).

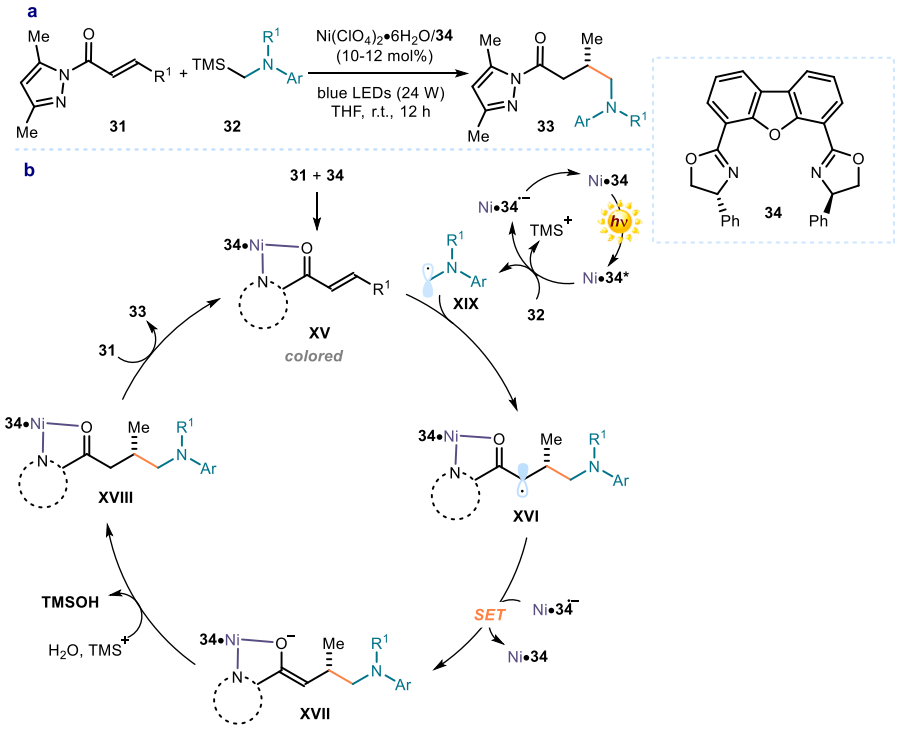

Figure 5.7. A nickel catalyst acting as bifunctional photoredox and chiral Lewis acid.

This complex, which could harvest the energy of visible light to promote a SET event and radical formation, catalyzed the enantioselective reactions between α-silylamines **32** and α,β-unsaturated carbonyl compounds **31**. The process did not need the presence of an external photoredox catalyst.[18] In the proposed mechanism, the colored Ni complex (Ni•**34**) absorbed light and, upon excitation, promoted SET oxidation of substrate **32** to generate the radical **XIX**. Concomitantly, Ni•**34** could also coordinate substrate **31** thus enhancing its electrophilicity and promoting the radical conjugate addition of **XIX**. This stereocontrolled step formed the radical **XVI**. SET reduction of **XVI** by [Ni•**34**]$^{\bullet-}$ followed by protonation delivered intermediate **XVIII**, which upon ligand exchange released the enantioenriched product **33** and restored **XV**.

[18] Shen, X.; Li, Y.; Wen, Z.; Cao, S.; Hou, X.; Gong, L. "A chiral nickel DBFOX complex as a bifunctional catalyst for visible-light-promoted asymmetric photoredox reactions" *Chem. Sci.*, **2018**, 9, 4562.

The Xiao group devised an alternative to precious metal catalysts designing an octahedral Co(II)-complex based on a chiral *N*4-ligand (**37**), which could drive an asymmetric radical conjugate addition (Figure 5.8).[19] DHPs **35** were selected as alkyl, benzyl, aryl, and acyl radical precursors, useful in the radical conjugate addition to enoates **26**. The organic photocatalyst **30** (see Figure 5.6), suitable for the SET oxidation of the DHPs, could be omitted when using DHP-acyl substrates, in analogy to our previous studies detailed in Figure 5.2.[3]

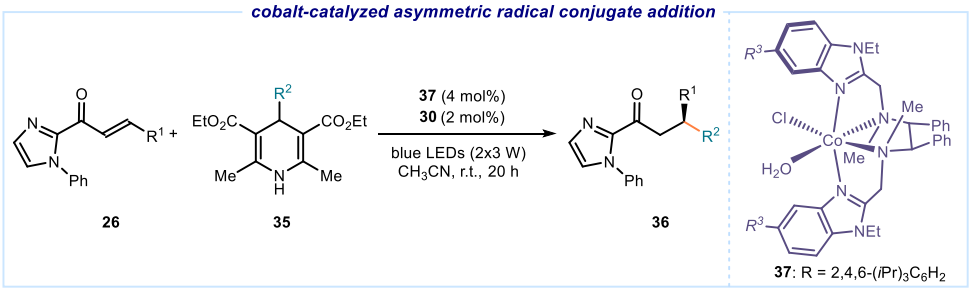

Figure 5.8. Asymmetric photochemical Giese reactions catalyzed by an octahedral chiral cobalt catalyst. Catalyst **30** is represented in Figure 5.6.

These examples showcase how modern photoredox catalysis could be harnessed to facilitate the development of catalytic enantioselective radical conjugate additions. In general, all the reported systems reported so far are limited by the need of preinstalling a particular anchoring group within the substrate to facilitate coordination of the chiral Lewis acid while ensuring optimal geometry control over the reactive intermediate.

5.2.2. Catalytic Asymmetric Radical Conjugate Additions with Organocatalysts

In addition to the previously described transition metal-systems, organic molecules have also been employed to achieve asymmetric catalytic radical conjugate addition processes. In 2005, Bach and his group described an intramolecular radical cyclization of pyrrolidine (**38**) into spirocyclic compound (**39**) catalyzed by the chiral ketone **40** (Figure 5.9).[20] Catalyst 40 bound substrate **38** through hydrogen-bonding interactions and effectively shielded one of the prochiral faces. UV-light irradiation of the benzophenone moiety within **40** promoted SET oxidation of the pyrrolidine unit that,

[19] Zhang, K.; Lu, L.-Q.; Jia, Y.; Wang, Y.; Lu, F.-D.; Pan, F.; Xiao, W.-J. "Exploration of Novel Chiral Cobalt Catalyst for Visible-Light-Induced Enantioselective Radical Conjugate Addition" *Angew. Chem. Int. Ed.* **2019**, *58*, 13375.

[20] Bauer, A.; Westkämper, F.; Grimme, S.; Bach, T. "Catalytic enantioselective reactions driven by photoinduced electron transfer" *Nature*, **2005**, *436*, 1139.

upon proton loss, generated the α-amino radical intermediate (**XX**). Cyclization and protonation delivered the enantioenriched spiro-product **39**.

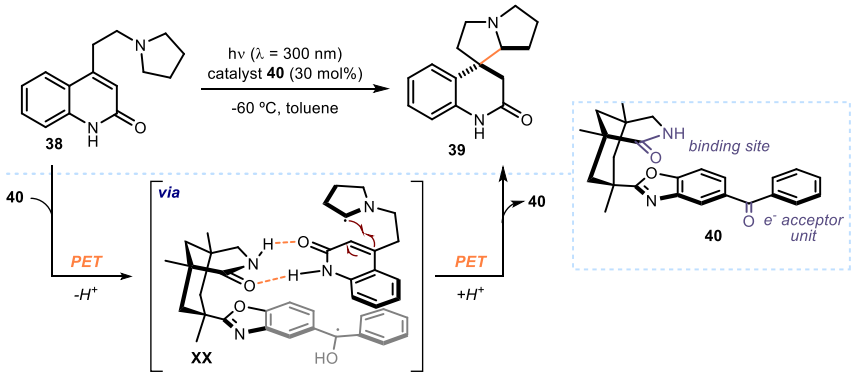

Figure 5.9. Enantioselective photoinduced-electron-transfer (PET)-catalyzed cyclization.

A strategy to functionalize more general scaffolds, such as cyclic enones **41**, was reported by our research group. In particular, we demonstrated that the combination of a chiral primary amine catalyst **44** and a photoredox catalyst (**PC**) could promote a radical conjugate addition to β-substituted cyclic enones **43** to forge quaternary stereocenters in a stereoselective fashion (Figure 5.10).[21] Overall, this system was driven by an electron-relay mechanism. The unstable 3π-radical cation **XXIII**, resulting from the addition of radical **XXII** to the electrophilic iminium ion **XXI**, underwent SET from an electron-rich carbazole moiety, purposely placed within the chiral organocatalyst **44**. The subsequent fast tautomerization from the enamine to the imine **XXIV** avoided a back-electron transfer. Finally, SET reduction of the carbazole radical cation **XXIV** from the reduced photocatalyst ($\mathbf{PC_{red}}$) restored the aminocatalyst **44** and delivered the enantioenriched β-difunctionalized product **43**.[22] The presence of a β-substituent in the enone substrate helped in hampering the racemic background reaction.

[21] Murphy, J. J.; Bastida, D.; Paria, S.; Fagnoni, M.; Melchiorre, P. "Asymmetric Catalytic Formation of Quaternary Carbons by Iminium Ion Trapping of Radicals." *Nature*, **2016**, *532*, 218.

[22] Bahamonde, A.; Murphy, J. J.; Savarese, M.; Brémond, E.; Cavalli, A.; Melchiorre, P. "Studies on the enantioselective iminium ion trapping of radicals triggered by an electron-relay mechanism" *J. Am. Chem. Soc.*, **2017**, *139*, 4559.

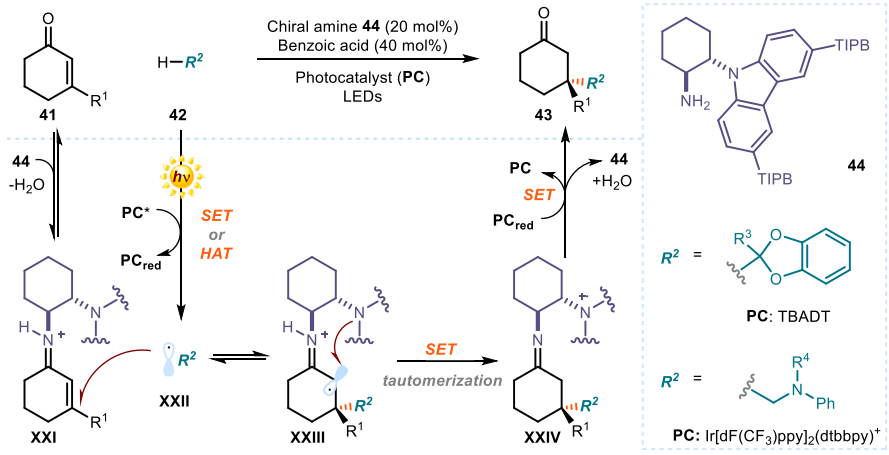

Figure 5.10. Photochemical organocatalytic strategy for the formation of quaternary stereocenters by radical conjugate addition to iminium ions. TBADT = tetrabutylammonium decatungstate; TIPB = triisopropylphenyl.

During this project, bright yellow crystals of the chiral iminium ion **XXI** were isolated from the condensation of the amine catalyst **44** and β-methyl cyclohexanone **41a**. X-ray crystallographic analysis[21,23] established that this coloration was elicited by the formation of an electron donor-acceptor (EDA) complex between the electron-rich carbazole unit and the electron-deficient iminium ion moiety (Figure 5.11). Capitalizing upon this observation, we found a way to exploit the visible-light photoactivity of the EDA complex **XXI** to trigger radical conjugate additions to β-substituted cyclic enones **41** without the need of an external photocatalyst.[24] Condensation of the modified carbazole catalyst **47** with a cyclic enone **41** formed a colored iminium ion **XXV**. Visible light irradiation induced a charge separation to form intermediate **XXVI**, which contained a persistent carbazole radical cation that acted as a SET oxidant (E_p^{ox} (**44**$^{\bullet+}$/**44**) = +1.09 V vs. Ag/Ag$^+$ in CH_3CN). Oxidation of substrate **45**, having a suitable fragmenting group and redox properties (E_p^{ox} < +1.09 V), led to radical **XXVII**, which was intercepted by the ground-state electrophilic chiral iminium ion **XXV** to afford the α-iminyl radical cation **XXVIII**. Subsequent intramolecular SET from the electron-rich carbazole in **XXVIII** reformed the carbazole radical cation in intermediate **XXIX**, which propagated the radical-chain process through oxidation of **45**.

[23] Crystallographic data for compound **XXI** has been deposited with the Cambridge Crystallographic Data Centre,

accession number CCDC 1437991.

[24] Cao, Z.-Y.; Ghosh, T.; Melchiorre, P. "Enantioselective radical conjugate additions driven by a photoactive intramolecular iminium-ion-based EDA complex" *Nat Commun*, **2018**, 9, 3274.

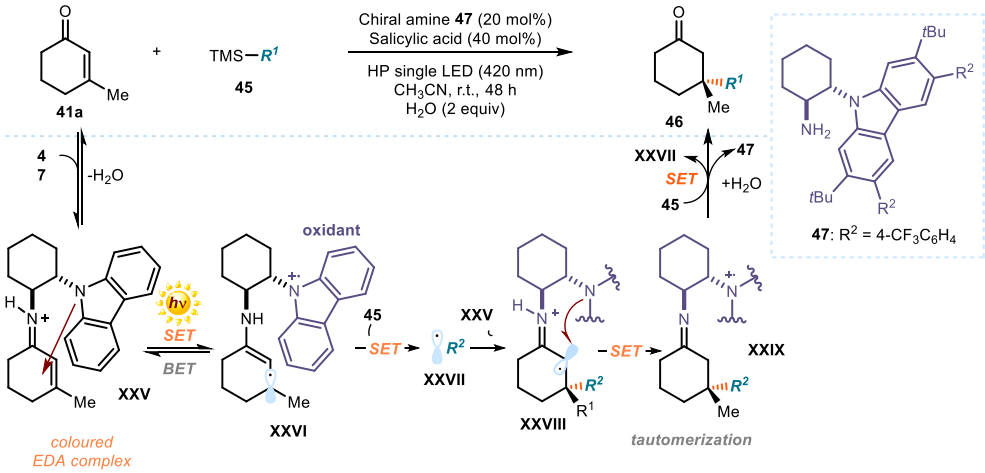

Figure 5.11. Intramolecular iminium ion-based EDA complex that triggers a photochemical asymmetric conjugate addition reaction. BET = Back-electron-transfer.

Overall, the reported organocatalytic strategies for asymmetric radical conjugate additions are limited to β-substituted cyclic enones.[21,24]

5.3. Targets of the Project

The present study was motivated by our interest in developing a general catalytic method for enantioselective radical conjugate additions to *unmodified acyclic* α,β-unsaturated carbonyl compounds. Previous methods relied on the Lewis acid-activation of purposely designed substrates, while iminium ion-based strategies were limited to cyclic enones and enals bearing an aromatic substituent at the β position.

Our target was to develop a general iminium ion-based system for radical conjugate additions to readily available *aliphatic* and *aromatic* enals. We planned to fill this gap in synthetic methodology by using a dual catalytic system in which the radical formation and the stereo-determining step were decoupled. Specifically, we envisioned the use of an external photoredox catalyst,[25] which generates radicals from a wide variety of stable radical precursors, in combination with a readily accessible chiral amine catalyst (Figure 5.12). Radical **XXX**, generated upon SET oxidation, would be trapped by the ground-state electrophilic chiral iminium ion **IV** in the stereodetermining step. The reduction of the resulting α-iminyl radical cation **XXXI**

[25] Zhao, J.-J.; Zhang, H.-H.; Shen, X.; Yu, S. Enantioselective Radical Hydroacylation of Enals with α-Ketoacids Enabled by Photoredox/Amine Cocatalysis. *Org Lett.* **2019**, *21*, 913–916.

would constitute the turnover event for the photocatalyst and would generate the β-functionalized chiral aldehyde **7**.

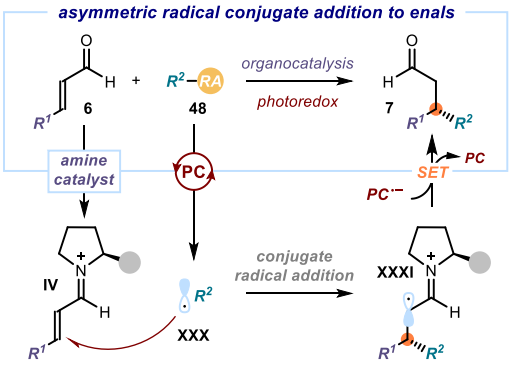

Figure 5.12. Our proposed strategy for a general radical conjugate addition to acyclic *aliphatic and aromatic* enals.

5.4. Results and Discussion

5.4.1. Optimization[26]

We commenced our studies by using the difluorinated secondary aminocatalyst **5** and 3,6-di-*tert*-butyl-9-mesityl-10-phenylacridinium tetrafluoroborate (**51**) as the photocatalyst (E^* (**51***/**51**$^{\bullet-}$) = +2.08 V, Table 5.1). The α-silylamine substrate **48a** bearing an oxidizable trimethylsilyl group in α-position to nitrogen was selected as the radical precursor due to its oxidation potential (E_p^{ox} (**48a**$^{\bullet+}$/**48a**) = +1.78 V) and the well-known ability of the ensuing α-amino radical to undergo addition to electron-deficient alkenes.[27] Crotonaldehyde **6a** was selected as the model acceptor since this substrate was unsuitable for the previously developed β-functionalization radical strategy based on the direct excitation of chiral iminium ions. In addition, the small size of the methyl fragment challenged the ability of the chiral catalyst to infer high stereoselectivity in the radical conjugate addition manifold. The experiments were conducted in CH_3CN using a blue high-power (HP) light-emitting-diode (LED, λ_{max} = 460 nm) with an

[26] Preliminary investigations were conducted by Dr. Catherine M. Holden.

[27] Nakajima, K.; Miyake, Y.; Nishibayashi, Y. "Synthetic Utilization of α-Aminoalkyl Radicals and Related Species in Visible Light Photoredox Catalysis" *Acc. Chem. Res.*, **2016**, 59, 1946.

irradiance at 60 mW/cm², as controlled by an external power supply[28] (details of the illumination set-up are reported in the experimental section).

Table 5.1. Optimization studies. [a]

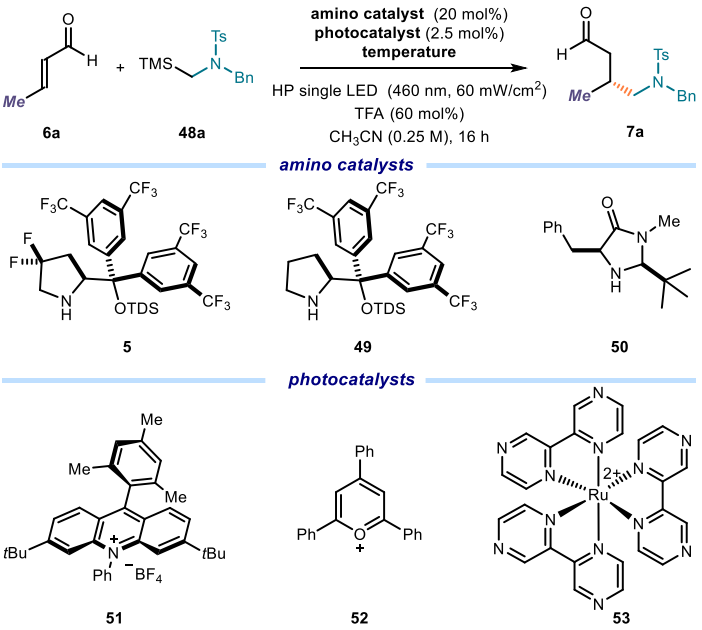

Entry	Amino catalyst	Photocatalyst	Temperature	Yield [%][b]	*ee* [%][c]
1	**5**	**51**	room temperature	complex mixture	--
2	**5**	**51**	-10 °C	99 (91)	91
3	**49**	**51**	-10 °C	31	33
4	**50**	**51**	-10 °C	99 (85)	64
5[d]	**5**	**52**	-10 °C	34	--
6	**5**	**53**	-10 °C	12	--
7[e]	**5**	**51**	-10 °C	0	--
8	**5**	**no**	-10 °C	0	--

[a] Reactions performed on a 0.1 mmol scale for 16 h using 0.4 mL of solvent under illumination by a single high-power (HP) LED (λ_{max} = 460 nm) with an irradiance of 60 mWcm^{-2}. [b] Yield of **7a** determined by ^{1}H NMR of the crude reaction mixture using trichloroethylene as the internal standard. Yields of isolated **7a** are reported in parentheses. [c] Enantiomeric excess determined by HPLC analysis on a chiral stationary phase. [d] Irradiation was performed by a single high-power (HP) LED (λ_{max}=420 nm). [e] No light.

[28] The vial was placed into an aluminum block on a 3D-printed holder, fitted with a 460 nm high-power single LED. This setup secured a reliable irradiation while keeping a distance of 1 cm between the reaction vessel and the light source. The temperature was kept at -10 °C using a chiller connected to the irradiation plate.

When performing the reaction at ambient temperature (Table 5.1, entry 1), a complex mixture of products was formed, likely arising from polar aminocatalytic processes of enal **6a**.[29] We then decided to lower the temperature to -10 °C (entry 2). To our delight, we could obtain the desired product **7a** in excellent yield (91% after isolation of **7a** by column chromatography purification) and enantiomeric excess (91%). We then tested if other widely used chiral secondary amine catalysts could induce similar levels of reactivity and stereocontrol in the model reaction. The thexyldimethylsilyl (TDS) protected version of the diarylprolinol silylether catalyst (**49**) substantially decreased the yield and the enantiomeric excess (entry 3, 31% yield, and 33% ee). The MacMillan 2nd generation amino catalyst **50** delivered product **7a** with the same yield as the difluorinated catalyst **5**, albeit with a lower enantiocontrol (entry 4, 64% ee). This trend in reactivity can be rationalized based on the higher electrophilicity of the ground-state iminium ion generated from catalyst **5** and **50** compared to **49.**[30] Other strongly oxidizing photocatalyst (E_{red}^* (**52***/**52**$^{\bullet-}$) = +2.3 V and E_{red}^* (**53***/**53**$^{\bullet-}$) = +1.86 V) did not improve the efficiency of the radical conjugate addition reaction (entries 5 and 6). Control experiments indicated that the photocatalyst and visible light irradiation were both essential for the reaction (entries 7-8).

5.4.2. Generality of the System

Adopting the optimized conditions described in Table 5.1, entry 2, we first demonstrated the versatility of our system evaluating a variety of *aliphatic* enals (Figure 5.13). The presence of a bulkier isopropyl group in the aliphatic chain (adduct **7b**) led to a substantial increase in enantioselectivity (97% ee). Extending the aliphatic chain to ethyl (product **7c**) or *n*-pentyl (**7d**) somehow decreased the yield (60%) while maintaining an excellent level of enantioselectivity. The introduction of a terminal aromatic ring (**7e**) or an olefin (**7f**) within the alkyl chain did not interfere with the reactivity. The use of β,β'-disubstituted (*E*)-3-phenyl-but-2-enal allowed us to forge a quaternary carbon stereocenter with moderate yield and selectivity (product **7g**).

---

[29] A dienamine-driven cyclisation, leading to aromatic aldehydes, is possible under the reaction conditions, see: Song, X.; Zhang, X.; Zhang, S.; Li, H.; Wang, W. "Direct Transformation of Simple Enals to 3,4-Disubstituted Benzaldehydes under Mild Reaction Conditions via an Organocatalytic Regio- and Chemoselective Dimerization Cascade" *Chem. Eur. J.*, **2012**, *18*, 9770.

[30] Lakhdar, S.; Tokuyasu, T.; Mayr, H. "Electrophilic Reactivities of α, β-Unsaturated Iminium Ions" *Angew. Chem. Int. Ed.* **2008**, *47*, 8723; b) Lakhdar, S.; Ammer, J.; Mayr, H. "Generation of α,β-Unsaturated Iminium Ions by Laser Flash Photolysis" *Angew. Chem. Int. Ed.* **2011**, *50*, 9953. While the electrophilicity of the iminium ion derived from catalyst **5** is not known, we expect that the incorporation of electron-withdrawing fluorine atoms would elicit an enhanced electrophilicity.

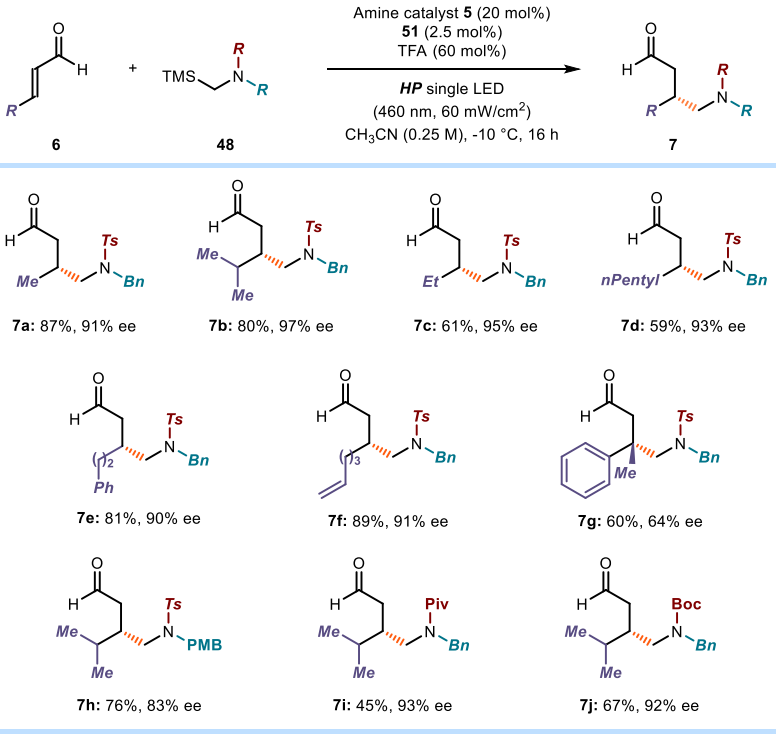

Figure 5.13. Survey of different alkyl enals **6** and radical precursors **48** that can participate in the enantioselective radical conjugate addition. Reactions performed on a 0.1 mmol scale at -10 °C for 16 h using 2 equiv. of enal **6**. Yields and enantiomeric excesses of the isolated products **7** are indicated below each entry (average of two runs per substrate). Enantiomeric excesses determined by HPLC analysis on a chiral stationary phase. Ts: toluenesulfonyl; Bn: benzyl; PMB: *p*-methoxybenzyl; Piv: pivaloyl; Boc: *tert*-butyloxycarbonyl.

As for the α-amino silyl radical precursor, the substitution of the *N*-benzyl group for a *para*-methoxybenzyl moiety resulted in a slight decrease in enantioselectivity (adduct **7h**). Replacing the *N*-tosyl moiety by a pivaloyl (Piv, **7i**) or a *tert*-butoxycarbonyl (Boc, **7j**) protecting group offered slightly decreased yields but excellent stereocontrol (93% and 92%, respectively).

To demonstrate the generality of our radical conjugate addition protocol, we tested the reactivity of enals bearing an aromatic β substituent (Figure 5.14). Cinnamaldehyde reacted smoothly with the α-silylamine radical precursor **48a**, leading to the corresponding product **7k** in high yield and stereocontrol (79% yield, 96% ee). We then wanted to make a direct comparison between the present dual catalytic protocol and the previously reported method based on the direct excitation of aromatic chiral iminium ions. The direct iminium ion excitation (λ = 420 nm, in the absence of the external photoredox catalyst) provided product **7k'**, arising from the reaction of

cinnamaldehyde, with a similar yield but lower stereoselectivity (83% yield and 87% ee). This result indicates that the dual photoredox/iminium ion catalytic system, besides accommodating aliphatic enals, provides better results with aromatic substrates too.

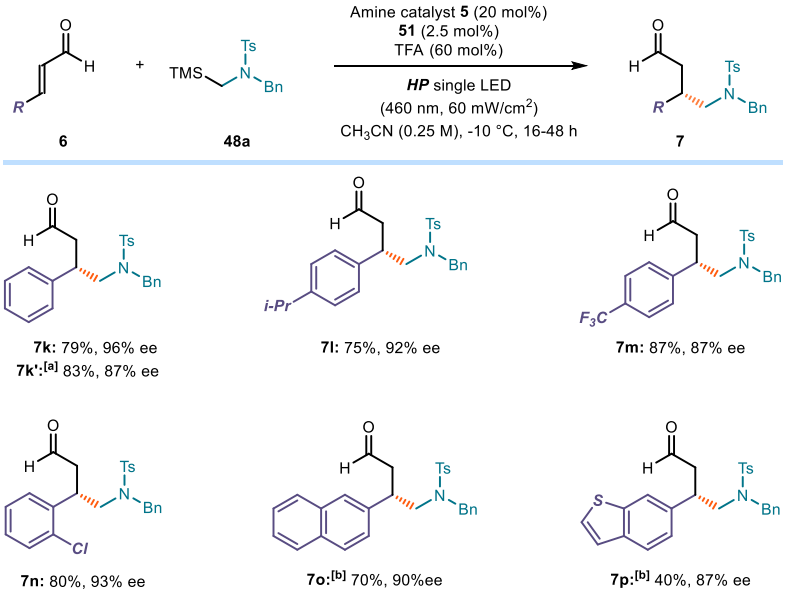

Figure 5.14. Survey of aromatic enals **6** that can participate in the enantioselective radical conjugate addition with α-silylamine **48a.** Reactions performed on a 0.1 mmol scale at -10 °C for 16 h using 2 equiv. of enal **6**. Yields and enantiomeric excesses of the isolated products **7** are indicated below each entry (average of two runs per substrate). Enantiomeric excesses by HPLC analysis on a chiral stationary phase. [a] Reactions performed with 3 equiv. of **6,** no photocatalyst **51,** on a 0.1 mmol scale at -10 °C for 16 h using 0.2 mL of solvent under illumination by a single high-power (HP) LED (λ_{max}=420 nm) with an irradiance of 60 mWcm^{-2}. [b] Reactions carried out for 48 hours.

As for the generality of the protocol, both electron-donating groups (product **7l**) and electron-withdrawing groups in *para* (**7m**) and *ortho* (**7n**) positions of the aryl ring were tolerated well. Extended π-aromatic (**7o**) and heteroaromatic (**7p**) systems reacted sluggishly but maintained high enantioselectivity.

We then wondered if other radicals, generated from different radical precursors, would be tolerated by our system (Figure 5.15). Theoretically, any radical precursors falling within the oxidation potential range of the photocatalyst **51** (E^{ox} < +2.08 V) should be suitable for this transformation. We first evaluated the use of non-stabilized alkyl radicals. Specifically, we tested whether a cyclopentyl fragment, generated by the trifluoroborate salt precursor, could be installed at the β position of aliphatic enals. The desired product **55a** could be obtained with a 64% yield and 82% ee. Other

trimethylsilyl radical precursors proved suitable for the stereoselective incorporation of a methylthiophenyl (adduct **55b**) or benzyl (**55c**) moieties. We are planning to study the feasibility of using dihydropyridine as radical precursors to fully explore the generality of the system.[31]

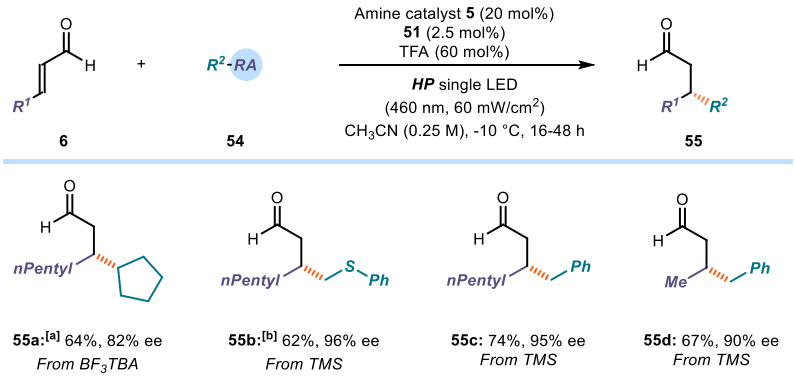

Figure 5.15. Survey of different radical precursors **54** amenable to the iminium-ion-mediated asymmetric radical conjugate addition. Reactions performed on a 0.1 mmol scale at -10 °C for 16 h using 2 equiv. of enal **54**. Yields and enantiomeric excesses of the isolated products **55** are indicated below each entry (average of two runs per substrate). Enantiomeric excesses by HPLC analysis on a chiral stationary phase. [a] Using 1.1 equiv. of enal **6**. [b] Using CH_3CN/H_2O (3:1) as solvent.

5.5. Mechanistic Investigations

Our proposed mechanism is depicted in Figure 5.16. Condensation of the chiral aminocatalyst **5** with the enal substrate delivers the electrophilic ground-state iminium ion **IV**. Simultaneously, SET oxidation of the radical precursor **48** (or **54**) by the excited state of the acridinium photocatalyst **51** would generate radical **XXX**. The ensuing radical intermediate **XXX** would undergo stereocontrolled conjugate addition to the chiral ground-state iminium ion **IV**, forming the 3π-radical cation **XXXI**. At this stage, SET reduction of **XXXI** from the reduced photocatalyst $\mathbf{51}^{\bullet-}$ would deliver the enamine **XXXIV**, which upon hydrolysis forms the enantioenriched β-functionalized product **7** and free aminocatalyst **5**.

[31] These studies are underway in our laboratories and conducted by other team members.

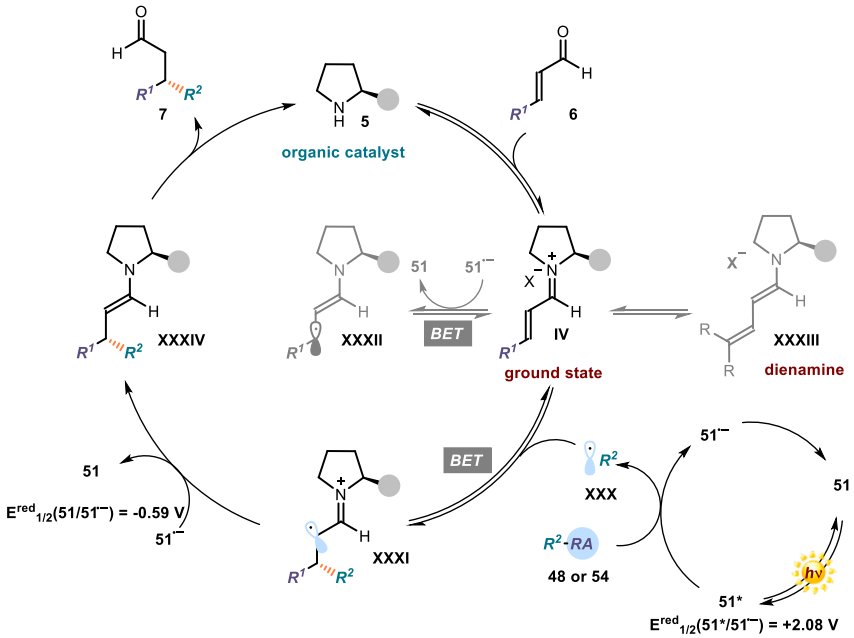

Figure 5.16. Proposed mechanism for the radical conjugate addition to simple enals.

Several side reactions could be associated with this catalytic cycle. First, the iminium ion **IV** (when adorned with an aliphatic β substituent) could be in equilibrium with the dienamine intermediate **XXXIII**, although we did not observe detectable amounts of this species during our studies. Second, the ground-state iminium ion **IV** may be reduced (E_{red}* (**IV***/**XXXII**) = −0.38 V) by the reduced formed of the photocatalyst to the 5π-intermediate **XXXII**. This pathway, although feasible, would most likely deliver back the ground-state iminium ion **IV** by back-electron-transfer from **XXXII**.

Finally, an alternative mechanistic scenario may rely on a *chain propagation* manifold, where the radical precursor **48** or **54** would be oxidized by the α-iminyl radical cation **XXXI** to form the enamine **XXXIV** and the propagating radical **XXX**, which would re-enter the chain. Previous studies estimated an oxidation potential for the 3π-intermediates of type **XXXV**[2] to the correspondent enamine **XXXVI** at about +0.9 V (vs Ag/Ag^+ in CH_3CN), as inferred by cyclic voltammetry studies on preformed enamines (Figure 5.17). Here, intermediate **XXXVI** mimics the actual enamine intermediate **XXXIV** involved in the mechanism. Consequently, the α-iminyl radical cation of type **XXXV** is not capable of oxidizing some of our radical precursors such as **48a,** which have a high redox potential (E_p^{ox} (**48a**$^{\bullet+}$/**48a**) = +1.78 V), therefore precluding a possible

radical chain propagation mechanism. Additionally, we measured the quantum yield[32] of the model reaction between 4-methylpent-2-enal and substrate **48a**, which was found to be as low as Φ = 0.02. This fractional value is far lower than the typical ones for chain propagation mechanisms (Φ > 1), suggesting that the closed catalytic cycle depicted in Figure 5.16 is the most plausible mechanism.

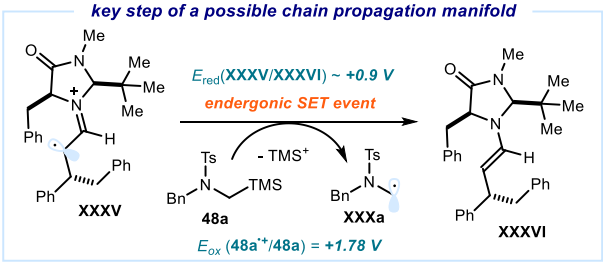

Figure 5.17. Cyclic voltammetry studies on the reduction of 3π-intermediates to the corresponding enamines.

5.6. Conclusions

In summary, we have developed a general iminium ion-based system for asymmetric radical conjugate additions to readily available aliphatic and aromatic enals. The method relies on the combination of a photoredox catalyst, which promotes the generation of radicals from stable precursors, and the highly electrophilic nature of ground-state chiral iminium ions, which can effectively trap the open-shell intermediates. The system delivers highly enantioenriched β-functionalized aldehydes, which cannot be accessed using previously reported strategies.

5.7. Experimental

5.7.1. General Information

The NMR spectra were recorded at 300 MHz, 400 MHz, and 500 MHz for ^{1}H or at 75 MHz, 101 MHz, and 126 MHz for ^{13}C, 376 MHz for ^{19}F, respectively. The chemical shifts (δ) for ^{1}H and $^{13}C\{^{1}H\}$ are given in ppm relative to residual signals of the solvents ($CHCl_3$ @ 7.26 ppm ^{1}H NMR, 77.00 ppm ^{13}C NMR). Coupling constants are given in Hz. The following abbreviations are used to indicate the multiplicity: s, singlet; d, doublet; t, triplet; q, quartet; m, multiplet; br s, broad signal.

[32] Details about quantum yield determination can be found in the experimental section 5.6.

High-resolution mass spectra (HRMS) were obtained from the ICIQ High-Resolution Mass Spectrometry Unit on MicroTOF Focus and Maxis Impact (Bruker Daltonics) with electrospray ionization. X-ray data were obtained from the ICIQ X-Ray Unit using a Bruker-Nonius diffractometer equipped with an APPEX 2 4K CCD area detector. Optical rotations were measured on a Polarimeter Jasco P-1030 and are reported as follows: $[\alpha]_D$ ambient temperature (c in g per 100 mL, solvent). Cyclic voltammetry studies were carried out on a Princeton Applied Research PARSTAT 2273 potentiostat offering compliance voltage up to ± 100 V (available at the counter electrode), ± 10 V scan range and ± 2 A current range.

General Procedures. All reactions were set up under an argon atmosphere in oven-dried glassware using standard Schlenk techniques unless otherwise stated. Synthesis grade solvents were used as purchased. Anhydrous solvents were taken from a commercial solvent purification system (SPS) dispenser. Chromatographic purification of products was accomplished using flash column chromatography (FC) on silica gel (35-70 mesh). For thin-layer chromatography (TLC) analysis throughout this work, Merck precoated TLC plates (silica gel 60 GF_{254}, 0.25 mm) were used, using UV light as the visualizing agent and either phosphomolybdic acid in EtOH, dinitrophenylhydrazine in EtOH/H_2O, *p*-anisaldehyde or basic aqueous potassium permanganate ($KMnO_4$), and heat as developing agents. Organic solutions were concentrated under reduced pressure on a Büchi rotary evaporator (*in vacuo* at 40 ºC, ~5 mbar).

Determination of Enantiomeric Purity: HPLC analysis on a chiral stationary phase was performed on an Agilent 1200 series HPLC, using Daicel Chiralpak IC-3, ID-3, and IG columns with *i*PrOH:*n*-hexane as the eluent. UPC² analysis on a chiral stationary phase was performed on a Waters Acquity instrument using CEL1 and IG chiral columns. The exact conditions for the analyses are specified within the characterization section. HPLC and UPC² traces were compared to racemic samples prepared by running the reaction in the presence of a catalytic amount (20 mol%) of an approximately 1:1 mixture of (2*R*, 5*R*)- and (2*S*, 5*S*)-2-*tert*-butyl-3-methyl-5-benzyl-4-imidazolidinone, which are commercially available from Sigma Aldrich.

Materials: Commercial grade reagents and solvents were purchased at the highest commercial quality from Sigma Aldrich, Fluka, Acros Organics, Fluorochem, or Alfa Aesar and used as received unless otherwise stated. Chiral secondary amine catalysts **5** and **49** were prepared according to the reported literature.[2] The photocatalyst **51** was

prepared according to the reported literature.[33] Enals **6a-d** and **6k** are commercially available, and they were distilled prior to use. Enals **6g** and **6m** were prepared according to the literature procedure.[2] Enal **6l, 6n,** and **6o** were prepared according to the literature procedure.[34] Enal **6e** was prepared according to the literature procedure.[35] Enal **6f** was prepared according to the literature procedure.[36] Radical precursor substrate **54b** was synthesized according to the reported procedure.[37] Radical precursor substrate **54a** was synthesized according to reported procedure washing with TBA-OH in H_2O:CH_2Cl_2 (1:1).[38] Substrate **48d** was synthesized according to the reported procedure.[39] Other tertiary amine substrates synthesis is detailed below.

5.7.2. Substrate Synthesis

Synthesis of tertiary amines 48[40]

Amines **48a** and **4c** were synthesized according to reported procedures, as shown in Figure 5.18:[40]

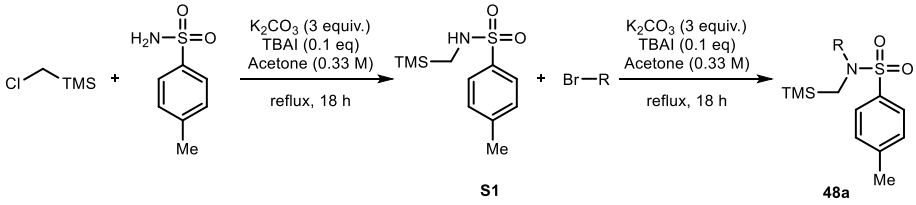

Figure 5.18. Preparation of tertiary amines **48.**

---

[33] White, A. R.; Wang, L.; Nicewicz, D. A. "Synthesis and Characterization of Acridinium Dyes for Photoredox Catalysis" *Synlett*, **2019**, *30*.

[34] Battistuzzi, G.; Cacchi, S.; Fabrizi, G. "An Efficient Palladium-Catalyzed Synthesis of Cinnamaldehydes from Acrolein Diethyl Acetal and Aryl Iodides and Bromides" *Org. Lett.* **2003**, *5*, 777.

[35] Franzoni, I.; Guénée, L.; Mazet, C. "Access to congested quaternary centers by Pd-catalyzed intermolecular γ-arylation of unactivated α,β-unsaturated aldehydes" *Chem. Sci.*, **2013**, *4*, 2619.

[36] Diedrich, M. K.; Klärner, F-G.; Beno, B. R.; Houk, K. N.; Senderowitz, H.; Still, C. W. "Experimental Determination of the Activation Parameters and Stereoselectivities of the Intramolecular Diels–Alder Reactions of 1,3,8-Nonatriene, 1,3,9-Decatriene, and 1,3,10-Undecatriene and Transition State Modeling with the Monte Carlo-Jumping Between Wells/Molecular Dynamics Method" *J. Am. Chem. Soc.*, **1997**, *119*, 10255.

[37] Ishibashi, H.; Nakatani, H.; Umei, Y.; Yamamoto, W.; Ikeda, M. "Reaction of [arylthio(chloro)methyl] trimethylsilanes with arenes and alk-1-enes in the presence of Lewis acid: syntheses of [aryl(arylthio)methyl]- and (1-arylthioalk-3-enyl)- trimethylsilanes." *J. Chem. Soc. Perkin Trans. 1*, **1987**, 589.

[38] Dreher, S. D.; Dormer, P. G.; Sandrock, D. L.; Molander, G. A. "Efficient Cross-Coupling of Secondary Alkyltrifluoroborates with Aryl Chlorides-Reaction Discovery Using Parallel Microscale Experimentation" *J. Am. Chem. Soc.*, **2008**, *130*, 9257.

[39] Sieburth, S. McN.; Somers, J. J.; O'Hare, H. K. "α-Alkyl-α-aminosilanes. 1. Metalation and Alkylation Between Silicon and Nitrogen" *Tetrahedron*, **1996**, *52*, 5669.

[40] Zhang, Y.-Y.; Wei, Y.; Tang, X.-Y.; Shia, M. "Dual-role of PtCl2 Catalysis in the Intramolecular Cyclization of (Hetero)Aryl-Allenes for the Facile Construction of Substituted 2,3-Dihydropyrroles and Polyheterocyclic Skeletons" *Chem. Commun.*, **2017**, *53*, 5966.

General Procedure A: To a flame dried round bottom flask were added 4-methylbenzenesulfonamide (1.2 equiv., 3.08 g, 18.00 mmol), potassium carbonate (3 equiv., 6.22 g, 45.00 mmol) and tetrabutylammonium iodide (0.1 equiv., 0.55 g, 1.5 mmol) in acetone (45 ml) under an argon atmosphere. Then was added (chloromethyl)trimethylsilane (1.0 equiv., 2.1 ml, 15 mmol) at room temperature, and the solution was refluxed overnight in a pressure flask. The solvent was then removed under vacuum, the residue was dissolved in EtOAc (120 mL), washed with aqueous HCl (1.0 M, 100 mL), then brine. The organic phase was dried over magnesium sulfate, filtered, and concentrated under vacuum. The crude material was purified by column chromatography (dry loading, SiO_2, hexane:EtOAc, 90:10) to afford 4-methyl-*N*-((trimethylsilyl)methyl)benzenesulfonamide (2.5g, 9.71 mmol, 65 % yield) as a white crystalline solid.

To a flame dried round bottom flask were added 4-methyl-*N*-((trimethylsilyl)methyl)benzenesulfonamide (1 equiv., 1.50 g, 5.83 mmol)), potassium carbonate (3 equiv., 2.42 g, 17.48 mmol) and tetrabutylammonium iodide (0.15 equiv., 0.32 g, 0.87 mmol) in acetone (18 ml) under an argon atmosphere. Then was added (bromomethyl)benzene (1.5 equiv., 1.50 ml, 8.74 mmol) at room temperature and the solution was refluxed in a pressure flask overnight. After filtration, the solvent was then removed under vacuum, and the crude material was purified by column chromatography (dry loading, SiO_2, hexane:EtOAc, 90:10) to afford *N*-benzyl-4-methyl-*N*-((trimethylsilyl)methyl)benzenesulfonamide (1.58 g, 4.54 mmol, 78 % yield) as a white crystalline solid.

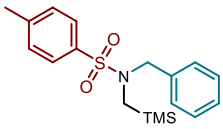

_N_-benzyl-4-methyl-_N_-((trimethylsilyl)methyl)benzene sulfonamide (48a)

Prepared according to the general procedure A.

^{1}H NMR (400 MHz, $CDCl_3$) δ 7.73 – 7.68 (m, 2H), 7.36 – 7.23 (m, 5H), 4.22 (s, 2H), 2.49 (s, 2H), 2.44 (s, 3H), -0.09 (s, 9H).

^{13}C NMR (101 MHz, $CDCl_3$) δ 143.14, 136.60, 135.26, 129.57, 128.46, 128.40, 127.68, 127.65, 55.23, 39.73, 21.52, -1.62.

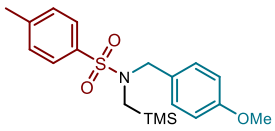

N-benzyl-N-(4-methoxybenzyl)-1-(trimethylsilyl) methanamine (48b)

Prepared according to the general procedure A using 1-(chloromethyl)-4-methoxybenzene (1.5 equiv., 0.32 ml, 2.33 mmol). The material was purified by column chromatography on silica gel (*n*-

hexane:EtOAc 90:10) to give the product as a pale yellow liquid (0.44 g, 50% over two steps).

^{1}H NMR (400 MHz, $CDCl_3$) δ 7.72 – 7.66 (m, 2H), 7.34 – 7.29 (m, 2H), 7.22 – 7.13 (m, 2H), 6.91 – 6.78 (m, 2H), 4.15 (s, 2H), 3.80 (s, 3H), 2.46 (s, 2H), 2.44 (s, 3H), -0.08 (s, 9H).

^{13}C NMR (101 MHz, $CDCl_3$) δ 159.22, 143.07, 135.34, 129.73, 129.55, 128.52, 127.63, 113.84, 55.29, 54.66, 39.40, 21.51, -1.57.

The following amine was synthesized using a reported procedure different from the general method described above.

N-benzyl-N-((trimethylsilyl)methyl)pivalamide (48c)[41]

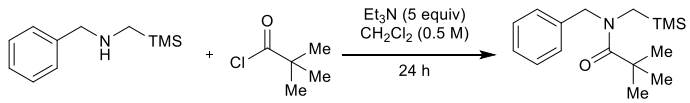

48c

Figure 5.19 Preparation of tertiary amine **48c.**

To a mixture of *N*-benzyl-1-(trimethylsilyl)methanamine[42] (1 equiv., 0.89 g, 4.65mmol) and triethylamine (1.5 equiv., 0.97 ml, 6.98 mmol) in DCM (40 ml) at room temperature were added 4-dimethylaminopyridine (0.002 equiv., 1.14 mg, 9.3 µmol), and di-tertbutyldicarbonate (1.2 equiv., 1.22 g, 5.58 mmol). The resulting solution was stirred for 48 hours at room temperature. After evaporation of the solvent, the mixture was dissolved in a mixture of methanol (10 mL) and NH_4OH (2 mL) and stirred for 2 h. The solution was diluted with H_2O (100 mL) and extracted twice with Et_2O. The combined organic layers were dried with $MgSO_4$, filtered, and concentrated under vacuum. The crude material was purified by column chromatography (SiO_2, hexanes:EtOAc, 90:10) to afford *tert*-butyl benzyl((trimethylsilyl)methyl)carbamate **48c** (1.093 g, 3.72 mmol, 80 % yield) as a clear oil.

[41] Zhou, S.; Junge, K.; Addis, D.; Das, S.; Beller, M. "A Convenient and General Iron-catalyzed Reduction of Amides to Amines" *Angew. Chem. Int. Ed.*, **2009**, *48*, 9507.

[42] Lim, S. H.; Yi, J.; Ra, S.; Nahm, K.; Cho, D. W.; Lee, G. Y.; Kim, J.; Yoon, C.; Mariano, P. S. "SET-promoted photoaddition reactions of N-a-trimethylsilylmethyl-N, N-dibenzylamines with fullerene C-60 Electronic factors that govern photoaddition efficiencies" *Tetrahedron Lett.*, **2015**, 56, 3014.

Synthesis of enals

Enal **6l** was synthesized as shown in Figure 5.20 following a reported procedure:[34]

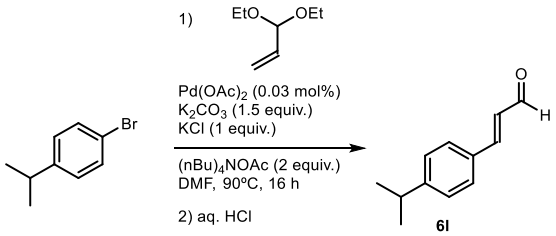

Figure 5.20. Preparation of enals.

To an oven-dried, argon purged, two neck round-bottomed flask fitted with a condenser was added an orange, cloudy mixture of 3,3-diethoxyprop-1-ene (3 equiv., 1.83 mL, 12.0 mmol), $Pd(OAc)_2$ (3 mol%, 27 mg, 0.12 mmol), K_2CO_3 (1.5 equiv., 0.83 g, 6.0 mmol), KCl (1.0 equiv., 0.30 g, 4.0 mmol), (n-Bu)$_4$OAc (2.0 equiv., 2.64 g, 8.0 mmol) and 1-bromo-4-isopropylbenzene (1.0 equiv., 0.65 mL, 4.0 mmol) in DMF (20 mL). The reaction mixture was heated to 90 °C. After 18 hours stirring, the black solution was allowed to cool to ambient temperature. HCl (Aq., 2 M, 15 mL) was added dropwise and the mixture was stirred for 15 minutes. Water (100 mL) was added and the mixture extracted with diethyl ether (100 mL). The organic layer was dried over $MgSO_4$ and concentrated to give a brown oil, which was purified by column chromatography (n-hexane:EtOAc 90:10) to give the product (0.50 g, 2.88 mmol, 72 % yield) as a yellow oil.

5.7.3. General Procedure for the Photochemical Radical Conjugate Addition

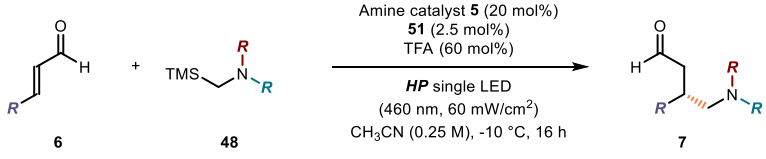

General Procedure B: To a 5 mL argon-purged glass vial, containing the amine catalyst **5** (14.1 mg, 0.02 mmol, 0.20 equiv.), photocatalyst **51** (1.4 mg, 2.5 µmol, 2.5 mol%) and the desired amine (0.1 mmol, 1 equiv.), was added enal **1** (0.2 mmol, 2 equiv.). Then 400 µL of an argon-sparged 0.2 M acetonitrile solution of TFA (4.6 µL, 0.06 mmol, 60 mol%) were added. The vial was sealed with Parafilm and then placed into an aluminum block on a 3D-printed holder, fitted with a 460 nm high-power single LED. The irradiance was fixed at 60±2 mW/cm², as controlled by an external power supply, and measured using a photodiode light detector at the start of each

reaction. This setup secured reliable irradiation while keeping a distance of 1 cm between the reaction vessel and the light source. The temperature was kept at -10 °C with a chiller connected to the irradiation plate (the setup is detailed in Figure 5.21)

The reaction was stirred for the indicated time (generally 16 hours), then the solvent was evaporated and the crude mixture was purified by flash column chromatography on silica gel to furnish the product **7**.

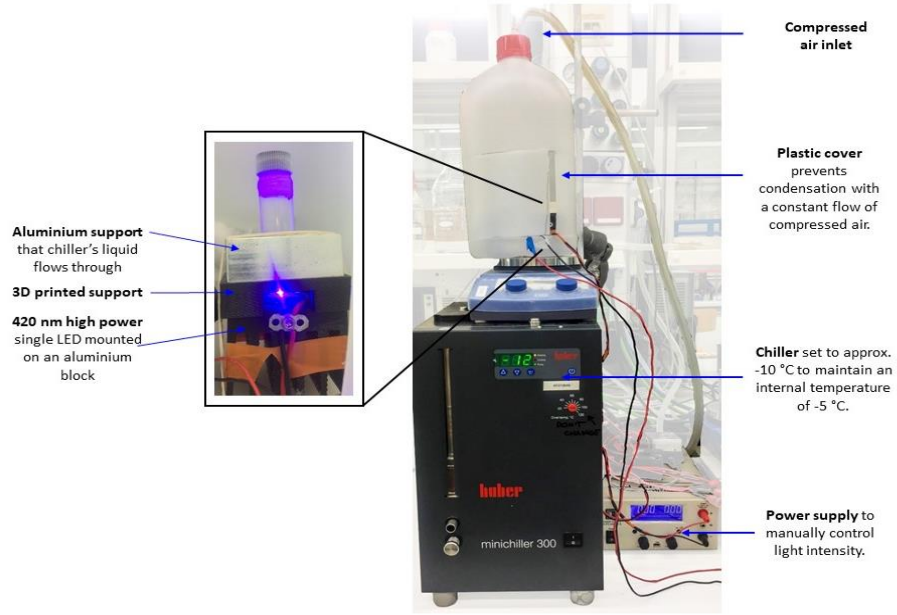

Figure 5.21. Detailed set-up and illumination system. The light source for illuminating the reaction vessel consisted of a single 460 nm high-power LED (LZ1-00DB00) purchased from Ledengin (more info).

5.7.4. Characterization of Products 7

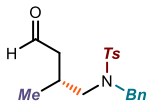

(*S*)-*N*-Benzyl-4-methyl-*N*-(2-methyl-4-oxobutyl)benzene sulfonamide (7a)

Prepared according to general procedure B from (*E*)-but-2-enal (16.5 µL, 0.2 mmol) and **48a** (34.8 mg, 0.1 mmol). The crude mixture was purified by column chromatography (SiO_2 gel, 95:5 to 85:15 hexanes:EtOAc) to afford the product as a colorless oil (32 mg, 91% yield, average of two runs, 91% ee). The enantiomeric excess was determined by HPLC analysis on a Daicel Chiralpak IC-3 column (70:30 *n*-hexane:*i*PrOH, 1.0 mL/min, 30 °C, λ = 230 nm: τ_1 = 30.55 min, τ_2 = 32.16 min).

^{1}H NMR (400 MHz, $CDCl_3$) δ 9.47 (dd, *J* = 2.0, 1.2 Hz, 1H), 7.75 – 7.69 (m, 2H), 7.37 – 7.33 (m, 2H), 7.33 – 7.24 (m, 5H), 4.39 (d, *J* = 14.8 Hz, 1H), 4.17 (d, *J* = 14.8 Hz, 1H), 3.08

(dd, *J* = 13.8, 8.3 Hz, 1H), 2.86 (dd, *J* = 13.9, 6.1 Hz, 1H), 2.46 (m, 4H), 2.13 – 2.02 (m, 2H), 0.79 (d, *J* = 6.4 Hz, 3H).

^{13}C NMR (101 MHz, $CDCl_3$) δ 201.80, 143.65, 136.42, 136.38, 129.93, 129.83, 128.75, 128.72, 128.13, 127.41, 54.92, 53.79, 48.03, 27.09, 21.66, 17.85.

HRMS (ESI) Calculated for $C_{23}H_{31}NNaO_3S$ [M+Na]$^+$: 424.1917, found: 424.1918.

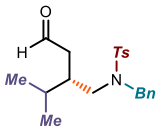

(*S*)-*N*-Benzyl-N-(2-isopropyl-4-oxobutyl)-4-methylbenzene sulfonamide (7b)

Prepared according to general procedure B from (*E*)-4-methylpent-2-enal (23.3 µL, 0.2 mmol) and **48a** (34.8 mg, 0.1 mmol). The crude mixture was purified by column chromatography (SiO_2 gel, 90:10 hexanes:EtOAc) to afford the product as a colorless oil (30 mg, 80% yield, average of two runs, 97% ee). The enantiomeric excess was determined by UPC^2 analysis on a chiral Daicel Chiralpak ID-3 (gradient: CO_2:*i*PrOH from 100:0 to 60:40 over 7.0 minutes, flow rate: 3.0 mL/min, 40 °C; λ = 240 nm, τ_1 = 4.93 min, τ_2 = 5.36 min).

^{1}H NMR (400 MHz, $CDCl_3$) δ 9.45 (t, *J* = 1.8 Hz, 1H), 7.73 – 7.66 (m, 2H), 7.35 – 7.31 (m, 2H), 7.30 – 7.23 (m, 5H), 4.30 (d, *J* = 14.8 Hz, 1H), 4.21 (d, *J* = 14.8 Hz, 1H), 2.99 (dd, *J* = 7.6, 3.5 Hz, 2H), 2.45 (s, 4H), 2.25 (td, *J* = 6.4, 1.8 Hz, 2H), 1.97 – 1.87 (m, 1H), 1.69 (pd, *J* = 6.9, 3.7 Hz, 1H), 0.69 (d, *J* = 6.9 Hz, 3H), 0.63 (d, *J* = 6.9 Hz, 3H).

^{13}C NMR (101 MHz, $CDCl_3$) δ 202.39, 143.64, 136.58, 136.32, 129.95, 129.91, 128.84, 128.77, 128.73, 128.63, 128.08, 127.44, 53.79, 51.19, 42.68, 36.75, 27.87, 21.67, 19.64, 17.98.

HRMS (ESI) Calculated for $C_{21}H_{27}NNaO_3S$ [M+Na]$^+$: 396.1604, found: 396.1599.

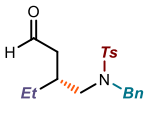

(*R*)-*N*-benzyl-*N*-(2-ethyl-4-oxobutyl)-4-methylbenzene sulfonamide (7b)

Prepared according to general procedure B from (*E*)-pent-2-enal (23.2 µL, 0.2 mmol) with **48a** (34.8 mg, 0.1 mmol). The crude mixture was purified by column chromatography (SiO_2 gel, 90:10 hexanes:EtOAc) to afford the product as an off-colorless oil (22.0 mg, 61%, average of two runs, 95% ee). The enantiomeric excess was determined by HPLC analysis on a Daicel Chiralpak ID-3 column (80:20 *n*-hexane:*i*PrOH, 0.6 mL/min, 20 °C, λ = 215 nm, τ_1= 41.35 min, τ_2 = 39.79 min).

^{1}H NMR (500 MHz, $CDCl_3$) δ 9.47 – 9.44 (m, 1H), 7.70 (d, *J* = 8.3 Hz, 2H), 7.33 (d, *J* = 8.0 Hz, 2H), 7.31 – 7.25 (m, 4H), 4.26 (dd, *J* = 43.0, 14.8 Hz, 2H), 2.99 (ddd, *J* = 20.1, 13.8, 7.5 Hz, 2H), 2.45 (s, 3H), 2.39 (ddd, *J* = 17.2, 5.6, 1.3 Hz, 1H), 2.20 (ddd, *J* = 17.2, 7.0, 2.1 Hz,

1H), 1.86 (dp, *J* = 12.8, 6.5 Hz, 1H), 1.34 – 1.26 (m, 1H), 1.15 (tt, *J* = 14.3, 7.3 Hz, 1H), 0.68 (t, *J* = 7.5 Hz, 3H);

^{13}C NMR (126 MHz, $CDCl_3$) δ 202.40, 143.87, 136.72, 136.55, 130.17, 129.02, 128.97, 128.35, 127.66, 54.10, 53.28, 45.91, 33.57, 25.00, 21.91, 11.25;

HR-MS (ESI) m/z Calculated for $C_{20}H_{25}NNaO_3S^+$ $[M+Na]^+$: 382.1453; found: 382.1446.

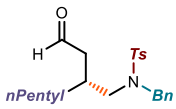

(*R*)-*N*-benzyl-4-methyl-*N*-(2-(2-oxoethyl)heptyl)benzene sulfonamide (7d)

Prepared according to general procedure B from (*E*)-oct-2-enal (29.8 µL, 0.2 mmol) and **48a** (34.8 mg, 0.1 mmol). The crude mixture was purified by column chromatography (SiO_2 gel, 90:10 hexanes:EtOAc) to afford the product as a colorless oil (24 mg, 59% yield, 93%ee). The enantiomeric excess was determined by HPLC analysis on a Daicel Chiralpak IC-3 column (70:30 *n*-hexane:*i*PrOH, 1.0 mL/min, 20 °C, λ = 230 nm τ_1 = 25.67 min, τ_2= 43.25 min)

^{1}H NMR (500 MHz, $CDCl_3$) δ 9.43 (dd, *J* = 2.2, 1.4 Hz, 1H), 7.71 – 7.66 (m, 2H), 7.34 – 7.30 (m, 2H), 7.30 – 7.22 (m, 5H), 4.31 (d, *J* = 14.8 Hz, 1H), 4.17 (d, *J* = 14.7 Hz, 1H), 3.04 (dd, *J* = 13.8, 8.9 Hz, 1H), 2.91 (dd, *J* = 13.8, 6.2 Hz, 1H), 2.43 (s, 3H), 2.42 – 2.34 (m, 1H), 2.18 (ddd, *J* = 17.2, 7.0, 2.2 Hz, 1H), 1.95 – 1.81 (m, 1H), 1.22 – 1.12 (m, 3H), 1.10 – 0.99 (m, 4H), 0.81 (t, *J* = 7.3 Hz, 3H).

^{13}C NMR (126 MHz, $CDCl_3$) δ 202.22, 143.64, 136.51, 136.36, 129.94, 128.80, 128.75, 128.12, 127.43, 53.89, 53.42, 46.13, 32.09, 31.93, 31.87, 26.39, 22.59, 21.66, 14.12.

HRMS (ESI) Calculated for $C_{23}H_{31}NNaO_3S$ $[M+Na]^+$: 424.1917, found: 424.1918.

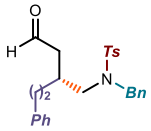

(*R*)-*N*-benzyl-4-methyl-*N*-(4-oxo-2-phenethylbutyl)benzene sulfonamide (7e)

Prepared according to general procedure B from (*E*)-5-phenylpent-2-enal (32.0 mg, 0.2 mmol) with **48a** (34.8 mg, 0.1 mmol). The crude mixture was purified by column chromatography (SiO_2 gel, 90:10 hexanes:EtOAc) to afford the product as a colorless oil (35.0 mg, 81%, average of two runs, 90% ee). The enantiomeric excess was determined by HPLC analysis on a Daicel Chiralpak ID-3 column (70:30 *n*-hexane:*i*PrOH, 1.0 mL/min, 20 °C, λ = 215 nm, τ_1= 21.35 min, τ_2 = 19.55 min).

^{1}H NMR (500 MHz, $CDCl_3$) δ 9.38 – 9.35 (m, 1H), 7.67 (d, *J* = 8.3 Hz, 126H), 7.34 – 7.28 (m, *J* = 6.3 Hz, 2H), 7.26 – 7.24 (m, *J* = 2.3, 1.7 Hz, 1H), 7.24 – 7.21 (m, 3H), 7.20 – 7.12 (m, 4H), 7.03 – 6.97 (m, 2H), 4.28 (d, *J* = 14.8 Hz, 68H), 4.13 (d, *J* = 15.0 Hz, 1H), 3.02 (ddd, *J*

= 20.1, 13.7, 7.6 Hz, 2H), 2.60 – 2.50 (m, 1H), 2.43 (s, 3H), 2.42 – 2.35 (m, 2H), 2.33 – 2.21 (m, 2H), 1.96 (dp, *J* = 19.1, 6.4 Hz, 1H), 1.53 – 1.48 (m, 1H), 1.48 – 1.38 (m, 1H);

^{13}C NMR (126 MHz, $CDCl_3$) δ 202.05, 143.91, 141.80, 136.66, 136.53, 130.20, 129.01, 128.78, 128.61, 128.35, 127.65, 126.32, 54.03, 53.48, 46.21, 33.86, 33.21, 31.78, 21.91

HR-MS (ESI) Calculated for $C_{26}H_{30}NO_3S^+$ $[M+H]^+$: 436.01946; found: 436.1940.

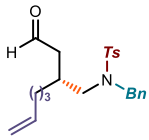

(*R*)-*N*-benzyl-4-methyl-*N*-(2-(2-oxoethyl)hept-6-en-1-yl)benzene sulfonamide (7f)

Prepared according to general procedure B from (*E*)-octa-2,7-dienal (24.8 mg, 0.2 mmol) with **48a** (34.8 mg, 0.1 mmol). The crude mixture was purified by column chromatography (SiO_2 gel, 90:10 hexanes:EtOAc) to afford the product as a colorless oil (36.0 mg, 89%, average of two runs, 91% ee). The enantiomeric excess was determined by UPC² analysis on a chiral Daicel Chiralpak IC-3 (gradient: CO_2:CH_3CN from 100:0 to 60:40 over 7.0 minutes, flow rate: 3.0 mL/min, 40 °C; λ = 230 nm, τ_1 = 4.56 min, τ_2 = 4.26 min).

^{1}H NMR (500 MHz, $CDCl_3$) δ 9.43 (dd, *J* = 2.0, 1.4 Hz, 1H), 7.67 (s, 2H), 7.31 (d, *J* = 7.9 Hz, 2H), 7.29 – 7.21 (m, 5H), 5.66 (ddt, *J* = 17.0, 10.3, 6.7 Hz, 1H), 4.94 – 4.89 (m, 1H), 4.89 – 4.87 (m, 1H), 4.24 (dd, *J* = 74.0, 14.8 Hz, 2H), 2.97 (ddd, *J* = 19.9, 13.8, 7.6 Hz, 2H), 2.47 – 2.37 (m, 4H), 2.18 (ddd, *J* = 17.3, 7.0, 2.1 Hz, 1H), 1.98 – 1.79 (m, 3H), 1.23 – 1.12 (m, 2H), 1.11 – 1.01 (m, 2H).

^{13}C NMR (126 MHz, $CDCl_3$) δ 202.25, 143.90, 138.67, 136.72, 136.54, 130.19, 129.04, 129.00, 128.39, 127.67, 115.06, 54.18, 53.59, 46.31, 33.96, 32.07, 31.84, 26.25, 21.91.

HR-MS (ESI) m/z Calculated for $C_{23}H_{30}NO_3S^+$ $[M+H]^+$: 400.1946; found: 400.1944 .

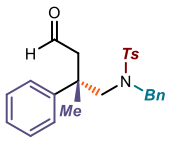

(*S*)-*N*-benzyl-4-methyl-*N*-(2-methyl-4-oxo-2-phenylbutyl) benzenesulfonamide (7g)

Prepared according to general procedure B from (*E*)-3-phenylbut-2-enal (29.2 mg, 0.2 mmol) and **48a** (34.8 mg, 0.1 mmol) for 24 h. The crude mixture was purified by column chromatography (SiO_2 gel, 90:10 hexanes:EtOAc) to afford the product as a colorless oil (26.0 mg, 60%, average of two runs, 64% ee). The enantiomeric excess was determined by UPC² analysis on a chiral Daicel Chiralpak ID-3 (gradient: CO_2: *i*PrOH from 100:0 to 60:40 over 7.0 minutes, flow rate: 3.0 mL/min, 40 °C; λ = 225 nm, τ_1 = 5.05 min, τ_2 = 5.53 min).

^{1}H NMR (500 MHz, $CDCl_3$) δ 9.45 (t, *J* = 2.5 Hz, 1H), 7.69 – 7.58 (m, 2H), 7.26 (dd, *J* = 5.5, 2.3 Hz, 4H), 7.24 – 7.20 (m, 3H), 7.18 – 7.13 (m, 1H), 7.13 – 7.07 (m, 2H), 6.65 – 6.58 (m, 2H), 3.97 (s, 2H), 3.48 (dd, *J* = 66.4, 14.8 Hz, 2H), 3.00 (dd, *J* = 16.1, 1.8 Hz, 1H), 2.64 – 2.59 (m, 1H), 2.42 (s, 3H), 1.51 (s, 3H).

^{13}C NMR (126 MHz, $CDCl_3$) δ 202.24, 144.21, 143.85, 137.68, 135.84, 130.09, 129.17, 128.58, 128.38, 127.78, 127.75, 127.30, 126.87, 59.56, 53.54, 52.97, 41.63, 24.00, 21.89.

HR-MS (ESI) m/z Calculated for $C_{25}H_{28}NO_3S^+$ $[M+H]^+$: 422.1712; found: 422.1783.

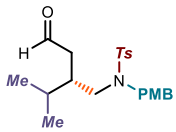

(*S*)-*N*-(2-isopropyl-4-oxobutyl)-*N*-(4-methoxybenzyl)-4-methylbenzene sulfonamide (7h)

Prepared according to general procedure B from (*E*)-4-methylpent-2-enal (23.3 µL, 0.2 mmol) and *N*-benzyl-*N*-(4-methoxybenzyl)-1-(trimethylsilyl) methanamine **48b** (37.8 mg, 0.1 mmol). The crude mixture was purified by column chromatography (SiO_2 gel, 87:13 hexanes:EtOAc) to afford the product as a colorless oil (30.7 mg, 76% yield, average of two runs, 83% ee). The enantiomeric excess was determined by HPLC analysis on a chiral Daicel Chiralpak ID-3 column (90:10 *n*-hexane:*i*PrOH, 1.0 mL/min, 20 °C, λ = 230 nm: τ_1 = 34.58 min, τ_2 = 40.36 min).

^{1}H NMR (400 MHz, $CDCl_3$) δ 9.49 (t, *J* = 1.8 Hz, 1H), 7.76 – 7.57 (m, 2H), 7.36 – 7.29 (m, 2H), 7.20 – 7.09 (m, 2H), 6.85 – 6.74 (m, 2H), 4.24 (d, *J* = 14.7 Hz, 1H), 4.13 (d, *J* = 14.7 Hz, 1H), 3.78 (s, 3H), 2.97 (m, 2H), 2.44 (s, 3H), 2.32 – 2.17 (m, 2H), 2.06 – 1.88 (m, 1H), 1.69 (pd, *J* = 6.9, 3.7 Hz, 1H), 0.70 (d, *J* = 6.9 Hz, 3H), 0.66 (d, *J* = 6.9 Hz, 3H).

^{13}C NMR (101 MHz, $CDCl_3$) δ 202.34, 159.39, 143.43, 136.27, 130.05, 129.78, 128.24, 127.29, 113.94, 55.30, 52.96, 50.68, 42.61, 36.69, 27.81, 21.52, 19.56, 17.91.

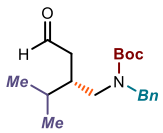

***tert*-butyl (*S*)-benzyl(2-isopropyl-4-oxobutyl)carbamate (7j)**

Prepared according to general procedure B from (*E*)-4-methylpent-2-enal (23.3 µL, 0.2 mmol) and **48d** (29.3 mg, 0.1 mmol). The crude mixture was purified by column chromatography (SiO2 gel, 90:10 hexanes:EtOAc) to afford the product as a colorless oil (21 mg, 67% yield, average of two runs, 92% ee). The enantiomeric excess was determined by HPLC analysis on a Daicel Chiralpak IC-3 column (90:10 *n*-hexane:*i*PrOH, 1.0 mL/min, 20 ºC, λ = 215 nm). τ_1 = 32.2 min, τ_2 = 30.6 min.

^{1}H NMR (400 MHz, $CDCl_3$) δ 9.70 (br. s, 1H), 7.41 – 7.14 (m, 5H), 4.58 – 4.12 (br. m, 2H), 3.48 – 2.91 (br. m, 2H), 2.53 – 2.18 (br. m, 3H), 1.71 (br. s, 1H), 1.53 – 1.34 (br. m, 9H), 0.86 (br. d, *J* = 6.9 Hz, 6H).

^{13}C NMR (101 MHz, $CDCl_3$) δ 202.56 (br.), 156.30, 138.34, 128.66, 127.37, 80.24, 50.59 (br.), 48.35 (br.), 43.87 (br.), 37.55, 29.40 (br.), 28.53, 19.95, 18.66 (br.).

HRMS (ESI) Calculated for $C_{19}H_{29}NNaO_3$ $[M+Na]^+$: 342.2040, found: 342.2038.

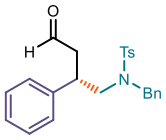

(*S*)-*N*-benzyl-4-methyl-*N*-(4-oxo-2-phenylbutyl)benzene sulfonamide (7k)

Prepared according to general procedure B from cinnamaldehyde with **48a** (34.8 mg, 0.1 mmol). The crude mixture was purified by column chromatography (SiO_2 gel, 90:10 hexanes:EtOAc) to afford the product as a colorless oil (32.0 mg, 79%, average of two runs, 96% ee). The enantiomeric excess was determined by HPLC analysis on a chiral Daicel Chiralpak IC-3 (70:30 *n*-hexane:*i*PrOH, 1.0 mL/min, 20 °C, λ = 215 nm, τ_1 = 24.68 min, τ_2 = 27.56 min).

^{1}H NMR (500 MHz, $CDCl_3$) δ 9.43 (dd, *J* = 2.2, 1.1 Hz, 1H), 7.69 – 7.65 (m, 2H), 7.32 – 7.26 (m, 5H), 7.25 – 7.16 (m, 5H), 7.01 – 6.94 (m, 2H), 4.19 (dd, *J* = 93.3, 14.7 Hz, 2H), 3.49 (dd, *J* = 14.1, 9.5 Hz, 1H), 3.21 (ddd, *J* = 14.9, 9.5, 5.6 Hz, 1H), 3.00 (dd, *J* = 14.1, 6.1 Hz, 1H), 2.86 (ddd, *J* = 17.3, 4.9, 1.1 Hz, 1H), 2.60 (ddd, *J* = 17.3, 9.5, 2.3 Hz, 1H), 2.43 (s, 3H).

^{13}C NMR (126 MHz, $CDCl_3$) δ 201.08, 143.83, 141.02, 136.60, 136.12, 130.08, 129.06, 129.04, 128.99, 128.42, 127.92, 127.58, 127.48, 54.36, 53.73, 46.93, 39.09, 21.80;

HRMS (ESI) Calculated for $C_{24}H_{25}NNaO_3S^+$ $[M+Na]^+$: 430.1453; found: 430.1437.

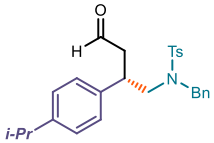

(*S*)-*N*-benzyl-*N*-(2-(4-isopropylphenyl)-4-oxobutyl)-4-methylbenzene sulfonamide (7l)

Prepared according to general procedure B from (*E*)-3-(4-isopropylphenyl)acrylaldehyde (34.8 mg, 0.2 mmol) with **48a** (34.8 mg, 0.1 mmol). The crude mixture was purified by column chromatography (SiO_2 gel, 90:10 hexanes:EtOAc) to afford the product as a colorless oil (33.8 mg, 75%, average of two runs, 92% ee). The enantiomeric excess was determined by HPLC analysis on a chiral Daicel Chiralpak IC-3 (70:30 *n*-hexane:*i*PrOH, 1.0 mL/min, 20 °C, λ = 215 nm, τ_1 = 66.98 min, τ_2 = 48.37 min).

^{1}H NMR (500 MHz, $CDCl_3$) δ 9.48 – 9.35 (m, 1H), 7.68 (d, *J* = 8.3 Hz, 2H), 7.33 – 7.26 (m, *J* = 5.9, 2.5 Hz, 5H), 7.19 – 7.16 (m, 2H), 7.08 (d, *J* = 8.1 Hz, 2H), 6.89 (d, *J* = 8.2 Hz, 2H), 4.20 (dd, *J* = 111.0, 14.7 Hz, 2H), 3.48 (dd, *J* = 14.1, 9.8 Hz, 1H), 3.26 – 3.12 (m, 1H), 2.98 (dd, *J* = 14.1, 5.8 Hz, 1H), 2.91 – 2.81 (m, 2H), 2.58 (ddd, *J* = 17.2, 9.6, 2.4 Hz, 1H), 2.43 (s, 4H), 1.20 (d, *J* = 6.9 Hz, 6H).

^{13}C NMR (126 MHz, $CDCl_3$) δ 201.00, 147.67, 143.40, 137.84, 136.24, 135.78, 129.66, 128.65, 128.57, 128.00, 127.40, 127.20, 126.68, 54.08, 53.32, 46.51, 38.31, 33.55, 23.82, 23.81, 21.40.

HRMS (ESI) Calculated for $C_{27}H_{31}NNaO_3S^+$ $[M+Na]^+$: 472.1922; found: 472.1901.

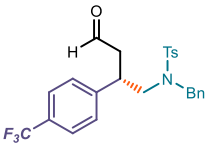

(*S*)-*N*-benzyl-4-methyl-*N*-(4-oxo-2-(4-(trifluoromethyl) phenyl)butyl)benzenesulfonamide (7m)

Prepared according to general procedure B from (E)-3-(4-(trifluoromethyl)phenyl)acrylaldehyde (40.0 mg, 0.2 mmol) with **48a** (34.8 mg, 0.1 mmol). The crude mixture was purified by column chromatography (SiO_2 gel, 90:10 hexanes:EtOAc) to afford the product as a colorless oil (41.5 mg, 87%, average of two runs, 87% ee). The enantiomeric excess was determined by UPC² analysis on a chiral Daicel Chiralpak ID-3 (gradient: CO_2:*i*PrOH from 100:0 to 60:40 over 7.0 minutes, flow rate: 3.0 mL/min, 40 °C; λ = 230 nm, τ_{major} = 4.03 min, τ_{minor} = 3.95 min).

^{1}H NMR (500 MHz, $CDCl_3$) δ 9.48 (s, 1H), 7.66 (d, *J* = 8.3 Hz, 2H), 7.44 (d, *J* = 8.1 Hz, 2H), 7.34 – 7.26 (m, 5H), 7.15 (dd, *J* = 7.6, 1.8 Hz, 2H), 7.05 (d, *J* = 8.1 Hz, 2H), 4.34 (d, *J* = 14.5 Hz, 1H), 4.04 (d, *J* = 14.5 Hz, 1H), 3.43 (dd, *J* = 14.0, 8.8 Hz, 1H), 3.32 (ddd, *J* = 14.3, 8.8, 6.4 Hz, 1H), 3.04 (dd, *J* = 13.9, 6.6 Hz, 1H), 2.88 (ddd, *J* = 17.7, 5.2, 0.7 Hz, 1H), 2.63 (ddd, *J* = 17.8, 8.9, 1.8 Hz, 1H), 2.43 (s, 3H).

^{13}C NMR (126 MHz, $CDCl_3$) δ 200.24, 145.31, 144.15, 136.17, 135.96, 130.24, 129.86, 129.61, 129.14, 128.63, 128.43, 127.70, 125.98, 125.47, 54.11, 47.14, 38.89, 21.89.

HRMS (ESI) m/z Calculated for $C_{25}H_{24}F_3NNaO_3S^+$ $[M+Na]^+$: 498.1327; found: 498.1320.

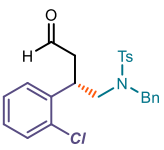

(*S*)-*N*-benzyl-*N*-(2-(2-chlorophenyl)-4-oxobutyl)-4-methyl benzenesulfonamide (7n)

Prepared according to general procedure B from (*E*)-3-(4-chlorophenyl)acrylaldehyde (33.2 mg, 0.02 mmol) with **48a** (34.8 mg, 0.1 mmol). The crude mixture was purified by column chromatography (SiO_2 gel, 90:10 hexanes:EtOAc) to afford the product as an off-white solid (35.5 mg, 80%, average of

two runs, 93% ee). The enantiomeric excess was determined by HPLC analysis on a chiral Daicel Chiralpak ID-3 (30:70 *i*PrOH:*n*-hexane 1.0 mL/min, 20 °C, λ = 215 nm, τ_1 = 29.49 min, τ_2 = 33.75 min).

^{1}H NMR (500 MHz, $CDCl_3$) δ 9.33 (dd, *J* = 2.5, 0.8 Hz, 1H), 7.67 – 7.64 (m, 2H), 7.32 – 7.26 (m, 8H), 7.21 – 7.08 (m, 3H), 4.52 (d, *J* = 15.0 Hz, 1H), 4.09 (d, *J* = 15.0 Hz, 1H), 3.91 – 3.73 (m, 1H), 3.45 (dd, *J* = 13.9, 10.1 Hz, 1H), 3.12 (dd, *J* = 13.9, 5.5 Hz, 1H), 2.94 (ddd, *J* = 17.4, 5.0, 0.9 Hz, 1H), 2.68 (ddd, *J* = 17.4, 9.5, 2.6 Hz, 1H), 2.42 (s, 3H).

^{13}C NMR (126 MHz, $CDCl_3$) δ 200.77, 143.94, 138.19, 136.62, 136.37, 134.37, 130.34, 130.19, 129.01, 129.00, 128.72, 128.46, 127.71, 127.62, 53.79, 53.28, 46.03, 21.89.

HRMS (ESI) m/z Calculated for $C_{24}H_{24}ClNNaO_3S$: 464.1058; found: 464.1059.

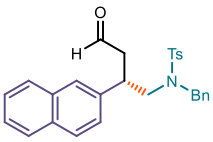

(*S*)-*N*-benzyl-4-methyl-*N*-(2-(naphthalen-2-yl)-4-oxobutyl)benzenesulfonamide (70)

Prepared according to general procedure B from (*E*)-3-(naphthalen-2-yl)acrylaldehyde (36.4 mg, 0.02 mmol) with **48a** (34.8 mg, 0.1 mmol). The crude mixture was purified by column chromatography (SiO_2 gel, 90:10 hexanes:EtOAc) to afford the product as an off-white solid (32.0 mg, 70%, average of two runs, 90% ee). The enantiomeric excess was determined by UPC² analysis on a Daicel Chiralpak IC-3 (gradient: CO_2:CH_3CN from 100:0 to 60:40 over 7.0 minutes, flow rate: 3.0 mL/min, 50 °C; λ = 223 nm, τ_1 = 5.55 min, τ_2 = 5.43 min).

^{1}H NMR (500 MHz, $CDCl_3$) δ 9.48 (dd, *J* = 2.1, 1.2 Hz, 1H), 7.77 (dd, *J* = 6.5, 2.7 Hz, 1H), 7.72 (d, *J* = 8.6 Hz, 1H), 7.70 – 7.67 (m, 1H), 7.66 – 7.62 (m, 2H), 7.48 – 7.40 (m, 2H), 7.35 (s, 1H), 7.30 – 7.27 (m, 3H), 7.23 (d, *J* = 8.0 Hz, 2H), 7.20 (dd, *J* = 6.5, 3.0 Hz, 2H), 7.11 (dd, *J* = 8.5, 1.8 Hz, 1H), 4.21 (dd, *J* = 82.6, 14.7 Hz, 2H), 3.56 (dd, *J* = 14.1, 8.9 Hz, 1H), 3.47 – 3.29 (m, 1H), 3.14 (dd, *J* = 14.1, 6.6 Hz, 1H), 2.90 (ddd, *J* = 17.4, 5.1, 1.1 Hz, 1H), 2.72 (ddd, *J* = 17.4, 9.3, 2.2 Hz, 1H), 2.40 (s, 3H).

^{13}C NMR (126 MHz, $CDCl_3$) δ 200.76, 143.63, 138.25, 136.50, 135.97, 133.51, 132.72, 129.88, 128.91, 128.82, 128.69, 128.27, 127.80, 127.73, 127.39, 126.73, 126.35, 126.00, 125.61, 54.09, 53.54, 46.92, 39.01, 21.64.

HRMS (ESI) Calculated for $C_{28}H_{27}NNaO_3S^+$ $[M+Na]^+$: 480.1604; found: 480.1605.

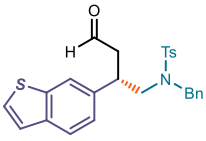

(*S*)-*N*-(2-(benzo[b]thiophen-6-yl)-4-oxobutyl)-*N*-benzyl-4-methyl benzenesulfonamide (7p)

Prepared according to general procedure B from (*E*)-3-(benzo[b]thiophen-6-yl)acrylaldehyde (37.6 mg, 0.02 mmol) with

48a (34.8 mg, 0.1 mmol). The crude mixture was purified by column chromatography (SiO_2 gel, 90:10 hexanes:EtOAc) to afford the product as a pale-yellow solid (19.0 mg, 40%, average of two runs, 87% ee). The enantiomeric excess was determined by UPC² analysis on a chiral Daicel Chiralpak ID-3 (gradient: CO_2: *i*PrOH from 100:0 to 60:40 over 7.0 minutes, flow rate: 3.0 mL/min, 40 °C; λ = 225 nm, τ_1 = 6.42 min, τ_2 = 6.31 min).

^{1}H NMR (500 MHz, $CDCl_3$) δ 9.44 (dd, *J* = 2.1, 1.1 Hz, 1H), 7.69 – 7.59 (m, 3H), 7.38 (d, *J* = 5.4 Hz, 1H), 7.35 – 7.32 (m, 1H), 7.29 – 7.26 (m, 3H), 7.26 – 7.25 (m, 2H), 7.24 – 7.23 (m, 1H), 7.22 – 7.12 (m, *J* = 6.6, 2.9 Hz, 2H), 6.97 (dd, *J* = 8.2, 1.6 Hz, 1H), 4.17 (dd, *J* = 78.3, 14.6 Hz, 2H), 3.52 (dd, *J* = 14.1, 8.8 Hz, 1H), 3.40 – 3.29 (m, 1H), 3.07 (dd, *J* = 14.1, 6.7 Hz, 1H), 2.86 (ddd, *J* = 17.3, 5.1, 1.1 Hz, 1H), 2.65 (ddd, *J* = 17.4, 9.3, 2.2 Hz, 1H), 2.40 (s, 3H).

^{13}C NMR (126 MHz, $CDCl_3$) δ 200.71, 143.67, 140.29, 138.88, 137.08, 136.54, 135.97, 129.91, 128.89, 128.83, 128.29, 127.39, 126.63, 124.03, 123.99, 123.62, 121.66, 54.27, 53.58, 47.14, 38.97, 21.66.

HR-MS (ESI) Calculated for $C_{26}H_{26}NO_3S_2^+$ $[M+H]^+$: 464.1349; found: 464.1345

5.7.5. Characterization of Products 55

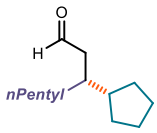

(*R*)-3-Cyclopentyloctanal (55a)

Prepared according to general procedure B from (*E*)-oct-2-enal (30.0 µL, 0.11 mmol) and cyclopentyl tetrabutylammonium trifluoroborate (**54a**) (37.9 mg, 0.1 mmol). The crude mixture was purified by column chromatography (SiO2 gel, 80:20 hexanes:CH_2Cl_2) to afford the product as a colorless oil (12.5 mg, 64% yield, average of two experiments, 82% ee). The enantiomeric excess of the corresponding 2,4-dinitrophenylhydrazone (obtained upon condensation with 2,4-dinitrophenylhydrazine) was determined by UPC² analysis analysis on a Daicel Chiralpak IG column (gradient: 1 min 100% CO2, 5 min, CO_2:EtOH from 100:0 to 60:40, flow rate: 2 mL/min, 30 °C; λ = 348 nm: τ_1 = 4.49 min, τ_2 = 4.68 min).

^{1}H NMR (400 MHz, $CDCl_3$) δ 9.80 (t, *J* = 2.5 Hz, 1H), 2.48 – 2.32 (m, 2H), 1.94 – 1.86 (m, 1H), 1.82 – 1.73 (m, 2H), 1.67 – 1.59 (m, 2H), 1.54 (ttd, *J* = 7.8, 3.9, 1.8 Hz, 2H), 1.48 – 1.42 (m, 1H), 1.37 – 1.23 (m, 8H), 1.20 – 1.05 (m, 2H), 0.90 (t, *J* = 6.9 Hz, 3H).

^{13}C NMR (126 MHz, $CDCl_3$) δ 203.23, 48.51, 45.17, 39.49, 33.45, 32.52, 30.80, 26.65, 25.63, 20.69.

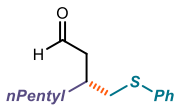

(*R*)-3-((Phenylthio)methyl)octanal (55b)

Prepared according to general procedure B from (*E*)-oct-2-enal (30.0 µL, 0.11 mmol) and trimethyl((phenylthio)methyl)silane (**54b**) (19.6 mg, 0.1 mmol, CH_3CN (300 uL), and H_2O (100 uL) . The crude mixture was purified by column chromatography (SiO_2 gel, 80:20 hexanes:CH_2Cl_2) to afford the product as a colorless oil (15.5 mg, 62% yield, average of two runs, 96% ee). The enantiomeric excess was determined by UPC² analysis analysis on a Daicel Chiralpak IG column (gradient: 1 min 100% CO2, 5 min, CO_2:*i*PrOH from 100:0 to 60:40, flow rate: 2 mL/min, 30 °C; λ = 253 nm: τ_1 = 2.70 min, τ_2 = 2.76 min).

^{1}H NMR (500 MHz, $CDCl_3$) δ 9.73 (t, *J* = 1.9 Hz, 1H), 7.35 – 7.23 (m, 4H), 7.20 – 7.13 (m, 1H), 3.05 (dd, *J* = 13.1, 5.4 Hz, 1H), 2.84 (dd, *J* = 13.1, 7.6 Hz, 1H), 2.65 (ddd, *J* = 17.0, 6.4, 1.7 Hz, 1H), 2.44 (ddd, *J* = 17.0, 6.5, 2.0 Hz, 1H), 2.24 (dtd, *J* = 7.6, 6.5, 5.3 Hz, 1H), 1.53 – 1.32 (m, 2H), 1.31 – 1.16 (m, 6H), 0.86 (t, *J* = 7.0 Hz, 3H).

^{13}C NMR (126 MHz, $CDCl_3$) δ 201.99, 132.39, 128.98, 126.78, 123.84, 47.72, 37.68, 33.75, 33.03, 31.80, 30.41, 25.83, 22.51.

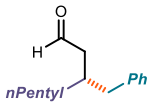

(*S*)-3-Benzyloctanal (55c)

Prepared according to general procedure B from (*E*)-oct-2-enal (30.0 µL, 0.11 mmol) and benzyl trimethylsilane (16.4 mg, 0.1 mmol). The crude mixture was purified by column chromatography (SiO2 gel, 80:20 hexanes:CH_2Cl_2) to afford the product as a colorless oil (16.2 mg, 74% yield, average of two runs, 95% ee). The enantiomeric excess of the corresponding 2,4-dinitrophenylhydrazone (obtained upon condensation with 2,4-dinitrophenylhydrazine) was determined by UPC² analysis on a Daicel Chiralpak IG column (gradient: 1 min 100% CO2, 5 min, CO_2:CH_3CN from 100:0 to 60:40, flow rate 2 mL/min, λ = 355 nm: τ_1 = 5.61 min, τ_2 = 6.30 min).

^{1}H NMR (500 MHz, $CDCl_3$) δ 9.64 (t, J = 2.0 Hz, 1H), 7.31 – 7.23 (m, 2H), 7.22 – 7.15 (m, 1H), 7.19 – 7.11 (m, 2H), 2.73 (dd, J = 13.6, 6.0 Hz, 1H), 2.48 (dd, J = 13.6, 7.8 Hz, 1H), 2.37 – 2.24 (m, 3H), 1.35 – 1.29 (m, 3H), 1.26 (ddd, J = 11.0, 5.4, 2.9 Hz, 5H), 0.87 (t, J = 7.0 Hz, 3H).

^{13}C NMR (126 MHz, $CDCl_3$) δ 204.06, 141.44, 129.61, 128.74, 126.52, 48.25, 40.98, 35.63, 34.46, 32.28, 31.26, 26.80, 22.93.

(*S*)-3-Methyl-4-phenylbutanal (55d)

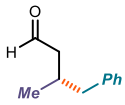

Prepared according to general procedure B from (*E*)-but-2-enal (16.6 uL, 0.2 mmol) and benzyl trimethylsilane (16.4 mg, 0.1 mmol). The crude mixture was purified by column chromatography (SiO_2 gel, 80:20 hexanes:CH_2Cl_2) to afford the product as a colorless oil (16.4 mg, 67% yield, average of two runs, 90% ee). The enantiomeric excess of the corresponding 2,4-dinitrophenylhydrazone (obtained upon condensation with 2,4-dinitrophenylhydrazine) was determined by UPC² analysis on a Daicel Chiralpak OJ column (gradient: 1 min 100% CO_2, 5 min, CO_2:CH_3CN from 100:0 to 60:40, flow rate 2 mL/min, λ = 351 nm: τ_1 = 4.07 min, τ_2 = 4.58 min).

^{1}H NMR (500 MHz, $CDCl_3$) δ 9.69 (dd, J = 2.5, 1.6 Hz, 1H), 7.31 – 7.11 (m, 5H), 2.62 – 2.51 (m, 2H), 2.46 – 2.30 (m, 2H), 2.23 (ddd, J = 15.8, 7.6, 2.5 Hz, 1H), 0.97 (d, J = 6.6 Hz, 3H).

^{13}C NMR (126 MHz, $CDCl_3$) δ 203.39, 140.87, 129.56, 128.73, 126.57, 50.61, 44.10, 30.61, 18.38.

5.7.6. Quantum Yield Determination

A ferrioxalate actinometer solution was prepared by following the Hammond variation of the Hatchard and Parker procedure[43] outlined in the *Handbook of Photochemistry*.[44] Ferrioxalate actinometer solution measures the decomposition of ferric ions to ferrous ions, which are complexed by 1,10-phenanthroline and monitored by UV/Vis absorbance at 510 nm. The moles of the iron-phenanthroline complex formed are related to the moles of photons absorbed. The values of the quantum yield of potassium ferrioxalate are related to concentration and wavelength.

The solutions were prepared and stored in the dark (red light):

1. **Potassium ferrioxalate solution 0.012M**: 147.4 mg of potassium ferrioxalate (commercially available from Alfa Aesar) and 69.5 µL of sulfuric acid (96%) were added to a 25 mL volumetric flask, and filled to the mark with water (HPLC grade).
2. **Phenanthroline solution**: 0.2% by weight of 1,10-phenanthroline in water (100 mg in 50 mL volumetric flask or 50 mg in 25 mL).

[43] Hatchard, C. G.; Parker, C. A. "A new sensitive chemical actinometer II. Potassium ferrioxalate as a standard chemical actinometer" *Proc. R. Soc. (London)*, **1956,** *A235*, 518.

[44] Montalti, M.; Credi, A.; Prodi, L.; Gandolfi, M. T. *Handbook of photochemistry*, Taylor&Francis, **2006,** 601.

3. **Buffer solution**: to a 100 mL volumetric flask 4.94 g of NaOAc and 1.0 mL of sulfuric acid (96%) were added and filled to the mark with water (HPLC grade).
4. **Internal standard solution**: 1.052 g of 1,3,5-trimethoxybenzene was added to a 5 mL volumetric flask which was filled up with HPLC grade acetonitrile (1.25 M).

Reaction setup:

1. **Reaction solution**: A Schlenk flask with stir bar was charged with amine catalyst **5** (35.3 mg, 0.05 mmol), **48a** (69.6 mg, 0.25 mmol), acetonitrile (1 mL). After three cycles of freeze pump thaw (with septum), TFA (11.5 µL, 0.15 mmol) and (*E*)-4-methylpent-2-enal (58.3 µL, 0.5 mmol) were added and the tube was sealed with parafilm and put in the HP-LED 460 nm at 1 cm distance at -10 °C with an irradiance of 38 mW/cm². Four different reactions were set up and irradiated for different times: 15 min, 30 min, 45 min, and 60 min. After each reaction was finished, the internal standard solution (200 µL, 0.25 mmol) was added. 500 µL of this solution was diluted with 4.5 mL of acetonitrile. From this solution were taken 100 µL, diluted to 1 mL, and analyzed by GC-FID.
2. **Actinometer solutions:** A Schlenk flask of the same dimensions as used for the reaction mixtures was loaded with 1.0 mL of actinometer solution and placed on the HP-LED the same light intensity as the reaction (without freeze pump thaw). Four different actinometer solutions were irradiated in sequence for 5 s, 10 s, 15 s, 20 s, and 25 s. To irradiate the Schlenk, it was placed on the holder with the light off and the light was turned on for the desired time. After each irradiation the actinometer solutions were carefully transferred into a 10 mL volumetric flask, then 0.5 mL of phenanthroline solution and 2.0 mL of buffer solution were added and the flask was filled up with water. The mixture was then analyzed by UV-Vis (Figure 5.22).[45]

[45] UV-Vis measurements were carried out on an Agilent Cary 60 UV-Vis spectrophotometer equipped with two silicon diode detectors, double beam optics and Xenon pulse light.

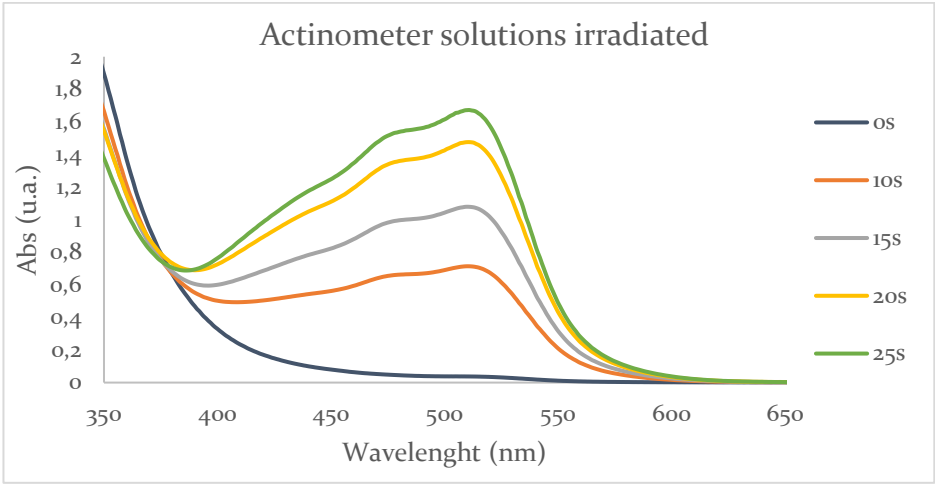

Figure 5.22. UV-Vis recorded spectra of the actinometer solutions irradiated for different periods of time.

The moles of Fe^{2+} formed for each sample are determined using Beers' Law (Eq. 5.1):

$$Moles\ of\ Fe(II) = \frac{V_1\ V_3\ \Delta A(510\ nm)}{10^3\ V_2\ l\ \epsilon(510\ nm)}\ (Eq.5.1)$$

where V_1 is the irradiated volume (1 mL), V_2 is the aliquot of the irradiated solution taken for the determination of the ferrous ions (1 mL), V_3 is the final volume after complexation with phenanthroline (10 mL), l is the optical path-length of the irradiation cell (1 cm), ΔA(510 nm) is the optical difference in absorbance between the irradiated solution and the one stored in the dark, ε(510 nm) is the extinction coefficient the complex $Fe(phen)_3^{2+}$ at 510 nm (11100 L mol^{-1} cm^1).

The moles of Fe^{2+} formed (x) are plotted as a function of time (t) (Figure 5.23). The slope of this line was correlated to the moles of incident photons by unit of time ($q^o_{n,p}$) by the use of the following Equation 3.4:

$$\Phi(\lambda) = \frac{dx/dt}{q^0_{n,p}[1 - 10^{-A(\lambda)}]}\ (Eq.5.2)$$

where dx/dt is the rate of change of a measurable quantity (spectral or any other property), the quantum yield (Φ) for Fe^{2+} at 458 nm is 1.11,[46] $[1\text{-}10^{-A(\lambda)}]$ is the ratio of absorbed photons by the solution, and A(λ) is the absorbance of the actinometer at the wavelength used to carry out the experiments (460 nm). The absorbance at 460 nm ($A(460)$) was 1.04.

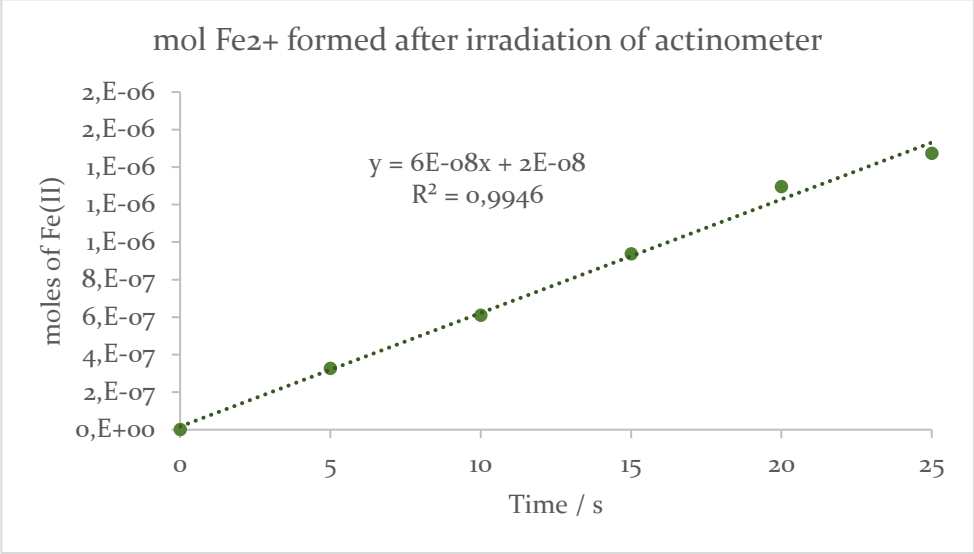

Figure 5.23. Plot of the moles of Fe^{2+} generated from the irradiation of the actinometer solutions, against time.

The photon flux, which is $q^{o}_{n,p}$, was determined to **1,81249x10^{-7} einstein s^{-1}**.

The moles of product per unit of time are plotted against the number of photons absorbed. The photons absorbed are correlated to the number of incident photons by the use of Equation 5.2. According to this, if we plot the moles of product (x-axis) versus the moles of incident photons ($q^{o}_{n,p}dt$), the slope is equal to:

$$\text{slope} = \Phi[1 - 10^{-A(460\ nm)}]\ (Eq.\ 5.3)$$

where Φ is the quantum yield to be determined and A(460 nm) is the absorption of the reaction under study. A(460 nm) was measured to be of 1.29 for the model reaction mixture.

[46] Holubov, C. A.; Langford, C. H. "Wavelength and Temperature Dependence in the Photolysis of the Chemical Actinometer, Potassium trisoxalatoferrate(III), at Longer Wavelengths" *Inorganica Chim. Acta*, **1981**, 53, 59.

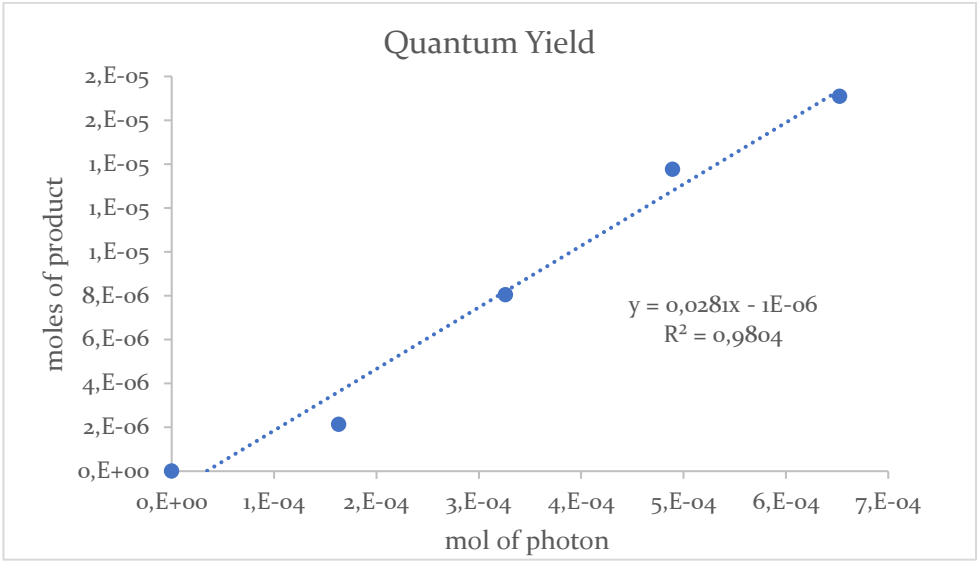

The quantum yield of the conjugate radical addition of **48a** to (*E*)-4-methylpent-2-enal was calculated to be **0.03**.

The procedure was repeated a second time to provide a similar value: quantum yield at 460 nm of **0.02**.

Chapter VI

General Conclusions

One of the most effective and used organocatalytic intermediates to achieve highly enantioselective transformations is the chiral iminium ion. Over the past twenty years, iminium ion activation has been widely explored in two-electron pathways to promote many enantioselective transformations. In contrast, less attention has been paid to processes involving radicals. Using the strong oxidizing power of photoexcited iminium ions recently demonstrated by our group, I succeeded in developing, during my research thesis, new enantioselective radical cascade processes. In a first example (*Chapter III*), we implemented a visible-light-mediated organocatalytic cascade based that combined two sequential radical-based bond-forming events in a single step and converted unactivated olefins and α,β-unsaturated aldehydes into complex chiral products. Additionally, we applied the photochemical activity of chiral iminium ions to activate allenes by SET oxidation (*Chapter IV*). This process delivers highly complex bicyclic structures in good enantioselectivities and excellent diastereoselectivity.

Finally, in *Chapter V* we addressed the main limitation of the previous excited iminium ion-based strategy: the need for an aromatic substituent at the β position of the enal substrate (such as cinnamaldehyde). We realized that a useful approach to overcome this limitation was to independently generate the radical with an external photoredox catalyst. The ensuing radical was then trapped by the ground-state chiral electrophilic iminium ion with high stereocontrol. The net reaction was a radical conjugate addition to linear aliphatic and aromatic enals via ground-state iminium ion-mediated catalysis, affording β-disubstituted chiral aldehydes. Different radical precursors such as trifluoroborate salts could be used to generate alkyl, benzyl, and α-heteroatom radicals and engage them in the enantioselective radical addition protocol.

Overall, these studies expanded the synthetic potential of iminium ion-mediated asymmetric catalysis from classical polar reactivity to include photochemistry and radical processes.

UNIVERSITAT ROVIRA I VIRGILI
COMBINING IMINIUM ION-MEDIATED CATALYSIS AND PHOTOCHEMISTRY TO DEVELOP ENANTIOSELECTIVE RADICAL PROCESSES
Pablo Bonilla Domínguez

UNIVERSITAT ROVIRA I VIRGILI
COMBINING IMINIUM ION-MEDIATED CATALYSIS AND PHOTOCHEMISTRY TO DEVELOP ENANTIOSELECTIVE RADICAL PROCESSES
Pablo Bonilla Domínguez

UNIVERSITAT ROVIRA I VIRGILI
COMBINING IMINIUM ION-MEDIATED CATALYSIS AND PHOTOCHEMISTRY TO DEVELOP ENANTIOSELECTIVE RADICAL PROCESSES
Pablo Bonilla Domínguez

UNIVERSITAT ROVIRA I VIRGILI
COMBINING IMINIUM ION-MEDIATED CATALYSIS AND PHOTOCHEMISTRY TO DEVELOP ENANTIOSELECTIVE RADICAL PROCESSES
Pablo Bonilla Domínguez